DEPARTMENT OF THE INTERIOR

UNITED STATES GEOLOGICAL SURVEY

GEOLOGICAL SOCIETY OF AMERICA
SHORT COURSE NOTES

Thermochronology: Applications to Tectonics, Petrology, and Stratigraphy

by

John F. Sutter[1], Peter K. Zeitler[2], and Robert D. Tucker[3]

[1] U.S. Geological Survey, 908 National Center, Reston, Virginia 22092

[2] Department of Earth and Environmental Sciences, Lehigh University, Bethlehem, Pennsylvania 18015-3188

[3] Geochronology Laboratory, Royal Ontario Museum, Toronto, Ontario M5S 2C6, Canada

TABLE OF CONTENTS

REVIEW OF ISOTOPE SYSTEMATICS

Cooling Ages and Diffusion
(P.K. Zeitler)

1. Introduction

Most geologists are familiar with the advances in igneous petrology and global dynamics that followed from developments in radiogenic tracer-isotope geochemistry. Fewer geologists seem to be aware that the advances made in geochronology in the 1970's and 1980's constituted an equally great leap forward for students of lithospheric processes. Because of the importance of heat transfer as a fundamental driving mechanism of tectonic activity, the fact that geochronological methods can reveal a sample's thermal history has given workers in metamorphic petrology and tectonics an important means for measuring the rates and timing of geological processes.

This short course in thermochronology and related aspects of geochronology has been organized around numerous case studies. However, before we proceed we will spend some time reviewing how the various dating systems used in thermochronology actually work. We will also review the theoretical basis for thermochronology, which amounts to a review of diffusion theory as applied to geochronological systems.

Perhaps ironically, the roots of thermochronology lie in the frequent violation of one of the fundamental assumptions of traditional geochronology. For an age determination to represent the formation age of a rock, the following assumptions must have held true: (1) decay of radioactive parent occurred at a constant rate unaffected by any environmental conditions experienced by the sample; (2) no isotopic fractionation occurred within the parent-daughter system; (3) correction can be made for any daughter isotope incorporated into the sample at the time of its formation; and (4) the parent-daughter system remained closed. In practice, requirement (4) is often not met and in many geological environments open-system behavior is virtually the rule. Thermochronology represents the attempt to exploit this widespread open-system behavior to obtain quantitative information about temperature (and other) histories.

Although we will provide specific references below, it is appropriate to note at this point that several good texts are available that provide basic information about geochronological methods and their applications. The textbook by Faure (2nd edition, 1986) covers nearly all dating methods and is a good general text. The book by McDougall and Harrison (1988) covers the $^{40}Ar/^{39}Ar$ method in detail, and also clearly explains the application of diffusion theory to $^{40}Ar/^{39}Ar$ thermochronology; the book is also a good introduction to solving problems involving the diffusive transfer of mass or heat. Mussett (1969) provides a useful review of diffusion and geochronology, and the articles by Giletti (1974a,b) are a useful introduction to measurement of kinetic parameters. Finally, the classic books by Crank (1975) and Carslaw and Jäger (1959) remain authoritative texts for obtaining fundamental solutions to a wide variety of diffusion problems.

2. Historical Perspective

The early work in geochronology, beginning with the first U-He age determinations made at the beginning of this century, was directed towards determining the formation ages of rocks and numerically calibrating the geologic time scale. However, it soon became apparent that in many cases measured ages were too low, particularly ages determined on mineral separates (as opposed to whole rocks). By the early- to mid-1960's, this phenomenon was widely recognized, and geochronologists were generally aware of the fact that many of the ages they determined were a function of the thermal histories of their samples. Classic papers from this period include those by Mason (1961), Hurley et al. (1962), Armstrong (1966), Westcott (1966), Harper (1967), and Dewey and Pankhurst (1970).

What followed this realization about the importance of thermal history was an increasing effort by geochronologists to place temperature constraints on the various mineral dating systems they used. For the most part, the initial efforts were made by means of geological calibrations carried out in contact aureoles and in slowly cooled terranes (Hart, 1964; Hanson and Gast; 1967, Jäger et al., 1967; Pankhurst et al., 1973; Wagner et al., 1977; Harrison et al., 1979). Throughout the 1970's, increasing numbers of laboratory experiments were also carried out (e.g., Foland, 1974; Giletti, 1974a; Harrison, 1981). This decade also saw publication of the seminal paper by Dodson (1973) setting out the mathematical basis for diffusion in slow cooling systems.

The 1980's were the decade in which methods began to catch up with theory. Fission-track dating became widely used, and because all of the mineral systems used with this method are very temperature sensitive, the potential for thermal history determination became more widely appreciated among the geological community. During the same period, $^{40}Ar/^{39}Ar$ dating underwent something of a resurgence as the technique increasingly was applied to terrestrial rocks, and as methods of analysis and interpretation were refined (Harrison, 1983). The decade ended with attempts to refine the accuracy and precision of thermochronological techniques, both from a theoretical and material-properties perspective, and with increasing attempts to examine and develop higher-temperature geochronological systems as thermochronometers.

3. A Hierarchy of Dating Systems

What happens when you apply the available dating techniques to samples having other than a simple geologic history? What you almost always get is a range of ages, and you find that by in large the various dating systems give consistently different results. In general, for a slowly cooled rock, you can arrange the dates you obtain as follows (after Dodson and McClelland-Brown, 1985):

Greatest age: U-Pb zircon
U-Pb monazite
U-Pb sphene
Nd-Sm garnet
U-Pb apatite, rutile
K-Ar hornblende

2

```
                         Rb-Sr muscovite
                         K-Ar muscovite
                         Rb-Sr biotite
                         K-Ar biotite
                         Fission-track sphene
                         K-Ar K-feldspar
                         fission-track zircon
                         fission-track apatite
Lowest age:              U-Th-He apatite
```

To make this point another way, we can look at the mineral age data of the sort obtained by Harrison et al., 1979 and Harrison and McDougall (1980) from large batholiths. When you plot measured ages against estimates of the "closure temperature" for each mineral system (we'll discuss closure temperature in a moment), you can see how the mineral ages define what is a very plausible thermal history for a cooling pluton (Figure 1).

The important point to realize is that mineral ages are best thought of as cooling ages. Because most rocks were hot or at least warm sometime in their lives, the safest course to take when you are confronted with an age determination is to be suspicious and take as a working hypothesis that your age is a cooling age. Of course you will then want to delve deeper: you need to consider what other complex thermal, geochemical, or metamorphic histories might be responsible for an age, or whether your age is in fact a primary age for some event. In the next two days, we would like to give you some feeling for how you can determine what your age might mean, and more important, how you can use the thermal (and "petrological") sensitivity of most mineral dating systems to place quantitative constraints on geological processes.

4. How Diffusion Explains Cooling Ages--Part I

What lies behind the frequent observation of cooling ages? Mostly the process of diffusion, and partly the geochemistry, thermodynamics, and kinetics that shape a sample's petrology. Thermally activated diffusion is so critical to thermochronometry that we really need to spend a bit of time establishing the basics.

(i) Diffusion is an inevitable natural process that is easy to understand. Matter (like heat) tends to flow down concentration gradients. If you live in a big house and someone leaves the front door open early in the autumn, leaves will begin to enter your home (if you have children you know that this is inevitable). Eventually, you will find leaves everywhere in your house. The leaves move randomly, and some leaves go out even as others are coming in. The point is that the leaves have diffused in, and they'll keep coming in until they're as dense inside as they are outside (to extend the analogy to its limits: think of the door sill as a partition coefficient, think of a potted plant in the house as a source term in the diffusion equation, and think of the amount of foot traffic in your house as an analogy for temperature: more feet, faster-moving leaves).

(ii) In geological materials, the rate of diffusion if strongly temperature dependent, and follows an Arrhenius relationship:

$$D = D_0 e^{-\frac{E}{RT}} \qquad (1)$$

The pre-exponential constant D_0 can be thought of as describing the relative ease of diffusion through a material, and the activation energy E can be thought of as describing the probability of an atom making a jump. Typically used units (which persist in the literature in non-SI form) are:

D_0 and D:	square centimeters per second
activation energy, E:	calories per mole
gas constant, R:	1.987 calories per degree Kelvin per mole;
temperature, T:	degrees Kelvin

In geological materials, the diffusion coefficient will typically vary by many orders of magnitude. For example, in the case of argon diffusion in a potassium feldspar, E might be 45000 cal/mole and D_0 might be 1 x 10^{-4} cm^2/s. Therefore, at 20°C (293.15 K) D will be 2.8 x 10^{-38} cm^2/s, but at 250°C (523.15 K) D would be 1.6 x 10^{-23} cm^2/s. That is over fourteen orders of magnitude higher!

(iii) Fick's Laws can be used to describe the state of diffusion in a geochronological system of interest. In such a system, Fick's First Law states that in the steady-state, the flux of diffusing isotope is directly proportional to the concentration gradient of that isotope. For the case of one-dimensional diffusion:

$$F = -D\frac{\partial C}{\partial x} \qquad (2)$$

Note that in this equation, the diffusion coefficient D is the constant of proportionality, and that the minus sign stems from the fact that diffusion occurs down the concentration gradient (like heat flows down a temperature gradient). Speaking of heat, note that Eqn. 2 is of the same form as the expression for steady-state heat flow.

For our purposes, the steady state is not relevant and is quite boring. In fact, it's hard to imagine a geochronological system that is in steady state, since radioactive decay keeps on providing daughter isotope relentlessly. At high temperatures, where daughter isotope can be lost as fast as it is produced, one can imagine a steady state being established, but that's only useful as a starting point for what we're interested in, which is to accumulate some daughter product and get an age!

The transient condition is what we need to worry about. Fick's Second Law is relevant here (again, for the one dimensional case; note that this equation is analogous to the equation for temperature distribution under transient conditions):

$$\frac{\partial C}{\partial t} = D \frac{\partial^2 C}{\partial x^2} \qquad\qquad (3)$$

It is straightforward to derive this equation from first principles, but a useful way to view it is to think of differentiating the steady-state equation (Eqn. 2) with respect to time. Fick's Second Law merely states that the change in concentration with respect to time is proportional to any gradient in the concentration gradient. If we remember that dating systems involve radioactive decay, we can add a source term A^* to Eqn. 3 to obtain a complete description (believe it or not) of a thermochronological system:

$$\frac{\partial C}{\partial t} = D \frac{\partial^2 C}{\partial x^2} + A^* \qquad\qquad (4)$$

How is this so? Eqn. 4 describes the loss (or possibly, gain) of daughter product by diffusion, and the gain of daughter product by decay. But there's more tucked away in this equation than that, especially when it comes down to choosing some boundary conditions and actually solving it. Specifically, recall from Eqn. (1) that the diffusion coefficient D is a function of temperature. Hence, temperature is an implicit part of Eqn. 4, and solutions can be obtained which reflect changes in concentration of daughter isotope as a function of thermal history. That's thermochronology!

Fortunately for those of us who are not mathematically agile, a wide range of solutions to Eqn. 4 are available, for both general cases and specific geochronological systems. Furthermore, many of these solutions can be expressed as simple algebraic formulae like this:

$$f = \frac{2}{\sqrt{\pi}} \sqrt{\frac{Dt}{a^2}} \qquad \textit{(for values of f<0.45)} \qquad (5)$$

Here f is the fractional diffusive loss of daughter isotope from a plane sheet having a diffusion dimension (half-width) a and having suffered a thermal event of duration t which was of sufficient temperature to yield a diffusion coefficient D. Crank (1975) offers many solutions of the diffusion equation, and many of the solutions in the classic book on heat transfer by Carslaw and Jäeger (1959) are direct analogs to diffusion problems. Finally, McDougall and Harrison (1988) provide a very useful tabulation and explanation of a number of solutions of varying complexity.

Eqn. 5 sneaks in a two very important points. First, in most solutions to the diffusion equation of interest to geochronologists, there is one other important parameter that must be considered besides D and t: what has often been called "grain size" but more properly should be referred to as "diffusion dimension" or "domain size" (daughter

isotope can be considered to have escaped from a crystal once it has reached any number of fast-diffusion pathways, only one of which may be a grain boundary). Second, in general, the parameter of importance in diffusion is Dt/a^2 and it is important to note that the three components of this parameter all have equivalent influence. Thus, if all that is known about a poorly characterized sample is that it has lost some daughter isotope, it is not possible to isolate the effects of temperature from that of heating duration or grain size. Another important point to make about the parameter Dt/a^2 is that in cases of geologically brief episodic heating (where production of daughter isotope by decay can be ignored), one can make the following substitution in solutions to the diffusion equation:

$$x = \frac{1}{a^2}\int^t D(t)dt \qquad (6)$$

where $D(t)$ is the diffusion coefficient as a function of time (e.g., thermal history), and where it is assumed that diffusion dimension is not time dependent. In other words, the good news is that it is only the integrated thermal history that matters in many calculations, and the bad news is that a single age determination cannot be used to differentiate between different styles of episodic heating.

4. How Diffusion Explains Cooling Ages--Part II

In his classic paper (Dodson, 1973) presented a solution to the diffusion equation which addressed the case of slow cooling. Dodson's equation provided a theoretical basis for the young ages that were frequently observed by geochronologists, and it also provided a quantitative framework with which to use the growing body of diffusion data. Let's examine both these aspects of Dodson's pivotal contribution to thermochronology.

Conceptually, what the closure-temperature theory does is balance the exponentially diminishing effectiveness of diffusion during slow cooling against the steady accumulation of daughter product from radioactive decay. Figure 2 shows what this statement means. Over geologically reasonable time scales, there are temperature ranges where a mineral system will be completely open, and there are temperature ranges where a mineral system will be completely closed. Between these two ranges will be a fuzzy temperature range where the mineral system is partly open: daughter isotopes accumulates, but not as rapidly as one would expect in a completely closed system. What Dodson's formula provides is a means to extrapolate back and extract the temperature of the system at the time given by its apparent age. This is an absolutely essential concept in thermochronology: it is the definition of the term "closure temperature."

Here's the equation for closure temperature (Figure 3 shows an annotated version):

The terms on the right-hand side of Eqn. 7 together define the closure temperature T_c E is activation energy, R is the gas constant, D_0 is the pre-exponential constant from the

$$T_c = \frac{(\frac{E}{R})}{\ln[\frac{AT_c^2(\frac{D_0}{a^2})}{(\frac{E}{R})(\frac{dT}{dt})}]} \qquad (7)$$

Arrhenius equation, and a is the diffusion dimension (the lumped parameter D_0/a^2 is sometimes referred to as the "frequency factor"). A is a diffusion-geometry term that is equal to 8.7 for infinite slabs, 27 for cylinders (radial diffusion geometry) and 55 for spheres. dT/dt is the cooling rate experienced by the sample while it was undergoing closure. Finally, T_c is ...closure temperature! The closure-temperature equation is iterative in nature, and you have to guess a value of T_c to get things rolling. Because of the nature of the natural log function, the equation converges rapidly, usually within two or three passes.

As an example, let's calculate a closure temperature for a hypothetical sample. Given:

pre-exponential term, D_0:	1 x 10^{-4} cm^2/s
diffusion dimension, a:	1 x 10^{-2} cm (100 μm)
activation energy, E:	45000 cal/mol
gas constant, R:	1.987 calories per degree Kelvin per mole;
geometry factor, plane sheet, A:	8.7
cooling rate, dT/dt:	10°C/m.y.

The first thing to do is to convert the cooling rate to degrees Kelvin per second: that would be 3.169 x 10^{-13} K/s. Next, let's guess a value for closure temperature of, say, 300°C, which is 573.15 K. Using this temperature, the value of the natural log term is 33.62 and E/R is 22647 K, so the first iteration yields a closure temperature estimate of 673.7 K (400.5°C). Substituting that estimate for closure temperature back into the equation yields a new estimate of 667.2 K; a third iteration using this estimate leads to a closure temperature of 667.6 K (394.5°C).

There are a number of things to note about closure temperature. First, it is important to realize that closure temperature is dependent not only on a sample's diffusion kinetics but also on cooling rate. Compared to slowly cooled samples, samples that cool quickly spend less time in the transitional, partially open state. Very roughly, the closure temperature of a sample will vary by about 10% per order of magnitude change in cooling rate (or a^2 or D_0). A second thing to note about closure temperatures is that they are only relevant to thermal histories involving continuous cooling. Citing a closure temperature when discussing whether or not a system should have survived a thermal resetting makes no sense whatsoever (this might seem obvious to you, but it is a common error). A third thing to realize about the term "closure temperature" is that

some people use the term "blocking temperature" as its synonym; this is fine if what is meant is in fact Dodsonian behavior based on volume diffusion or first-order kinetics. However, it can be argued that use of the term "blocking temperature" for isotopic systems could be misleading, because (1) paleomagnetic systems have much higher activation energies and thus are far more temperature sensitive than isotopic systems (e.g., only a very short time spent at the magnetic blocking temperature will erase a magnetization), and (2) as a consequence, in paleomagnetic systems it is appropriate to think of blocking and unblocking as occurring at a single temperature, whereas this is not the case for isotopic systems. Finally, it should be recognized that closure-temperature theory applies not only to thermochronological systems, but to many petrological systems as well, where closure can be thought to represent, for example, the "freezing in" of exchange reactions.

5. Diffusion Profiles

One consequence of diffusion is that anything other than a completely straightforward thermal history consisting of very fast cooling will result in a sample developing appreciable diffusion gradients in its radiogenic daughter isotopes. This is because the boundary conditions superimposed on our samples are (1) a finite or rate-limited supply of daughter product, and (2) a grain boundary immersed in an infinite sink having effectively a zero concentration of daughter isotope. As a result, it is reasonable to expect that many natural samples will have diffusion profiles set up within their diffusion domains. For many geochronological methods, this information is of academic interest only, for it is likely that diffusion domains will be on the order of microns or even less, and the technological means do not exist to cleanly sample such small domains. However, the $^{40}Ar/^{39}Ar$ method is potentially an exception, in that it uses diffusion itself to pump natural diffusion gradients out of samples in the laboratory. Therefore, it is worth knowing that in theory the diffusion profiles developed in a slowly cooled minerals can be used to constrain segments of temperature-time paths, as each position along a diffusion profile can be thought of as having a position-dependent closure temperature (Dodson, 1986). We will return to this topic again when we discuss the $^{40}Ar/^{39}Ar$ dating of potassium feldspars.

6. References

Armstrong, R. L., 1966, K-Ar dating of plutonic and volcanic rocks in orogenic belts. *In*: Schaeffer, O. A. & Zahringer, J. (eds.) *Potassium-Argon Dating*. Springer-Verlag, Berlin, 117-133.

Carslaw, H.S. & Jaeger, J.C., 1959, *Conduction of Heat in Solids (2nd ed.)*. Oxford University Press, New York.

Crank, J., 1975, *The Mathematics of Diffusion (2nd ed.)* Oxford University Press, New York.

Dewey, J.F. & Pankhurst, R.P., 1970, The evolution of the Scottish Caledonides in relation to their radiometric age patterns. *Transactions of the Royal Society of Edinburgh*, 69, 361-389.

Dodson, M.H., 1973, Closure temperatures in cooling geochronological and petrological systems. *Contributions to Mineralogy and Petrology*, 40, 259-274.

Dodson, M.H., 1986, Closure profiles in cooling systems. *Materials Science Forum*, 7, 145-153.

Dodson, M.H. & McClelland-Brown, E., 1985, Isotopic and palaeomagnetic evidence for rates of cooling, uplift and erosion. *In*: Snelling, N.J. (ed.) *The Chronology of the Geological Record*. Memoir Geological Society London, 10, 315-325.

Faure, G., 1986, *Principles of Isotope Geology (2nd. ed.)*. Wiley, New York.

Foland, K.A., 1974, ^{40}Ar diffusion in homogeneous orthoclase and an interpretation of Ar diffusion in K-feldspar. *Geochimica et Cosmochimica Acta*, 38, 151-166.

Giletti, B.J., 1974a, Studies in diffusion, I. Argon in phlogopite mica. *In*: Hofmann, A.W., Giletti, B.J., Yoder, H.S. & Yund, R.A. (eds.) *Geochemical Transport and Kinetics*. Carnegie Institution, Washington, D. C., 107-116.

Giletti, B.J., 1974b, Diffusion related to geochronology. *In*: Hofmann, A.W., Giletti, B.J., Yoder, H.S. & Yund, R.A. (eds.) *Geochemical Transport and Kinetics*. Carnegie Institution, Washington, D. C., 61-76.

Hanson, G.N. & Gast, P.W., 1967, Kinetic studies in contact metamorphic zones. *Geochimica et Cosmochimica Acta*, 31, 1119-1153.

Harper, C.T., 1967, The geological interpretation of potassium-argon ages of metamorphic rocks from the Scottish Caledonides. *Scottish Journal of Geology*, 3, 46-66.

Harrison, T.M., 1981, Diffusion of ^{40}Ar in hornblende. *Contributions to Mineralogy and Petrology*, 70, 324-331.

Harrison, T.M., 1983, Some observations on the interpretation of ^{40}Ar/^{39}Ar spectra. *Chemical Geology (Isotope Geoscience Section)*, 1, 319-338.

Harrison, T.M. & McDougall, I., 1980, Investigation of an intrusive contact in NW Nelson, New Zealand. I. Thermal, chronological and isotopic constraints. *Geochimica et Cosmochimica Acta*, 44, 1985-2003.

Harrison, T.M., Armstrong, R.L., Naeser, C.W. & Harakal, J.E., 1979, Geochronology and thermal history of the Coast Plutonic Complex near Prince Rupert, British Columbia. *Canadian Journal of Earth Sciences*, 16, 400-410.

Hart, S.R., 1964, The petrology and isotopic mineral age relations of a contact zone in the Front Range, Colorado. *Journal of Geology*, 72, 493-525.

Hurley, P.M., Hughes, H., Pinson, W.H., Jr. & Fairbairn, H.W., 1962, Radiogenic argon and strontium diffusion parameters in biotite at low temperatures obtained from Alpine fault uplift in New Zealand. *Geochimica et Cosmochimica Acta*, 26, 67-80.

Jäger, E., Niggli, E. & Wenk, E., 1967, Rb-Sr Alterbestimmungen an Glimmern der Zentralalpen. *Beitrage zur Geologisches Karte der Schweiz*, 134, 1-67.

Mason, B., 1961, Potassium-argon ages of metamorphic rocks and granites from Westland, New Zealand. *New Zealand Journal of Geology and Geophysics*, 4, 352-356.

McDougall, I. & Harrison, T.M., 1988, *Geochronology and Thermochronology by the ^{40}Ar/^{39}Ar Method*. Oxford University Press, New York.

Mussett, A.E., 1969, Diffusion methods and the potassium-argon method of dating. *Geophysical Journal of the Royal Astronomical Society*, 18, 257-303.

Pankhurst, R.J., Moorbath, S., Rex, D.C. & Turner, G., 1973, Mineral age patterns in ca. 3700 m.y. old rocks from West Greenland. *Earth and Planetary Science Letters*, 20, 157-170.

Wagner, G.A., Reimer, G.M. & Jäger, E., 1977, Cooling ages derived by apatite fission track, mica Rb-Sr and K-Ar dating: the uplift and cooling history of the Central Alps. *Memoir of the Institute of Geology and Petrology of the University of Padova*, 30, 1-27.

Westcott, M.R., 1966, Loss of argon from biotite in a thermal metamorphism. *Nature*, 210, 83-84.
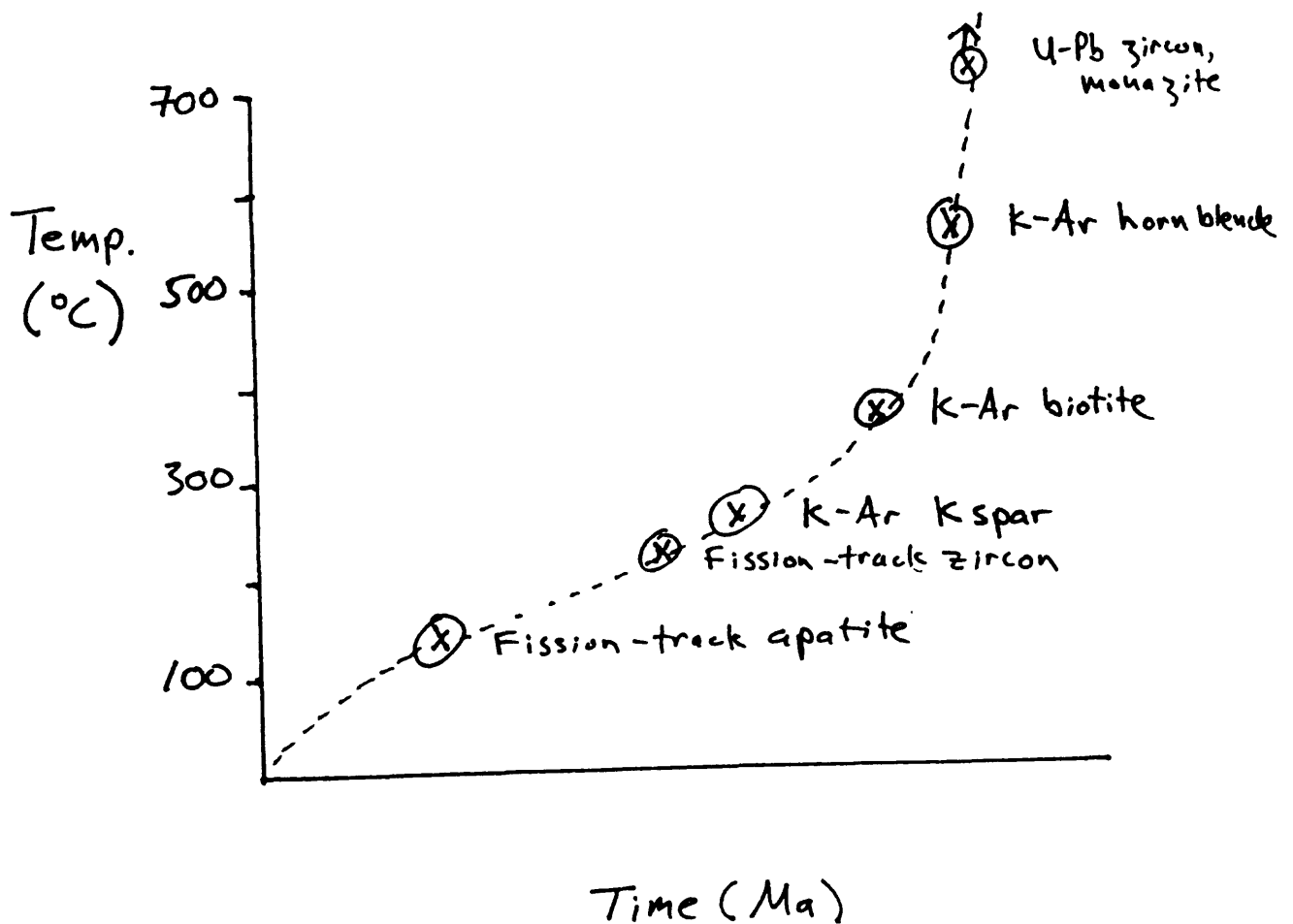
1. Sketch showing the thermal history to be expected from a cooling intrusion (dashed line), and the typical results that one would obtain from dating a suite of thermochronometers from the intrusion. The "ages" for each mineral system have been plotted against their estimated closure temperatures to yield an empirically derived cooling curve.
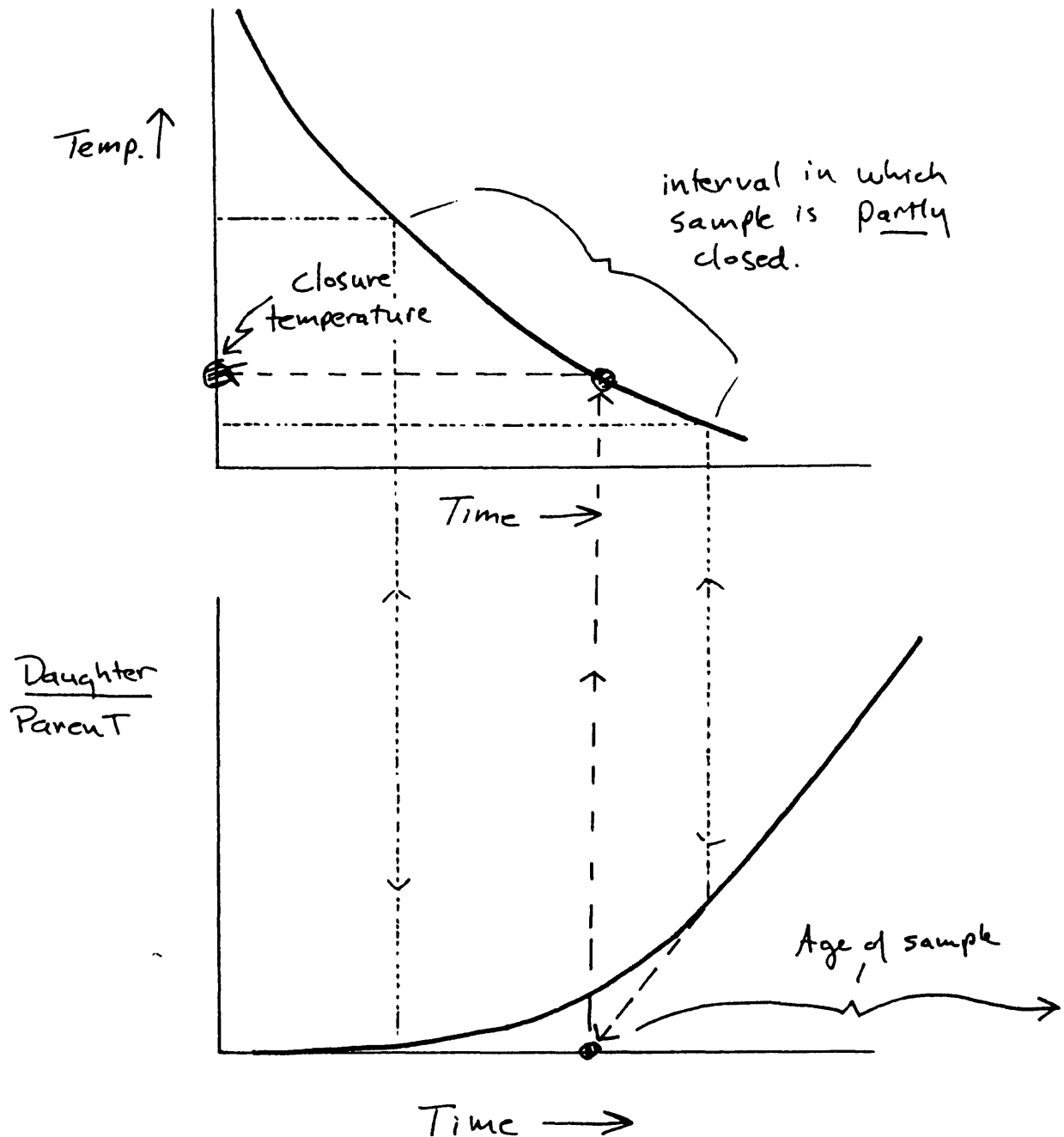
2. A graphical representation of the closure phenomenon. The top figure shows the temperature history experienced by a sample, and the bottom panel shows the value of the parent-daughter ratio as a function of thermal history. The closure temperature represents the temperature of the system at the time given by its apparent age. Note that at high temperatures the sample is completely open (no daughter product is retained), and that at low temperatures the sample is completely closed (all daughter product is retained). In the transitional interval, some of the daughter produced by decay is retained (in the centers of grains). Note also that for the isotopic systems typically used in thermochronometry, for times near and within the closure interval, the growth of the daughter/parent ratio can be approximated as a linear function of time.

12

Closure Temperature

Parameters of geological interest:
- → Closure temperature
- → Cooling rate
- → Diffusion dimension (? = grain size?)

$$T_c = \frac{E/R}{\ln\left[\dfrac{A \cdot T_c^2 \cdot D_0/a^2}{E/R \cdot dT/dt}\right]}$$

Knowable Material properties:
- → Activation energy (ease of jump)
- → Diffusion coefficient (... holes in cheese)
- → Diffusion dimension

Note #1: ↑ $\frac{dT}{dt}$ by 10x, ↑ T_c by 10%

Note #2: all we need is $\boxed{D_0/a^2}$

3. Annotated copy of closure-temperature equation.

Blank

.

Samarium-Neodymium and Uranium-Lead
(R. Tucker)

Introduction

This chapter is intended to introduce to the nonspecialist the principles of isotopic dating, and to illustrate with real examples the range of geological problems that may be studied by the U-Pb method as it is practiced in many laboratories today. The chapter is divided into two parts. The first part, covering Day 1 AM, is a review of the principles of isotopic dating, introducing the fundamentals of the method using both the Sm-Nd and U-Pb systems as examples. The second part of the chapter is a brief survey of some geological applications of the U-Pb method, done by the isotope dilution method, using selected examples of the author (some unpublished). Space limitations preclude a comprehensive review or discussion of the U-Pb technique practiced by the crystal evaporation (Kober 1986, 1987) or ion-microprobe methods (*e.g.* Compston *et al.* 1984, Kinney *et al.* 1988, Bowring *et al.* 1989), and for this, the reader is referred to selected listings in the references or to a recent review article by Heaman and Parrish (1991).

PART I. DAY 1, AM: REVIEW OF ISOTOPE SYSTEMATICS

An isotopic age may be determined for a mineral or a suite of cogenetic minerals and rocks provided that neither radioactive parent nor radiogenic daughter were lost or gained from the sample over its lifetime, that each sample had an identical initial daughter isotopic ratio at their time of formation, and that parent and daughter are present in sufficient abundance to enable meaningful measurements to be made. In practice, the method of isotopic dating selected for use depends on the type of age information that is sought, as well as a host of geological factors that may favor or preclude one method over another. Although the principles and assumptions of most methods are the same, the type of extractable age information is not, primarily because of inherent differences in the chemical properties of parent and daughter nuclides. The task for the geologist is to learn the strengths and limitations of each dating method, and to understand how geological processes magnify or diminish these strengths for a given application. No single method or technique can be applied with equal success to all dating projects and, in some instances, full appreciation of the complexity of a problem will only come with a multidisciplinary approach. That said, over thirty years of experience in the isotope community has demonstrated that some methods of dating enjoy distinct advantages over others for the same application and, with appropriate attention to collecting and analytical technique, these methods can be applied to most geological problems to yield highly precise and accurate ages.

The Samarium-Neodymium Method

The fundamental principle of the Sm-Nd, Rb-Sr, and Re-Os methods is that the production of radiogenic daughter isotope, D, occurs at a constant rate through time,

with the amount of the daughter produced being proportional to the amount of radioactive parent isotope (P) present. As can be seen in Equation 1, the decay equation predicts that the amount of daughter atoms present today (D_{total}) is the sum of the daughter isotopes present initially (D_{inital}) and the radiogenic component, P $(e^{\lambda t}-1)$, produced during time t.

$$D_{total}=D_{initial}+P(e^{\lambda t}-1)_{rad} \qquad (8)$$

As we can only measure isotopic ratios in mass spectrometers, it is convenient to reference both P and D_{total} relative to a stable isotope of the daughter element such that Equation 1 becomes:

$$\left.\frac{D_{total}}{D_{ref}}\right]_{meas} = \left.\frac{D_{init}}{D_{ref}}\right]_{initial} + \left.\frac{P}{D_{ref}}(e^{\lambda t}-1)\right]_{rad} \qquad (9)$$

which has the general form of the equation for a straight line. Note that in this form, the amount of the daughter isotope present (D_{meas}) is the sum of the radiogenic daughter plus the nonradiogenic component present in the sample at $t=0$ (the *initial* daughter). Also present at the time of mass spectrometric measurement is the nonradiogenic contaminant contributed by the laboratory during analysis (the laboratory blank) which, for the present discussion, we shall assume to have a value much less than $D_{initial}$.

The solution for t may be obtained two ways. If the number of atoms produced through decay (radiogenic component) greatly exceeds that initially present (the initial component), then t can be determined from the abundance of P and D without precise knowledge of the initial daughter isotopic composition. This form of solution was recognized by Goldschmidt (1937) and Hahn *et al.* (1937) over thirty years ago, and an early application of the method was for dating Rb-rich lepidolite using the decay of ^{87}Rb to ^{87}Sr (Ahrens 1946). The second solution, having far greater application for geological materials, is to analyze several samples of the same age and initial daughter isotopic composition, but different ratios of P/D_{ref}, to construct the familiar isochron diagram (Allsopp 1961, Nicolaysen 1961, Faure 1986). If all rocks and minerals behaved as closed-systems, had the same initial isotopic ratio and age, they will define a straight line, the slope of which corresponds to the age of the system.

As can be seen in Equation 2, the precision of an isochron may be improved by obtaining an array exhibiting a large spread in P/D_{ref}. For the Sm-Nd system, Equation 2 becomes:

$$\left.\frac{^{143}Nd}{^{144}Nd}\right]_{meas} = \left.\frac{^{143}Nd}{^{144}Nd}\right]_{initial} + \left.\frac{^{147}Sm}{^{144}Nd}(e^{\lambda_{147}t}-1)\right]_{rad} \qquad (10)$$

where ^{147}Sm/^{144}Nd is the measure of P/D_{ref}. Unlike the Rb-Sr, Re-Os, and U-Th-Pb systems, however, parent (^{147}Sm) and daughter (^{143}Nd) are not fractionated strongly in

nature which results in modest variations of the $^{147}Sm/^{144}Nd$ ratio and only small long-term variations in the value of $^{143}Nd/^{144}Nd$. The typical range of the Sm/Nd ratio (by weight) in rocks is from about 0.1 to 0.6 (Richard *et al.* 1976, Zindler *et al.* 1982), and about 0.4 for common rock-forming and accessory minerals, although xenotime and garnet may have $^{147}Sm/^{144}Nd$ ratios somewhat greater than one (Mearns 1986). This small variation in parent/daughter ratios means that all ages determined by the Sm-Nd method must be done using the isochron approach which, with currently-achieved measurement precisions of about ±0.003%, results in an optimum age uncertainty at the 95% confidence level of about 20 m.y (DePaolo 1988).

The quality of an isochron is evaluated by the degree to which individual analyses plot within analytical uncertainty of a least-squares regression line (*e.g.* York 1969). The samples comprising the isochron my either be minerals plus whole-rock from a single sample or many whole-rocks collected from a single formation or geological unit. To be a valid determination the isochron must satisfy the assumptions of the method, namely: 1) all samples are of the same age, 2) each sample had the identical initial isotopic ratio, and 3) that there has been no loss or gain of parent or daughter isotopes since time=0. If one or more of these conditions is not met, then the analyses will not conform to the regression (within reasonable expectation; *cf.* Brooks *et al.* 1972, McIntyre *et al.* 1966), in which case statistical treatment and analysis of the data may be applied to evaluate the reliability of the "age", to infer the geological basis of the uncertainty, and to investigate the disturbance of the system.

Use of minerals ("internal") or whole-rocks ("external") to define an isochronous relationship depends on the geological problem and the extent to which all of the above conditions will be met by the choice of samples. Internal isochrons, for example, may be the preferred method for dating igneous intrusions with single-stage cooling histories because the likelihood of post-crystallization exchange is small and the probability that each mineral had the same initial isotopic composition is high (see, however, Johnson 1989 and Cortini and van Calsteren 1985 for examples of isotopic disequilibrium between minerals and whole-rocks in recent tuffs). In the case of a metamorphosed intrusion, however, the whole-rock approach may be preferred because it is improbable that whole-rock isotopic compositions will be modified significantly (especially in the Sm-Nd system) even if small-scale exchange between minerals has occurred. Nevertheless, an all-too common problem with whole-rock dating, is demonstrating that all samples are isochronous and had the same initial isotopic ratio. Variations in initial $^{87}Sr/^{86}Sr$ ratios for suites of young lavas from a single volcano have been reported (Chen and Frey 1983, Hildreth *et al.* 1991), suggesting that the assumption of identical initial ratios for many suites of rocks is difficult to defend and cannot automatically be made. This is especially troublesome in the Sm-Nd system where variation in the initial $^{143}Nd/^{144}Nd$, larger than analytical uncertainty, may produce totally spurious ages. Moreover, if petrologically unrelated rocks or minerals are grouped to construct an isochron, or if a mixing line is constructed from two reservoirs whose isotopic compositions are very different, then meaningless ages or poor quality isochrons may result (Cattell *et al.* 1984).

17

Applications of Sm-Nd Geochronology

The Sm-Nd system has been applied successfully to determine crystallization ages for mafic and ultramafic terrestrial rocks and, perhaps most successfully, to date lunar and extraterrestrial materials (see Shirey 1991 for a very useful summary). Specific examples are too numerous to cite but, in general, the whole-rock and mineral isochron approach has dated ultramafic, mafic and felsic volcanic rocks (particularly of Archean age), high grade gneisses and granulites, anorthositic rocks and layered mafic intrusions, and ophiolites.

Sm-Nd mineral isochrons can be useful for dating the time of metamorphism in mafic granulites and tectonites, particularly amphibolite-facies and higher grade tectonites, where total isotopic exchange between minerals has occurred by thermal diffusion, dynamic recrystallization, and new mineral growth. Garnet, titanite, hornblende, and clinopyroxene exhibit the greatest range in $^{147}Sm/^{144}Nd$, and they have proved useful for dating eclogites (Griffin and Brueckner 1980, 1985; Mørk and Mearns 1986, Mørk *et al.* 1988, Beard et al 1991), garnet peridotites (Mearns 1986, Brueckner *et al.* 1991, Li Shanguang *et al.* 1991), coronitic anorthosite and gabbro (Cohen *et al.* 1988), and pelitic gneisses (van Breemen and Hawkesworth 1980). In a novel approach, Vance and O'Nions (1990) and Burton and O' Nions (1991) have used the Sm-Nd method to determine the timing of garnet growth zone and reaction-rim formation to model the P-T-time history of greenschist- and amphibolite-facies pelites. This type of application is useful because it attempts to date the growth of a mineral or mineral pair for which temperature and pressure estimates are obtained. The results must be evaluated carefully, however, because garnet is a known refractory mineral, capable of surviving intense periods of metamorphism, and it commonly grows new domains over old, each of a different age (*cf.* Brueckner *et al.* 1991). In instances such as these, microscopic characterization of garnet types, coupled with replicate isotopic analysis, is necessary to demonstrate that total isolation and identification of component parts has been achieved.

In another application, Gromet (1991) and Getty and Gromet (*in press*) apply the mineral isochron approach using the Sm-Nd, Rb-Sr, and U-Pb systems to date directly the time of recrystallization and strain-fabric formation in middle- and upper-amphibolite-facies gneisses. This is an especially useful approach, because all isotopic measurements were made from aliquots of the same mineral fractions, and thus the completeness of the isotopic initialization for each system could be evaluated on a mineral-by-mineral basis.

The Uranium-Lead Method

The U-Pb method is unique among all decay series in that two isotopes of U, ^{238}U and ^{235}U, decay at nonequal rates to two different isotopes of Pb (^{206}Pb and ^{207}Pb, respectively). This allows for the calculation of three ages ($^{206}Pb/^{238}U$, $^{207}Pb/^{235}U$, and $^{207}Pb/^{206}Pb$ ages) from a single isotopic analysis, which provides an internal check of the reliability of the age determination. Moreover, the natural variation of the U/Pb ratio in common accessory minerals (*e.g.* zircon, monazite, baddeleyite) may exceed many thousands, resulting in enormous variation in the isotopic composition of Pb over time. This, in turn, permits precise determination of the time of mineral formation essentially

independent of an assumed initial daughter isotopic composition. Common accessory minerals useful as geochronometers are found in most igneous, metamorphic, and sedimentary rocks over a wide compositional and textural range. With experience and a keen eye, the trained geologist can learn to identify and collect samples appropriate for mineral separation and U-Pb analysis which, by reference to field observations, can be used to date a variety of geological events.

The Concordia Diagram and Discordant Analyses

The key to the success of the U-Pb method is that, in addition to the high initial parent/daughter ratios, many U-bearing minerals such as zircon and monazite are both refractory and retentive, neither loosing nor gaining their parent and daughter isotopes over time and under most geological conditions. When carefully selected and prepared, these minerals approach closed isotopic systems, the condition when all three isotopic ages agree. This condition is commonly illustrated on the "Concordia" (Wetherill 1956a) or Tera-Wasserburg (Tera and Wasserburg 1972) diagrams which are graphical representations of time as measured by the decay of ^{235}U to ^{207}Pb and ^{238}U to ^{206}Pb. Since the half-live of ^{235}U ($\lambda = 703.8$ m.y) is much less than that of ^{238}U ($\lambda = 4468.3$ m.y.) (Jaffey *et al*. 1971), the production of ^{207}Pb is faster than ^{206}Pb and the line representing the locus of equal ages ("concordia") is a curve (Fig. 1). The shape of "concordia" is a function of the $^{238}U/^{235}U$ ratio, which has been ever-changing throughout geological time, but which has a modern-day value of 137.88 (Shields 1960, Steiger and Jäger 1977).

Analyses that plot above or below concordia (in excess of analytical uncertainty) signify deviation from closed-system behavior, either by gain or loss of U or Pb. Most of a mineral's U is bound within the lattice, and radiogenic-Pb is in an ∝-damaged site, hence deviation from closed-system behavior is generally caused by loss of radiogenic-Pb, and almost always in a sense that the $^{207}Pb/^{206}Pb$ age $> {}^{207}Pb/^{235}U$ age $> {}^{206}Pb/^{238}U$ age (Fig. 1; but, for an exception, see Williams *et al*. 1984). Moreover, it is commonly observed that a suite of analyses (*e.g.* of zircon) will form a linear array (a discordia line) whose intercepts with concordia define meaningful geological events. Many mechanisms have been proposed to explain discordant behavior, and most of them involve radiogenic Pb-loss (*e.g.* Wetherill 1956 b, Wetherill 1963; Tilton 1960, Silver *et al*. 1963, Wasserburg 1963, Allègre *et al*. 1974, Goldich and Mudrey 1972). Incorporation of old xenocrystic minerals in multigrain fractions or old components in any single grain (so called "inheritance") may also produce discordant analyses, and generate mixing lines between components of different ages (Fig. 1). In some cases, the "inherited" component can be easily observed in transmitted light and simply avoided during sample selection. In other cases, the source of the inheritance may not be observable directly and the inheritance may only be detected if the analysis yields an unusually old isotopic age (which, of course, implies that the resolution of the measurement exceeds the age difference between core and overgrowth). In practice, all cases indicating discordant behavior must be evaluated carefully on a case-by-case basis, and the most favorable solution to the problem of discordance is to eliminate it (as much as possible) through careful grain selection and preparation (Krogh 1982 a). Total elimination is not always possible but,

through replicate analysis of parts of minerals, it is possible to eliminate some sources of discordance and thereby better interpret the real age pattern.

Diffusion and the Concept of Closure Temperature

The U-Pb method has proven to be the preferred method for dating high-grade metamorphic events, as well as events predating and slightly post-dating high-grade metamorphism of many crustal rocks. This is because U-bearing minerals such as zircon and monazite are stable under amphibolite-facies conditions, and also because they are retentive to loss or gain of parent and daughter isotopes during and after high-grade metamorphic events. Because temperature and pressure estimates are *not* obtained directly from these minerals, however, the concept of a mineral's closure-temperature has proven to be a useful convenience to relate an isotopic mineral age to the P-T-t history of a sample. This concept, when used in conjunction with isotopic ages of other minerals in other samples, has been commonly employed as a means to construct the regional P-T-t history of orogenic belts.

The interpretation of concordant U-Pb mineral ages, or indeed any mineral age, is not always straight-forward because it has been observed in many studies that the apparent dates of some metamorphic minerals more closely reflect their cooling ages rather than their primary crystallization ages; that is they represent the apparent time elapsed since the mineral closed to diffusion of daughter isotopes following a regional heating event. Armstrong (1966) and Harper (1967) initially developed the concept, and its general acceptance has followed from the observations of Hart (1964), Hanson and Gast (1967), Purdy and Jäger (1976), Harrison and McDougall (1980), and Mezger *et al.* 1989. In 1973, Dodson (1973) presented the mathematical foundation for the closure-temperature concept which is illustrated in Figure 2.

At a high initial temperature (T_i), it is assumed that the radiogenic daughter isotope diffuses out of a mineral as fast as it is produced, but that with continued near-monotonic cooling (constant dT/dt), the mineral enters a transitional temperature interval (the partial retention interval) where some of the radiogenic daughter isotope is retained and some is lost. At a lower temperature on the cooling path (T_f), the loss of radiogenic daughter isotope is negligible and the mineral begins to accumulate radiogenic daughter at the rate which it is produced. In determining an age for a system we, in effect, extrapolate the "closed-system" segment of the D/P back to the time axis, as shown by the intersection of the broken line to t_c in Figure 2. The solution for T_c, the closure temperature, is shown graphically as the temperature on the cooling curve which is defined by the apparent age of the mineral (t_c).

A mineral's closure-temperature age is based on the concept of progressive diminution of diffusive transport during monotonic cooling, and it should not be expected to be sharply defined in nature because it is dependent strongly on the magnitude of dT/dt as well as the effective diffusional radius. In the case of old minerals recrystallized during a younger event, application of the closure-temperature model presumes that the last event was hot enough and of a duration long enough to reset the mineral, and that the mineral lattice not be disrupted by subsequent deformational processes (*e.g.* creep and glide at the sub-grain scale). Moreover, it is well known that many minerals can

form at temperatures well below their estimated blocking temperatures (*e.g.* zircon, titanite and monazite) in which case the apparent age will date the time of mineral growth. All of these factors complicate the interpretation of an isotopic mineral age, and the reader is advised to use the closure-temperature concept with caution and only in those instances where the assumptions of the model apply.

Data Evaluation

Realistic assessment of uncertainties in U-Pb and ^{207}Pb/^{206}Pb isotopic ages is essential to determine whether the analysis is concordant or discordant and, if discordant, to assign appropriate errors to intercept ages. For analyses truly discordant outside of analytical uncertainty, the computation of ages and errors is done by line-fitting techniques (York 1969, Cumming 1969, Cumming *et al.* 1972, Ludwig 1982a, 1985, Davis 1982, Briqueu and de la Boisse 1990) which use the isotopic ratios, and their correlated uncertainties, to construct the "best fit" discordia line to the Concordia curve. Methods for calculating the uncertainty of a U-Pb analysis can be found in Ludwig (1980, 1982b) and Roddick (1987), and a review of the fundamental sources of error in U-Pb analyses is given by Mattinson (1987). The following discussion draws heavily from their work, introducing new diagrams to give emphasis where appropriate.

The ^{207}Pb/^{206}Pb, or Pb-Pb, age is the time-integrated measure of the initial ^{235}U/^{238}U ratio, and it is calculated directly from the Pb isotopic composition without knowledge of the U or Pb concentration. It is a useful measure of a mineral's age because the ^{235}U/^{238}U and ^{207}Pb/^{206}Pb ratios cannot be modified by isotopic fractionation in nature (provided that secular equilibrium between intermediate daughters is maintained), and the ^{207}Pb/^{206}Pb ratio for most samples can be measured with a precision that corresponds to an age uncertainty of ± 3 Ma (provided that the signal/noise level of the measurement is high and that the isotopic fractionation is carefully controlled and well-known). For samples containing appreciable amounts of common-Pb, however, random errors in the ^{207}Pb/^{206}Pb age arise from two sources: 1) the uncertainty in the measured ^{207}Pb/^{204}Pb ratio, and b) the uncertainty in the composition of the initial common-Pb. The error contribution from both of these sources diminish as the value of the ^{207}Pb/^{204}Pb ratio becomes large, and the effect is illustrated graphically in Figure 3 for samples 100 m.y.,500 m.y.,and 2500 m.y. old.

To obtain age precision of ± 4 Ma for a 2500 m.y. old concordant zircon, the analysis must have an uncorrected ^{207}Pb/^{204}Pb ratio of 60 (or greater) and it must be known to better than ± 1.0%. If the ^{207}Pb/^{204}Pb ratio of the analysis is less than 60, for example 40, then an uncertainty of 2% (a reasonable value, *cf.* Mattinson 1987) on the initial ^{207}Pb/^{204}Pb isotopic composition will yield an uncertainty of *ca.* 9 m.y. on the ^{207}Pb/^{206}Pb age. For younger samples this effect is magnified (because of the large variation of ^{207}Pb/^{206}Pb over an equivalent period), and for a 100 Ma sample with a ^{207}Pb/^{204}Pb ratio of 40, a 2% uncertainty on the initial ^{207}Pb/^{204}Pb ratio would produce a *ca.* 17 m.y. uncertainty on the ^{207}Pb/^{206}Pb age.

Figure 3 illustrates that age precision of ± 3-5 m.y. on the ^{207}Pb/^{206}Pb age may be obtained for most samples provided that the measured ^{207}Pb/^{204}Pb ratio is greater than 75 and that the measurement precision exceeds 1%. For measured ^{207}Pb/^{204}Pb ratios less

than 75, the uncertainty on the initial $^{207}Pb/^{204}Pb$ ratio becomes the principal source of error, and the magnitude of the $^{207}Pb/^{206}Pb$ age error is dependent on how well the initial $^{207}Pb/^{204}Pb$ ratio is known. The magnitude of the age error may, in some cases, be reduced by measuring the initial-Pb composition from a cogenetic, U-poor minerals (*e.g.* leached K-feldspar) and assuming that its composition matches the initial-Pb in the sample. In many cases, however, the complexity of the sample's history precludes this assumption, and the sample's initial-Pb may only be approximated from a model composition (*e.g.* Stacey and Kramers 1975, Cummings and Richards 1975). In reality, the initial-Pb composition of any analysis can never be known absolutely, and the best means to minimize this source of age uncertainty is to reduce the addition of ^{204}Pb to each analysis.

Concept of the Sample/Blank Ratio

The principal sources of lead isotope ^{204}Pb in an isotopic analysis are: 1) the initial Pb in the sample (Pb in the crystal lattice, cracks, inclusions, and adhered grains), and 2) the Pb introduced into the sample during analysis in the laboratory (so-called *blank* Pb). Other possible sources, including evolved-Pb contributed to the sample from the dissolution vessel (so-called "memory Pb") are not commonly observed, and they can be virtually eliminated with careful monitoring and cleaning. Results of years of study of zircon, including tests with abrasion techniques (Krogh 1982a) and the Kober evaporation technique (Kober 1986,1987), indicate that the initial-Pb abundance in high-quality zircon is generally less than a part per million, indicating that most of the observed ^{204}Pb is attributable to the laboratory blank whose isotopic composition should be rather well known (ca. ± 1 %). The observed $^{207}Pb/^{204}Pb$ ratio of a sample is thus a measure of the amount of sample (the dominant source of radiogenic ^{207}Pb) relative to the laboratory blank, as expressed by the following relationship,

$$\left.\frac{^{207}Pb}{^{204}Pb}\right|_{meas} = \frac{^{207}Pb_{rad} + {}^{207}Pb_{blank}}{^{204}Pb_{blank}} = 75 \qquad (11)$$

Equation 4 illustrates that by reducing the amount of laboratory blank it is possible to analyze a proportionally smaller amount of sample without compromising the integrity of the age determination. Developing the capability to analyze ultra-small samples (perhaps weighing only a few millionths of a gram) is, of course, advantageous because greater sample selectivity is achieved and more diverse applications of the technique become possible. These may include provenance studies using detrital single-zircon (Krogh and Keppie 1990, Davis *et al.* 1990) or monazite (Ross *et al.* 1991), dating of complex rocks with multi-generational zircon populations (Moser *et al.* 1991), or dating rocks with low mineral yields such as mafic and ultramafic intrusions (LeCheminant and Heaman 1989), many felsic volcanic rocks, and extraterrestrial samples. To illustrate the point, the following discussion and diagram applies to zircon where the uncertainty in the composition of the common-Pb is restricted to the blank-Pb isotopic composition.

Figure 4 shows the growth of uranogenic Pb_{total} (^{207}Pb and ^{206}Pb, expressed as ppm) through time as a function of a sample's U concentration (ppm). Contours of Pb_{total} are indicated as dotted lines, which were calculated from the relationship:

$$Pb_{total}^{rad} = {}^{206}Pb^{rad} + {}^{207}Pb^{rad} = {}^{238}U(e^{\lambda^{238}t}-1) + {}^{235}U(e^{\lambda^{235}t}-1) \tag{12}$$

and

$$U_{total} = {}^{238}U + {}^{235}U = {}^{238}U\left(1+\frac{1}{137.88}\right) \tag{13}$$

Also shown are curves of equal $^{207}Pb/^{204}Pb$ ratio ($=75$) for a specified sample size and constant laboratory blank, which can be calculated from Equation 4.

Figure 4 illustrates the dependence of the sample/blank ratio to the age of the zircon, its U abundance, and the absolute abundance of the laboratory blank. It has been known for nearly thirty years that there exists a negative correlation between zircon grain-size and age discordance (Silver and Deutsch 1963), and a positive correlation between magnetic susceptibility and U abundance (Silver 1963, Krogh 1982b, Krogh and Davis 1974). As a general rule (but by no means firm), severe to moderate degrees of age discordance are observed in zircons of Archean age when their U abundance exceeds ca. 200 ppm, and likewise for Paleozoic zircons where their U abundances are greater than 1000 ppm. Moreover, the natural U abundance in zircon is rarely less than 40 ppm, and thus a field depicting the range of zircons likely to yield concordant analyses is drawn in the inset to Figure 4. For most of geological time, the total uranogenic Pb abundance in concordant zircon ranges between 5-100 ppm, with most falling in the range between 10-50 ppm.

Shown also on Figure 4 are curves of constant $^{207}Pb/^{204}Pb$ ($=75$) for samples weighing between 5-10 μg with blank levels of 2,100, and 200 pg. This size range was chosen to represent the likely range (by weight) of single zircons in many medium-grained plutonic rocks (10 μg) as well as fine-grained volcanic rocks (<5 μg). The key point to the figure is that there exists in nature a real limit as to the type of zircon which will yield a meaningful age, and that to determine the age of small amounts (<20 μg) of zircon, without compromising the result, the analyst must achieve a laboratory blank that is on the order of a few picograms of Pb. This level of laboratory blank has been achieved (and maintained) in several laboratories around the world, and the remaining portion of these notes will be used to highlight examples where this capability has been utilized to study a variety of geological problems.
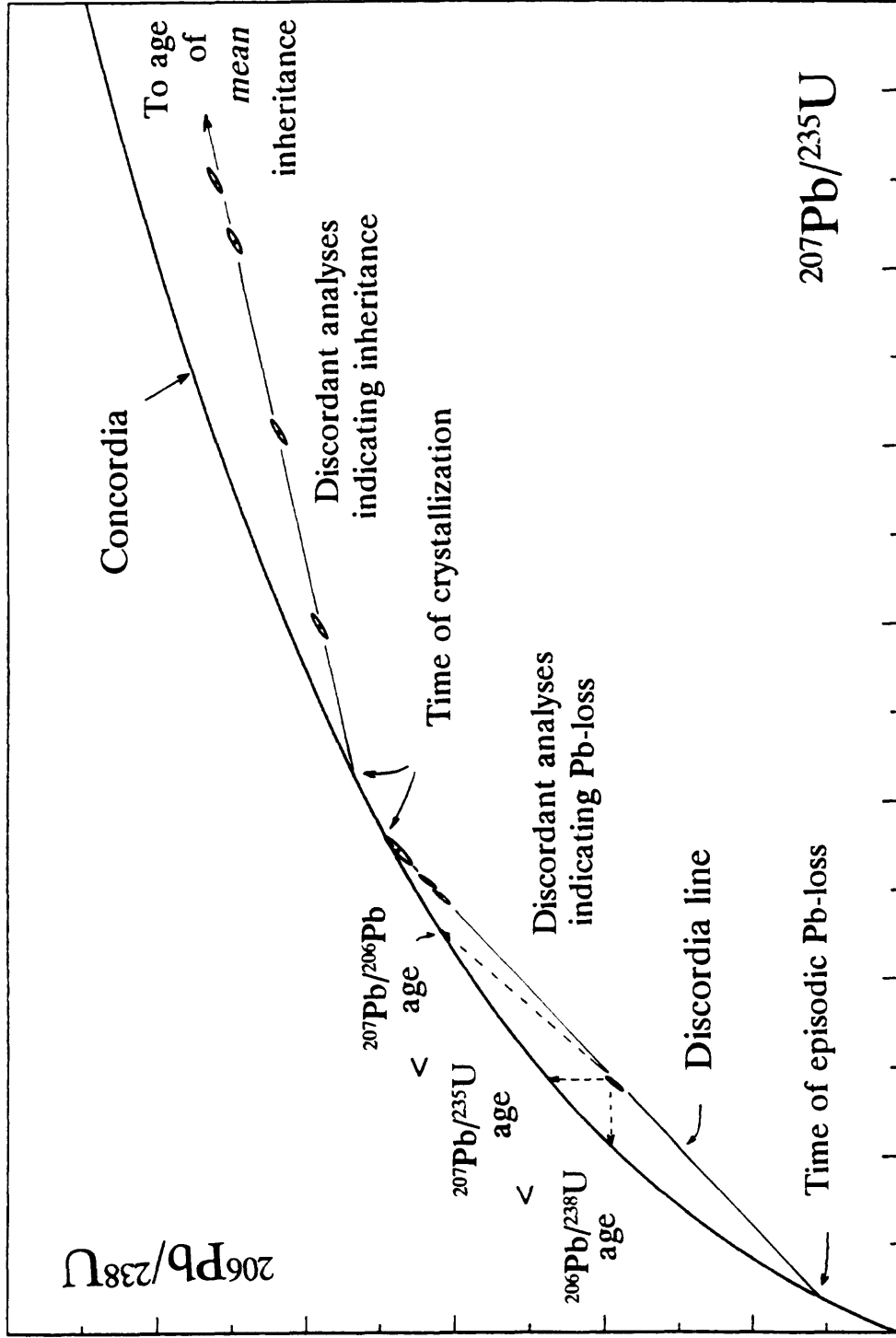
FIGURE 1. Conventional concordia diagram (Wetherill 1956) illustrating some of the terms used in the text. Concordia is the locus of points for which the $^{206}Pb/^{238}U$ age equals the $^{207}Pb/^{235}U$ age, and has its curved form because of the different half-lives of ^{238}U and ^{235}U, and the changing ratio of $^{238}U/^{235}U$ throughout time.
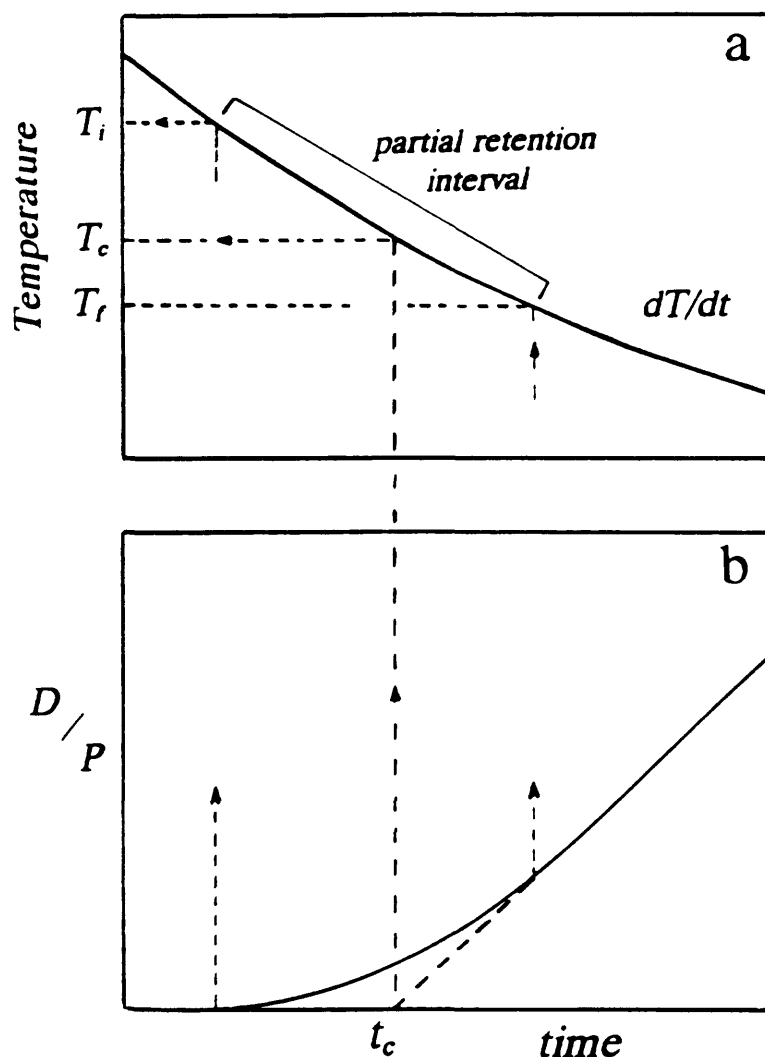
24

FIGURE 2. Graphical illustration of closure-temperature concept modified from Dodson (1973). (a) The cooling curve (dT/dt) over the time interval of interest is linear, and the partial retention interval is that segment of the curve where daughter isotopes begin to accumulate but where diffusion is ongoing. For minerals cooling through this interval, the closure temperature (T_c) is defined by the apparent age (t_c) of the system. (b) The accumulation curve, showing the retention of daughter (D) relative to parent (P) over time. Broken lines indicate the approximate limits of the partial retention interval, as well as the extrapolation of the apparent mineral age (t_c) to the cooling curve (dT/dt).
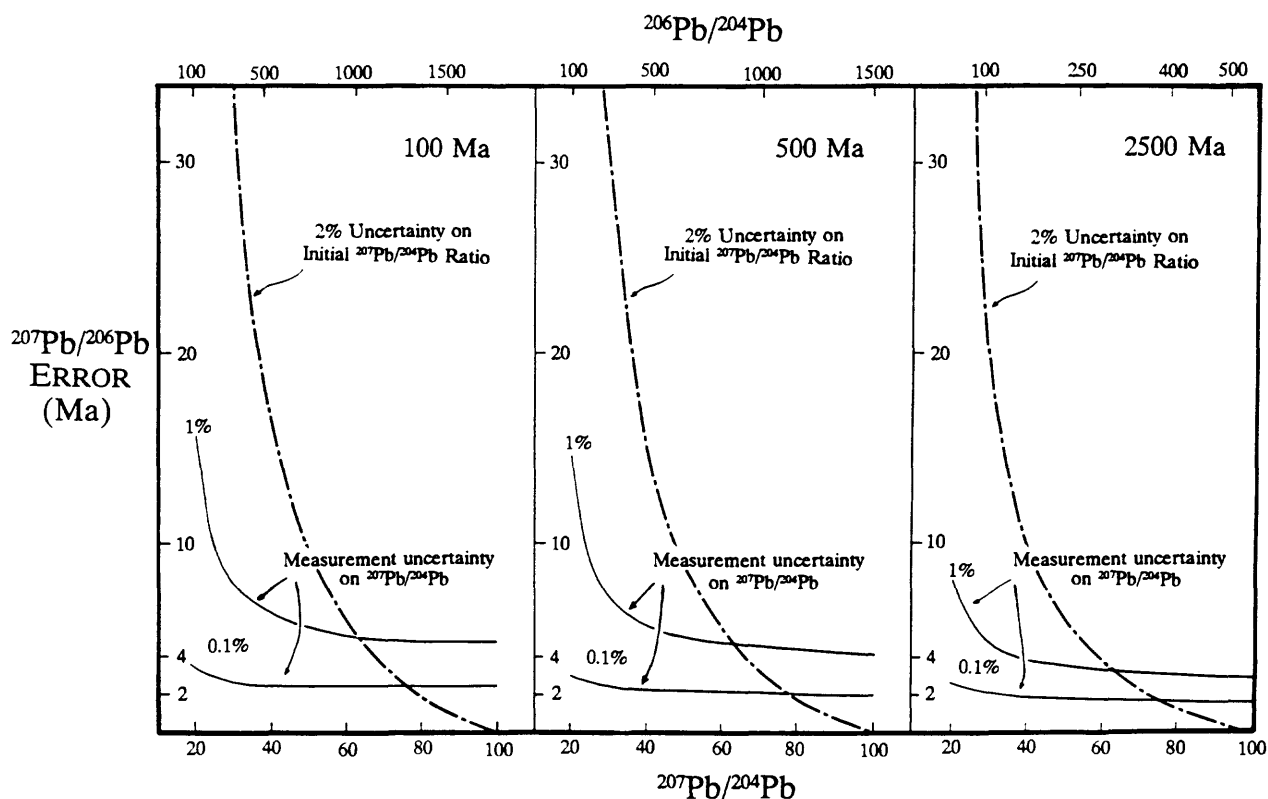
FIGURE 3. Absolute errors (Ma) of the $^{207}Pb/^{206}Pb$ age as a function of the measured, uncorrected $^{207}Pb/^{204}Pb$ ratio for 100 Ma, 500 Ma, and 2500 Ma samples. Two different sources of error are plotted together: the measurement precision of the uncorrected $^{207}Pb/^{204}Pb$ ratio (thin solid lines) and the error generated by a 2% uncertainty in the initial $^{207}Pb/^{204}Pb$ (thick dashed line). Absolute age errors arising from 0.1% and 1% measurement uncertainties were calculated by determining the $^{207}Pb/^{206}Pb$ age for a given $^{207}Pb/^{204}Pb$ ratio, then again using the $^{207}Pb/^{204}Pb$ ratio plus the indicated error. Similarly, absolute age errors arising from a 2% uncertainty in the initial-Pb were calculated by determining the $^{207}Pb/^{206}Pb$ age for a given $^{207}Pb/^{204}Pb$ ratio assuming a Stacey and Kramers' (1975) model-Pb, then again using a 2% larger initial $^{207}Pb/^{204}Pb$ (cf. Mattinson 1987), and taking the difference. Note that is it convenient to reference $^{207}Pb/^{206}Pb$ age errors relative to the measured $^{207}Pb/^{204}Pb$, rather than the $^{206}Pb/^{204}Pb$ (also shown in the upper abscissa), because of the smaller variation of $^{207}Pb/^{204}Pb$ over time.
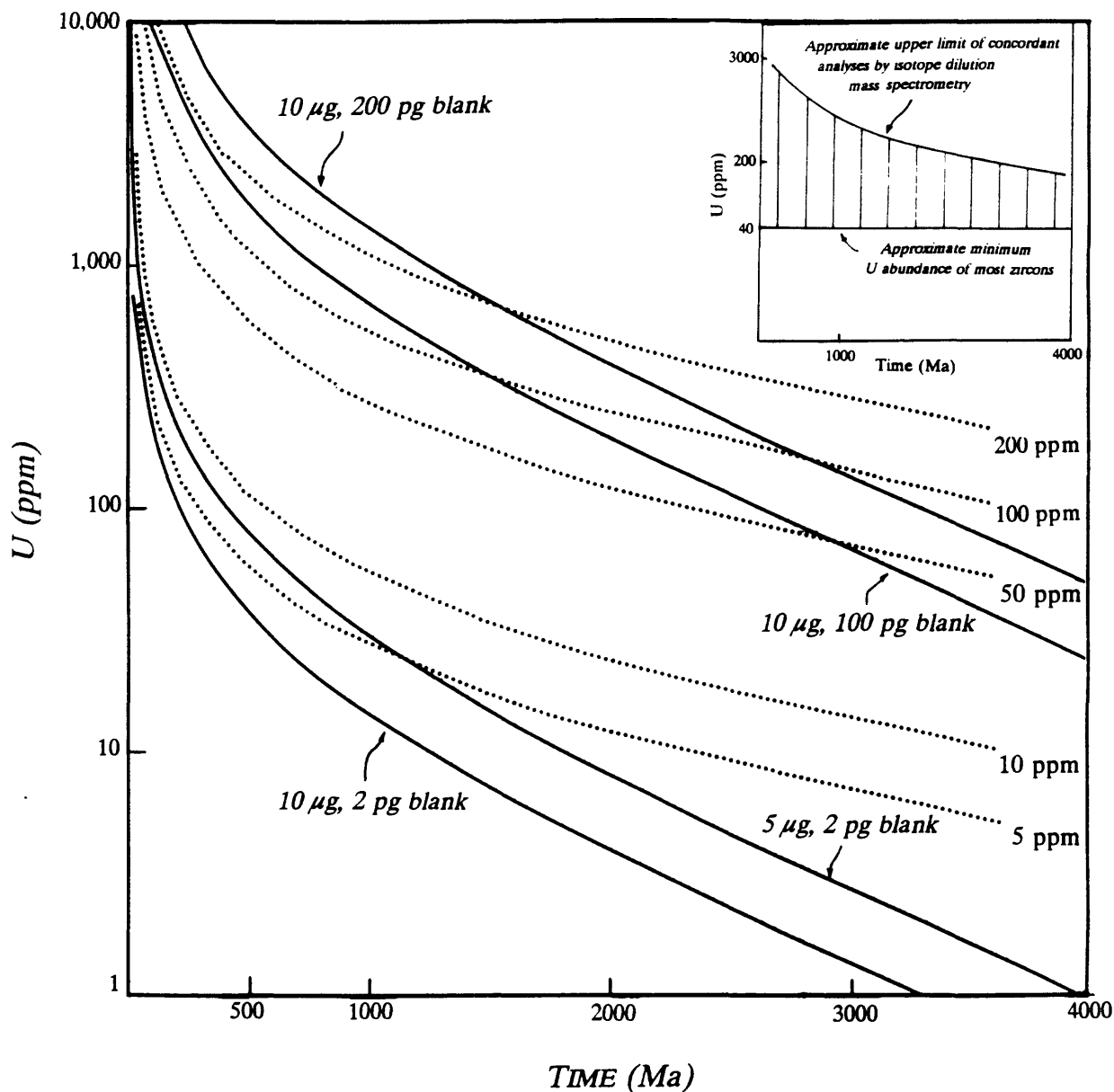
FIGURE 4. Growth of uranogenic Pb (^{206}Pb and ^{207}Pb) in zircon as a function of uranium abundance (plotted logarithmically) and age. Contours of uranogenic Pb$_{total}$ are shown as dotted lines at concentrations of 5, 10, 50, 100, and 200 ppm. Shown as solid lines are contours of equal ^{207}Pb/^{204}Pb (sample/blank = 75; see text and Fig. 3) for samples weighing 5 and 10 μg with laboratory blanks of 2, 100, and 200 pg, respectively (calculated using Equation 4 and an assumed laboratory blank of ^{206}Pb/^{204}Pb = 18.3, ^{207}Pb/^{204}Pb = 15.6). Points to the right and left of a given curve indicate ^{207}Pb/^{204}Pb values greater and less than 75, respectively. Note that the constant sample/blank curves are in ppm (= μg/pg, mg/ng, etc.) making the conversion to different sample sizes and blank levels convenient (e.g. 5 μg/2pg = 5 mg/2 ng). Shown in the inset is the field of naturally-occurring, concordant zircons, defined approximately by the collective observations of the ROM geochronology laboratory over the past 10 years. Note that for most zircons of late Proterozoic and younger age, uncompromised single-grain ($\leq$ 10 μg) analyses may be achieved only if blank levels are ca. 25 pg or less.

2-7-

Blank

$^{40}Ar/^{39}Ar$ dating technique

The $^{40}Ar/^{39}Ar$ dating technique is a variant of the conventional K-Ar method. To obtain an age by this technique, the sample of unknown age and a standard of known age are irradiated together in a nuclear reactor to produce ^{39}Ar from ^{39}K by fast neutron bombardment. After irradiation, the $^{40}Ar/^{39}Ar$ ratios of sample and standard are measured. The age of a sample can be calculated from its $^{40}Ar/^{39}Ar$ ratio when compared to the $^{40}Ar/^{39}Ar$ ratio of the standard. Most importantly, only the isotopic composition of argon need be measured and this is done by gas-source mass spectrometry, potentially a very precise analytical technique. In contrast, for a conventional K-Ar date, both ^{40}K and ^{40}Ar must be measured quantitatively. To do this, argon in one aliquant of the sample is measured by isotope-dilution, gas-source mass spectrometry. Potassium in a different aliquant of sample is determined by some other analytical method such as flame photometry, X-ray fluorescence, or isotope-dilution solid-source mass spectrometry. Thus, one inherent problem of the conventional K-Ar technique is the necessity of measuring isotopic abundances for separate aliquants of the same sample. This poses the danger that, because of sample inhomogeneity, different potassium and/or argon contents may exist in each aliquant. Two major advantages of the $^{40}Ar/^{39}Ar$ dating method are: only isotopic ratios of argon need be determined, and all measurements are made on the same sample aliquant, thus avoiding the question of homogeneity. In addition, by the $^{40}Ar/^{39}Ar$ method, it is possible to obtain a series of dates on a single sample when the argon is extracted by step heating. The combination of these advantages potentially increases the precision of the $^{40}Ar/^{39}Ar$ method over the conventional K-Ar technique. However, the $^{40}Ar/^{39}Ar$ technique will suffer if proper corrections are not made for interfering radiation-induced isotopes.

29

$^{40}Ar/^{39}Ar$ age equation

Details of the $^{40}Ar/^{39}Ar$ dating technique have been discussed by Dalrymple et al. (1981). For the purposes of this study, a summary of the formulation of the age equation is presented below. This summary is germane to understanding how some variables can be optimized to improve the precision of the technique.

The age of a sample is calculated according to the relationship:

$$t_u = \frac{1}{\lambda} ln \ (JF + 1), \qquad (1)$$

where t_u is the calculated age of the unknown sample, λ is the decay constant for decay of ^{40}K, J is related to the neutron flux during irradiation, and F is the ratio of $^{40}Ar_R$ (radiogenic ^{40}Ar) to $^{39}Ar_K$ (potassium-derived ^{39}Ar) of the sample. The decay constants used in this study are those recommended by Steiger and Jäger (1977), i.e., $\lambda_\epsilon = 0.581 \times 10^{-10}$/yr, $\lambda_{\beta-} = 4.962 \times 10^{-10}$/yr, and $\lambda = \lambda_\epsilon + \lambda_{\beta-} = 5.543 \times 10^{-10}$/yr. The flux parameter, J, is calculated according to the relationship:

$$J = (e^{\lambda t_m} - 1)/(^{40}Ar_R/^{39}Ar_K)_m, \qquad (2)$$

where t_m is the age of the primary flux monitor (i.e., standard), and $(^{40}Ar_R/^{39}Ar_K)_m$ is the measured ratio of the standard. The standard for this experiment is hornblende MMhb-1 with the percent of $K = 1.555$, $^{40}Ar_R = 1.624 \times 10^{-9}$ mole/g, and K-Ar age = 519.4 m.y. (Alexander et al., 1978; Dalrymple et al., 1981).

In reality, the determination of an age by the $^{40}Ar/^{39}Ar$ technique is not a simple matter of measuring $^{40}Ar_R$ and $^{39}Ar_K$. As in the conventional K-Ar technique, a correction for the presence of atmospheric ^{40}Ar must be made by using ^{36}Ar and the recommended atmospheric $^{40}Ar/^{39}Ar$ ratio of 295.5 (Steiger and Jäger, 1977). Just as importantly, corrections must be made for irradiation-produced ^{40}Ar (from ^{40}K), ^{39}Ar (from ^{42}Ca), and ^{36}Ar (from ^{40}Ca). Corrections for each are reactor-specific and are made by measuring argon production ratios on irradiated, pure potassium and calcium salts. For this study, the samples were irradiated in the TRIGA reactor of the U. S. Geological Survey, Denver, Colorado. Argon production ratios for these samples are $(^{36}Ar/^{37}Ar)_{Ca}$ = 2.67 ± 0.017 × 10^{-4} (25 determinations), $(^{39}Ar/^{37}Ar)_{Ca}$ = 6.73 ± 0.037 × 10^{-4} (25 determinations), and $(^{40}Ar/^{39}Ar)_K$ = 0.59 ± 0.072 × 10^{-2} (4 determinations) (Dalrymple et al., 1981). The production ratios were confirmed for this study. No correction was made for ^{36}Ar produced from chlorine, an interference recently pointed out by Roddick (1983), but calculations based on his work, and the fact that the muscovites of this study contain little or no chlorine, show that this interference is negligible. The only additional correction made was for the decay of unstable, reactor-produced ^{37}Ar, which has a half-life of about 35.1 days. Thus, the actual $(^{40}Ar_R/^{39}Ar_K)$ ratio or F is calculated from the relationship:

$$F = \frac{^{40}Ar_R}{^{39}Ar_K} = \{(^{40}Ar/^{39}Ar) - 295.5[(^{36}Ar/^{39}Ar)$$

$$- (^{36}Ar/^{37}Ar)_{Ca}(^{37}Ar/^{39}Ar)] - (^{40}Ar/^{39}Ar)_K\}/$$

$$1 - (^{39}Ar/^{37}Ar)_{Ca}(^{37}Ar/^{39}Ar), \quad (3)$$

after a correction for ^{37}Ar decay is made.

31

$^{40}Ar/^{39}Ar$ age spectra

The $^{40}Ar/^{39}Ar$ method was first used in total fusion experiments in which an irradiated sample was completely melted and all isotopes of argon measured in a single analysis to calculate an age for the sample. This total fusion age is roughly analogous to a conventional K-Ar age of the sample except that no isotopic concentration measurements are required. Very soon after the first uses of the $^{40}Ar/^{39}Ar$ method, it was realized that a sample could be progressively degassed in temperature increments (Turner, 1968). An age could be calculated for each increment of gas released and the ages of all temperature increments of a sample were plotted against percent of released argon to form an age spectrum. The character of the spectrum can be evaluated within a theoretical framework to interpret the apparent distribution of potassium and argon within the sample. Turner (1968) showed that some spectra of meteorites display characteristics that would be expected if volume diffusion were the dominant mechanism controlling the loss of argon from a sample in the geologic environment. Since that time, many studies have shown that meaningful ages of samples could be determined by the age spectrum technique even though some loss of $^{40}Ar_R$ had occurred during the sample's geologic history. It should be noted here that loss or gain of $^{40}Ar_R$ by a sample will result in an erroneous conventional K-Ar age. Furthermore, since loss or gain of $^{40}Ar_R$ in a sample is generally thermally controlled, samples from thermally complex regions (such as ore deposits) should be analyzed by $^{40}Ar/^{39}Ar$ age spectrum techniques.

Fission-Track Dating
(P.K. Zeitler)

1. Introduction

Not every atom of uranium decays to lead. Occasionally, once per every two million or so ^{238}U atoms that undergoes α-decay to Pb, a ^{238}U atom will decay by spontaneous fission into two halves of subequal mass. These two fragments fly apart with high initial velocity, and as they slow down and transfer energy to the host lattice, they inflict a linear damage trail that is on the order of 10-15 microns in length. The density of such fission tracks is proportional to U content and age, and thus the spontaneous fission of ^{238}U provides us with a geochronological method. After chemical etching these tracks become visible and thus countable using an optical microscope at magnifications of 500-1500 X. Further, it turns out that the strained portion of the crystal lattice that constitutes a fission track is susceptible to repair via diffusion, and it is observed in the common U-bearing accessory minerals that fission tracks "fade" or "anneal" at low to moderate temperatures. Thus the minerals used in fission-track dating are all useful as low-temperature thermochronometers.

The book by Fleischer, Price, and Walker (1975), although somewhat dated, provides a thorough overview of charged particle tracks. Naeser (1979) and Naeser et al. (1989) include concise summaries of the fission-track method as well as examples of applications. Hurford and Green (1982, 1983) discuss several important aspects having to do with methods and calibration of fission-track analysis. Finally, papers by Gleadow et al. (1983, 1986) and by Green et al. (1989) are a good introduction to the thermochronological uses of confined fission-track lengths.

2. Methods and Materials

In principle any U-bearing mineral can be dated by the fission-track method, but in practice apatite, zircon, and to a lesser extent sphene are the minerals that are commonly used and well calibrated. Because of the heterogeneity of U concentration within and between mineral grains, almost all fission-track determinations are now done using the "external detector method." This involves mounting, polishing, and etching of a sample to reveal the spontaneous fission tracks, and then the covering of this grain mount with a thin wafer of detector material, usually muscovite. This package is sent to the reactor for irradiation by thermal neutrons, which cause some of the ^{238}U in the sample to undergo fission. Upon return to the laboratory, the detector is removed and etched to reveal the tracks induced in the reactor. This procedure allows individual grains and parts of individual grains to be dated by comparing the ratio of spontaneous to induced tracks in the area of interest, and then the use of some protocol to reference this ratio to that of an age standard.

Because in fission-track dating relatively few tracks are counted (something like 500 to 1000 tracks might be typical for an analysis), the uncertainties associated with an individual analysis are dominated by the Poisson statistics that must be used when counting radioactive decay events. For a Poisson distribution, the standard deviation is given by the square root of the mean; for example, 1000 tracks must be counted to attain

a 3% uncertainty on a track density. What this means in practical terms is that it quickly takes an intolerable increase in analytical effort to achieve a modest reduction in uncertainties. Furthermore, in young samples it is often not possible to find many more than 50 or 100 tracks. When all sources of uncertainty are included, realistic uncertainties for a fission-track age determination will range from 5 to 10%.

It is important not to let the apparently large uncertainties associated with fission-track dating overshadow the method's advantages. First, fission-track dating remains one of the few geochronological techniques to routinely allow age determinations to be made on individual grains. Second, although the method is imprecise, it is worth keeping in mind that a single spontaneous fission track represents the fossilized remains of a single atom of U: the method is clearly very sensitive! Third, the great temperature sensitivity of fission tracks in apatite provide us with a very low-temperature thermochronometer that is of great use in structural and basin studies; it is also worth noting that apatite fission-track is the one thermochronometer that can and has been directly calibrated by means of deep boreholes. The key point to remember when using fission-track dating (as with any other method, for that matter) is simply to pose questions the method can answer; there are numerous geologic problems that can be usefully constrained even with a 10% level of uncertainty.

3. Fission-Track Annealing and Thermochronology

Early in the development of fission-track dating it was noted that tracks fade when a sample is heated. Calk and Naeser's (1969) classic study of the overprinting associated with intrusion of a basaltic plug into a felsic pluton demonstrated just how systematic and potentially useful this annealing behavior could be (Figure 1). At about the same time, geochronologists working in the Alps showed how the great temperature sensitivity of the fission-track method could be brought to bear on problems of tectonics and unroofing, since one of the consequences of even relatively minor tectonic activity is uplift and erosion, which in turn will cool rocks at depth (Wagner and Reimer, 1972).

By means of laboratory annealing experiments and geological calibrations (including sampling of deep boreholes in which the density of spontaneous fission tracks can be observed to go to zero (e.g., Naeser, 1981)), the closure behavior of the minerals used in fission-track dating has been reasonably well constrained. At a cooling rate of 10°C/m.y., apatite has a closure temperature of about 110 ± 10°C, zircon has a closure temperature of about 200 ± 40°C (Naeser et al., 1989), and sphene has a closure temperature of somewhere between 250 and 300°C (sphene ages usually come out to be fairly close to K-Ar biotite ages). A great deal of laboratory work is currently underway to more precisely calibrate the annealing kinetics of apatite, which lends itself well to laboratory study (unlike zircon and sphene, which cannot be meaningfully studied by laboratory heating experiments for technical reasons having to do with the way accumulated radiation damage influences their etching behavior (Gleadow, 1978).

4. Track Lengths and Thermochronology

For reasons that are not well understood, fission-track annealing occurs by the shortening of tracks (as tracks shorten they will have a lower probability of intersecting

the etched surface, and thus the observed track density decreases as shortening progresses even though the numbers of tracks may not decrease). In the case of apatite, it has been found that the distribution of fission-track lengths in a group of samples provides a data set that is powerfully complementary to the distribution of measured ages. The apparent track-length distribution seen at the surface of a mount is strongly biased by the fact that most of the tracks are dipping steeply, and also by the fact that most of these tracks have been amputated during the polishing process. Therefore, what is specifically measured are the lengths of horizontal confined tracks found within crystals; such tracks are surprisingly common and develop when etchant penetrates along other fission tracks (tracks in tracks, or TINTs) or along features such as cleavages or partings (tracks in cleavages, or TINCLEs).
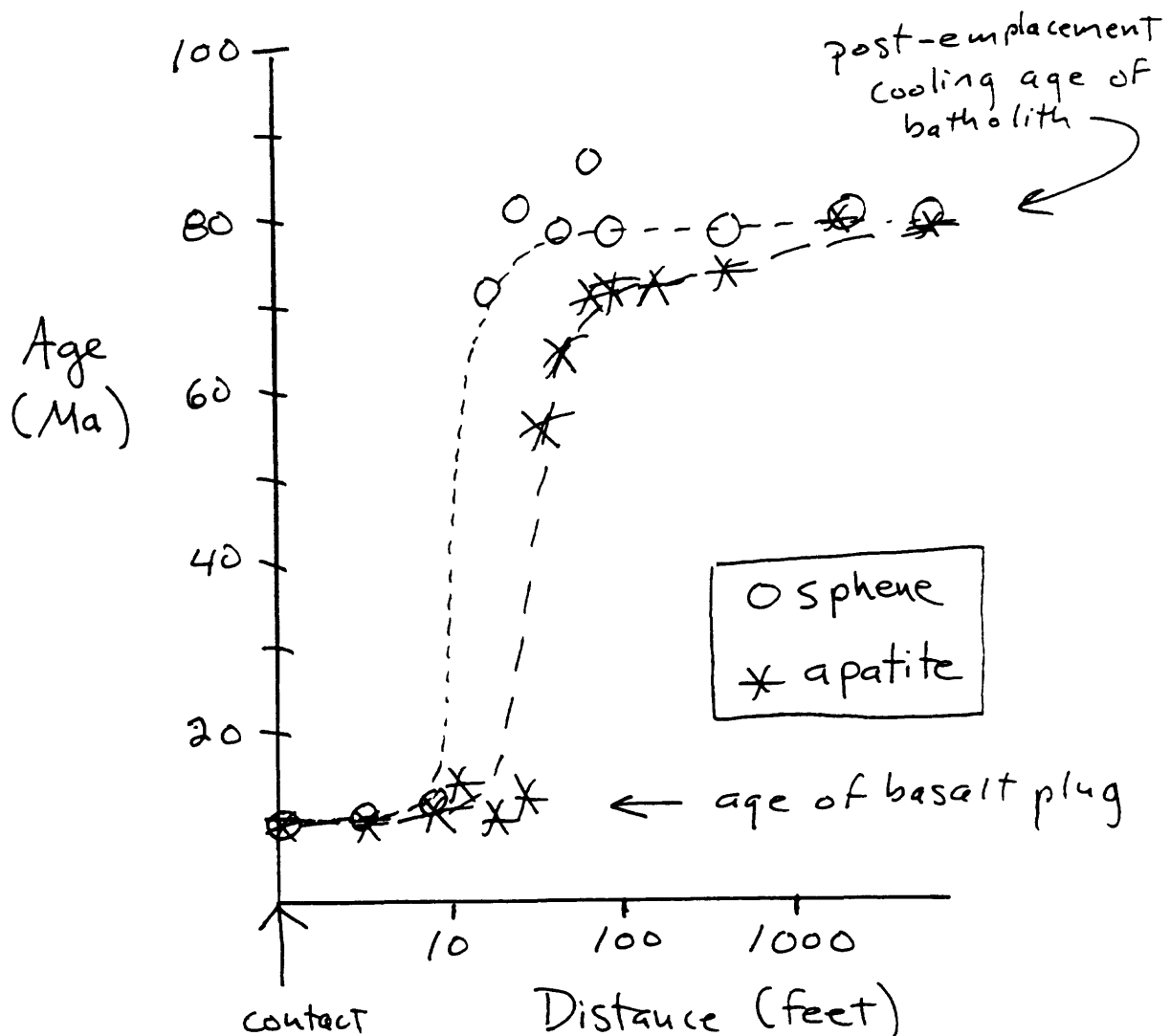
Track-length histograms are roughly analogous to diffusion profiles in that they can record some of the details of a sample's thermal history. Fission-tracks generally vary in length for the simple reason that each track is formed at a different time. Thus, early-formed tracks suffer through much more of a sample's history than tracks formed, say, just before etching in the laboratory. During very slow cooling, tracks formed just as a sample enters the closure interval will suffer significant shortening before the sample reaches the end of this interval, and such a sample will show a broadened distribution of track lengths (Figure 2). On the other hand, during rapid cooling, hardly any tracks will form during the sample's brief passage through the closure interval, and such a sample will tend to have a tight distribution of long tracks. A number of other possibilities exist, as shown by Figure 2.
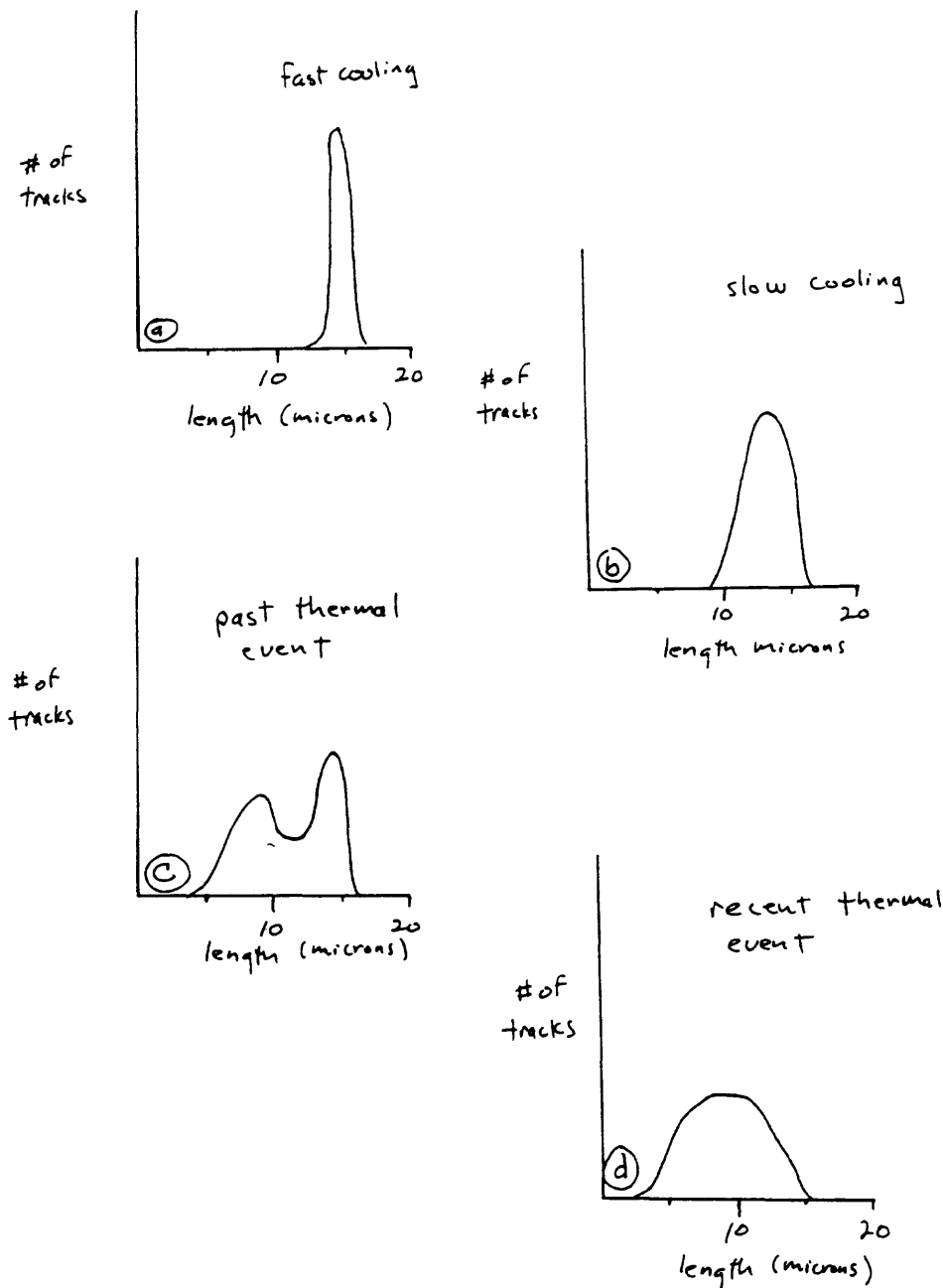
5. Areas of Research and Controversy

Much of the current research in fission-track dating is being directed towards a better understanding of annealing kinetics in apatite, largely because of the utility this low-temperature thermochronometer has in constraining the thermal evolution of sedimentary basins (although the slow-cooling closure temperature of apatite is around 110°C, for geologic time scales the partial track stability zone extends to as low as 70°C and to as high as 150°C, a temperature range of great interest to petroleum geologists interested in hydrocarbon maturation). It has been found (e.g., Crowley et al., 1990) that the composition of apatite can have a moderate influence on annealing behavior, with chlorapatites being somewhat more resistant to annealing. This finding has led workers to repeat previous annealing studies in an effort to remove the effects of sample variability that might have clouded these studies. A related effort has been to develop a fundamental model to predict annealing behavior theoretically; currently, annealing models involve merely empirical best-fits through measured data. Finally, several workers have begun to develop inverse models of track-length distribution in an attempt, first, to get a feeling for how adequately track-length data can constrain a thermal history, and second, to increase the degree of objectivity in the interpretation of thermal histories.

5. References

Calk, L.C. & Naeser, C.W., 1973, The thermal effect of a basalt intrusion on fission tracks in quartz monzonite. *Journal of Geology*, 81, 189-198.

Crowley, K.D., Cameron, M., & McPherson, B.J., 1990, Annealing of fission tracks in apatite: geometry of the Arrhenius plot and effects of composition. *Geological Society of America Abstracts With Programs*, 22, A261.

Fleischer, R.L., Price, P.B. & Walker, R.M., 1975, *Nuclear Tracks in Solids*, University of California Press, Berkeley, 605 pp.

Gleadow, A.J.W., 1978, Anisotropic and variable track etching characteristics in natural sphenes, *Nuclear Track Detection*, 2, 105-117.

Gleadow, A.J.W., Duddy, I.R. & Lovering, J.F., 1983, Fission-track analysis: a new tool for the evaluation of thermal histories and hydrocarbon potential. *Australian Petroleum Exploration Association Journal*, 23, 93-102.

Gleadow, A.J.W., Duddy, I.R., Green, P.F. & Lovering, J.F., 1986, Confined fission track lengths in apatite: A diagnostic tool for thermal history analysis. *Contributions to Mineralogy and Petrology*, 94, 405-415.

Green, P.F., Duddy, I.R., Gleadow, A.J.W. & Lovering, J.F., 1989, Apatite fission-track analysis as a paleotemperature indicator for hydrocarbon exploration. In: Naeser, N.D. & McCulloh, T.H. (eds.) *Thermal History of Sedimentary Basins*. Springer, New York, 181-196.

Hurford, A.J., and Green, P.F., 1982, A user's guide to fission-track dating calibration. *Earth and Planetary Science Letters*, 59, 343-354.

Hurford, A.J., and Green, P.F., 1983, The zeta age calibration of fission-track dating. *Chemical Geology (Isotope Geoscience Section)*, 1, 285-317.

Naeser, C.W., 1979, Fission-track dating and geologic annealing of fission tracks. In: Jäger, E. and Hunziker, J. C. (eds.) *Lectures in Isotope Geology*. Springer, 154-169.

Naeser, C.W., 1981, The fading of fission tracks in the geologic environment: Data from deep drill holes. *Nuclear Tracks*, 5, 248-250.

Naeser, N.D., Naeser, C.W. & McCulloh, T.H., 1989, The application of fission track dating to the depositional and thermal history of rocks in sedimentary basins. In: Naeser, N.D. & McCulloh, T. H. (eds.) *Thermal History of Sedimentary Basins*. Springer, New York, 157-180.

Wagner, G.A. and Reimer, G.M., 1972, Fission-track tectonics: the tectonic interpretation of fission-track apatite ages. *Earth and Planetary Science Letters*, 14, 263-268.

100

Age (Ma)

80

60

40

20

post-emplacement cooling age of batholith →

O sphene

✳ apatite

← age of basalt plug

contact

10   100   1000

Distance (feet)

1. Resetting profile of apatite and sphene fission-track ages in quartz monzonite located immediately adjacent to a basaltic intrusion. Data from Calk and Naeser (1973). Note that: (1) near the intrusion, both apatite and sphene provide good estimates for the time of intrusion; (2) at distance from the intrusion, apatite and sphene ages reflect the regional cooling history of the host batholith; and (3) at moderate distances from the intrusion, sphene and apatite give different ages consistent with their different resistances to fission-track annealing (the apatite is reset further from the contact because of its greater temperature sensitivity).

Fast cooling

\# of tracks

10   20
length (microns)

slow cooling

\# of tracks

10   20
length microns

past thermal event

\# of tracks

10   20
length (microns)

recent thermal event

\# of tracks

10   20
length (microns)

2. Schematic track-length distributions for confined tracks in apatite, for various thermal histories. (a) Under conditions of fast cooling, all tracks are nearly full length, as most tracks form when the sample is cool. (b) Under conditions of slow cooling, some of the tracks that formed as the sample entered the partial stability zone will have shortened by the time the sample has cooled out of this zone. Hence, the distribution is broadened, although full length tracks formed at low temperatures are still abundant. (c) Should a sample experience a mild thermal event sometime in the past, the previous complement of fission tracks will be shortened; following the event all new tracks will be of full length, resulting in a bimodal length distribution. (d) A sample that has experienced an episodic heating event in the recent past will contain few or no long tracks, resulting in a broad distribution of lengths that is shifted to low values. Note (1) that full length for a spontaneous track in apatite is about 15 microns, (2) that a track-length analysis usually consists of the measurement of 100 lengths, and (3) that the distributions pictured above are best thought of end-members, with intermediate distributions being very probable.

38

K-Feldspar ^{40}Ar/^{39}Ar Thermochronology
(P.K. Zeitler)

1. Introduction

The K-Ar dating of potassium feldspars has long endured a bum rap, starting in the 1950's when geologists became disgruntled by the fact that the mineral always seemed to give ages that were far too young. This myth of unreliability became deeply entrenched, and the point was reached where K-feldspar was blamed for leaking Ar even at room temperature! We now know that ^{40}Ar/^{39}Ar dating of K-feldspar is a thermochronometric system of enormous potential in constraining temperature histories in the range 150°C to over 300°C. How did such a shift in opinions come about?

It's taken some fifteen years to rehabilitate K-feldspar's reputation among (most) K-Ar geochronologists. The study by Foland (1974) of Ar diffusion kinetics in orthoclase led the way. Foland showed that Ar loss from feldspar occurs in an orderly fashion and that given large enough grains, K-feldspar could be quite retentive of Ar; Foland also pointed out that a likely cause for low ages were the perthite lamellae and other microstructural features that are nearly ubiquitous in feldspars-they would tend to diminish the effective grain size in a sample and lead to enhanced Ar loss at lower temperatures. Perhaps the next important step forward was the ^{40}Ar/^{39}Ar study by Harrison and McDougall (1982) of microclines from a slowly cooled batholith. They found that their samples all yielded continuously rising "staircase" age spectra, which they interpreted to reflect diffusion profiles resulting from slow cooling. Further, Harrison and McDougall also applied an approach (also being used by Berger and York (1981) at about the same time) in which the loss of ^{39}Ar during laboratory heating was exploited to determine diffusion parameters specific to the sample under analysis. They found that their samples had low closure temperatures of roughly 150°C, consistent with the samples' ages and the thermal history of their host rock.

2. Summary of K-Feldspar Systematics

What does theory have to say about the nature of ^{40}Ar/^{39}Ar age spectra? A sample that has been episodically overprinted or slowly cooled should yield a convex-up age spectrum (Figure 1). This assumes that the sample is composed of grains all having the same diffusion dimension. If a range of diffusion dimensions is present, then, as first shown by Turner (1968), the age spectra resulting from episodic Ar loss are quite different and for moderate to high losses are concave-up (Figure 1). This change in shape occurs because (1) for a specified degree of Ar loss from the bulk sample, the smaller grains will tend to be completely overprinted whereas the larger grains will tend to be untouched, and (2) Ar from the smaller grains will dominate during the early stages of gas extraction in the laboratory.

Theory also predicts that the age spectrum from a continuously cooled sample should have "relief" about equal to the time it took to cool about 70°C to 100°C (Dodson, 1986). Actually, Dodson's work on closure profiles addressed concentration profiles; it was not until the publication of the paper by Lovera et al. (1989) that a solution was available for calculating theoretical age spectra for the case of slow cooling.

How do natural samples behave? Slowly cooled samples do indeed yield age spectra that reflect the presence of diffusion profiles (e.g., Figure 2). Episodically overprinted samples not only show evidence for marked diffusion profiles but also behave like they contain a range of diffusion dimensions (Harrison et al., 1986; Gillespie et al., 1982; Zeitler, 1987; Figure 3). It would seem that K-feldspar has great potential as a complex thermochronometer.

The papers by Lovera et al. (1989, 1991) synthesized the work of the previous decade and took several important steps further, including development of a closed-form solution for calculating slow-cooling age spectra. Of most relevance to K-feldspar systematics, Lovera et al. showed (1) that slow-cooling age spectra modelled using a range of diffusion dimensions fit observed data far better than traditional models, and predict segments of thermal histories in better agreement with independent constraints, (2) that the distribution of diffusion-domain sizes found in their samples tend to consist of three or four discrete sizes, not a continuum, (3) that this distribution of sizes is evident in both the release of reactor-produced, laboratory-outgassed ^{39}Ar, and in the age-spectrum systematics of radiogenically derived ^{40}Ar, and (4) that the smallest diffusion domains must be micron or submicron in size (in fact, Lovera et al. (1991) were able to show that a single large sand-sized grain of feldspar exhibited the same behavior as a bulk separate).

It appears then that most K-feldspar grains contain several diffusion domains of varying sizes. Thus, the shape of a K-feldspar age spectrum will be a function not only of thermal history but also of domain size distribution. Fortunately, examination of the laboratory release kinetics of ^{39}Ar allows one to make an independent determination of the domain-size distribution. In the ideal situation, the presence of a range of differently sized diffusion domains allows a considerable portion of a sample's cooling path to be constrained, as each domain will record some 70°C to 100°C of the cooling path (Dodson, 1986; there is usually, of course, some overlap between the temperature segments constrained by each domain).

4. Some Final Comments on K-feldspar Thermochronometry and Domain Theory

One of the most important realizations to emerge from all of the renewed interest in the K-Ar dating of K-feldspar is that the closure temperature of K-feldspar is not 150°C (a number we geochronologists tossed around quite a bit a few years ago). Of course no thermochronometric system has a single closure temperature associated with it, dependent as closure temperature is on sample-specific properties like diffusion dimension, activation energy, diffusivity, and cooling rate. But in the case of K-feldspar, this is especially true, for each domain will a closure temperature. Furthermore, it's been found that few domains in few samples have slow-cooling closure temperatures as low as 150°C.

A second thing to recognize if you're feeling uncomfortable with the notion of diffusion domains is that the "domain theory" is firmly supported by a large body of observations, and that's the bottom line, not all the fancy math and theory that can be trotted out in the theory's favor. If variations in diffusion dimension bother you, note that all of the observations of domain theory could be explained by having regions within

a crystal of varying diffusivity, rather than having regions of constant diffusivity but varying size. Note however that if you do this, you're still stuck with the notion of domains, only this time they'd be diffusivity domains, rather than size domains.

5. Areas of Research and Controversy

Current research in K-feldspar thermochronology has several foci. One area of study is the refinement of conceptual models of Ar diffusion systematics. In this regard, Harrison et al. (1991) have found evidence that different diffusion domains within a sample may have varying activation energies, which provides an explanation for some of the types of deviant spectra that are sometimes measured, but which will complicate the modelling of spectra. Other researchers are attempting to understand what diffusion domains actually are, particularly the smaller ones. This is an important area, as some controversy over the nature of Ar diffusion in K-feldspar has emerged: for example, Parsons et al. (1988) claimed that Ar diffusion in feldspars is controlled not by regular geometric features, but instead by what they termed "micropores." Finally, attempts are being made to invert K-feldspar spectra to determine temperature-time paths free from the uncertainties and assumptions inherent in the forward modelling that is currently done.

6. References

Berger, G.W. and York, D., 1981, Geothermometry from ^{40}Ar/^{39}Ar dating experiments. *Geochimica et Cosmochimica Acta*, 45, 795-811.

Dodson, M.H., 1986, Closure profiles in cooling systems. *Materials Science Forum*, 7, 145-153.

Foland, K.A., 1974, ^{40}Ar diffusion in homogeneous orthoclase and an interpretation of Ar diffusion in K-feldspar. *Geochimica et Cosmochimica Acta*, 38, 151-166.

Gillespie, A.R., Huneke, J.C. and Wasserburg, G.J., 1982, An assessment of ^{40}Ar/^{39}Ar dating of incompletely degassed xenoliths. *Journal of Geophysical Research*, 87, 9247-9257.

Harrison, T.M. and McDougall, I., 1982, The thermal significance of potassium feldspar K-Ar ages inferred from ^{40}Ar/^{39}Ar age spectrum results. *Geochimica et Cosmochimica Acta*, 46, 1811-1820.

Harrison, T.M., Morgan, P. and Blackwell, D.P., 1986, Constraints on the age of heating at the Fenton Hill site, Valles Caldera, New Mexico. *Journal of Geophysical Research*, 91, 1899-1908.

Harrison, T.M., Lovera, O.M. and Heizler, M.T., 1991, ^{40}Ar/^{39}Ar results for alkali feldspars containing diffusion domains with differing activation energy. *Geochimica et Cosmochimica Acta*, 55, 1435-1448.

Lovera, O.M., Richter, F.M, and Harrison, T.M., 1989, The ^{40}Ar/^{39}Ar thermochronology for slowly cooled samples having a distribution of diffusion domain sizes. *Journal of Geophysical Research*, 94, p. 17,917-17,931.

Lovera, O.M., Richter, F.M, and Harrison, T.M., 1991, Diffusion domains determined by ^{39}Ar released during step heating. *Journal of Geophysical Research*, 96, p. 2057-2070.
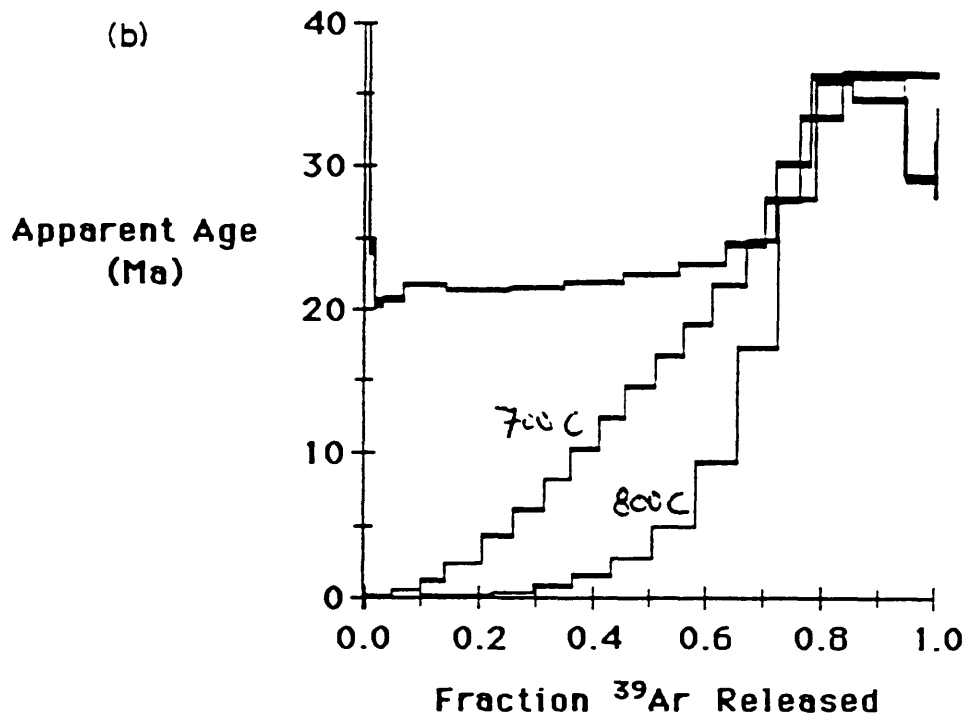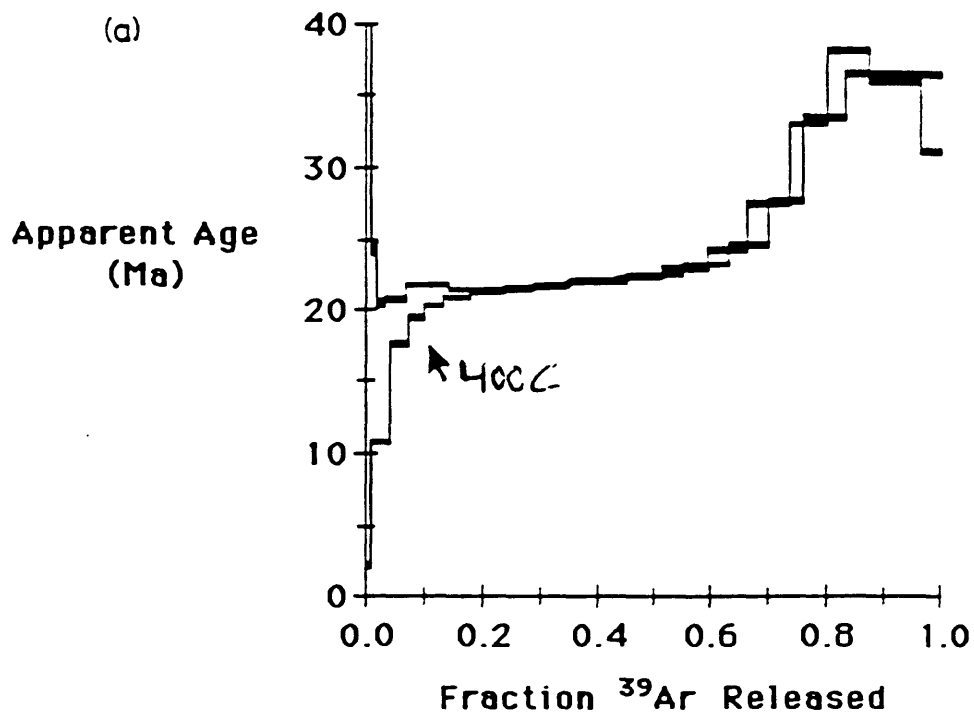
Parsons, I., Rex, D.C., Guise, P. and Halliday, A.N., 1988, Argon-loss by alkali feldspars. *Geochimica et Cosmochimica Acta*, 52, 1097-1112.

Turner, G., 1968, The distribution of potassium and argon in chondrites. In: Ahrens, L.H. (ed.) *Origin and Distribution of the Elements*, Pergamon, New York, 387-398.

Zeitler, P.K., 1987, Argon diffusion in partially outgassed alkali feldspars: insights from $^{40}Ar/^{39}Ar$ analysis. *Chemical Geology (Isotope Geoscience Section)*, 65, 167-181.

Zeitler, P.K., Sutter, J.F., Williams, I.S., Zartman, R.E. and Tahirkheli, R.A.K., 1989, Geochronology and temperature history of the Nanga Parbat-Haramosh Massif, Pakistan. *In*: Malinconico, L.L. & Lillie, R. J. (eds.) *Tectonics of the Western Himalaya*, Geological Society of America Special Paper 232, p. 1-22.
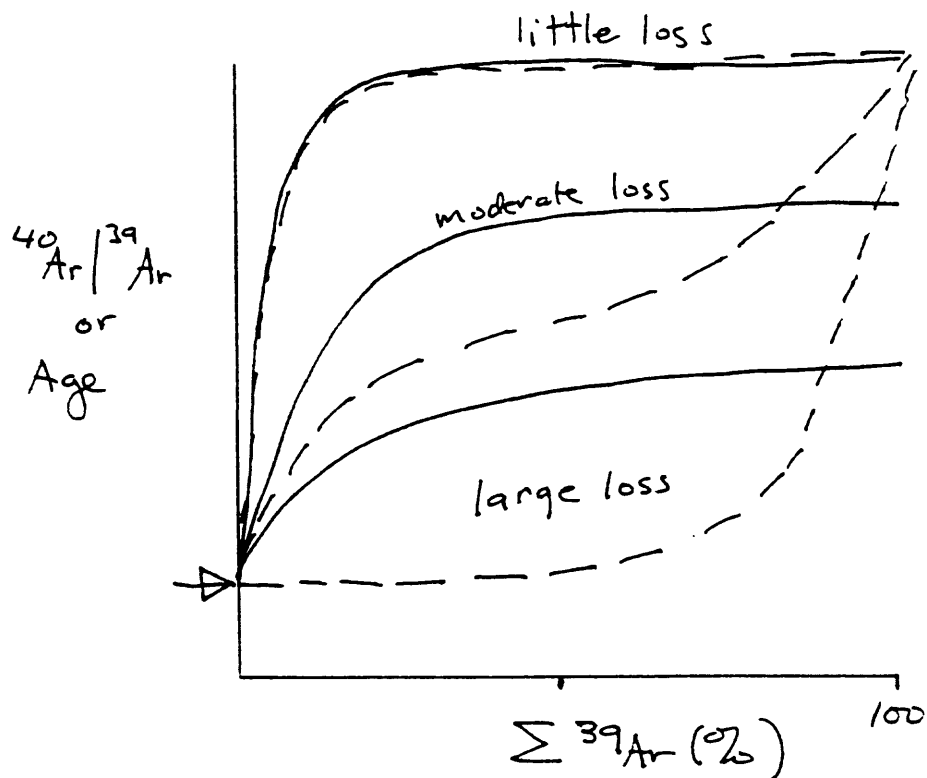
1. Theoretical age spectra for the case of slow cooling/episodic loss (solid lines), and episodic loss experienced by a sample containing domains having a range of diffusion dimensions (dashed lines).
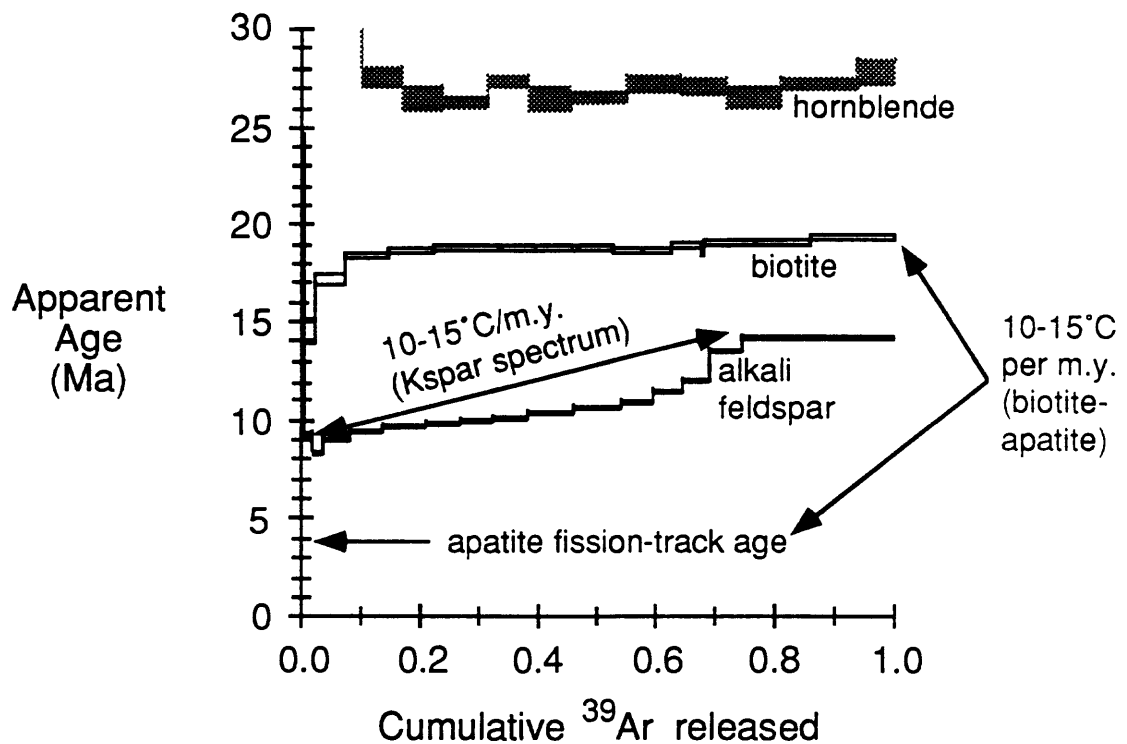
2. Age spectra for samples from a Himalayan tonalite. The hornblende, biotite, and apatite fission-track ages show that the sample experienced relatively slow cooling through the interval 320°C through 110°C, from 27 Ma to 4 Ma. Essentially the same cooling history is preserved internally within the K-feldspar age spectrum, for the period 11-14 Ma. Data from Zeitler et al., 1988)

43

(a)

Apparent Age
(Ma)

Fraction ^{39}Ar Released

(b)

Apparent Age
(Ma)

Fraction ^{39}Ar Released

3. Age spectra from several aliquots of purified K-feldspar subjected to heating prior to irradiation. The samples heated to high temperatures yield strongly concave-up spectra, with the youngest ages being indistinguishable from zero (thank goodness!). Compare these results to the theoretical curves shown in Figure 1. The nature of the spectra is consistent with the presence of a range of diffusion dimensions within each sample. After Zeitler (1987).

44

CASE STUDY TOPICS

I. CHRONOSTRATIGRAPHY

Siwalik Molasse, Himalayas, Pakistan
(P.K. Zeitler)

1. Introduction. Tracks and the Time Scale-Oil and Water?

Some people have grave reservations at seeing the term "fission-track dating" juxtaposed anywhere near the holy word "chronostratigraphy." Is such skepticism justified? Maybe yes, maybe no.

First, for very young rocks less than a million years in age, the fission-track method can compete successfully against other methods. Second, the justification for using fission-track dating in attacking a chronostratigraphic problem depends on the problem and the time resolution that is required. In applications such as the one presented below, all that is required is an approximate fix in time, in order to allow a magnetostratigraphic section to be correlated to the magnetic polarity reversal time scale. Third, the fission-track method does have the advantage that it allows individual grains to be dated. Thus, it is sometimes possible to detect and ameliorate the effects of detrital contamination, which is very common in volcanic ashes. Finally, fission-track dating can serve as a useful cross-check on a date obtained by another method, both in terms of age, and in terms of identifying any unsuspected potential thermal disturbances which might have affected other dating systems as well.

The drawback to fission-track dating remains the rather large uncertainties that are typical of fission-track ages. An age of 150 ± 15 Ka (10% error) might be useful for some of the goals of Quaternary geology, but an age of 400 ± 40 Ma (10% error) is unlikely to be of much use to most geologists. With some exceptions for young samples, it is probably best to just say no to any suggestion of doing direct "time scale work" using the fission-track method.

2. Case Study: Magnetostratigraphy of a Neogene Foreland Basin, Pakistan

Some ten kilometers of molasse sediments (Siwalik molasse) occur in the foredeep which runs the length of the Himalayan chain. These terrestrial clastic sediments are very important for several reasons. First, in their facies and in their petrology, these rocks provided an integrated record of the latter phases of the Himalayan Orogeny in the hinterland. Second, particularly in Pakistan, where there is abundant salt in the Phanerozoic platform section of the northern Indian plate, the Siwalik molasse has become highly deformed, and this deformation serves as a detailed record of tectonic events in the foreland. Finally, specimens of *Ramapithecus* have been found in the Siwalik sediments.

The only geochronological tool capable of providing a detailed chronology for the fluvial sandstones and shales of the Siwalik Group is magnetic polarity reversal stratigraphy. Throughout the 1970's and 1980's, teams from Dartmouth College,

Lamont-Doherty, and Yale University erected a detailed conventional and magnetic stratigraphy for these rocks. However, what was needed were widely available tie points with which to lock the observed magnetic sections into the magnetic-reversal time scale. Fortunately, at several levels in the Siwalik section, thin (usually 5-10 cm) bentonites can be found (Johnson et al., 1982). The source of these bentonites was probably the Dacht-e-Nawar volcanic complex, located about 600 km to the west in eastern Afghanistan.

The bentonites found within the Siwaliks proved to be useless for K-Ar dating: what little feldspar remained was heavily contaminated by detrital material, and the sometimes plentiful biotites were thoroughly vermiculitized. However, the bentonites also contained euhedral crystals of light pink zircon, which proved straightforward to date using the fission-track method. By dating the zircons, even with precision on the order of ±10% or more, it was possible to justify the correlations that been made to the reversal time scale (Figure 1). Thus, although both the fission-track analysis and the interpretation of the resulting dates were simple, the work was of great importance to the larger project. A sampling of some of the work that reports on and discusses the implications of the detailed Siwalik Group chronology is given below.

3. References

Johnson, G.D., Johnson, N.M., Opdyke, N.D., & R.A.K. Tahirkheli, 1979, Magnetic reversal stratigraphy and sedimentary tectonic history of the Upper Siwalik Group, eastern Salt Range and southwestern Kashmir. *In*: A. Farah and K.A. De Jong (eds.), *Geodynamics of Pakistan*. Geological Survey of Pakistan, Quetta, 149-165.

Johnson, G.D., Zeitler, P., Naeser, C.W., Johnson, N.M., Summers, D.M., Frost, C.D., Opdyke, N.D. & R.A.K. Tahirkheli, 1982, The occurrence and fission-track ages of Late Neogene and Quaternary volcanic sediments, Siwalik Group, northern Pakistan. *Palæogeography, Palæoclimatology, and Palæoecology*, 37, 63-93.

Johnson, G.D., Opdyke, N.D., Tandon, S.K. & A.C. Nanda, 1983, The magnetic polarity stratigraphy of the Siwalik Group at Haritalyangar (India) and a new last appearance datum for *Ramapithecus* and *Sivapithecus* in Asia. *Palæogeography, Palæoclimatology, and Palæoecology*, 44, 223-249.

Johnson, G.D., Raynolds, R.G.H. & D.W. Burbank, 1986, Late Cenozoic tectonics and sedimentation in the northwestern Himalayan foredeep: I. Thrust ramping and associated deformation in the Potwar region, *in* P.A. Allen and P. Homewood, (eds.) *Foreland Basins*, International Association of Sedimentologists Special Publication 8, 203-221.

Johnson, N.M., Opdyke, N.D., Johnson, G.D., Lindsay, E.H., & R.A.K. Tahirkheli, 1982, Magnetic polarity stratigraphy and ages of Siwalik Group rocks of the Potwar Plateau. Pakistan. *Palæogeography, Palæoclimatology, and Palæoecology*, 37, 17-42.

Johnson, N.M., Stix, J., Tauxe, L., Cerveny, P.F., & R.A.K. Tahirkheli, 1985, Paleomagnetic chronology, fluvial processes and tectonic implications of the Siwalik deposits near Chinji Village, Pakistan. *Journal of Geology*, 93, 27-40.
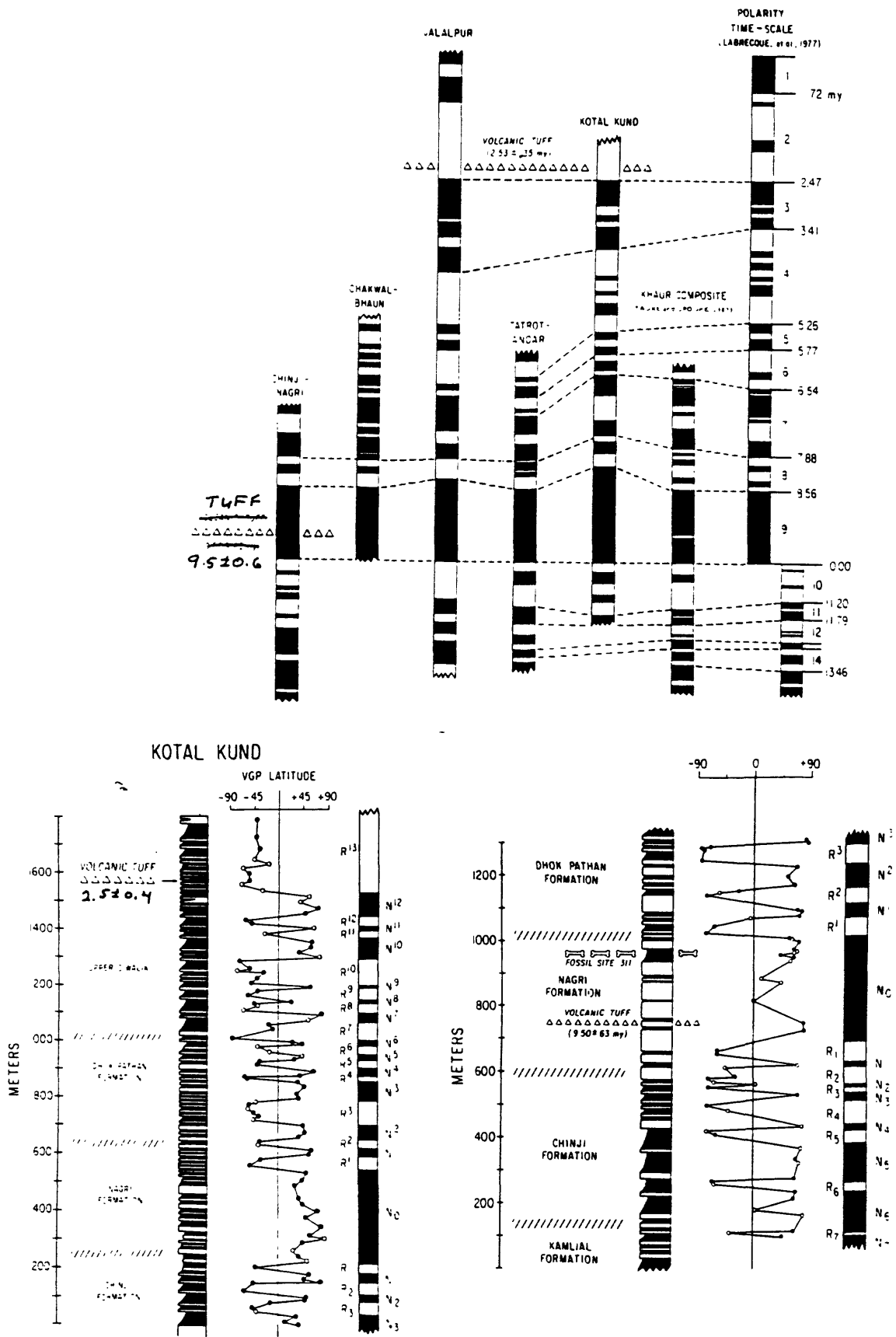
1. (Top) Correlation of local Siwalik Group magnetostratigraphies for the Potwar Plateau, Pakistan, with the magnetic polarity reversal time scale. Note how the fission-track ages of volcanic ashes, although not very precise, do a good job of aiding the correlations. (Bottom) Example of measured data from two localities.

Blank

.

High-precision ^{40}Ar/^{39}Ar sanidine geochronology of ignimbrites in the Mogollon-Datil volcanic field, southwestern New Mexico

William C McIntosh[1], John F Sutter[2], Charles E Chapin[1], and Laura L Kedzie[1]

[1] N. M. Bureau of Mines and Mineral Resources, N. M. Institute of Mining and Technology, Socorro, NM 87801, USA
[2] U. S. Geological Survey, Reston, VA 22092, USA

Abstract. ^{40}Ar/^{39}Ar age spectra have been obtained from 85 sanidine separates from 36 ignimbrites and one rhyolitic lava in the latest Eocene-Oligocene Mogollon-Datil volcanic field of southwestern New Mexico. Of the 97 measured age spectra, 94 yield weighted-mean plateau ages each giving single-spectrum 1σ precision of ±0.25%–0.4% (±0.07–0.14 Ma). Replicate plateau age determinations for eight different samples show within-sample 1σ precisions averaging ±0.25%. Plateau ages from multiple ($n = 3$–8) samples of individual ignimbrites show 1σ within-unit precision of ±0.1%–0.4% (±0.04–0.13 Ma). This within-unit precision represents a several-fold improvement over published K-Ar data for the same ignimbrites, and is similar to the range of precisions reported from single-crystal laser fusion studies. A further indication of the high precision of unit-mean ^{40}Ar/^{39}Ar ages is their close agreement with independently established stratigraphic order. Two samples failed to meet plateau criteria, apparently due to geologic contamination by older feldspars. Effects of minor contamination are shown by six other samples, which yielded slightly anomalous plateau ages. ^{40}Ar/^{39}Ar plateau ages permit resolution of units differing in age by 0.5% (0.15 Ma) or less. This high resolution, combined with paleomagnetic studies, has helped to correlate ignimbrites among isolated ranges and has allowed development of an integrated time-stratigraphic framework for the volcanic field. Mogollon-Datil ignimbrites range in age from 36.2 to 24.3 Ma. Ignimbrite activity was strongly episodic, being confined to four brief (<2.6 m.y.) eruptive episodes separated by 1–3 m.y. gaps. Ignimbrite activity generally tended to migrate from the southeast toward the north and west.

Introduction

The need for high-resolution ^{40}Ar/^{39}Ar geochronology is acute in mid-Tertiary silicic volcanic fields where ma-

jor ignimbrites (ash-flow tuffs) have in some cases been erupted at intervals of 0.2 Ma or less, and differences in eruption ages are unresolvable by conventional K-Ar geochronology. Under the best circumstances, conventional K-Ar dating yields within-sample 1σ precisions near ±1.0% (Lanphere 1988); in practice, however, within-unit standard deviations of reported K-Ar ages from individual ignimbrites may exceed ±5% (e.g., Marvin et al. 1987).

^{40}Ar/^{39}Ar dating techniques can yield ages which are several times more precise than the best conventional K-Ar ages. This high precision chiefly results from the ability to simultaneously measure radiogenic ^{40}Ar and ^{40}K (as reactor-produced ^{39}Ar) on a single aliquot of sample (Turner 1968; Roddick 1983). Furthermore, the ^{40}Ar/^{39}Ar method can provide accurate ages without extracting all Ar from a sample, thereby overcoming the chronic problem of incomplete ^{40}Ar extraction in K-Ar dating of sanidine and anorthoclase (McDowell 1983).

Currently, the two variations of the ^{40}Ar/^{39}Ar method used for high-precision age determinations are age spectra (e.g., Lanphere 1988) and laser-heating total fusions (e.g., Dalrymple and Duffield 1988). Age spectra offer two advantages. First, the shape of the age spectrum allows identification of samples which have been affected by Ar loss or excess Ar. Second, precision can be increased by statistically treating incremental-heating-step data using plateau or isotope correlation methods. On the other hand, the laser-heating, total-fusion method offers advantages of small blank, single-grain sample size, rapid analysis, and easy identification of contamination. Within-sample and within-unit 1σ precisions of about ±0.5% have reported for ^{40}Ar/^{39}Ar age spectra from biotites (e.g., Lanphere 1988), and even higher precision has been reported from laser-heating, ^{40}Ar/^{39}Ar total-fusion dating of small samples or single crystals of sanidine (Dalrymple and Duffield 1988; Deino and Best 1988; Deino 1989).

This paper reports the results of a ^{40}Ar/^{39}Ar sanidine age spectra study of regional ignimbrites in the Mogollon-Datil volcanic field of southwestern New Mexi-

49

co. The application of this data to Mogollon-Datil volcanic stratigraphy and to calibration of the mid-Tertiary magnetic polarity time scale is discussed elsewhere (McIntosh 1989; McIntosh et al. 1986, in press).

Mogollon-Datil volcanic field

The Mogollon-Datil volcanic field is the northern tip of a once contiguous late Eocene-Oligocene volcanic field that extended from southwestern New Mexico into Chihuahua, Mexico (Fig. 1). This relatively accessible volcanic field has been the focus of numerous mapping, stratigraphic, geochemical, petrologic, and isotopic studies (e.g., see references in Ratté et al. 1984; Osburn and Chapin 1983b). The general history of Mogollon-Datil activity resembles that of the San Juan volcanic field of Colorado (Lipman et al. 1978). Activity began with andesitic volcanism from about 40 to 36 Ma, which was followed by episodic bimodal silicic and basaltic andesite activity from 36 to 24 Ma (Cather et al. 1987; Elston 1984). The silicic sequence includes about 25 widespread (> 1000 km³), voluminous (50-1300 km³), high- and low-silica rhyolitic ignimbrites. Source cauldrons have been identified for many of

these ignimbrites (Osburn and Chapin 1983a; Elston 1984), but regional correlations of outflow sheets have been problematic. Although local stratigraphic sequences have been established by detailed mapping (e.g., Ratté et al. 1984; Seager et al. 1982), regional correlations have been hampered by extensional faulting and tectonism and by lithogic similarities among units (McIntosh et al. 1986; Hildreth and Mahood 1985).

Conventional K-Ar and fission-track data have proven too imprecise to allow reliable correlation of many Mogollon-Datil regional ignimbrites. For most units, only a small number of K-Ar dates are available, and these data in many cases disagree with independently established stratigraphic relationships (e.g., Clemens 1976). Where several K-Ar or fission-track dates have been determined for individual units, within-in-unit standard deviations generally exceed ±5%, or about ±1.4 Ma (e.g., Marvin et al. 1987). For many of the units, sanidine K-Ar dates are significantly younger than biotite K-Ar ages, apparently reflecting incomplete extraction of Ar from sanidine (McDowell 1983).

$^{40}Ar/^{39}Ar$ age spectra from Mogollon-Datil ignimbrites yield plateau ages far more precise than published K-Ar data. $^{40}Ar/^{39}Ar$ dating and paleomagnetic studies have helped to correlate ignimbrites among isolated ranges, thereby solving some long-standing strati-
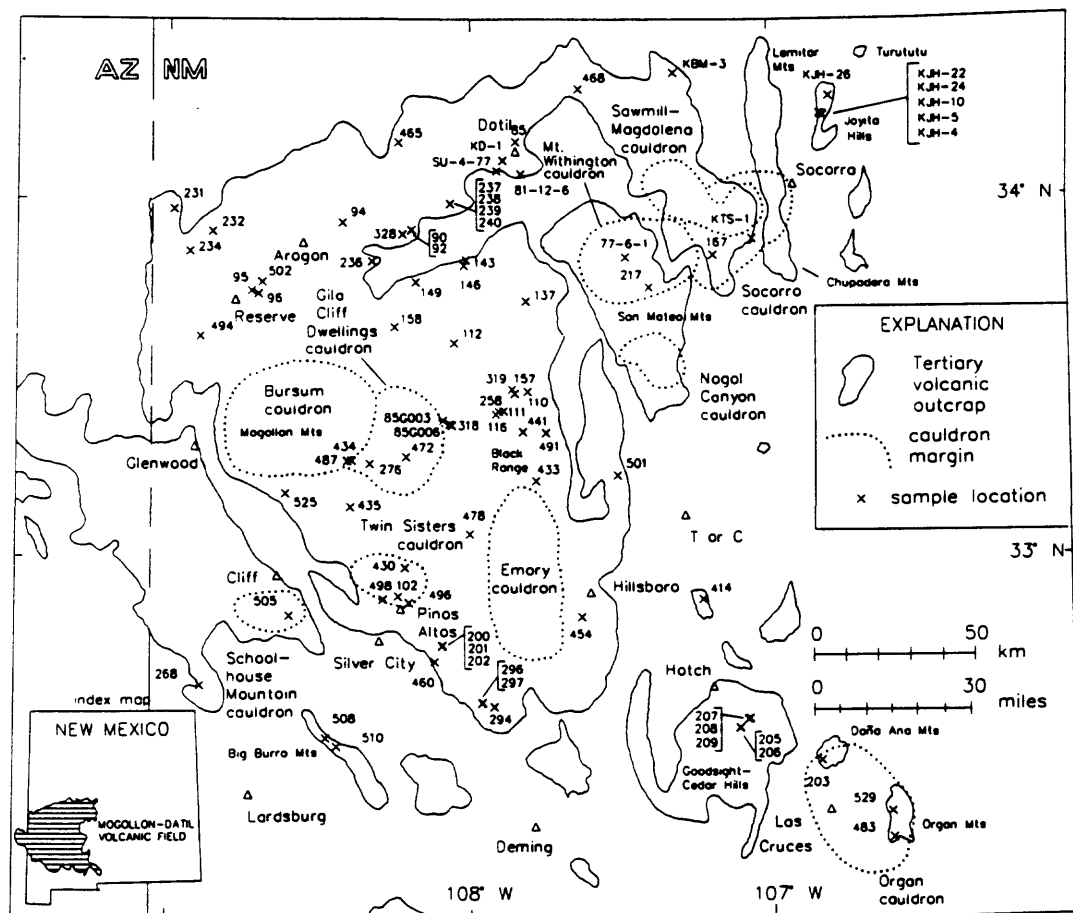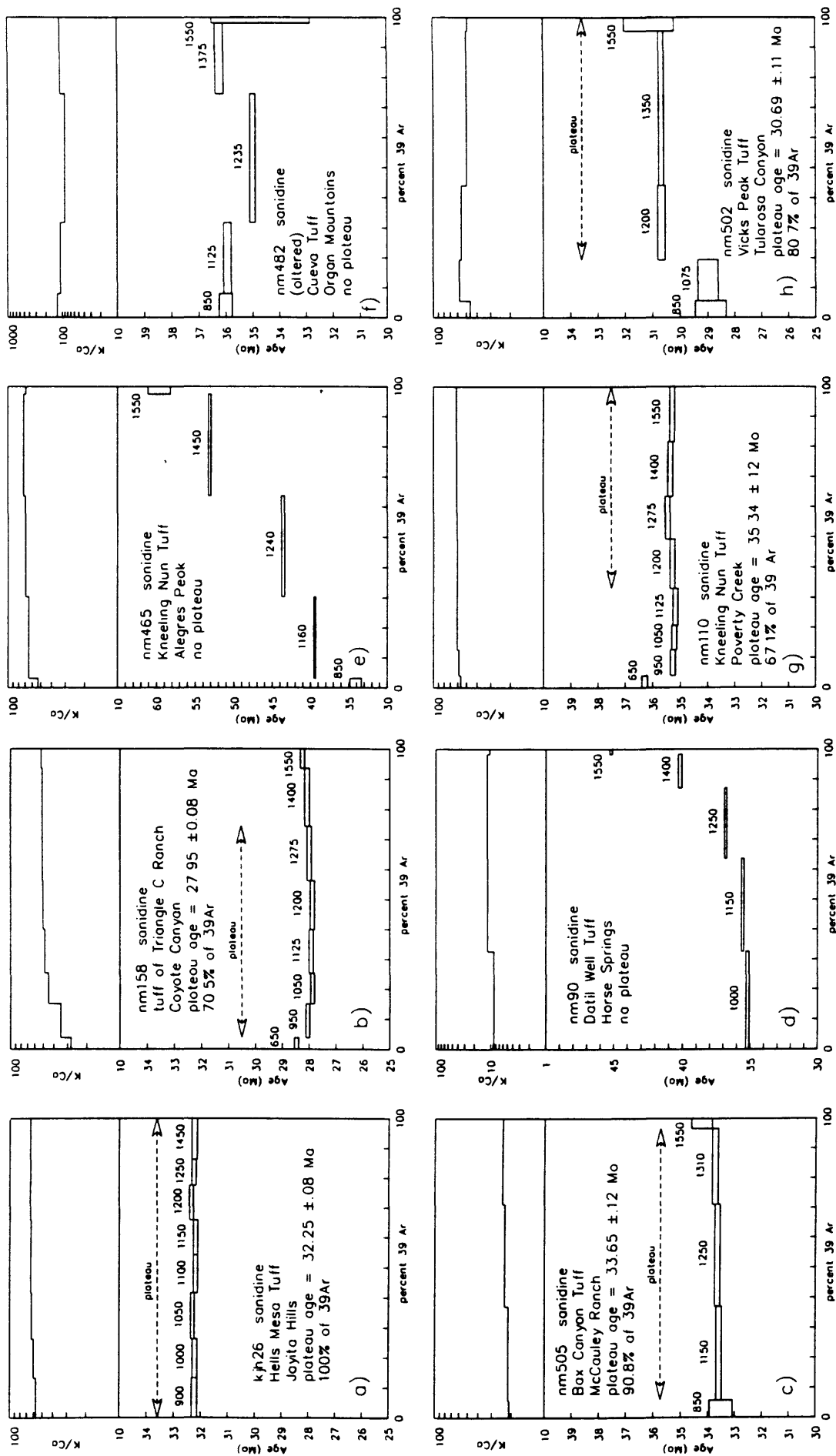

Fig. 1. Map of $^{40}Ar/^{39}Ar$ dating samples from the Mogollon-Datil volcanic field. *Numbered crosses* show sample locations (precise locations in McIntosh and Kedzie, in press)

5 0

Fig. 5a–h. Representative age spectra from Mogollon-Datil sanidines. a Concordant plateau age spectrum and flat K/Ca spectrum typical of 80% of analyzed sanidines. b Concordant plateau age spectrum accompanied by a somewhat discordant K/Ca spectrum. c Age spectrum that climbs in age slightly with increasing temperature. d Steeply climbing age spectrum. e Steeply climbing age spectrum; both d and e indicate contamination by older K-feldspar. f Irregular discordant age spectrum of an altered sanidine. g Concordant plateau age spectrum of an apparently contaminated sample. h Somewhat discordant age spectrum, still meeting plateau criteria, of an apparently contaminated sample

Fig. 7

independently established stratigraphic sequence

| S. Canyon |
| Lemitar |
| Caronita |
| Bloodgood |
| Shelly Pk. |
| Garcia C. |
| Vicks Pk. |
| La Jencia |
| Mud Hole |
| L.M.Creek |

3
2
1
8
1
1
3
4
1
1

apparently contaminated by older K-feldspar

$^{40}Ar/^{39}Ar$ age (Ma)

29.5 29.0 28.5 28.0 27.5 27.0

Fig. 7. The order of $^{40}Ar/^{39}Ar$ ages from this 29.0–27.4 Ma sequence of nine ignimbrites agrees closely with independently determined stratigraphic order (*column*), except for the apparently contaminated sample of Shelly Peak Tuff. The number of dated samples per unit is shown right of each error bar

Fig. 6

fission track zircon: 28 2 ±2 1 Ma

fission track sphene: 28 1 ±2 2 Ma

K-Ar sonidine: 26 9 ±1 3 Ma

K-Ar biotite: 28 8 ±1 4 Ma

$^{40}Ar/^{39}Ar$ sonidine: 28 05 ±0.04 Ma

BLOODGOOD CANYON TUFF

$^{40}Ar/^{39}Ar$ — sanidine

K-Ar — [S] sonidine, [B] biotite

fission track — [Z] zircon, [T] sphene
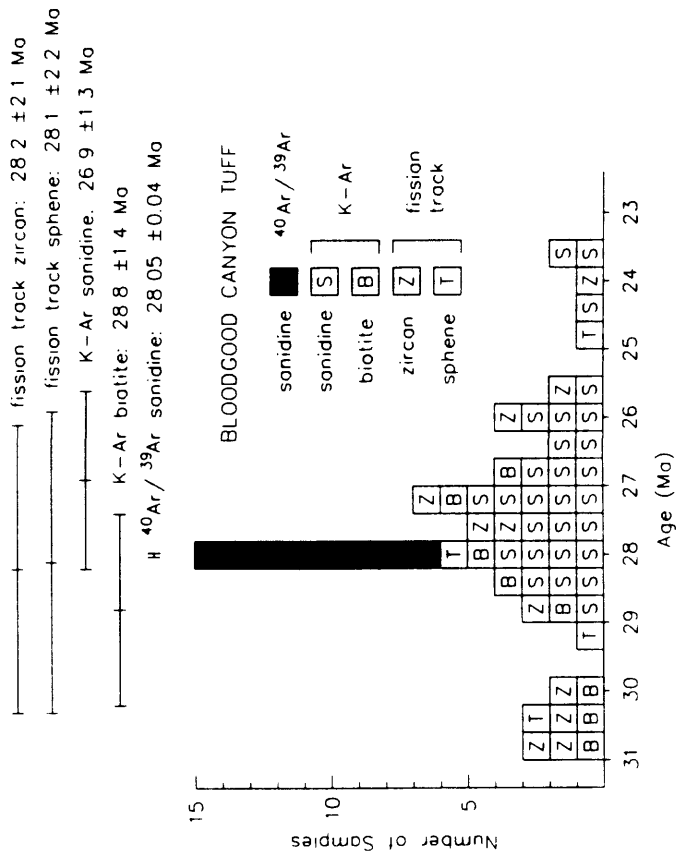
Age (Ma)

23 24 25 26 27 28 29 30 31

Number of Samples

Fig. 6. A comparison of eight $^{40}Ar/^{39}Ar$ sanidine plateau ages with published conventional K-Ar and fission track ages from the Bloodgood Canyon Tuff (Marvin et al. 1987). Each box denotes a single age determination. The large standard deviation of the published data in part reflects its acquisition from several different laboratories
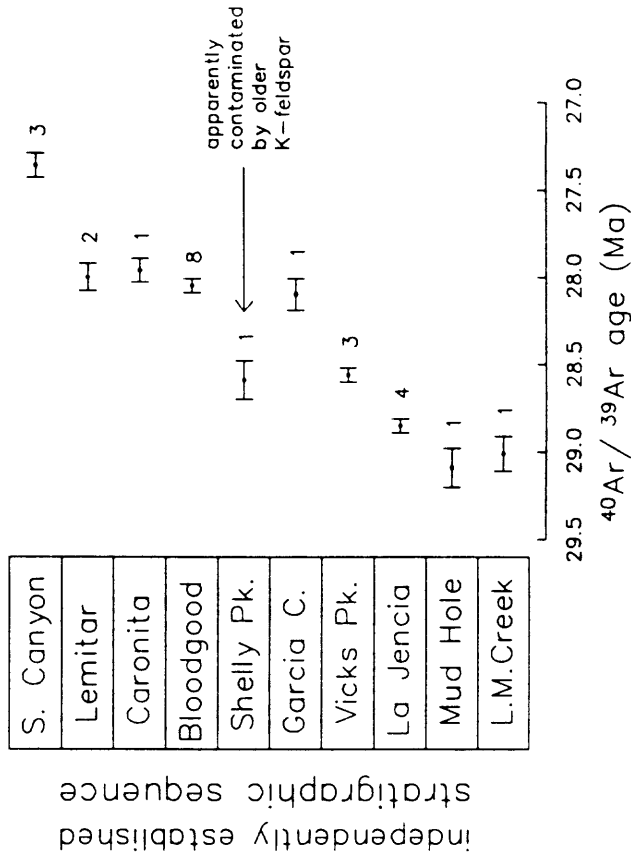
5 2

Table 4. Summary of $^{40}Ar/^{39}Ar$ age data for Mogollon-Datil ignimbrites

Stratigraphic Unit	Ref.	Extent (km)	Volume (km³)	$^{40}Ar/^{39}Ar$ plateau age		
				n	Ma	σ (Ma)
EPISODE 4						
Turkey Springs[a]	5	62		2	24.33	±0.03
EPISODE 3						
Slash Ranch[a]	14	22		1	26.10	±0.12
South Canyon	9	135	700	3	27.36	±0.07
Walking X Canyon[a]	8			1	27.58	±0.10
Lemitar	9	78	450	2	28.00	±0.08
Caronita Canyon	9	40	50	1	27.96	±0.07
Triangle C Ranch[a]	10	58		1	28.05	±0.14
Apache Springs	11	35	1200	1	27.98	±0.09
Bloodgood Canyon	11	155	1000	8	28.05	±0.04
Diablo Range	12	10		1	28.05	±0.08
Shelly Peak	11	96	100-200	1	28.59[b]	±0.11 (28.1)
Garcia Camp	4	25		1	28.10	±0.09
Vicks Peak	9	200	1050	3	28.56	±0.04
Lookout Mountain[a]	18			2	28.69	±0.03
La Jencia	9	158	1250	4	28.85	±0.04
Davis Canyon	11	125	200-400	2	29.01	±0.11
Mud Hole[a]	7			1	29.09	±0.11
Little Mineral Creek[a]	18			1	29.01	±0.10
EPISODE 2						
u. Tadpole Ridge	6	28		1	31.39	±0.11
Caballo Blanco	17	143		5	31.65	±0.06
Hells Mesa	9	152	1200	4	32.06	±0.10
EPISODE 1						
Box Canyon	2	225	>100	7	33.51	±0.13
Blue Canyon	9	135		2	33.66	±0.03
Table Mountain[a]	2			1	33.89	±0.12
Rock House Canyon	9	142		1	34.42	±0.12
Mimbres Peak	3			1	34.57	±0.12
Lebya Well[a]	13	72		1	34.70	±0.10
Kneeling Nun	3	213	>900	4	34.89	±0.05
Bell Top 4	1	112		3	34.96	±0.04
Upper Sugarlump	17	50?		1	35.17	±0.12
Farr Ranch[a]	13	143		1	35.57	±0.13
Datil Well	18	140		2	35.48	±0.07
Doña Ana	16	8		1	35.49	±0.11
Bell Top 3	1	41		2	35.69	±0.02
Squaw Mountain	15	11		1	35.75	±0.12
Cueva	15	13		1	36.20	±0.13

Regional ignimbrites are underlined. [a] denotes informal unit name; [b] indicates $^{40}Ar/^{39}Ar$ age affected by xenocrystic contamination (age in parentheses is based on stratigraphic constraints). Extent is maximum exposed width (extents based on uncertain correlations are queried). Volume estimates are after McIntosh et al. (1986), Ratté et al. (1984), and Elston et al. (1975). n is number of plateau ages used in mean. σ is standard deviation of multiple ages or analytical error of single ages.

1, Clemons (1976); 2, Elston (1957); 3, Elston et al. (1975); 4, Duffield et al. (1987); 5, Ferguson (1986); 6, Finnell (1976); 7, R Harrison, personal communication 1988; 8, Hedlund (1978); 9, Osburn and Chapin (1983b); 10, J Ratté, personal communication 1988; 11, Ratté et al. (1984); 12, Ratté and Gaskill (1975); 13, Ratté et al. (1989); 14, Richter (1978); 15, Seager and McCurry (1988); 16, Seager et al. (1976); 17, Seager et al. (1982); 18, Woodard (1982)

^{40}Ar/^{39}Ar plateau ages determined from Mogollon-Datil ignimbrites range from 36.2 to 24.3 Ma indicate that ignimbrite activity was strongly episodic. Activity was confined to four brief (<2.6 m.y.) eruptive episodes separated by 1-3-m.y. gaps during which no ignimbrites were erupted (Table 4, Fig. 8). The generalized history of the four Mogollon-Datil ignimbrite eruptive episodes are summarized below. Details of ignimbrite timing, distribution, and stratigraphy are presented in McIntosh (1989) and McIntosh et al. (in press).

Episode 1 (36.2-33.5 Ma). Mogollon-Datil ignimbrite activity commenced at the southeast edge of the field with eruption of the Organ Mountains/Doña Ana Cauldron complex and associated outflow sheets from 36.2-35.5 Ma. During the next 2 m.y. at least five regional ignimbrites were erupted in the southern portion of the field (Table 4, Fig. 8), including the >900-km^3 Kneeling Nun Tuff at 34.9 Ma. Four 35.6-33.7-Ma outflow sheets are also present in the northern portion of the field (Datil Well, Farr Ranch, Lebya Well, and Blue Canyon tuffs in Table 4), although their calderas have not yet been identified.

Episode 2 (32.1-31.4 Ma). After a 1.4-m.y. hiatus, three low-silica rhyolitic ignimbrites were erupted i.e., the Hells Mesa (32.1 Ma, 1200 km^3), Caballo Blanco (31.7 Ma), and Tadpole Ridge (31.4 Ma) tuffs.
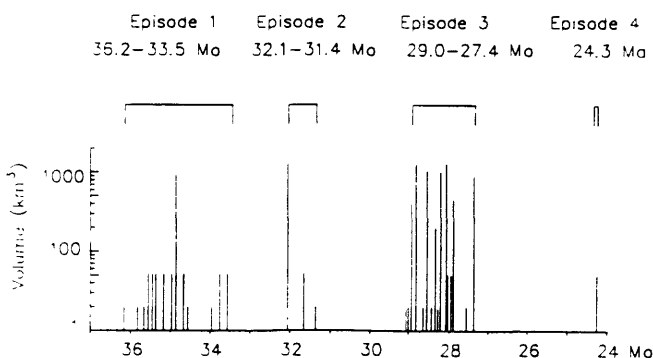

Fig. 8. Time distribution of well-dated Mogollon-Datil ignimbrites, showing episodic nature of volcanism. *Vertical lines* each represent a dated ignimbrite, with length proportional to estimated volume from Table 4. Units with no available volume estimate are conservatively shown as 50 km^3 for regional units (lateral extent >40 km) and 20 km^3 for more local units

Conclusions

^{40}Ar/^{39}Ar age spectra from 85 sanidine separates yield weighted average plateau ages with single-spectrum 1σ precision of ±0.3%-0.4% (±0.07-0.14 Ma) and within-unit 1σ precision of ±0.1%-0.4% (±0.04-0.13 Ma). Depending on the number of dated samples per unit, ^{40}Ar/^{39}Ar plateau ages presently allow resolution of units differing in age by less than 0.5% (0.12-0.15 Ma), and offer potential resolution of less than 0.2% (0.03-0.04 Ma).

^{40}Ar/^{39}Ar age spectra from eight sanidine separates show elevated apparent ages which apparently reflect contamination by older xenocrystic or lithic K-feldspar. Two of these spectra show ages which increase with extraction temperature, but six meet the plateau criteria of Fleck et al. (1977).

The within-unit precision of Mogollon-Datil sanidine ^{40}Ar/^{39}Ar plateau ages far exceeds that of published K-Ar and fission-track data, and shows good agreement with independently established stratigraphic order. Furthermore, plateau ages from some of the better studied units show within-unit precisions which are similar to those reported from laser-fusion ^{40}Ar/^{39}Ar dating studies. These plateau ages have helped resolve many of the long-standing ignimbrite correlation problems in the Mogollon-Datil volcanic field. The combination of ^{40}Ar/^{39}Ar plateau ages, paleomagnetic studies, and existing stratigraphic data has allowed the development of a comprehensive, ignimbrite-based, time-stratigraphic framework for the Mogollon-Datil volcanic field.

^{40}Ar/^{39}Ar plateau data indicate that Mogollon-Datil ignimbrite activity ranged from 36.2 to 24.3 Ma and was strongly episodic, being confined to four brief (<2.6-Ma) eruptive episodes separated by 1-3-Ma gaps during which no caldera-forming eruptions occurred.

54

References

Bogaard PVD, Hall CM, Schmincke H, York D (1987) $^{40}Ar/^{39}Ar$ Laser dating of single grains: ages of Quaternary tephra from the East Eifel volcanic field, FRG. Geophys Res Lett 14:1211–1214

Cather SM, Johnson BD (1984) Eocene tectonics and depositional setting of west-central New Mexico and eastern Arizona. NM Bur Mines Miner Resour Circ 192:1-33

Cather SM, McIntosh WC, Chapin CE (1987) Stratigraphy, age, and rates of deposition of the Datil Group (Upper Eocene-Lower Oligocene), west-central New Mexico. NM Geol 9:50-54

Chapin CE, Lindley JI (1986) Potassium metasomatism of igneous and sedimentary rocks in detachment terranes and other sedimentary basins: Economic implications. Ariz Geol Soc Dig 16:118-126

Clemons RE (1976) Sierra del las Uvas ash-flow field, south central New Mexico. NM Geol Soc Spec Pub 6:115-121

Dalrymple GB, Duffield WA (1988) High-Precision $^{40}Ar/^{39}Ar$ dating of Oligocene rhyolites from the Mogollon-Datil volcanic field using a continuous laser system. Geophys Res Lett 15:463-466

Dalrymple GB, Lanphyre MA (1969) Potassium-argon dating. Principles, techniques, and applications to geochronology. WH Freeman, San Francisco

Dalrymple GB, Lanphere MA (1988) Correlation diagrams in $^{40}Ar/^{39}Ar$ dating: is there a correct choice? Geophys Res Lett 15:589-591

Dalrymple GB, Alexander EC, Lanphyre MA, Kraker GP (1981) Irradiation of samples for $^{40}Ar/^{39}Ar$ dating using the Geological Survey TRIGA reactor. US Geol Surv Prof Pap 1176:1-55

Deino AL (1989) Single-crystal $^{40}Ar/^{39}Ar$ dating as an aid in correlation of ash flows: examples from the Chimney Spring/New Pass Tuffs and the Nine Hill/Bates Mountain Tuffs of California and Nevada. Continental magmatism abstracts. NM Bur Mines Miner Res Bull 131:70

Deino AL, Best MG (1988) Use of high-precision single-crystal $^{40}Ar/^{39}Ar$ ages and TRM data in correlation of an ash-flow deposit in the Great Basin. Geol Soc Am Abstr with Progr 20:397

Duffield WA, Richter DH, Preist SS (1987) Preliminary geologic map of the Taylor Creek Rhyolite, Catron and Sierra Counties, New Mexico. US Geol Surv, Open File Rep 87-515, 1:50,000

Elston WE (1957) Geology and mineral resources of Dwyer quadrangle, Grant, Luna, and Sierra Counties, New Mexico. NM Bur Mines Miner Res Bull 37:1-88

Elston WE (1984) Mid-Tertiary ash flow tuff cauldrons, southwestern New Mexico. J Geophys Res 89:8733-8750

Elston WE, Seager WR, Clemons RE (1975) Emory Cauldron, Black Range, New Mexico: source of the Kneeling Nun Tuff. NM Geol Soc Field Conf Guideb 26:283-292

Ferguson CA (1986) Geology of the east-central San Mateo Mountains, Socorro County, New Mexico. NM Bur Mines Miner Res Open File Rep 252:1-135

Finnell TL (1976) Geologic map of the Twin Sisters quadrangle, Grant County, New Mexico. US Geol Surv, Miscellaneous Field Studies MF-779, 1:24,000

Fleck RJ, Sutter JF, Elliot DH (1977) Interpretation of discordant $^{40}Ar/^{39}Ar$ age-spectra of Mesozoic tholeiites from Antarctica. Geochim Cosmochim Acta 41:15-32

Foland KA (1974) ^{40}Ar diffusion in homogeneous orthoclase and an interpretation of Ar diffusion in K-feldspars. Geochim Cosmochim Acta 38:151-166

Goldich SS, Fischer LB (1986) Air-abrasion experiments in U-Pb dating of zircon. Isotope Geosci 58:195-215

Harrison TM, Bé K (1983) $^{40}Ar/^{39}Ar$ age spectrum analysis of detrital microclines from the southern San Joaquin Basin, California: an approach to determining the thermal evolution of sedimentary basins. Earth Planet Sci Lett 64:244-256

Hedlund DC (1978) Geologic map of the C-Bar Ranch quadrangle, Grant County, New Mexico. US Geol Surv, Miscellaneous Field Studies MF-1039, 1:24,000

Hildreth W, Mahood G (1985) Correlation of ash-flow tuffs. Geol Soc Am Bull 96:968-974

Hildreth W, Mahood G (1986) Ring fracture eruption of the Bishop Tuff. Geol Soc Am Bull 97:396-403

Kedzie LL (1984) High precision $^{40}Ar/^{39}Ar$ dating of major ash-flow tuff sheets, Socorro, New Mexico. MS Dissertation, NM Institute of Mining and Technology, Socorro

Kroll H, Ribbe PH (1987) Determining (Al, Si) distribution and strain in alkali feldspars using lattice parameters and diffraction-peak positions: A review. Am Mineral 72:491-506

Kunk MJ, Sutter JF, Naeser CW (1985) High-precision $^{40}Ar/^{39}Ar$ ages of sanidine, biotite, hornblende, and plagioclase from the Fish Canyon Tuff, San Juan volcanic field, south-central Colorado. EOS Trans AGU 17:636

Lanphere MA (1988) High-resolution $^{40}Ar/^{39}Ar$ geochronology of Oligocene volcanic rocks, San Juan Mountains, Colorado. Geochim Cosmochim Acta 52:1425-1434

Lindley JI (1985) Potassium metasomatism of Cenozoic volcanic rocks near Socorro, New Mexico. Ph D Dissertation, Univ North Carolina, Chapel Hill

Lipman PW, Doe BR, Hedge CE, Steven TA (1978) Petrologic evolution of the San Juan volcanic field, southwestern Colorado: Pb and Sr isotopic evidence. Geol Soc Am Bull 89:59-82

Lippolt HJ, Fuhrmann U, Hradetzky H (1986) $^{40}Ar/^{39}Ar$ age determinations on sanidines of the Eifel volcanic field (Federal Republic of Germany): constraints on age and duration of a middle Pleistocene cold period. Chem Geol 59:187-204

Lo Bello P, Féraud G, Hall CM, York D, Lavina P, Bernat M (1987) $^{40}Ar/^{39}Ar$ step-heating and laser fusion dating of a Quaternary pumice from Neschers, Massif Central, France: the defeat of xenocrystic contamination. Chem Geol 66:61-71

Marvin RF, Naeser CW, Bikerman M, Mehnert HH, Ratté JC (1987) Isotopic ages of post-Paleocene igneous rocks within and bordering the Clifton 1° x 2° quadrangle, Arizona-New Mexico. NM Bur Mines Miner Res Bull 118:1-63

McDowell FW (1983) K-Ar dating: incomplete extraction of radiogenic argon from alkali feldspar. Isot Geosci 1:119-126

McIntosh WC (1989) Ages and distribution of ignimbrites in the Mogollon-Datil volcanic field: a stratigraphic framework using $^{40}Ar/^{39}Ar$ dating and paleomagnetism. Ph D Dissertation, NM Institute of Mining and Technology, Socorro

McIntosh WC, Kedzie LL (1990) Paleomagnetic and $^{40}Ar/^{39}Ar$ dating database for Mogollon-Datil ignimbrites, southwestern New Mexico. NM Bur Mines Miner Res Bull 135 (in press)

McIntosh WC, Sutter JF, Chapin CE, Osburn GR, Ratté JC (1986) A stratigraphic framework for the Mogollon-Datil volcanic field based on paleomagnetism and high-precision $^{40}Ar/^{39}Ar$ dating of ignimbrites - a progress report. NM Geol Soc Field Conf Duideb 37:183-195

McIntosh WC, Chapin CE, Ratté JC, Sutter JF (1990) Ages and distribution of ignimbrites in the Mogollon-Datil volcanic field, southwest New Mexico: a stratigraphic framework using $^{40}Ar/^{39}Ar$ dating and paleomagnetism. Geol Soc Am Bull (in press)

Osburn GR, Chapin CE (1983a) Ash-flow tuffs and cauldrons in the northeast Mogollon-Datil volcanic field: a summary. NM Geol Soc Field Conf Guideb 34:197-204

Osburn GR, Chapin CE (1983b) Nomenclature for Cenozoic rocks of the northeast Mogollon-Datil volcanic field, New Mexico. NM Bur Mines Miner Res Strat Chart 1:1-7

Ratté JC, Gaskill DL (1975) Reconnaisance geologic map of the Gila Wilderness study area, southwestern New Mexico. US Geol Surv, Miscellaneous Investigations I-886, 1:50,000

Ratte JC, Marvin RF, Naeser CW (1984) Calderas and ash-flow tuffs of the Mogollon Mountains. J Geophys Res 89:8713-8732

Ratte JC, McIntosh WC, Houser BB (1989) Geologic map of the Horse Springs West quadrangle. US Geol Surv, Open File Rep 89-210, 1:24,000

Richter DH (1978) Geologic map of the Spring Canyon quadrangle, Catron County, New Mexico. US Geol Surv, Miscellaneous Field Studies MF-966, 1:24,000

Roddick JC (1983) High precision inter calibration of $^{40}Ar/^{39}Ar$ standards. Geochim Cosmochim Acta 47:887-898

Roddick JC, Cliff RA, Rex DC (1980) The evolution of excess argon in Alpine biotites - $^{40}Ar/^{39}Ar$ analysis. Earth Planet Sci Lett 48:185-208

Samson SD, Alexander CE (1987) Calibration of the interlaboratory $^{40}Ar/^{39}Ar$ dating standard, MMhb-1. Isot Geosci 66:27-34

Seager WR, McCurry M (1988) The cogenetic Organ cauldron and batholith, south central New Mexico: evolution of a large-volume ash flow cauldron and its source magma chamber. J Geophys Res 93:4421-4433

Seager WR, Kottlowski FE, Hawley JW (1976) Geology of the Doña Ana Mountains, New Mexico. NM Bur Mines Miner Res Circ 147:1-35

Seager WR, Clemons RE, Hawley JW, Kelley RE (1982) Geology of the northwest part of Las Cruces 1° x 2° sheet, New Mexico. NM Bur Mines Min Res, Geologic Map GM-53, 1:125,000

Snow E, Yund RA (1985) Thermal history of a Bishop Tuff Section as determined from the width of cryptoperthite lamellae. Geology 13:50-53

Turner G (1968) The distribution of potassium and argon in chondrites. In: Ahrens LH (ed) Origin and distribution of the elements. Pergamon, London

Woodard TW (1982) Geology of the Lookout Mountain area, Black Range, Sierra County, New Mexico. MS Dissertation, Univ New Mexico, Albuquerque

Zeitler PK (1987) Argon diffusion in partially outgassed alkali feldspars: insights from $^{40}Ar/^{39}Ar$ analysis. Chem Geol 65:167-181

Ordovician and Silurian Stratotypes of Britain
(R.D. Tucker)

Because the U-Pb dating method has the ability to apply an independent check on the reliability of an age determination, it is an inherently superior method for determining ages of many geological samples. One approach gaining wide appeal, has been to apply the technique to Paleozoic and younger sedimentary strata to obtain absolute ages of the fossils contained therein. Application of the method depends on the presence of widespread eruptive igneous rocks, either explosive Plinian-type air falls or near-vent rhyolitic flows, which serve as reliable time-markers within the stratified sequence. In most felsic eruptive rocks, zircon is the preferred mineral for dating (Samson *et al.* 1990, Tucker *et al.* 1990, Claoué-Long *et al.* 1991) but in rare instances, especially in peraluminous rocks, monazite may be suitable (Roden *et al.* 1990, Oberli and Meier, 1991).

The technique cannot be attempted by all laboratories because of the restrictions previously discussed. Inherited zircon is a common component in many felsic ashes, and the inheritaned component may exist as xenocrysts, detrital grains, or inherited zircon cores in any single grain. Assurances must be made, therefore, that the determined age is reliable and free of age biases resulting from these components and radiogenic Pb-loss. This can best be achieved by replication (at 1-2 Ma resolution) of concordant analyses obtained on ultra-small zircon samples representing the true eruption population.

The lower Paleozoic stratotypes of Great Britain, including the Borderlands, South Wales, and Scotland, provide a unique setting in which separately established frameworks of relative time (graptolites and shelly biostratigraphies) and absolute time (altered volcanic ash beds) can be combined into a common temporal framework (Fig. 5). Nine volcanic ash samples from the Ordovician and Lower Silurian stratotypes of Britain, some of which were previously dated by the zircon and apatite fission-track method (Ross *et al.* 1976, Ross *et al.* 1982), have yielded improved U-Pb zircon ages that are entirely consistent with their known stratigraphic positions. Another sample from the Middle Ordovician (Rocklandian) of the central United States was also dated to determine its absolute positioning within the type Ordovician (British) sequence.

The new zircon ages indicate that significant reproportioning of the Ordovician Period is required (*cf.* McKerrow *et al.* 1985, Odin 1985). The Llandeilo stage, for example, can be no longer than a few (*ca.* 3-4) million years in duration, and the combined duration of the Middle and Late Ordovician epochs is less than half of the entire Ordovician Period. In another case, the volcanic ash from Middle Ordovician (Rocklandian) strata of North America is in excellent age agreement with a Caradocian ash from Britain, demonstrating the age equivalence of the two sedimentary sequences which lack directly comparable fauna. Two of the Silurian ages are the first U-Pb zircon determinations from the stratotype in the Borderlands, and the youngest age of 419.7 ± 2 Ma is from a bentonite in the upper Ludfordian a few meters below the Ludlow - Přídol í boundary.
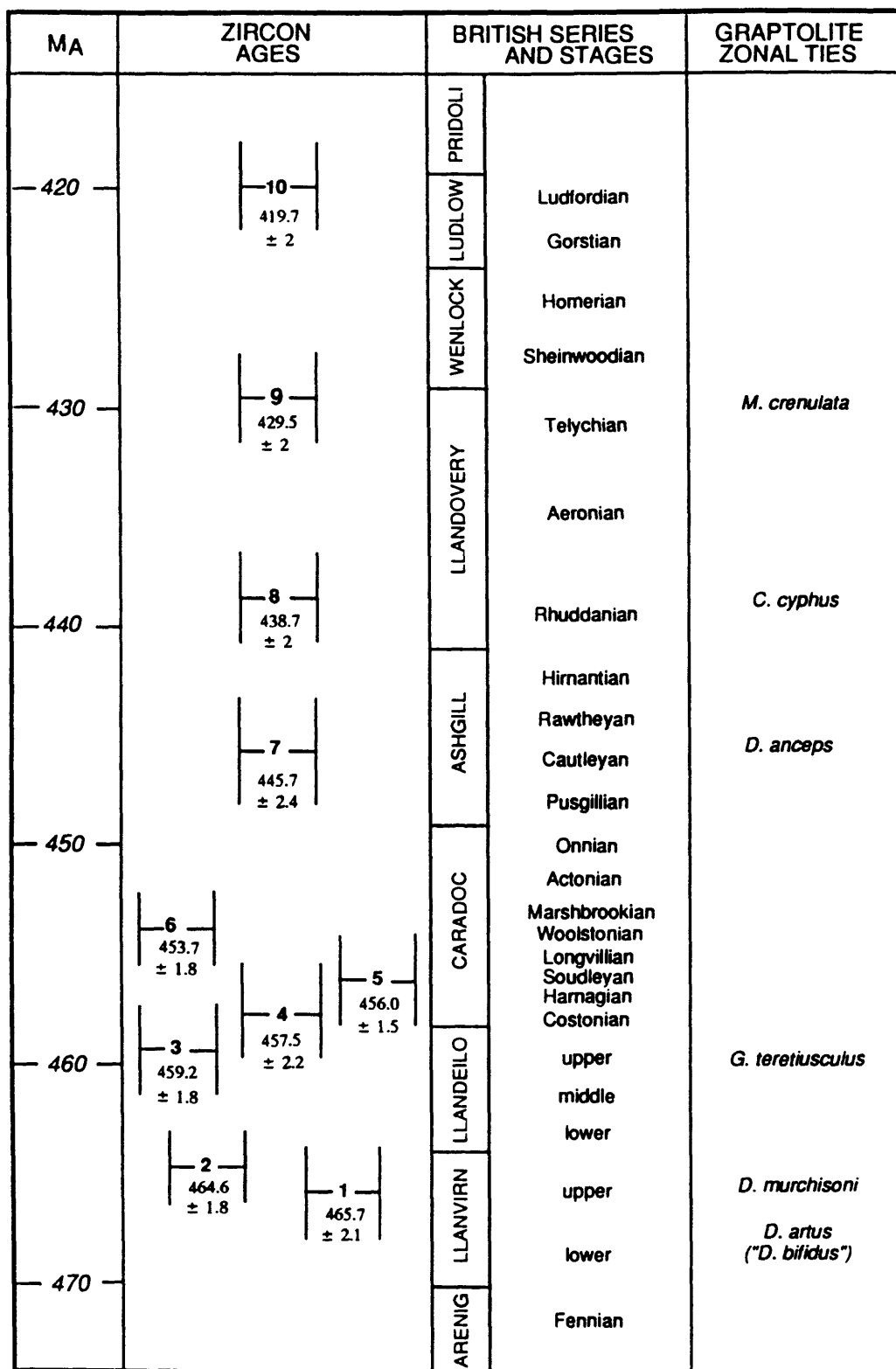
MA	ZIRCON AGES		BRITISH SERIES AND STAGES		GRAPTOLITE ZONAL TIES
— 420 —	—10— 419.7 ± 2		PRIDOLI		
			LUDLOW	Ludfordian Gorstian	
			WENLOCK	Homerian Sheinwoodian	
— 430 —	—9— 429.5 ± 2		LLANDOVERY	Telychian	M. crenulata
				Aeronian	
— 440 —	—8— 438.7 ± 2			Rhuddanian	C. cyphus
	—7— 445.7 ± 2.4		ASHGILL	Hirnantian Rawtheyan Cautleyan Pusgillian	D. anceps
— 450 —			CARADOC	Onnian Actonian Marshbrookian Woolstonian Longvillian Soudleyan Harnagian Costonian	
	—6— 453.7 ± 1.8	—5— 456.0 ± 1.5			
— 460 —	—3— 459.2 ± 1.8	—4— 457.5 ± 2.2	LLANDEILO	upper middle lower	G. teretiusculus
	—2— 464.6 ± 1.8	—1— 465.7 ± 2.1	LLANVIRN	upper lower	D. murchisoni D. artus ("D. bifidus")
— 470 —			ARENIG	Fennian	

FIGURE 5. Absolute age of altered volcanic ash beds in the Ordovician and Silurian stratotypes of England, Wales and Scotland referenced to their series, stages, and graptolite biozones (Tucker *et al.* 1990 and *in prep.*). Also show is the age of the K-bentonite (6) from the Spechts Ferry Shale (Mohawkian Series, Rocklandian Stage) determined as a Middle Ordovician datum in the North American section.

58

II. Uplift/Denudation/Burial

Denudation History of Young Orogens
(P.K. Zeitler)

1. General Comments

    The use of thermochronology to study the unroofing history of mountains belts was pioneered by European workers who applied fission-track dating as well as Rb-Sr and K-Ar dating of micas to the study of Alpine tectonics (Wagner and Reimer, 1972; Purdy and Jäger, 1976; Wagner et al., 1977). Figure 1a shows schematically how mineral cooling ages can be used to constrain tectonic and erosional histories.

    Two main approaches can be taken. First, a series of minerals can be dated from one sample. If the dated minerals have different closure temperatures, it is possible to construct a cooling curve using measured ages together with estimates of closure temperature. The sample's cooling history can be compared to that of other samples for tectonic purposes, or it can be converted to a denudation history in an attempt to constrain the sample's uplift path. The disadvantages of this method are (1) that closure temperatures must be accurately and precisely known in order to make possible a meaningful internal comparison, and (2) that a geothermal gradient must be known or assumed in order translate the cooling history into an unroofing history.

    A second approach is to exploit the fact that samples taken from higher elevations will have older cooling ages because mountain summits should have cooled earlier than the valley floors below them. The advantage of this method is that an apparent unroofing rate can be determined directly from the measured age-elevation gradient, without any need to know either the closure temperature of the system in use, or the geothermal gradient.

    However, it is important to realize some of the assumptions that are made when using either one of these approaches. One major assumption is that conduction has been the dominant mode of heat transfer. In dealing with rocks undergoing metamorphism, dewatering, and melting, this assumption could be questionable. Even if the assumption of conductive heat transfer is valid, large potential troubles continue to loom because of the way in which unroofing perturbs the thermal structure of the crust. Parrish (1982) discussed potential problems in detail; among these are (1) the fact that as uplift and erosion proceed, the near-surface thermal gradient is steepened and made strongly non-linear, (2) the fact that isotherms will respond to abrupt changes in uplift/erosion history only sluggishly, with considerable lag time, and (3) the fact that different isotopic systems closing at different temperatures and thus different crustal levels will respond to an identical uplift/erosion history in different ways. As one example, near-instantaneous uplift and erosion of a block of rock will result in a thermal history that is much more muted and which will not at face value suggest the occurrence of any rapid event. As another example, a thermal history marked by accelerating cooling may actually reflect uplift and erosion of a sample at a constant rate along a steepened, non-linear temperature gradient (Figure 1b).

2. Case Study: Thermochronology of NW Himalaya, Pakistan

    Abstract. Cooling history of the NW Himalaya, Pakistan
    (Zeitler, 1985)

59

INSERT ZEITLER 1985 ABSTRACT HERE

Abstract. Geochronology and temperature history of the Nanga Parbat-Haramosh Massif, Pakistan
(Zeitler et al., 1989)

INSERT ZEITLER ET AL. 1989 ABSTRACT HERE

General comments : Northern Pakistan represents a natural laboratory in which we can examine recent and ongoing tectonic processes associated with collisional orogenesis. The two studies presented here represent an initial, broad-scale reconnaissance using mostly fission-track dating, and a later follow-up study on an area of what appear to exceptionally rapid unroofing rates. A comparison of the two studies, which were conducted at two very different levels of detail, using different thermochronologic systems, demonstrates the different kinds of questions that are both solved and created by such investigations.

Summary of main points:

(1) Apatite fission-track ages show significant regional variations that vary smoothly and generally don't coincide with known structures.

(2) Zircon fission-track ages show significant regional variations, and often vary rapidly, with frequent discontinuities that sometimes coincide with major structures.

(3) Zircon ages "see" the Main Mantle Thrust Suture zone, but apatite ages don't. This implies activity along this structure was underway at about 20 Ma, but had ceased by 15 Ma.

(4) Cooling rates determined both by comparison of dating systems and by age-elevation analysis imply that rates of uplift/erosion to have varied greatly over space and time.

(5) The Nanga Parbat-Haramosh Massif, a "half-window" of Indian-plate Precambrian basement which possesses the greatest continental relief on earth (~ 7 km) is a region of very young ages. Its western boundary is defined by a high-angle reverse fault across which there is a sharp discontinuity in ages as determined by all isotopic systems.

(6) The thermochronological data imply recent denudation rates of at least several mm/yr, and together with metamorphic petrology imply at least 15-20 km of unroofing within no more than 15-20 Ma.

(7) Recent detailed work in the core of the massif, at the base of Nanga Parbat itself, suggests that this area has experienced a very recent metamorphic episode at 3-4 Ma. Some of our new data call into question some of our earlier conclusions based on assumptions about heat transfer within the Nanga Parbat Massif.

COOLING HISTORY OF THE NW HIMALAYA,
PAKISTAN

Peter K. Zeitler[1]

Department of Earth Sciences, Dartmouth
College, Hanover, New Hampshire 03755

Abstract. Fission-track and $^{40}Ar/^{39}Ar$
cooling ages indicate that the late-
Tertiary cooling history of the Himalayan
ranges of northern Pakistan is largely a
function of uplift and erosion. Inter-
pretation of cooling ages which range
from under 0.5 Ma to over 80 Ma suggests
that during the late Tertiary, long-term
uplift rates at least doubled, from under
0.2 mm/yr to in some cases well over 0.5
mm/yr. Uplift rates show strong and sys-
tematic regional variations as well which
reflect the greater uplift of eastern and
northern regions. The association of
very rapid uplift and erosion with the
Nanga Parbat-Haramosh Massif can be
explained by a locally vigorous collision
of India with Eurasia near a promontory
of Indian crust. The resultant rapid
uplift of the Nanga Parbat-Haramosh
Massif reactivated the Main Mantle Thrust
melange zone with a reversed sense of
motion. Discontinuities in the cooling-
age distribution along the Main Mantle
Thrust in the southern Swat-Hazara region
may be the result of the thermal effects
of overthrusting.

[1]Now at Research School of Earth Sci-
ences, Australian National University,
Canberra.

INTRODUCTION

The mountains of northern Pakistan
record the recent and ongoing collision
of India with Eurasia. Situated as they
are astride this major plate boundary,
they offer an opportunity to understand a
number of the diverse phenomena which
characterize continental collision.

As a step toward such understanding, I
wish to summarize here the results of a
fission-track and $^{40}Ar/^{39}Ar$ dating study
of northern Pakistan's thermal history.
Because cooling is an inevitable result
of many geological processes, knowledge
of a region's thermal history offers
insight into its magmatic, metamorphic,
and tectonic evolution. Isotopic methods
can provide this knowledge, because the
dating of mineral separates is in essence
a form of geothermometry. This follows
from the fact that each dateable phase
within each isotopic system can be
assigned a characteristic closure tem-
perature below which daughter products
are no longer lost [Dodson, 1973, 1979].
Thus, using the $^{40}Ar/^{39}Ar$ method on horn-
blende and micas and the fission-track
method on zircon and apatite, a rock's
thermal history can be sampled at tem-
peratures of roughly 500°C, 300°C, 200°C,
and 100°C, respectively.

Geochronology and temperature history of the Nanga Parbat-Haramosh Massif, Pakistan

Peter K. Zeitler*
Research School of Earth Sciences, Australian National University, GPO Box 4, Canberra, ACT 2601, Australia
John F. Sutter
U.S. Geological Survey, National Center, Reston, Virginia 22092
Ian S. Williams
Research School of Earth Sciences, Australian National University, GPO Box 4, Canberra, ACT 2601, Australia
Robert Zartman
U.S. Geological Survey, Box 25046, Denver Federal Center, Denver, Colorado 80225
R.A.K. Tahirkheli
Center of Excellence in Geology, University of Peshawar, Peshawar, NWFP, Pakistan

ABSTRACT

The gneisses of the Nanga Parbat-Haramosh Massif (NPHM), Pakistan, experienced peak metamorphic temperatures in the interval from 25 to 30 Ma, as revealed by $^{40}Ar/^{39}Ar$ cooling ages of hornblende and the ages of the youngest intrusions of the Kohistan batholith located immediately adjacent to the NPHM. $^{40}Ar/^{39}Ar$ and fission-track mineral ages indicate that the postmetamorphic cooling history of the NPHM has been controlled over the past 5 to 10 m.y. by active tectonism associated with the Raikhot Fault, although passive uplift and erosion in response to overthrusting of the NPHM by the Kohistan Arc has been underway as well. Net cooling rates for NPHM gneisses exposed today along the Indus River at low elevations have accelerated, from 20°C/m.y. at ~20 Ma to 300°C/m.y. at 0 to 0.4 Ma. Following emplacement of aplite dikes at about 30 to 35 Ma, portions of the Kohistan Batholith adjacent to the NPHM experienced cooling rates similar to the NPHM of about 20°C/m.y. over the period 25 to 10 Ma, but the net cooling rates for the batholith of ~30°C/m.y. over the past 10 m.y. have been much lower than those experienced within the NPHM. Ion microprobe and conventional U/Pb analyses of zircon show that the protoliths for the Iskere Gneiss and the structurally lower Shengus Gneiss of the NPHM are, respectively, ~1850 Ma and 400 to 500 Ma in age. Zircons from the Iskere Gneiss have thin, relatively high U rims that yield ages from 2.3 to 11 Ma. These rims indicate that metamorphism of the NPHM gneisses is Tertiary, not Precambrian, in age. The ages and Concordia systematics of analyses of Shengus Gneiss zircons suggest that this gneiss may be a metamorphosed equivalent of the Mansehra Granite and other Paleozoic S-type granites found throughout the Himalaya.
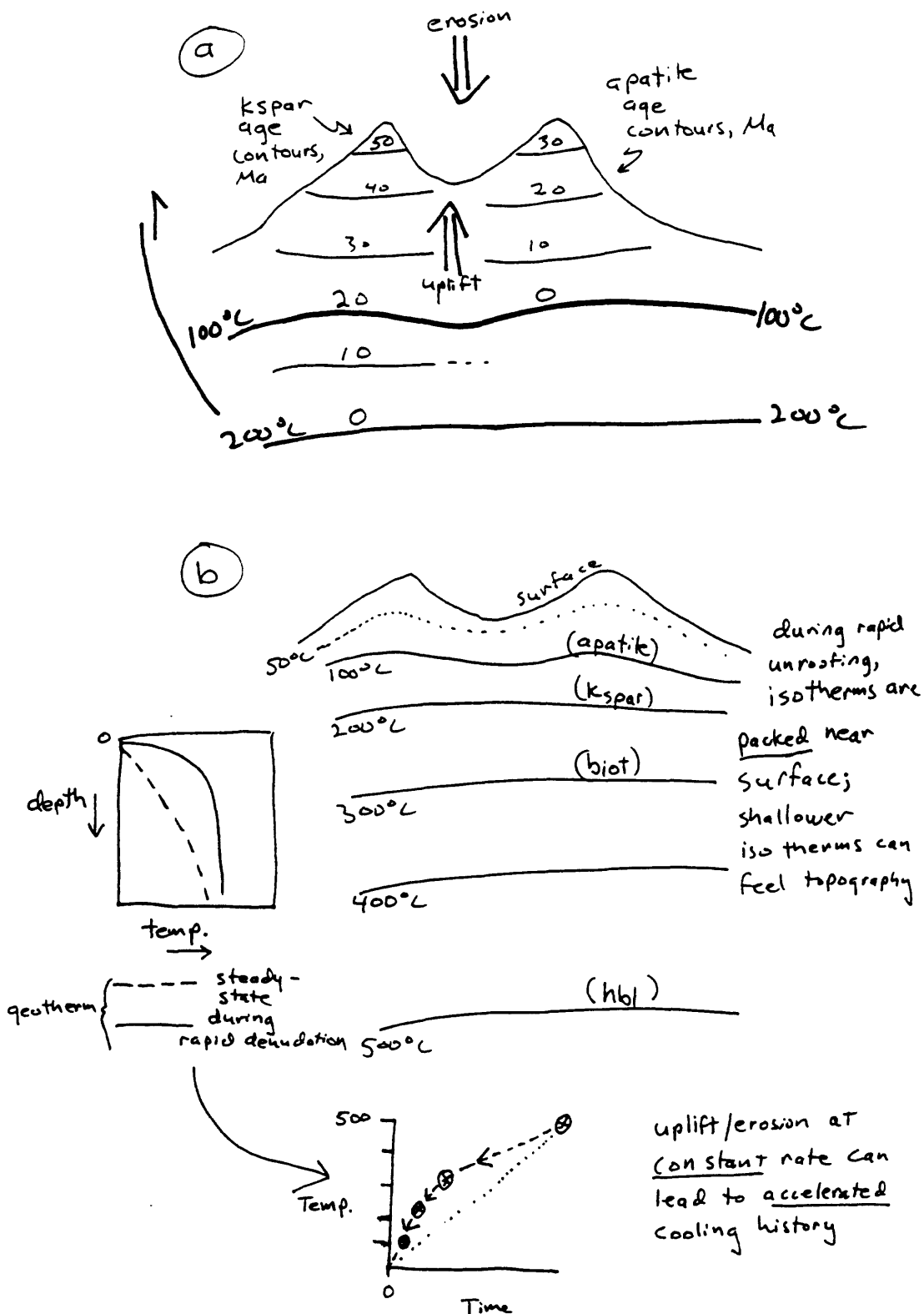
INTRODUCTION

The Nanga Parbat-Haramosh Massif lies within the Himalayan chain's northwestern syntaxis, at the focus of the great orogenic knot defined by the ranges of central Asia. A portion of the Indian plate comprising mostly high-grade metamorphic rocks, the Nanga Parbat-Haramosh Massif (hereafter referred to as NPHM), juts with anomalous north-south strike from the foothills of the Himalaya toward the Karakorum (Fig. 1). It contains the mountain Nanga Parbat (8,126 m), which together with the Indus River, serves to define the greatest continental relief on Earth (~7,000 m).

Present address: Department of Geological Sciences, Williams Hall 31, Lehigh University, Bethelem, Pennsylvania 18015-3188.

3. References

Butler, R.W.H.; and Prior, D.J., 1988, Tectonic controls on the uplift of the Nanga Parbat Massif, Pakistan Himalayas: Nature, v. 333, p. 247-250.

Chamberlain, C. P., Zeitler, P. K., and Jan, M. Q., 1987, Pressure-temperature-time paths in the Nanga Parbat Massif: Constraints on the tectonic development of the northwest Himalayas. In: Malinconico, L. L. and Lillie, R. J. (eds.) Tectonics of the Western Himalaya, Geological Society of America Special Paper 232, p. 23-32.

Coward, M. P.; Jan, M.; Rex, D.; Tarney, J.; Thirwall, M.; and Windley, B. F., 1982, Geotectonic framework of the Himalaya of northern Pakistan: Journal of Geological Society of London, v. 139, p. 299-308.

Chamberlain, C.P., Zeitler, P.K., and Erickson, E., 1991, Constraints on the tectonic evolution of the northwestern Himalaya from geochronologic and petrologic studies of the Babusar Pass, Pakistan. Journal of Geology, in press.

Parrish, R. R., 1982, Cenozoic thermal and tectonic history of the Coast Mountains of British Columbia as revealed by fission-track and geological data and quantitative thermal models. Unpublished Ph.D. thesis, University of British Columbia, Vancouver.

Smith, H.A.; Chamberlain, C.P.; and Zeitler, P.K., 1990, Young monazite U-Pb ages from schists in the Nanga Parbat Syntaxis, Himalayas, northwestern Pakistan (abstr.): Geological Society of America Abstracts with Programs, v. 22, p. A97.

Tahirkheli, R. A. K., Mattauer, M., Proust, F., and Tapponier, P., 1979, The India-Eurasia suture zone in northern Pakistan: Some new data for an interpretation at plate scale, in Farah, A., and De Jong, K. A., eds., Geodynamics of Pakistan: Quetta, Geological Survey of Pakistan, p. 125-130.

Wagner, G. A. & Reimer, G. M. 1972, Fission-track tectonics: the tectonic interpretation of fission-track apatite ages. Earth and Planetary Science Letters, v. 14, p. 263-268.

Wagner, G. A., Reimer, G. M. & Jäger, E. 1977, Cooling ages derived by apatite fission track, mica Rb-Sr and K-Ar dating: the uplift and cooling history of the Central Alps. Memoir of the Institute of Geology and Petrology of the University of Padova, v. 30, p. 1-27

Zeitler, P. K., 1983, Uplift and cooling history of the NW Himalaya, northern Pakistan--evidence from fission-track and ^{40}Ar/^{39}Ar cooling ages: Unpublished Ph.D. thesis, Dartmouth College (Hanover, NW).

Zeitler, P. K., 1985, Cooling history of the NW Himalaya: Tectonics, v. 4, p. 127-151.

Zeitler, P. K., and Chamberlain, C. P., 1991, Petrogenetic and tectonic significance of young leucogranites from the northwestern Himalaya, Pakistan: Tectonics, v. 10, p. 729-741.

Zeitler, P. K., Sutter, J. F., Williams, I. S., Zartman, R. E. & Tahirkheli, R. A. K., 1989, Geochronology and temperature history of the Nanga Parbat-Haramosh Massif, Pakistan. In: Malinconico, L. L. and Lillie, R. J. (eds.) Tectonics of the Western Himalaya, Geological Society of America Special Paper 232, p. 1-22.

Zeitler, P. K. and Chamberlain, C. P., 1991, Quaternary anatexis at Nanga Parbat, Pakistan (abstract). Geological Society of America Abstracts with Programs, v. 23, p. A135.

(a)

erosion

kspar age contours, Ma

apatite age contours, Ma

50   30

40   20

3.   10

uplift

20   0

100°C   100°C

10   - - -

200°C   0   200°C

(b)

surface

50°C   (apatite)   during rapid unroofing, isotherms are packed near surface; shallower isotherms can feel topography

100°C

(kspar)

200°C

(biot)

300°C

400°C

depth

temp.

geotherm { - - - - steady-state   (hbl)
         during rapid denudation   500°C

500

Temp.

0   Time

uplift/erosion at constant rate can lead to accelerated cooling history

1. Cartoon showing relationship between denudation and cooling ages. (a) Relationship between cooling ages and topography: older ages are found at higher elevations. (b) Influence of rapid denudation on geotherm and consequences for cooling histories derived from thermochronology. Rapid uplift packs isotherms near the surface (because hot rock is moving towards the surface faster than heat can conduct), creating a strongly non-linear geotherm (the effect is proportional to the velocity of the uplift). Note that uplift is used here to refer to motion of rock towards the surface, not increase in surface elevation.

64
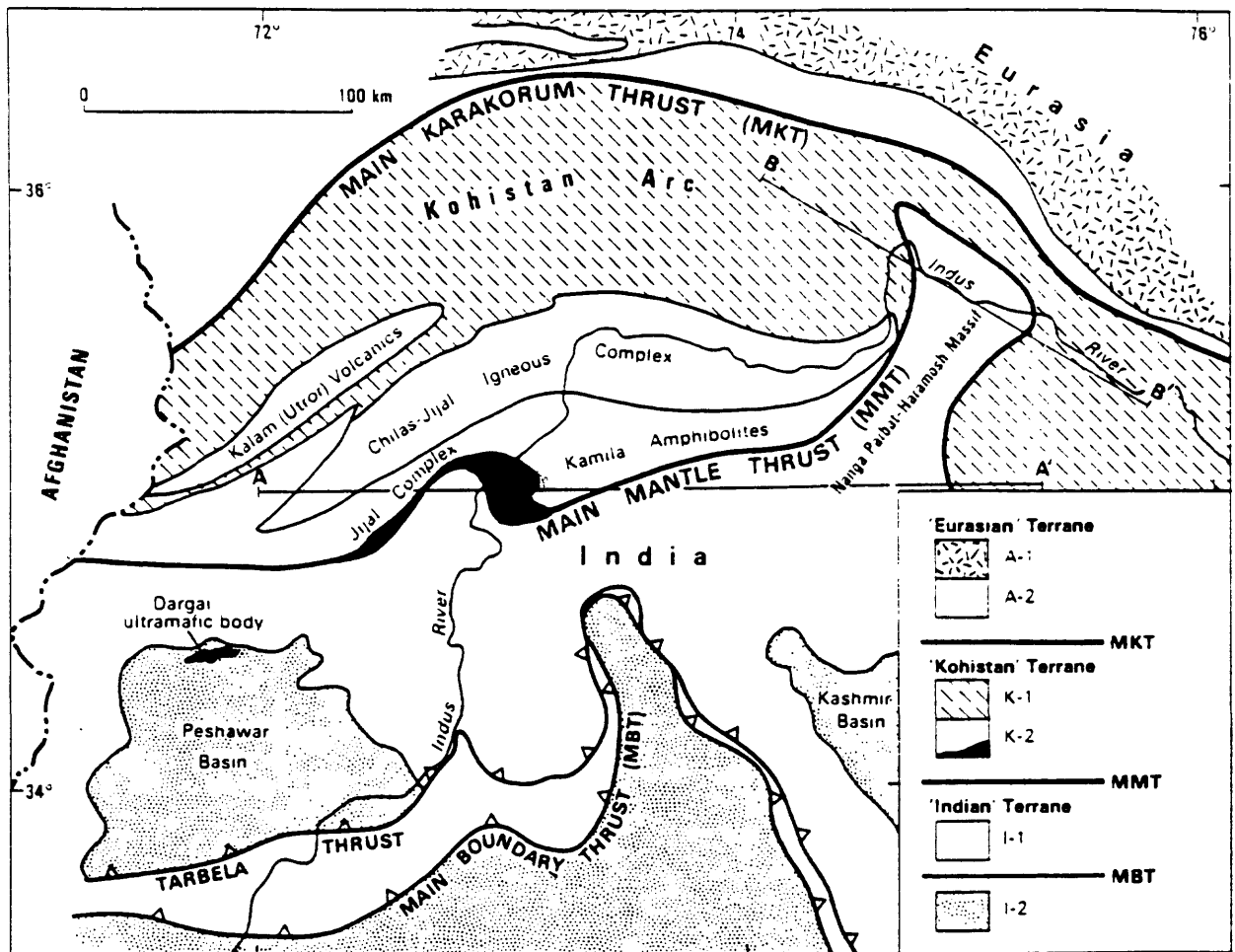
2. Sketch map of the NW Himalaya in Pakistan (from Zeitler, 1985). Two sutures (the Main Mantle Thrust (south) and the Main Karakorum Thrust (north) divide the region into three terranes: the Indian plate (south), the Kohistan island-arc terrane, and the Asian plate (north). Note also the prominent northward-projecting region of the Indian plate, called the Nanga Parbat-Haramosh Massif. A–1, Karakorum Batholith (late Cretaceous to Early Tertiary); A–2, pelitic metasedimentary rocks (Precambrian to lower Paleozoic). K–1, intermediate to felsic intrusives, volcanics (Utror Volcanics shown in white), sediments, metasediments and metavolcanics (largely Cretaceous to Early Tertiary); K–2, igneous and metaigneous rocks (Cretaceous). The Chilas-Jijal Complex comprises mafic, pyroxene-granulite facies layered intrusives. The unit shown in black is the Jijal Ultramafic Complex. I–1, granites and granite gneisses (Precambrian; early Cambrian augen gneisses are common; several small Carboniferous alkaline intrusions are also present); I–2, Neogene molasse sediments of the Rawalpindi and Siwalik Groups, and basin fills of the Peshawar and Kashmir intermontane basins.

65
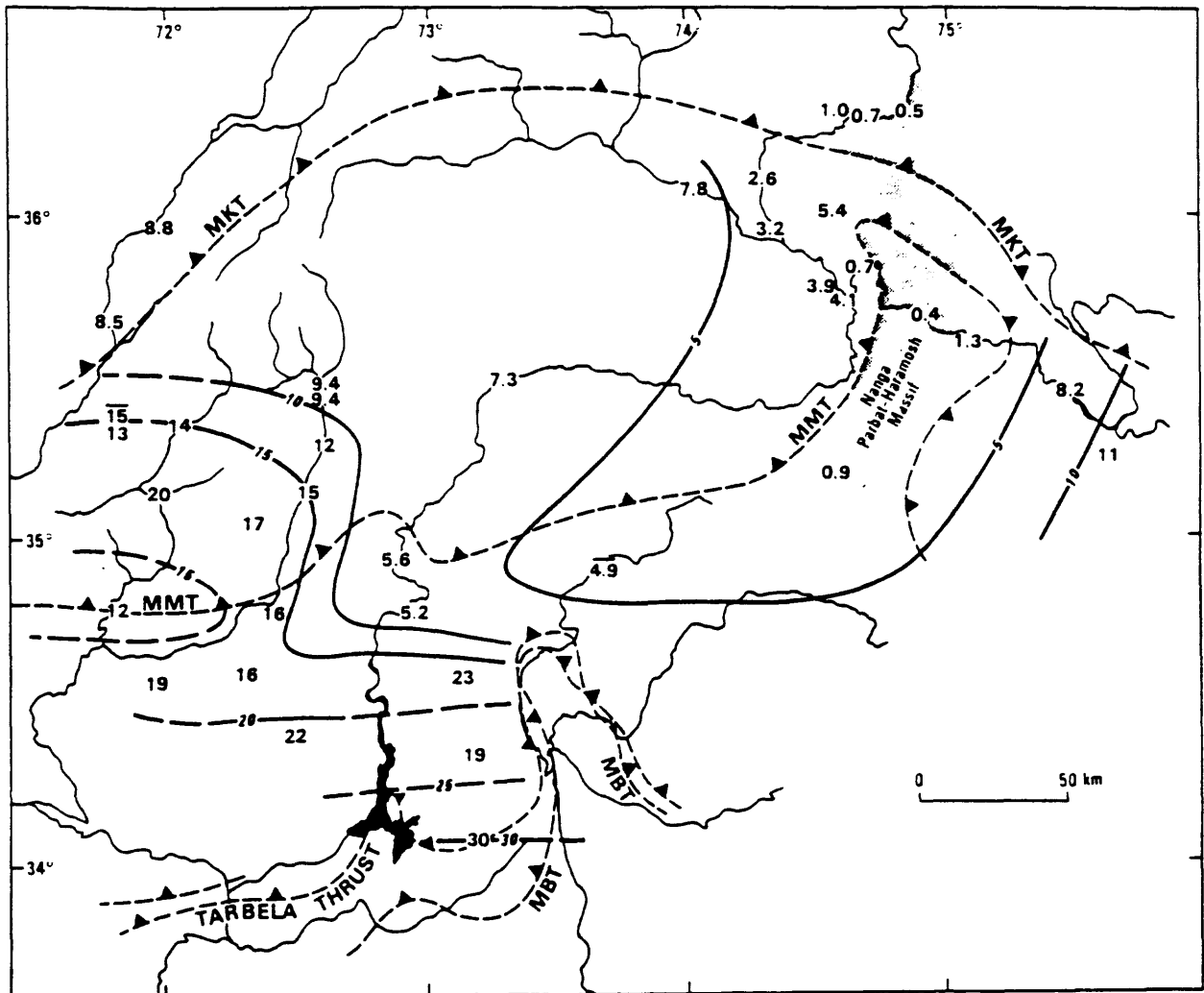
3. Apatite fission-track ages of samples taken from low elevations (local base level). Contour interval is 5 Ma. Note that the smooth variation in apatite ages does not seem to be offset by structures, with the exception of the Nanga Parbat-Haramosh Massif. Note also that there is no apparent discontinuity across the Main Mantle Thrust (southern suture).

66
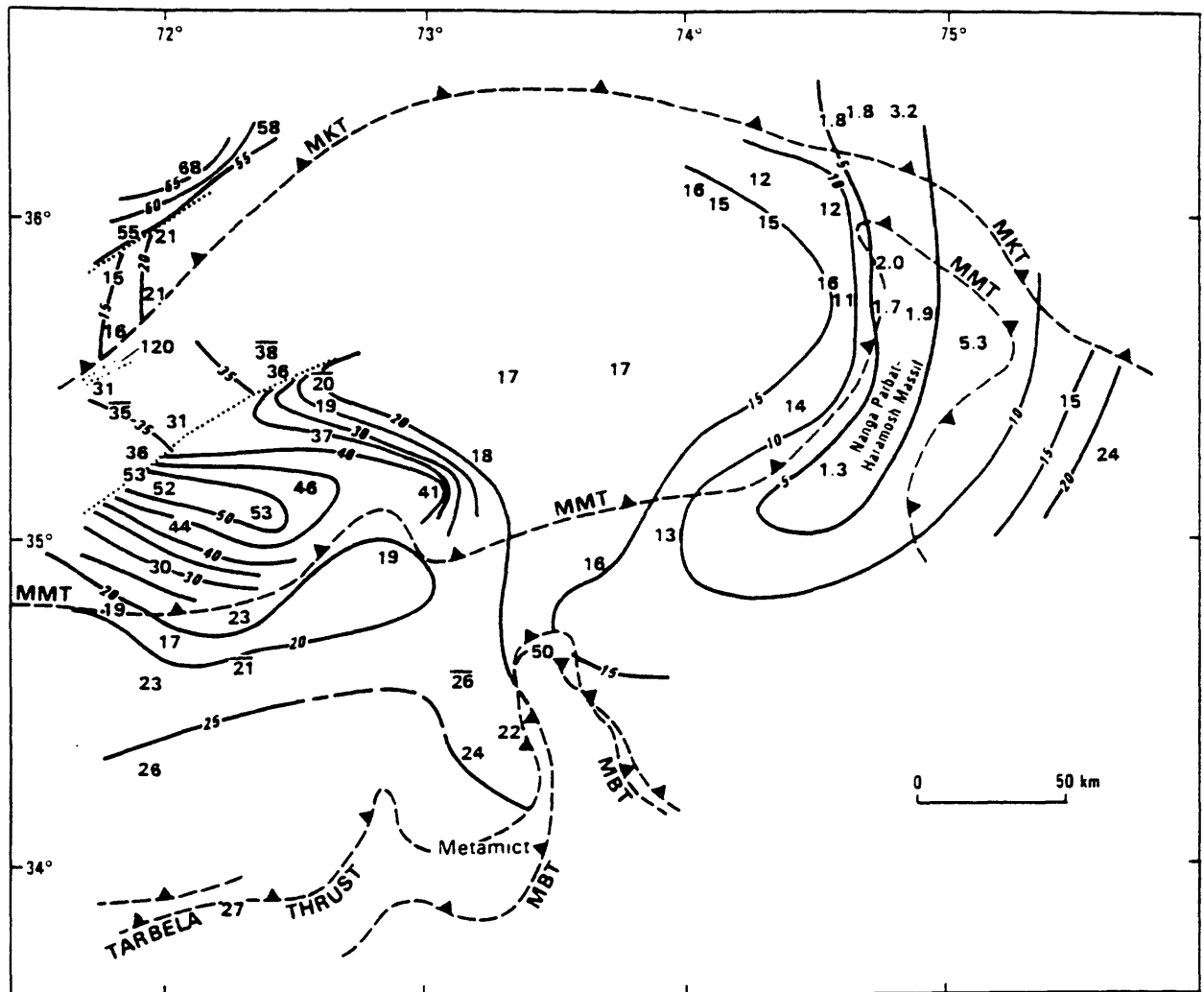
4. Zircon fission-track ages of samples taken from low elevations (local base level). Contour interval is 5 Ma. The dotted lines highlight discontinuities in age. In contrast to the pattern in apatite ages, variations in zircon fission-track age correlate much more strongly with structure and lithology. The geology of northern Pakistan suggests that the region has been differentially uplifted, with western areas underlain by a variety of supracrustal rocks and eastern regions underlain by basement rocks; the zircon results are consistent with there having been less denudation in the west. Note that there is a discontinuity in zircon ages across the Main Mantle Thrust in western areas which does not seem to be present farther to the east. Along the western boundary of the Nanga Parbat-Haramosh Massif, the polarity of this age discontinuity is reversed.

67
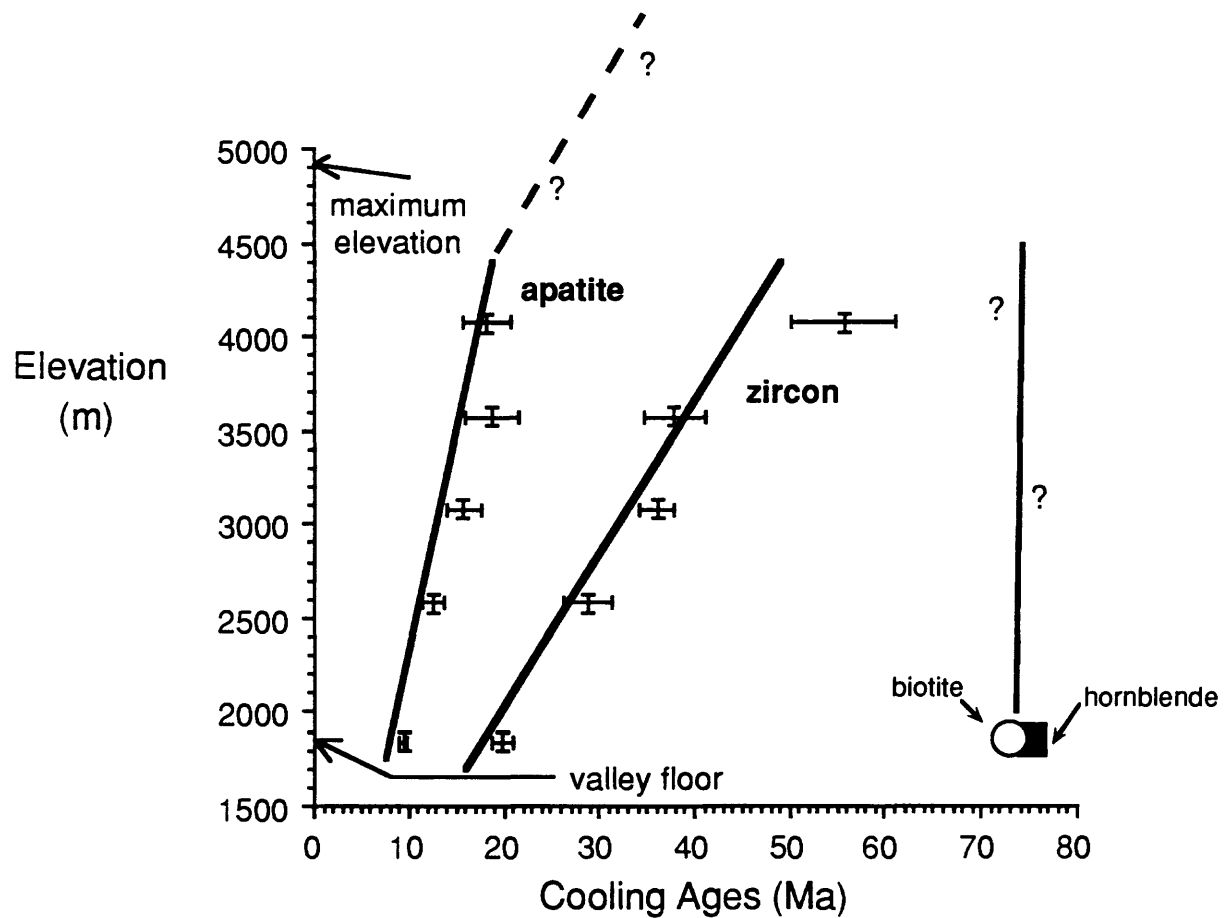
5. Variation of fission-track ages with elevation, northern Swat Valley (located in the west-central portion of the Kohistan terrane). At face value, the apatite and zircon results suggest unroofing rates of 0.22±0.07 and 0.08±0.009 mm/yr, respectively. The biotite and hornblende results date the age of the tonalitic pluton underlying the ridge that was sampled.

6 8
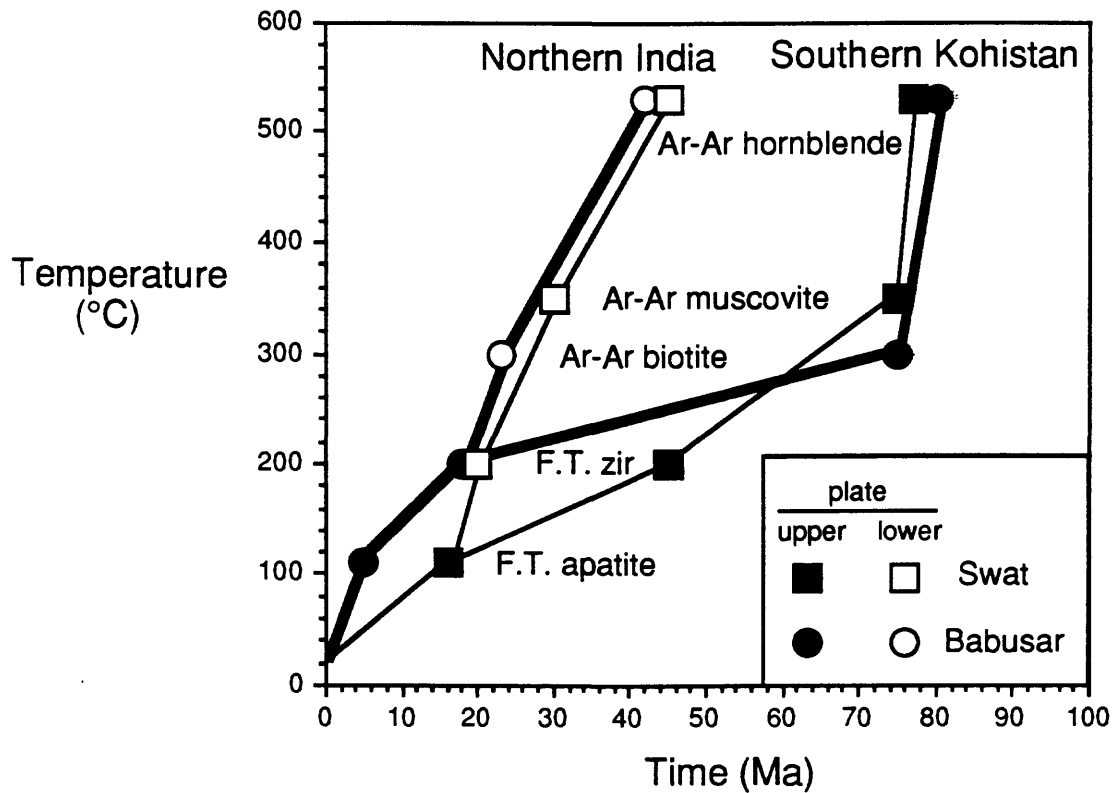
6. Net cooling curves for localities on the Indian plate and Kohistan terrane that are closely juxtaposed across the Main Mantle Thrust. Results from two regions are shown: near the Swat valley (a western area) and in the vicinity of Babusar Pass (an area 50 km SW of Nanga Parbat). Note that for both regions, the thermal histories of the two terranes become shared at about 15-20 Ma and is divergent before that time. What is different about the two regions is the closure isotherm (=crustal level?) at which this convergence of thermal histories is recorded. At Babusar, similar zircon ages are common to both terranes but biotite ages are very different; at Swat, apatite ages are similar but zircon ages are different.

69
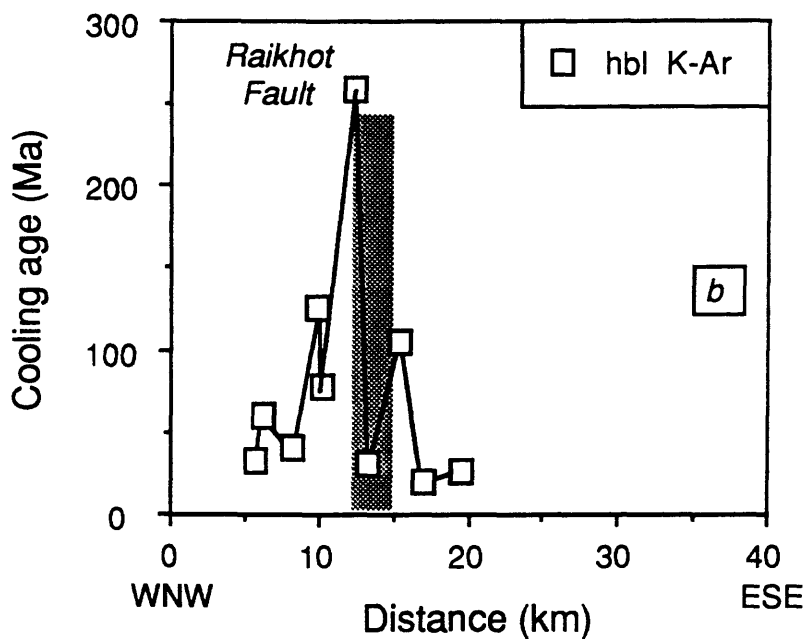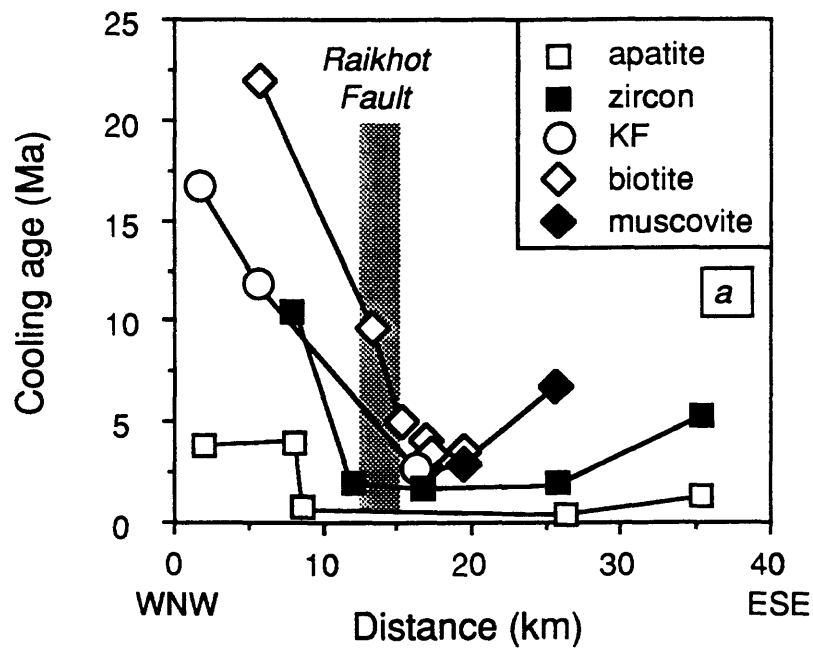
7. Cooling-age profile across the western boundary of the Nanga Parbat-Haramosh Massif. (a) Lower-temperature thermochronometers. There is about a sevenfold difference in ages across the Raikhot Fault. (b) Amphibole ages. These ages reflect incorporation of excess ^{40}Ar—it appears that the Raikhot Fault zone, a major and active ductile shear zone, has served as a conduit for metamorphic fluids, one of which is ^{40}Ar.
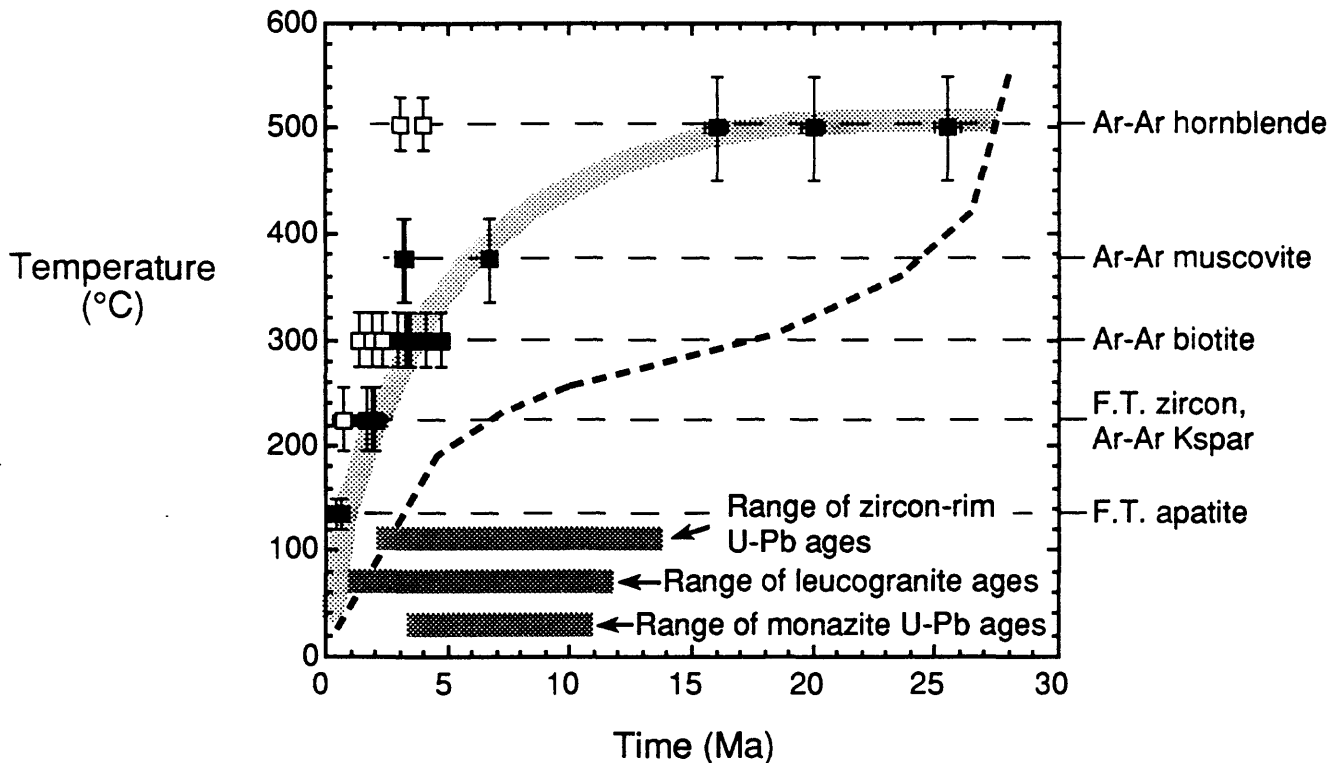
8. General thermal history of the Nanga Parbat-Haramosh Massif. The strongly non-linear cooling history could be explained by fairly constant denudation at rates of 1 mm/yr or higher, although the very youngest ages suggest some acceleration of denudation rate. Open symbols are for recent results from the Tato River section at the base of Nanga Parbat itself; there is evidence here for very young igneous activity and metamorphism in the range 1-4 Ma. This raises the question as to how much of the thermal history seen elsewhere at Nanga Parbat is due to denudation, and how much might be due to a thermal overprint centered on the core of the massif.

7-1

Blank

.

U-Pb Dating in the Scandinavian Caledonides
(R.D. Tucker)

The Caledonides of Norway are a fascinating orogenic belt in three respects: 1) they are characterized by exceedingly far-travelled nappe units which form a near-continuous sequence along strike for over 1,000 km, 2) the vertical succession of nappes (tectonostratigraphy) is remarkably consistent along the length of the belt, having been only locally broken and disrupted by faults and shear zones, unlike their counterparts in East Greenland, and 3) the orogen is characterized by a deep level of erosion, particularly along the west coast, which exposes a number of windows and culminations through the nappes into underlying Proterozoic gneisses of the former Baltoscandian Shield. In this lowest structural level of the tectonostratigraphy, metamorphosed high-P mafic rocks (internal and external eclogites, as well as garnet peridotites) are exposed which attest to the high-pressure metamorphism attained in the lowest structural plate during continental collision approximately 400 m.y. ago.

Detailed mapping in the largest and southernmost of these gneissic terranes reveals that the exposure is not a simple window but rather a structural culmination exposing Proterozoic gneisses and a deeply infolded and progressively metamorphosed sequence of rocks identical to the nappe stratigraphy of the eastern foreland sequence. This terrane, termed the Western Gneiss Region (WGR), has been a classic area for metamorphic (Eskola 1921, Ramberg 1943) and structural studies (Hansen 1971) for over 75 years, and has proved to be a remarkable natural laboratory for documenting Pb-diffusion in zircon, baddeleyite, particularly titanite (Tucker *et al.* 1987, Tucker *et al.* 1991).

Geologic Setting

Figure 6 is a generalized geological map of the northern part of the WGR, showing the distribution of metamorphosed supracrustal nappe units (locally containing *ca.* 480 Ma volcanic rocks) together with undivided Proterozoic gneissic rocks. Throughout the area of Figure 6, Caledonian reworking was pervasive and intense enough to produce a Pennine-style arrangements of bedrock units involving km-scale recumbent fold- and thrust nappes (here, involving Proterozoic gneisses) that are themselves refolded by three and locally four phases of recumbent and upright folds. In the east where Caledonian folding is least complex, the metamorphic grade is at greenschist facies, whereas, in the west, regional metamorphism is amphibolite facies retrogressive from eclogite facies. Indeed, field observations and published thermo-barometry (Krogh 1980, Griffin *et al.* 1985) are consistent with a model of westward subduction (present-day direction) of the WGR under Laurentia (Greenland) near end Silurian time, consistent with Sm-Nd ages of the 'external' eclogites dated throughout the WGR (Krogh *et al.* 1974, Griffin and Brueckner 1980, 1985, Gebauer *et al.* 1985, Mearns 1986, Mørk and Mearns 1986). Following partial continental subduction, mineralogical and isotopic disequilibrium was quenched-in by rapid uplift of the WGR, possibly along a continental-scale detachment fault presently situated southeast of the islands of Hitra and Smøla, and the Fosen peninsula (Figure 6, Tucker and Krogh 1986).

In the northern part of the WGR, garnet-bearing dolerites, and gabbros commonly bear coronitic textures reflecting their incomplete transformation to eclogite (Mørk 1985). These bodies appear as mafic dikes and sills several tens of meters thick, commonly boudinaged and broken up, but with locally developed granophyric patches produced *in situ* igneous differentation. One such rock near Selsnes was selected for U-Pb geochronology in order to ascertain the time of mafic dike emplacement and coronite formation. In addition, a sample of garnet-orthopyroxene eclogite from Hareidland, in the district of Stadt, was redated (from the sample of Krogh *et al.* 1974) to compare and contrast the time of zircon formation in eclogite and gabbro coronite in two related but widely separated rocks of the WGR.

Metamorphic Growth of Zircon and the Response of Baddeleyite and Zircon to a Pb-Diffusion Event

From the coronitic gabbro near Selsnes, two varieties of zircon were recovered as well as a population of baddeleyite (monoclinic ZrO_2) exhibiting unusual morphological characteristics (Figs. 7 a and b). The baddeleyite in the coronitic gabbro occurs in two forms: brown striated plates free of adhered grains, and brown plates overgrown by microcrystalline zircon (*cf.* Fig. 6 and Davidson and van Breemen, 1988). Also, zircon occurs in two forms: clear slightly cracked skeletal crystals, and as a microcrystalline variety commonly (but not always always) replacing baddeleyite (Fig. 7b). Optical petrography and scanning electron microscopy of the latter type of baddeleyite clearly demonstrates: 1) the monoclinic habit of microcrystalline aggregates, 2) the presence of twinned baddeleyite with surrounding untwinned zircon aggregrate, and 3) the presence of faceted zircon 'pegs' projecting into baddeleyite (and *vice versa*), indicating that zircon is not an additive growth on baddeleyite but a partial replacement of it.

Isotopic analyses performed on all varieties of baddeleyite and zircon (Fig. 8) demonstrate clear age differences between them, indicating that metamorphism of the gabbro postdated significantly the crystallization of the magma. Skeletal zircon and prismatic baddeleyite, which represent primary igneous minerals, are least discordant from the upper intercept age of 1462 ± 2 Ma, interpreted as the time of dike emplacement and igneous crystallization of the gabbro protolith. Replicate analyses of both minerals suggest only small degrees of Pb-loss (*ca.* 12%), and baddeleyite and zircon exhibit comparable amounts of radiogenic-Pb loss.

Near the lower age intercept at *ca.* 401 ± 2 Ma, microcrystalline zircon is slightly discordant with a [207]Pb/[206]Pb age of 425 Ma which might be because of incorporation of radiogenic initial-Pb or minute amounts (< 1%) of primary baddeleyite enclosed within the minerals analyzed. The lower intercept age is thus interpreted as the time of new zircon growth around primary baddeleyite, and presumably the time of coronitic mineral growth in the metagabbro. Predictably, the fraction of consisting of mixtures of baddeleyite and zircon plots on a mixing line between 1462 Ma and 401 Ma, and the amount of end-member components present in the multigrain fraction may be estimated by use of the lever rule.

Previous efforts to date the formation of eclogites have utilized the Sm-Nd mineral isochron method (Griffin and Brueckner 1980, Mearns 1986, Mørk and Mearns

1986) or the U-Pb zircon method (Krogh *et al.* 1974, Gebauer *et al.* 1985) with general agreement of about 430-400 Ma. Most of the Sm-Nd determinations were done on clinopyroxene-garnet pairs suggesting formation ages of around 425 ± 25 Ma, although one sample yielded a cate of *ca.* 880 Ma which was interpreted as having two generations of garnet. In fact, detailed petrographic work where done (Mørk and Mearns 1986) indicates that eclogite and protolith olivine gabbro are quite mineralogically complex, and that replicate Sm-Nd isochron ages are difficult to achieve. Moreover, as the abundance of Sm and Nd in omphacite and garnet are typically quite low (< 4-1 ppm), large multigrain fractions are required for analysis, which imposes the added difficulty of having to analyze 5-100 mg multigrain mineral fractions, possibly with significant amounts of included mineral phases.

Zircon from the Hareidland eclogite was earlier analyzed by Krogh *et al.* (1974) which were reported to contain inclusions of omphacite (Jd = 35-40), rutile, and quartz, but not sedondary minerals common in the eclogite. A preliminary age of 401 ± 20 Ma was reported based on the $^{206}Pb/^{238}U$ age from the largest sample analyzed (*ca.* 5 mg), and a maximum age of 600 ± 100 Ma is indicated by a rather imprecise $^{207}Pb/^{206}Pb$ age. Four multigrain fractions of zircon (0.7-0.4 mg) yielded replicate, concordant analyses (Fig. 7b) defining an age of 401 ± 2 Ma. The Hareidland zircons are low in U (< 50 ppm), low in Th relative to U (Th/U = 0.02; typical of metamorphic zircon), and have a morphology characteristic of metamorphic zircon, namely clear, colorless, multifaceted, and equant.

Petrographic observations, SEM imaging, and precise U-Pb geochronology thus indicate that synchronous growth of metamorphic zircon in mafic precursors, probably by different metamorphic reactions, but presumably in response to the same high-pressure event. The recovery of both primary skeletal zircon and baddeleyite in the same sample allows for a comparative test of the response of baddeleyite and zircon to a short-lived metamorphic event; the data suggest that baddeleyite and zircon lost nearly equal amounts of radiogenic-Pb during the diffusion event, each about 12% of their radiogenic-Pb budget. Interestingly, the reactions producing microcrystalline zircon from igneous baddeleyite were probably domainal, at a scale of a few mm, because some baddeleyite grains were completely replaced, others only partially replaced, and a few were totally replaced in the transformation to metamorphic zircon (Fig. 7a). The reaction resulting in the replacement of baddeleyite to zircon in the coronitic gabbro was probably,

$$2 \, ZrO_2 + Si = ZrSiO_4 + Zr$$

which suggests that the replacement was in response to increased local silica activity, possibly because of the breakdown of igneous plagioclase, olivine, or clinopyroxene, or any of the corona-forming silicates. Moreover, the synchroneity of the zircon-producing event across a wide area (and see below) suggests that the zircon-producing (and eclogite-forming) event was relatively short-lived and in fair agreement with the Sm-Nd mineral isochron age.

75

Titanite as a Indicator of Rapid, Tectonic Burial and Uplift

To determine the response of zircon, titanite, and monazite to the Caledonian metamorhpic event, a variety of gneissic rocks ranging in composition from gabbro to granite (most are tonalite) were sampled from throughout the WGR across the regional metamorphic gradient (Fig. 6). Many of the orthogneisses contain two types of titanite (distinguishable by optical inspection) that are very different in their isotopic compositions. One type, comprising clear, faceted, and generally inclusion-free titanite, is concordant in nearly all cases at *ca.* 395 Ma, whereas the other type, comprising dark-brown turbid titanite, commonly contained as cores within clear faceted, titanite has grossly discordant and older U-Pb ages. Multi- and single-grain analyses of dark-brown titanite from 38 gneissic rocks across the Caledonian field gradient are evenly distributed along a single discordia with intercepts of 1657 ±3 Ma (upper intercept) and 395 ±2 Ma (lower intercept; Fig. 9). These intercept ages are known to be the times of igneous emplacement and profound metamorphic resetting (respectively) of the orthogneisses on the basis of detailed zircon, metamorphic monazite, and clear-faceted titanite dating throughout the region (Tucker *et al.* 1987, 1991).

The extent of age discordance shown by the dark titanites varies systematically with the degree of Caledonian metamorphism: at lowest greenschist-facies grade dark-brown titanites are least discordant from their primary age (1657 Ma), and at highest metamorphic grade (amphibolite-facies) they are most discordant or entirely reset (at *ca.* 395 Ma; Fig. 6). Comparison of the response of titanite to zircon across the region, indicates that zircon is comparatively more discordant than titanite at lowest metamorphic grades, but achieves a threshold of *ca.* 30% discordance (for highest-quality grains) at low amphibolite-facies where titanite is totally reset (or nearly so) under the same conditions.

Figure 6 is best interpreted as an oblique and elongated crustal cross-section - wherein to the southwest, in deep structural levels, rocks are at amphibolite-facies grade, and to the northeast, in shallow structural levels, rocks are at upper greenschist-facies grade. The fact that titanites from all crustal levels regress to single discordia line implies that the onset of Caledonian metamorphism, as recorded in titanite, occurred at approximately the same time throughout this section of the crust, and that both deep- and shallow-level rocks cooled at nearly the same time. These data thus suggest that a thick portion of the former Baltoscandian shield, together with a stacked-up assembly of nappe units, was depressed, heated to a range of temperatures above the closure-temperature of titanite, and cooled almost synchronously, and that the period of Pb-diffusion through titanite (the partial retention interval) was on the order of the uncertainty of the lower intercept age (*ca.* 4 Ma). The area is thus a remarkable, natural laboratory that is ideally suited for studying the diffusive loss of Pb in established geochronometers.
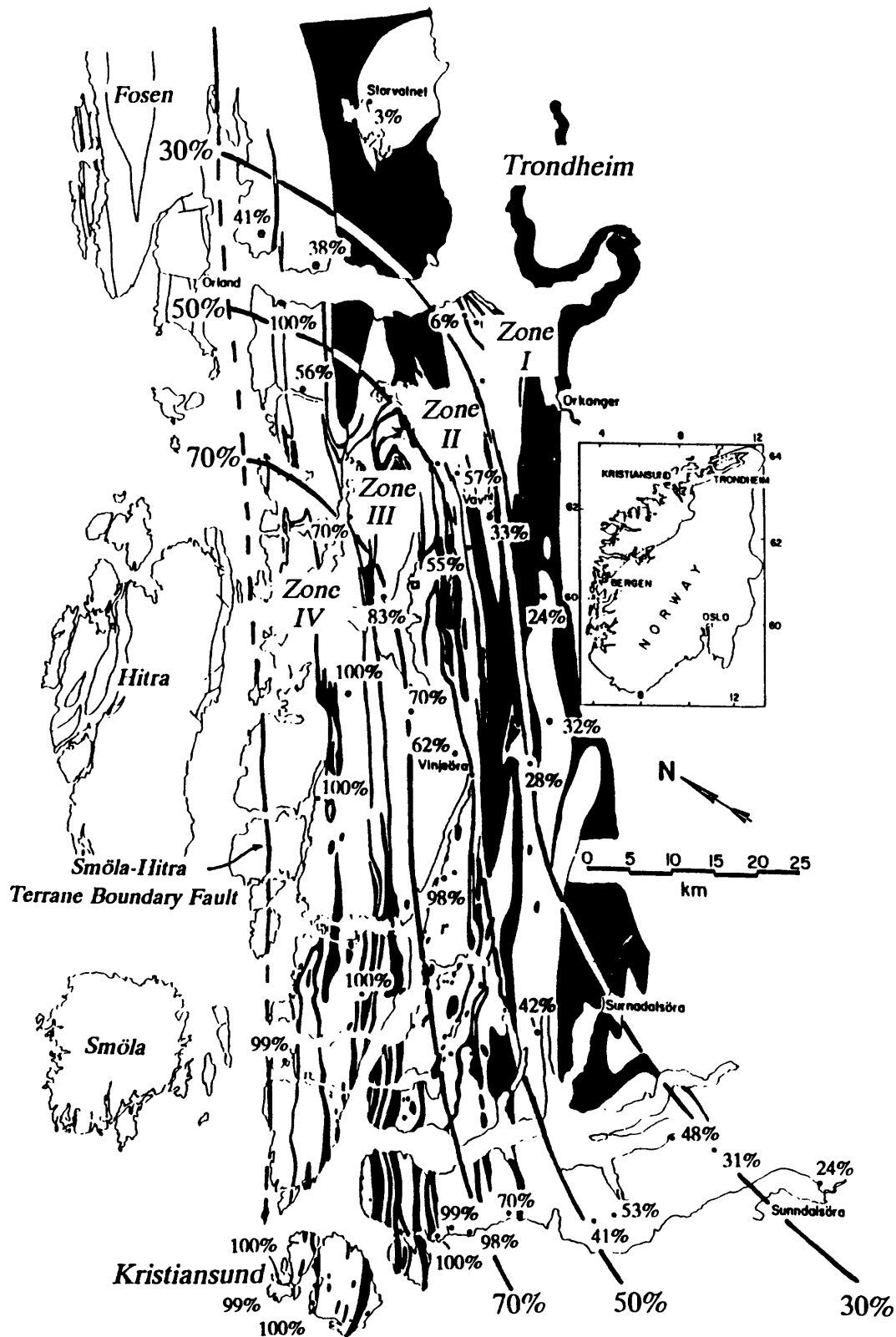
FIGURE 6. Simplified geologic map of the central part of the Western Gneiss Region, Norway, showing the distribution of supracrustal nappe units (black) and autochthonous orthogneisses (white). Contours labeled 30%, 50%, and 70% refer to the percent discordance of titanite analyses on a discordia line from 1657 Ma to 395 Ma (Fig. 9) Individual titanite analyses, with their percent discordance, are also indicated.
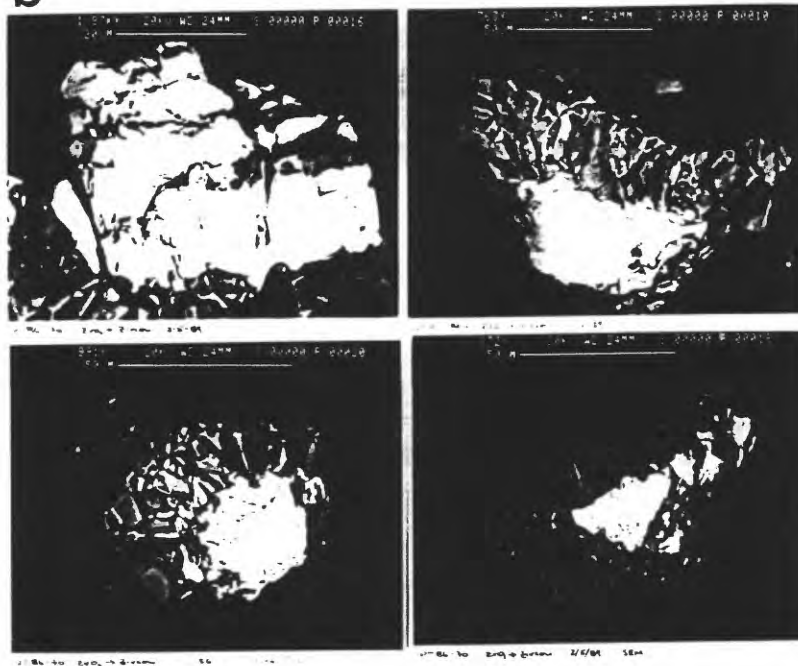
77

FIGURE 7. Mineral grains analyzed from the Selsnes coronitic gabbro photographed in plane light (a) and by SEM imaging (b). (a) Grains of baddeleyite (upper left), skeletal zircon (lower left), microcrystalline zircon (upper right) and composite grains consisting of baddeleyite and microcrystalline zircon (lower right). (b) SEM images of composite baddeleyite-zircon grains analyzed for isotopic age determination. Note the details of the reaction surface (upper left image) between baddeleyite (white) and zircon (removed), showing the molded surface of baddeleyite produced by the replacing zircon 'pegs'.
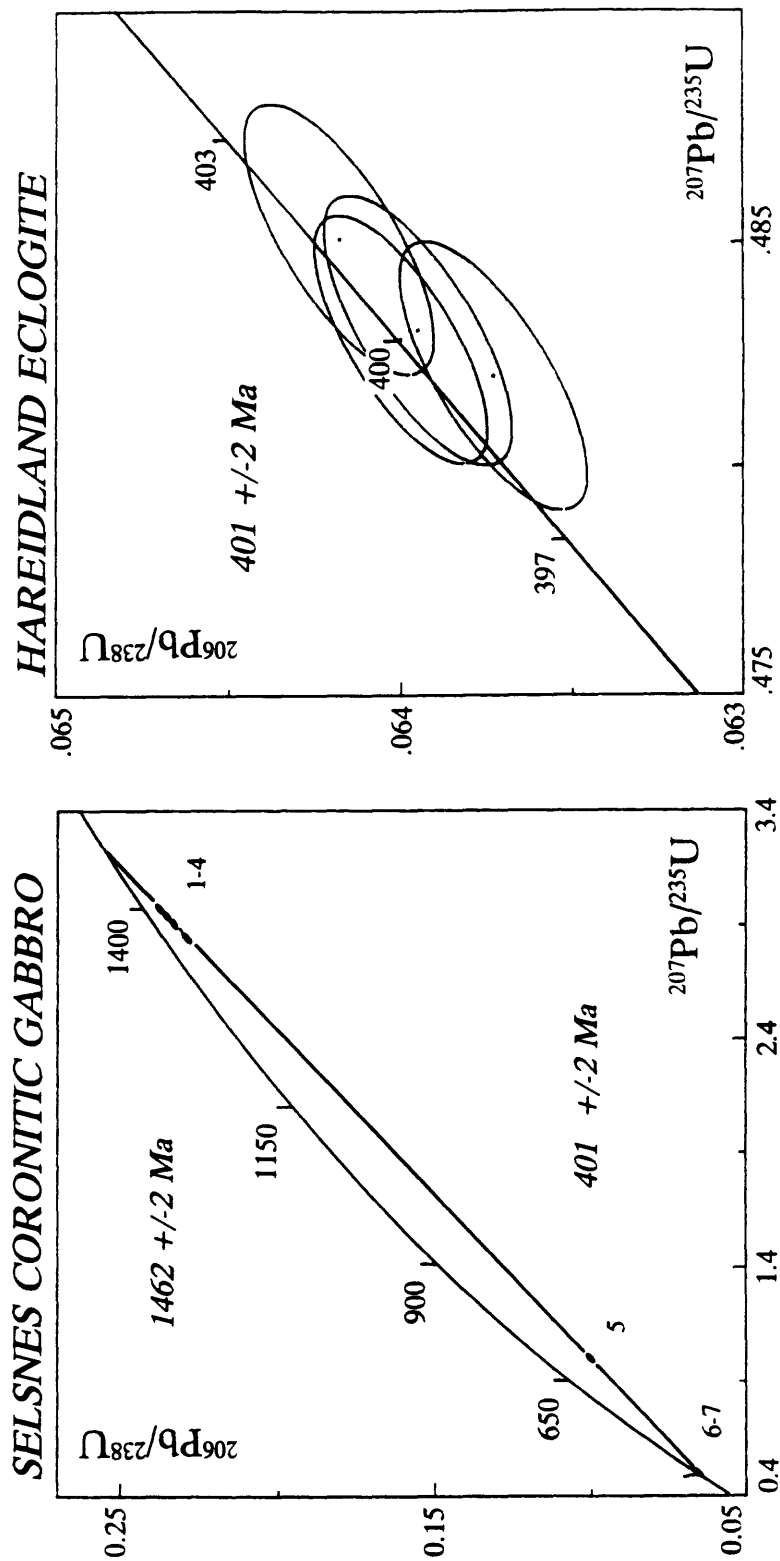
FIGURE 8. Concordia diagram of Selsnes coronite gabbro (a) and Hareidland eclogite (b). (a) Skeletal zircon and baddeleyite (1-4), composite baddeleyite + zircon (5), and microcrystalline zircon (6-7) define the discordia line with upper- and lower-intercept ages of 1462 ± 2 Ma and 401 ± 2 Ma, respectively. These correspond to the time of mafic dike emplacement and corona formation, respectively. (b) Four concordant and coincident zircon analyses define the eclogite age of 401 ± 2 Ma, identical to the time of zircon-growth in the Selsnes coronitic gabbro (above).

WESTERN GNEISS REGION - TITANITES
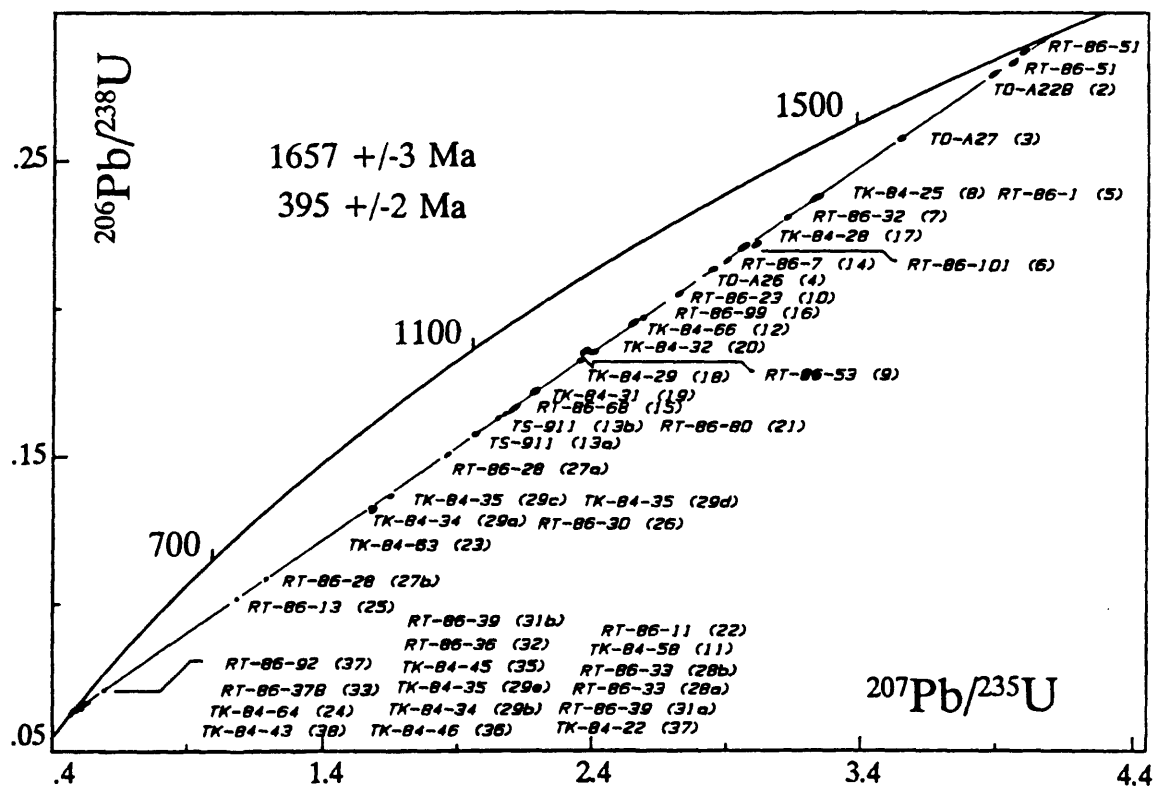
FIGURE 9. Concordia diagram of titanite analyses from 38 orthogneisses collected across the Western Gneiss Region, Norway (see Fig. 5). Most titanite analyses conform to a single discordia line with intercepts of 1657 Ma (upper) and 395 Ma (lower), corresponding to the time of igneous emplacement and regional, high-grade metamorphism, respectively. Titanites from greenschist-facies rocks are near concordant to ca. 30% discordant from the upper intercept, whereas titanites from amphibolite-facies and higher grade rocks are nearly to completely reset at 395 Ma. Titanites from intermediate metamorphic grades display moderate degrees of age discordance. The discordant analyses are interpreted as resulting from a short-lived diffusive Pb-loss event at ca. 395 Ma that affected an area of at least 10,000 km^2 (Fig. 5).

80

Evidence for Late-Paleozoic brine migration in Cambrian carbonate rocks of the central and southern Appalachians: Implications for Mississippi Valley-type sulfide mineralization

PAUL P. HEARN, JR., JOHN F. SUTTER and HARVEY E. BELKIN

U.S. Geological Survey, Reston, VA 22092, U.S.A.

Abstract—Many Lower Paleozoic limestones and dolostones in the Valley and Ridge province of the central and southern Appalachians contain 10 to 25 weight percent authigenic potassium feldspar. This was considered to be a product of early diagenesis, however. $^{40}Ar/^{39}Ar$ analyses of overgrowths on detrital K-feldspar in Cambrian carbonate rocks from Pennsylvania, Maryland, Virginia, and Tennessee yield Late Carboniferous–Early Permian ages (278–322 Ma). Simple mass balance calculations suggest that the feldspar could not have formed isochemically, but required the flux of multiple pore volumes of fluid through the rocks, reflecting regional fluid migration events during the Late-Paleozoic Alleghanian orogeny.

Microthermometric measurements of fluid inclusions in overgrowths on detrital K-feldspar and quartz grains from unmineralized rocks throughout the study area indicate homogenization temperatures from $100°$ to $200°C$ and freezing point depressions of $-14°$ to $-18.5°C$ (18–21 wt.% NaCl equiv). The apparent similarity of these fluids to fluid inclusions in ore and gangue minerals of nearby Mississippi Valley-type (MVT) deposits suggests that the regional occurrences of authigenic K-feldspar and MVT mineralization may be genetically related. This hypothesis is supported by the discovery of authigenic K-feldspar intergrown with sphalerite in several mines of the Mascot-Jefferson City District, E. Tennessee. Regional potassic alteration in unmineralized carbonate rocks and localized occurrences of MVT mineralization are both explainable by a gravity-driven flow model, in which deep brines migrate towards the basin margin under a hydraulic gradient established during the Alleghanian orogeny. The authigenic K-feldspar may reflect the loss of K during disequilibrium cooling of the ascending brines. MVT deposits are probably localized manifestations of the same migrating fluids, occurring where the necessary physical and chemical traps are present.

INTRODUCTION

MANY OCCURRENCES of authigenic K-feldspar have been reported in Lower Paleozoic rocks of the mid-continent area and the Appalachian Basin during the past 60 years (DALY, 1912; TESTER and ATWATER, 1934; WOODARD, 1972; BUYCE and FRIEDMAN, 1975). Far from being a geologic rarity, authigenic K-feldspar is now known to be a common constituent in Cambrian carbonate rocks throughout the Appalachians (BUYCE and FRIEDMAN, 1975; HEARN and SUTTER, 1985; HEARN et al., 1985). This phenomenon was once thought to be the product of early diagenesis involving potassium-rich brines (MAZULLO, 1975); however, recent $^{40}Ar/^{39}Ar$ analyses of authigenic K-feldspar in Cambrian rocks of the Valley and Ridge Province of the central and southern Appalachians have yielded Late Carboniferous ages (HEARN and SUTTER, 1985; HEARN et al., 1985). This paper will present evidence in support of the hypothesis that the authigenic K-feldspar is genetically related to nearby occurrences of MVT mineralization, and thus may allow constraints to be placed on both the timing and the chemistry of ore formation.

EXPERIMENTAL METHODS

$^{40}Ar/^{39}Ar$ age-spectrum analysis

Pure (>95%, the remainder being quartz) mineral separates of detrital K-feldspar grains with authigenic overgrowths were obtained by removing carbonates in dilute HCl and sieving to the 63–150 μm size fraction, followed by gravity separation in a mixture of bromoform and dimethyl formamide (specific gravity = 2.60). The ages of the authigenic overgrowths in these samples were determined by the $^{40}Ar/^{39}Ar$ age-spectrum technique (LANPHERE and DALRYMPLE, 1971; DALRYMPLE and LANPHERE, 1974). Two age-spectra were generated for each sample: one from a split of detrital K-feldspar with authigenic overgrowths. and a second from a split of the same sample whose overgrowths had been removed in a solution of 5 percent hydrofluoric acid. After the HF treatment, detrital cores were examined optically to ensure that the authigenic overgrowths had been completely removed. The ages of the authigenic overgrowths were determined using a method employed by HEARN and SUTTER (1985), which is based on the assumption that the samples represent physical mixtures of phases with different ages but having similar argon-diffusion systematics. For a sample of igneous K-feldspar cores with authigenic K-feldspar overgrowths, the age of the authigenic overgrowths is expressed by the equation:

$$A_o = \frac{A_t - M_c A_c}{M_o} \qquad (1)$$

where:

A_t = apparent age of total sample
A_c = age of core
A_o = age of overgrowth
M_c = mass fraction of core
M_o = mass fraction of overgrowth.

The mass fraction of cores and overgrowths were determined in the following manner. A representative split of each sample was imbedded in epoxy and then ground and polished to ex-
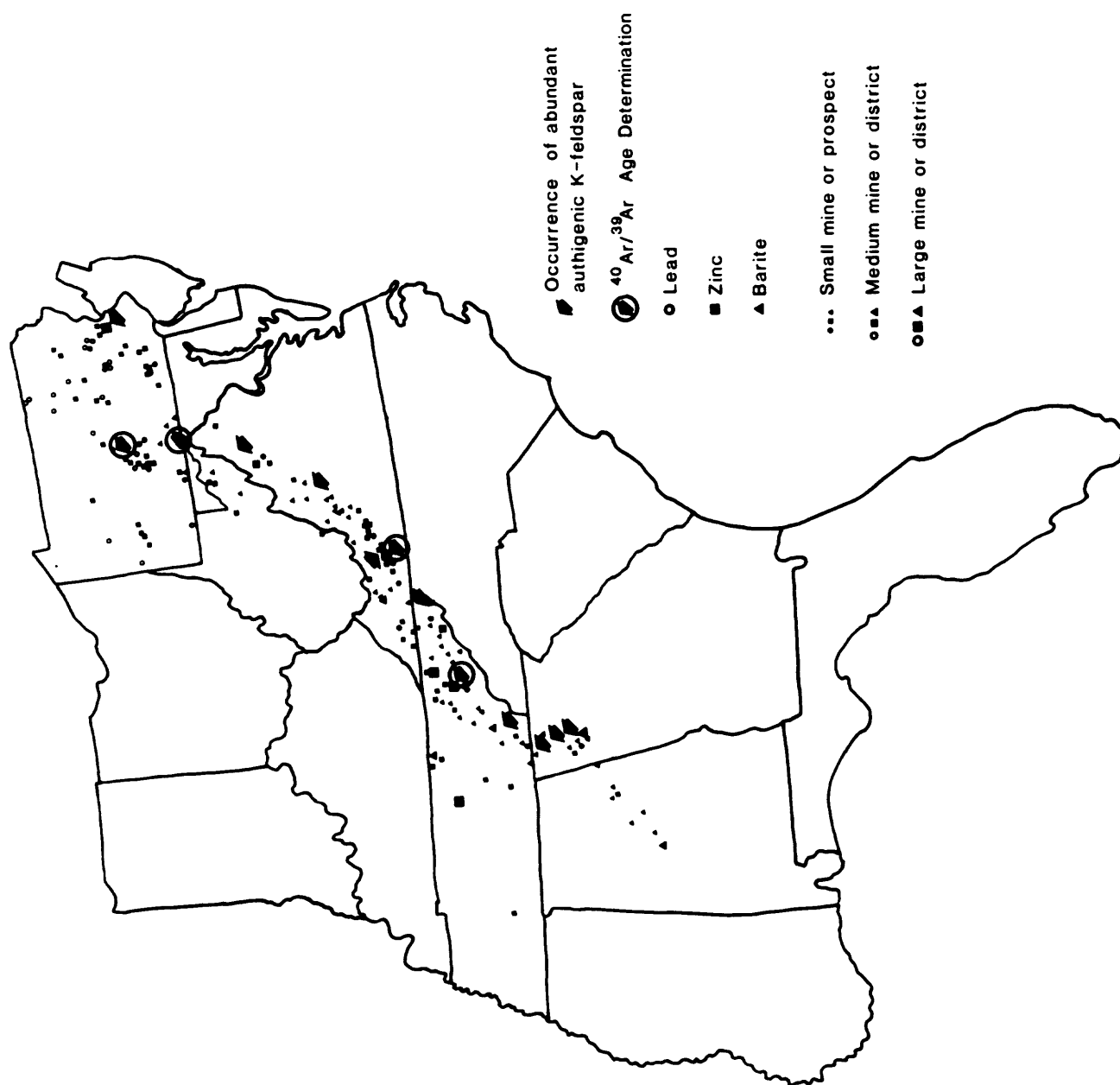
FIG. 1. Map showing sampled occurrences of authigenic K-feldspar and locations of deposits and occurrences of zinc, lead, and barium mineralization in Lower Paleozoic sedimentary rocks of the central and southern Appalachians. Locations of ore deposits and occurrences were taken from CLARK (in press).
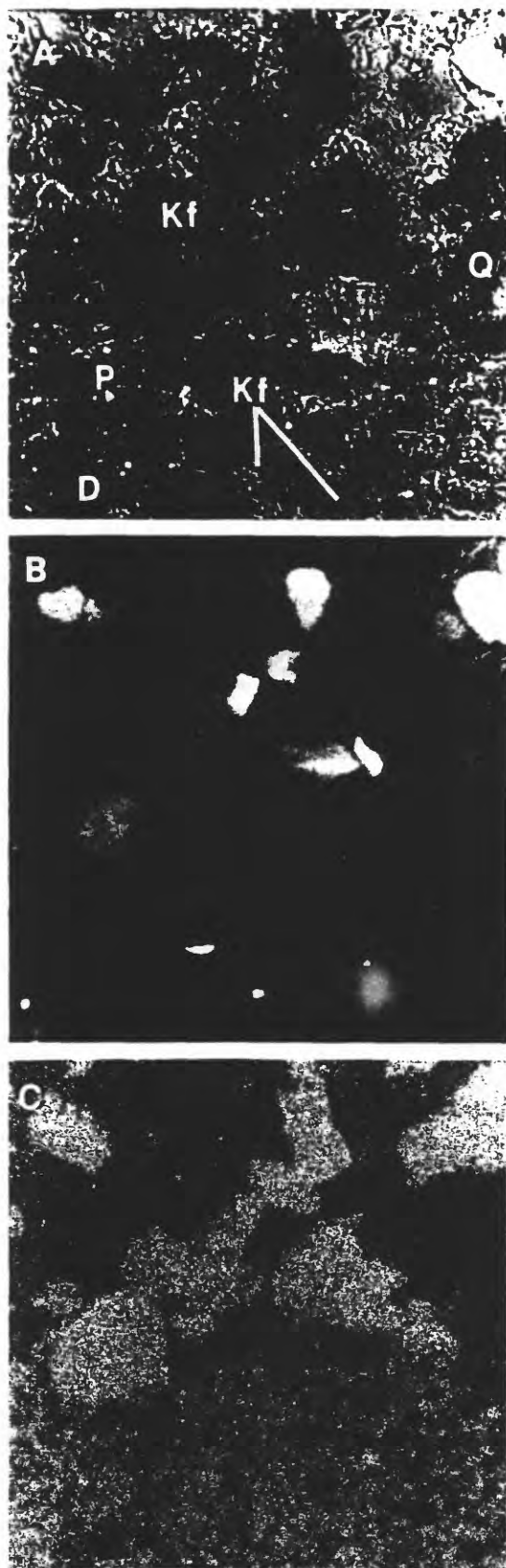
FIG. 2. Scanning electron micrographs of feldspathized dolostone from the Maynardsville Formation, near Jefferson City, Tennessee. All micrographs are of the same area. Scale
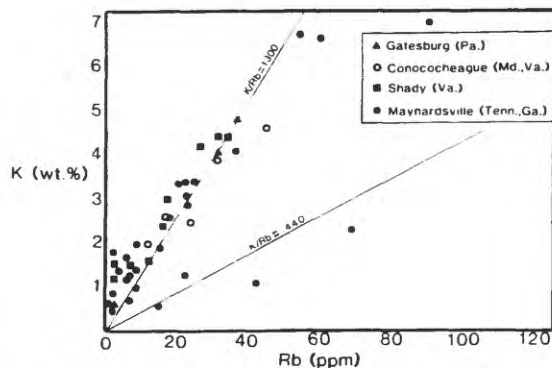

FIG. 3. Plot of whole-rock potassium and rubidium concentrations for samples of Cambrian limestones and dolostones from the Valley and Ridge province of the central and southern Appalachians.

to as much as 90 ppm. Optical and X-ray diffraction analyses of these samples indicate that K-feldspar is the major potassium containing phase and that illite and muscovite are either absent or present in only minor amounts. The plot of potassium *versus* rubidum shows most samples to fall along a line defined by a K/Rb ratio of approximately 1300 (Fig. 3). The marked depletion in Rb indicated by these data suggests that a significant proportion of the K-feldspar in these rocks is authigenic—a conclusion consistent with petrographic observations.

Authigenic K-feldspar in mineralized rocks

Authigenic K-feldspar has been identified as a primary component of jasperoid gangue in three mines of the Mascot-Jefferson City district in eastern Tennessee (New Market, Young, and Immel mines). All of these occurrences are in the Beekmantown dolomite, the major host formation for MVT mineralization in the Appalachians. The jasperoids are thinly banded, dark gray, shaley to cherty zones which are often intimately associated with ore. These zones are believed to have formed during silicification events in the early part of the paragenetic sequence–prior to the deposition of sphalerite (McKORMICK *et al.*, 1971). Authigenic K-feldspar in the jasperoids is typically intergrown with silica and dolomite, and occurs as broad zones of coalescing overgrowths on grains of detrital K-feldspar (Fig. 4). In all the cases observed, the nature of grain contacts between authigenic K-feldspar and sphalerite

bar = 100 micrometers. A) Backscattered electron image showing interface between coarse-grained limestone interbed and fine-grained dolostone interbed. Note intergrowths of dolomite and authigenic K-feldspar in dolostone layer. Key: K-feldspar (Kf); quartz (Q); dolomite (D); calcite (C); pyrite (P). B) Cathodoluminescence image showing detrital (luminescing) K-feldspar grains. C) Potassium X-ray map showing distribution of authigenic and detrital K-feldspar. X-ray diffraction analysis of the <63 µm fraction of the insoluble residue of this sample showed K-feldspar and quartz to be the primary phases present; no clay minerals were found.
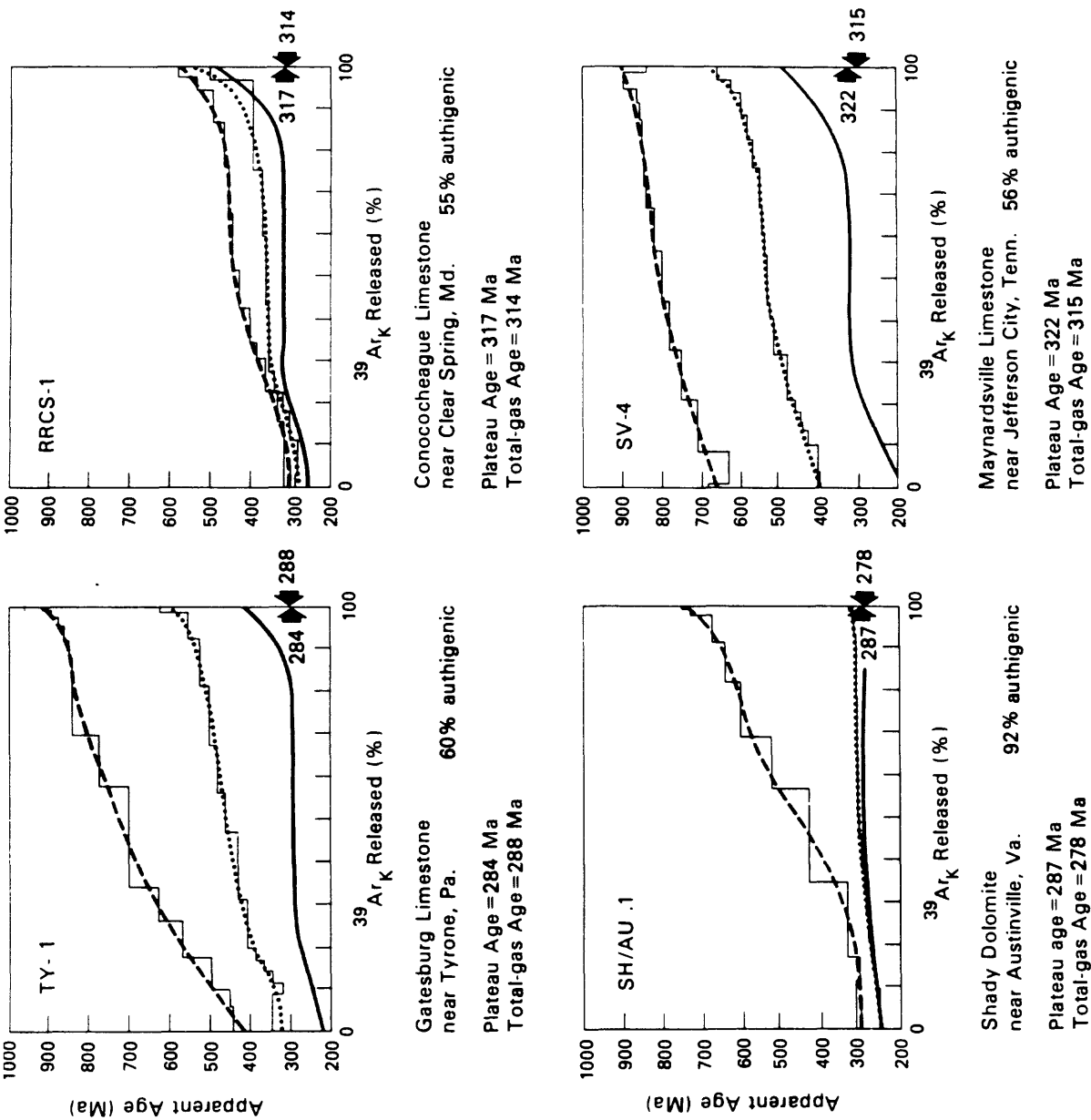
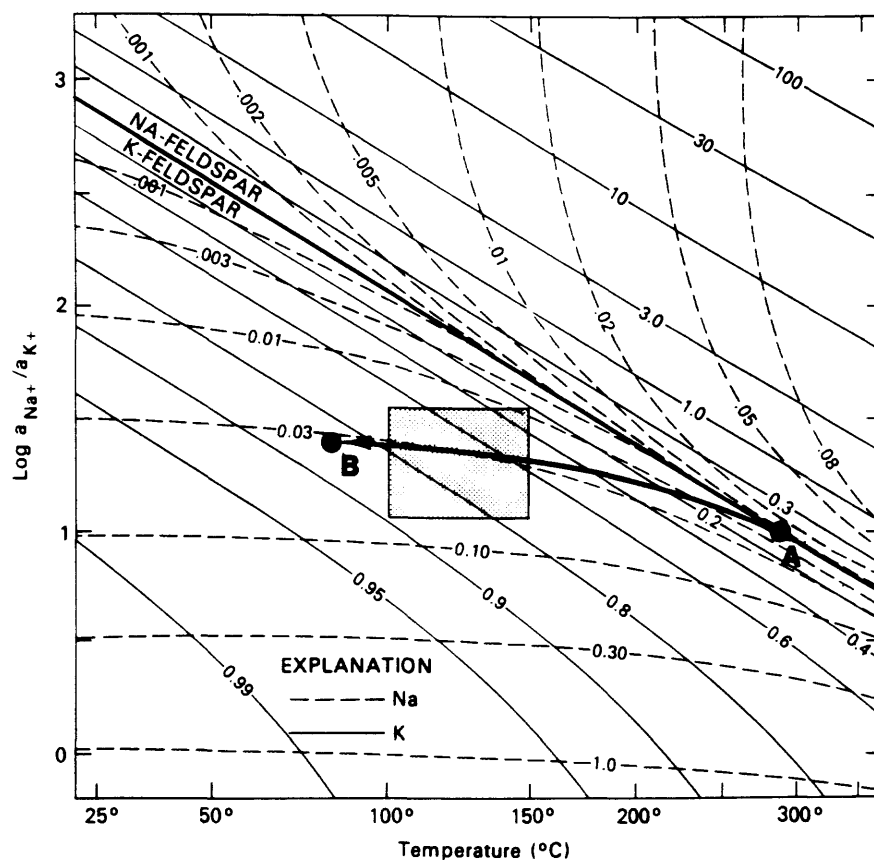FIG. 5. ^{40}Ar/^{39}Ar age spectra of K-feldspar separates.

84

Fig. 9. Relative proportions of alkali ions produced (+) or consumed (−) during isothermal equilibration of a solution with a given Na/K activity ratio with respect to a full equilibrium assemblage containing both Na- and K-feldspars (activity coefficients for both species are assumed to be equal); The curved arrow represents a hypothetical cooling trajectory for an ascending hydrothermal fluid (modified slightly from GIGGENBACH, 1984; see this reference for a detailed treatment of the derivation of this figure). The shaded area represents range of reported trapping temperatures and Na/K ratios for fluid inclusions in Mississippi Valley-type ore deposits from the data of VIETS et al.. (1984), and ROEDDER (1972).

margin for fluids to rise towards the surface in these areas. At the Pine Point deposit, which has been attributed to emplacement by gravity-flow, the ore is hosted in rocks which are structurally undeformed (GARVEN, 1985).

The lack of extensive mineralization in sediments younger than Middle Ordovician is not convincing evidence that ore emplacement did not occur significantly later than this time. The collapse structures which appear to be necessary for ore formation are largely absent in carbonate rocks above the Middle Ordovician unconformity. Furthermore, numerous minor occurrences of lead and zinc mineralization have been cited in rocks as young as Carboniferous in Tennessee, Kentucky, and Pennsylvania (JEWELL, 1947; KYLE, 1976; HOWE 1981).

CONCLUSIONS

1) $^{40}Ar/^{39}Ar$ age-spectrum analyses of authigenic K-feldspar in Cambrian carbonate rocks of the Valley and Ridge province of the central and southern Ap-

palachians yield Late Carboniferous–Early Permian ages (278–322 Ma). Simple mass-balance calculations suggest that the K-feldspar did not form isochemically, but involved the flux of multiple pore-volumes of fluid through these rocks. These observations are believed to reflect the regional migration of basinal brines in response to tectonic activity during the Late-Paleozoic Alleghanian Orogeny.

2) Microthermometric measurements of fluid inclusions in overgrowths on K-feldspar and quartz grains in unmineralized carbonate rocks indicate that these phases precipitated from a hot ($100°-200°C$) and saline (18–21 weight percent NaCl equivalent) fluid. The apparent similarity of these fluids to fluid inclusions in ore and gangue minerals of nearby MVT deposits suggests that both the mineralization and the regional occurrences of authigenic K-feldspar were emplaced during basin-wide fluid migration events.

3) The suggestion that authigenic K-feldspar in unmineralized rocks and MVT ore deposits were emplaced by similar fluids is also supported by the discovery of authigenic K-feldspar intergrown with

sphalerite in several mines of the Mascot-Jefferson City District in eastern Tennessee. Textural observations suggest that the authigenic K-feldspar predates the ore and formed during a silicification event in the early part of the paragenetic sequence.

4) The genesis of MVT deposits in the central and southern Appalachians as well as regional occurrences of authigenic K-feldspar in unmineralized rocks can be explained by the migration of basinal brines in a gravity-driven flow system established by Alleghanian tectonism. The presence of authigenic K-feldspar in Valley and Ridge dolostones is believed to reflect the loss of potassium from ascending basinal fluids as they cooled and attempted to move towards equilibrium in the K-feldspar-albite system. We believe that MVT deposits in the central and southern Appalachians do not represent isolated or discrete fluid movements, but rather are localized manifestations of a regional fluid migration event where the specific physical and chemical traps necessary for ore formation were present.

REFERENCES

BACHTADSE V., VAN DER VOO R., KESTLER S. E. and HAYNES F. M. (1985) Carboniferous remagnetization of the Lower Ordovician Knox Group, East Tennessee (abstr.). *EOS* **66**, 258.

BASKIN Y. (1956) A study of authigenic feldspars. *J. Geol.* **64**, 132-155.

BETHKE C. M. (1985) A numerical model of compaction-driven groundwater flow and heat transfer and its application to the paleohydrology of intracratonic sedimentary basins. *J. Geophys. Res.* **90B**, 6817-6828.

BETHKE C. M. (1986) Hydrologic constraints on genesis of the Upper Mississippi Valley mineral district from Illinois Basin brines. *Econ. Geol.* **81**, 233-249.

BROKAW A. L. and JONES C. L. (1946) Structural control on ore bodies in the Jefferson City area, Tennessee. *Econ. Geol.* **41**, 160-165.

BUYCE M. R. and FRIEDMAN G. M. (1975) Significance of authigenic K-feldspar in Cambrian-Ordovician carbonate rocks of the Proto-Atlantic shelf in North America. *J. Sediment. Petrol.* **45**, 808-821.

CARPENTER A. B., TROUT M. L. and PICKETT E. E. (1974) Preliminary report on the origin and chemical evolution of lead- and zinc-rich oil field brines in central Mississippi. *Econ. Geol.* **69**, 1191-1206.

CATHLES L. M. and SMITH A. T. (1983) Thermal constraints on the formation of Mississippi Valley-type lead-zinc deposits and their implications for episodic basin dewatering and deposit genesis. *Econ. Geol.* **78**, 983-1002.

CHURNET H. G. (1985) Fluid inclusion evidence for fluid mixing, Mascot-Jefferson City zinc district, Tennessee—A discussion. *Econ. Geol.* **80**, 1440-1443.

CLARK S. H. B. (in press) Zinc, lead, and barium deposits and occurrences in Paleozoic sedimentary rocks, East-Central United States. U.S. Geol. Surv. Misc. Inv. Series Map I-1773.

CRAWFORD J. and HOAGLAND A. D. (1968) The Mascot-Jefferson City Zinc District, Tennessee. In *Ore Deposits of the United States 1933-1967—The Graton-Sales Volume*. (ed. J. D. RIDGE), pp. 242-256. Amer. Inst. Mining Metall. Petroleum Engineers, Maple Press.

COX G. H. (1911) The origin of the lead and zinc ores of the Upper Mississippi Valley district. *Econ. Geol.* **6**, 427-448, 582-603.

CUNNINGHAM C. G. JR. and COROLLO C. (1980) Modification of a fluid-inclusion heating/freezing stage. *Econ. Geol.* **75**, 335-337.

CURRIER L. W. (1935) Structural relations of southern Appalachian zinc deposits. *Econ. Geol.* **30**, 260-286.

DALRYMPLE G. B. and LANPHERE M. A. (1974) ^{40}Ar/^{39} age spectra of some undisturbed terrestrial samples. *Geochim. Cosmochim. Acta* **38**, 715-738.

DALY R. A. (1912) Stratigraphy and structure of the Clark Range: in America Cordillera-Forty-ninth Parallel. *Geol. Survey Can. Mem.* **38**, 47-57.

DAUBREE A. (1887) *Les Eaux Souterraines, aux Epoques Anciennes et à l'Époque actuelle*. Paris, Dunod, 3 vol.

DEMICCO R. V. and MITCHELL R. W. (1982) Facies of the Great American Bank in the central Appalachians. In *NE-SE GSA '82 Field Trip Guidebooks* (ed. P. T. LYTTLE), pp. 171-266. Amer. Geol. Inst.

DOZY J. J. (1970) A geologic model for the genesis of the lead-zinc ores of the Mississippi Valley, U.S.A. *Trans. Inst. Mining Metall.* **79**, sec. B, 163-170.

FOLEY N. K. (1980) Mineralogy and geochemistry of the Austinville-Ivanhoe district, Virginia. Master thesis, Virginia Polytechnic Institute and State University.

GARVEN G. (1985) The role of regional fluid flow in the genesis of the Pine Point deposit, Western Canada sedimentary basin. *Econ. Geol.* **80**, 307-324.

GARVEN G. and FREEZE R. A. (1984a) Theoretical analysis of the role of groundwater flow in the genesis of stratabound ore deposits. 1. Mathematical and numerical model. *Amer. J. Sci.* **284**, 1085-1124.

GARVEN G. and FREEZE R. A. (1984b) Theoretical analysis of the role of groundwater flow in the genesis of stratabound ore deposits. 2. Quantitative results. *Amer. J. Sci.* **284**, 1125-1174.

GIGGENBACH W. D. (1984) Mass transfer in hydrothermal alteration systems—a conceptual approach. *Geochim. Cosmochim. Acta* **48**, 2693-2711.

HANOR J. S. (1979) The sedimentary genesis of hydrothermal fluids. In *Geochemistry of Hydrothermal Ore Deposits* (ed. H. L. BARNES), Chap. 4, pp. 137-172. Holt, Rinehart, and Winston.

HARRIS A. G., HARRIS L. D. and EPSTEIN J. B. (1978) Oil and gas data from Paleozoic rocks in the Appalachian Basin: Maps for assessing hydrocarbon potential and thermal maturity (Conodont color alteration isograds and overburden isopachs). U.S. Geol. Surv. Misc. Inv. Series Map I-917-E.

HEARN P. P. JR. and SUTTER J. F. (1985) Authigenic potassium feldspar in Cambrian carbonates: evidence of Alleghanian brine migration. *Science* **228**, 1529-1531.

HEARN P. P. JR., SUTTER J. F., KUNK M. J. and BELKIN H. E. (1985) Evidence for Alleghenian brine migration in the central and southern Appalachians: implications for Mississippi Valley-type sulfide mineralization (abstr.). *Geol. Soc. Amer. Abstr. Prog.* **17**, 606.

HEIER K. S. and TAYLOR S. R. (1959) Distribution of Li, Na, K, Rb, Cs, Pb, and Tl in southern Norwegian pre-Cambrian alkali feldspars. *Geochim. Cosmochim. Acta* **15**, 284.

HILL W. T. (1969) Mine geology of the New Market Zinc Company's Flat Gap Mine at Treadway in the Copper Ridge district. *Tenn. Geol. Div. Rept. Inv.* **23**, 76-90.

HOWE S. S. (1981) Mineralogy, fluid inclusions, and stable isotopes of lead-zinc occurrences in Central Pennsylvania. Masters thesis, Pennsylvania State Univ.

JACKSON S. A. and BEALES F. W. (1967) An aspect of sedimentary basin evolution: The concentration of Mississippi

Valley-type ores during the late stages of diagenesis. *Can. Petrol. Geol. Bull.* **15**, 393–433.

JEWELL W. B. (1947) Barite, fluorite, galena, sphalerite veins of Central Tennessee. *Tenn. Div. Geol. Bull. 51*, 114p.

KASTNER M. (1971) Authigenic feldspars in carbonate rocks. *Amer. Mineral.* **56**, 1403–1442.

KASTNER M. and SIEVER R. (1979) Low temperature feldspars in sedimentary rocks. *Amer. J. Sci.* **279**, 435–479.

KENDALL D. L. (1960) Ore and sedimentary features, Jefferson City Mine, Tennessee. *Econ. Geol.* **55**, 985–1003.

KYLE J. R. (1976) Brecciation, alteration, and mineralization in the central Tennessee Zinc District. *Econ. Geol.* **71**, 892–903.

LANPHERE M. A. and DALRYMPLE G. B. (1971) $^{40}Ar/^{39}Ar$ technique of K/Ar dating: A comparison with the conventional technique. *Earth Planet. Sci. Lett.* **12**, 300–308.

LEACH D. L. and ROWAN E. L. (1986) Genetic link between Ouachita fold-belt tectonism and the Mississippi Valley-type lead-zinc deposits of the Ozarks. *Geology* **14**, 931–935.

McCORMICK J. E., EVANS L. L., PALMER R. A. and RASNICK F. D. (1971) Environment of the zinc deposits of the Mascot-Jefferson City District, Tennessee. *Econ. Geol.* **66**, 757–762.

MAZULLO S. J. (1976) Significance of authigenic K-feldspar in Cambrian-Ordovician carbonate rocks of the proto-Atlantic shelf in North America: A discussion. *J. Sediment. Petrol.* **46**, 1035–1040.

MECKEL L. D. (1970) Paleozoic alluvial deposition in the central Appalachians: a summary. In *Studies of Appalachian Geology, Central and Southern* (eds. G. W. FISHER, F. J. PETTIJOHN, J. C. READ and K. N. WEAVER), pp. 49–64. Wiley Interscience.

OHLE E. L. (1980) Some considerations in determining the origin of ore deposits of the Mississippi Valley type. Part II. *Econ. Geol.* **75**, 161–172.

REINHARDT J. and HARDIE L. A. (1976) Selected examples of carbonate sedimentation, Lower Paleozoic of Maryland. Guidebook for the 1976 NE-SE Joint Sectional meeting of the Geological Society of America, 53p.

ROEDDER E. (1972) Composition of fluid inclusions. In *Data of Geochemistry* (ed. M. FLEISCHER), *U.S. Geological Survey Professional Paper 440-JJ*, 164p.

ROEDDER E. (1976) Fluid-inclusion evidence on the genesis of ores in sedimentary and volcanic rocks. In *Ores in Sediments, Sedimentary and Volcanic Rocks* (ed. K. H. WOLF), Vol. 2, Chap. 4, pp. 67–110. Elsevier.

ROEDDER E. (1984) *Fluid Inclusions, Reviews in Mineralogy* Vol. 12, 644p. Mineral. Soc. Amer.

SHARP J. M. JR. (1978) Energy and momentum transport model of the Ouachita basin and its possible impact on formation of economic mineral deposits. *Econ. Geol.* **73**, 1057–1068.

TAYLOR M., KELLY W. C., KESLER S. E., McCORMICK J. E., RASNICK F. D. and MELLON W. V. (1983) Relationship of zinc mineralization in East Tennessee to Appalachian orogenic events. In *International Conference on Mississippi Valley-type Lead-Zinc Deposits. Proceedings Volume* (eds. G. KISVARSANYI, S. K. GRANT, W. PRATT and J. W. KOENIG), pp. 271–278. Missouri-Rolla Press.

TAYLOR M., KESLER S. E., CLOKE P. L. and KELLEY W. C. (1985) Fluid inclusion evidence for fluid mixing, Mascot-Jefferson City Zinc district, Tennessee—A reply. *Econ. Geol.* **80**, 1442–1443.

TESTER A. C. and ATWATER G. I. (1934) The occurrence of authigenic feldspars in sediments. *J. Sediment. Petrol.* **4**, 23–31.

VAN DER VOO R. (1977) Age of Alleghenian folding in the Central Appalachians. *Geology* **7**, 297–298.

VIETS J. G., ROWAN L. and LEACH D. L. (1984) Composition of fluids extracted from sphalerite, galena, and dolomite in Mississippi Valley-type deposits of the mid-continent: implications for the origin of the fluid (abstr.). *Geol. Soc. Amer. Abstr. Prog.* **16**, 682.

WOODARD H. H. (1972) Syngenetic sanidine beds from Middle Ordovician St. Peter sandstone, Wisconsin. *J. Geol.* **82**, 116–119.

WOODWARD H. (1957) Chronology of Appalachian folding. *Bull. Amer. Assoc. Petrol. Geol.* **41**, 2312–2327.

Blank

.

III. Metamorphism: Detrital/Prograde/Retrograde

Hinterland Thermochronology from Analysis of Foreland Clastics
(P.K. Zeitler)

1. Introduction

Usually, geochronologists avoid detrital material like the plague. Whether in primary form, as a contaminant in a volcanic ash, or in some more subtle form, inherited material can be a real nuisance. Of course, one can fight back, look for the silver lining to the cloud, and recognize that detrital grains can carry with them very useful information about provenance. Over the years, numerous studies have in fact taken this approach and used the ages of detrital grains to learn something about the source areas of sediments and granites. Improvements in analytical techniques have extended the range of methods by which one can do detrital geochronology, and currently it is possible to do single-grain analyses of U-Pb in zircon, Ar in feldspars and micas, and fission-tracks in zircon and apatite.

There's a neat, thermochronological twist that one can add to the geochronology of detrital material. In a mountain belt that's undergoing unroofing, it is very true that what goes up, in the form of uplifting basement in the hinterland, comes down in the from of clastic sediments in the foreland. Now, if we sample some of the basement just as it arrives at the surface, we claimed earlier that we can sniff out something about the sample's thermal history, using thermochronology. Well, why stop there just because some of our sample has escaped and washed downhill to join the molasse? If we can date single grains, then the age of any such grains entrained in a sandstone should tell us something about the unroofing history of that sandstone's source area(s). That in itself is interesting, but if the sandstone we are studying happens to be of well-known age, then we can learn something about the state of the hinterland at the time of sandstone deposition. Furthermore, if we examine an entire clastic wedge, we should be able to learn something about the evolution of the hinterland through time, and of course, we can also obtain heavy-mineral and facies data to compare with the story extracted for the hinterland. Figure 1 illustrates this approach in cartoon form.

Needless to say, you need to make several assumptions when trying to do detrital thermochronology. The exact nature of these assumptions depends a little on what you're trying to accomplish, but typically you might want to assume that transport from outcrop to basin is rapid, that little or no reworking is underway in the foredeep, and that the inferred source areas are constrained and well characterized. In many cases, a test of these assumptions itself makes for an interesting and geologically informative study.

2. Case Study: Fission-Track Dating of Detrital Zircons, Siwalik Molasse, NW Himalaya, Pakistan

Abstract. History of uplift and relief of the Himalaya during the past 18 million years: Evidence from fission-track ages of detrital zircons from sandstones of the Siwalik Group
(Cerveny et al., 1988)

History of Uplift and Relief of the Himalaya During the Past 18 Million Years: Evidence from Fission-Track Ages of Detrital Zircons from Sandstones of the Siwalik Group

P.F. Cerveny, N.D. Naeser, P.K. Zeitler, C.W. Naeser, and N.M. Johnson

Abstract

Fission-track dating of individual detrital zircon grains can be used to characterize both ancient and modern sedimentary provenance. Ages of zircons in the modern Indus River drainage system of northern Pakistan are controlled dominantly by uplift rates of the source rocks in the Himalaya. Young detrital zircons come from rapidly rising terrain, whereas old zircon ages imply slow or negligible uplift. Modern Indus River sands contain a distinctive population of young, 1 to 5 Ma, zircons that are derived from the Nanga Parbat-Haramosh Massif, an area of rapid uplift (5 m/10³ yr). Sandstones of the Siwalik Group deposited by the ancestral Indus River over the past 18 million years contain zircons that are only 1 to 5 million years older than the depositional age of the sandstones. Therefore, young zircons have been a consistent component of Himalayan surface rocks for the past 18 million years. These ages imply that a series of uplifted blocks or "massifs," analogous to the contemporary Nanga Parbat area, have been continually present in the Himalaya since 18 Ma, and that over that time the elevation and relief of the Himalaya, on a broad scale, have been essentially constant.

Introduction

This paper describes the relief and uplift in the upper Indus River watershed during the past 18 million years, based on fission-track ages of detrital zircons derived from the sediments of the present Indus River of northern Pakistan and from sandstones of the Siwalik Group, which originated from sediments deposited by the ancestral Indus River during Neogene time. The data analysis represents a new methodology in the study of source terrain. Previous studies have used fission-track dating of detrital zircons to identify source area based on the ages of the detrital grains (e.g., Hurford *et al.* 1984; Johnson 1984; Yim *et al.* 1985; Baldwin *et al.* 1986). However, none of these studies was directly concerned in detail with using the ages of the detrital grains in sedimentary rocks to interpret the *tectonic history* of the source terrain. Detailed interpretation of the tectonic history is the central purpose of this paper.

Zeitler (1985) and Zeitler *et al.* (1982b,c) have demonstrated that in the Himalaya, areas characterized by rapid uplift rates have zircons with young fission-track ages (Fig. 3.1). Zeitler *et al.* (1982a) showed further that young zircons are present in the detrital zircon suite currently being eroded from the Himalaya. These data suggest that by dating detrital zircons separated from Siwalik Group sandstones of known stratigraphic age, it would be possible to determine the ages of zircon that were being eroded from the basement source terrain in northern Pakistan at selected intervals during Neogene time, and that the detrital zircons might thus be a vehicle through which uplift rates from the geologic past could be assessed (Zeitler *et al.* 1982a). This possibility is explored in this paper. The primary objective of the present study is to determine if zircons with young ages, which are indicative of high uplift rates, have been present in the Himalaya over the past 18 million years.

Geography and Geologic Setting

The study area in the Punjab region of northern Pakistan (Fig. 3.2) contains the type sections for most of the formations of the Siwalik Group (Fatmai 1974), which consists of sandstones derived from

INSERT CERVENY ET AL. ABSTRACT HERE

General Comments : Figure 1 in the section on Himalayan denudation provides a geologic setting for this study, and the regional thermochronology presented there is the baseline for the study by Cerveny et al. (see above). It is interesting to note the Copeland and Harrison (1990) obtained a very similar style of results from 40Ar/39Ar analysis of K-feldspars taken out of sediments of the Bengal Fan (this fan is far from the Himalaya, but nonetheless dominated by their debris). What they found is that at every stratigraphic horizon, there were always very young grains present that would have had close to a zero age at the time of deposition. It is instructive to compare the studies by Cerveny et al. (1988) and Copeland and Harrison (1990) to see how the advantages and disadvantages of the fission-track and ^{40}Ar/^{39}Ar methods match up in an application like this.

Summary of main points :

(1) Modern detrital zircons yield an age spectrum very close to that obtained from hard-rock samples in the hinterland. This implies that time spent in transport in negligible (looking at some of the rivers tells you that, too!).

(2) There are always very young (0-2 Ma) zircon grains present in the sediments arriving in the foredeep (when ages are corrected for stratigraphic age of the sampled horizon).

(3) A look at the hinterland today shows that such young ages are only found in regions of extreme relief of over 5 km; this suggests that very prominent relief has been present in the NW Himalaya for at least the past 15 m.y.
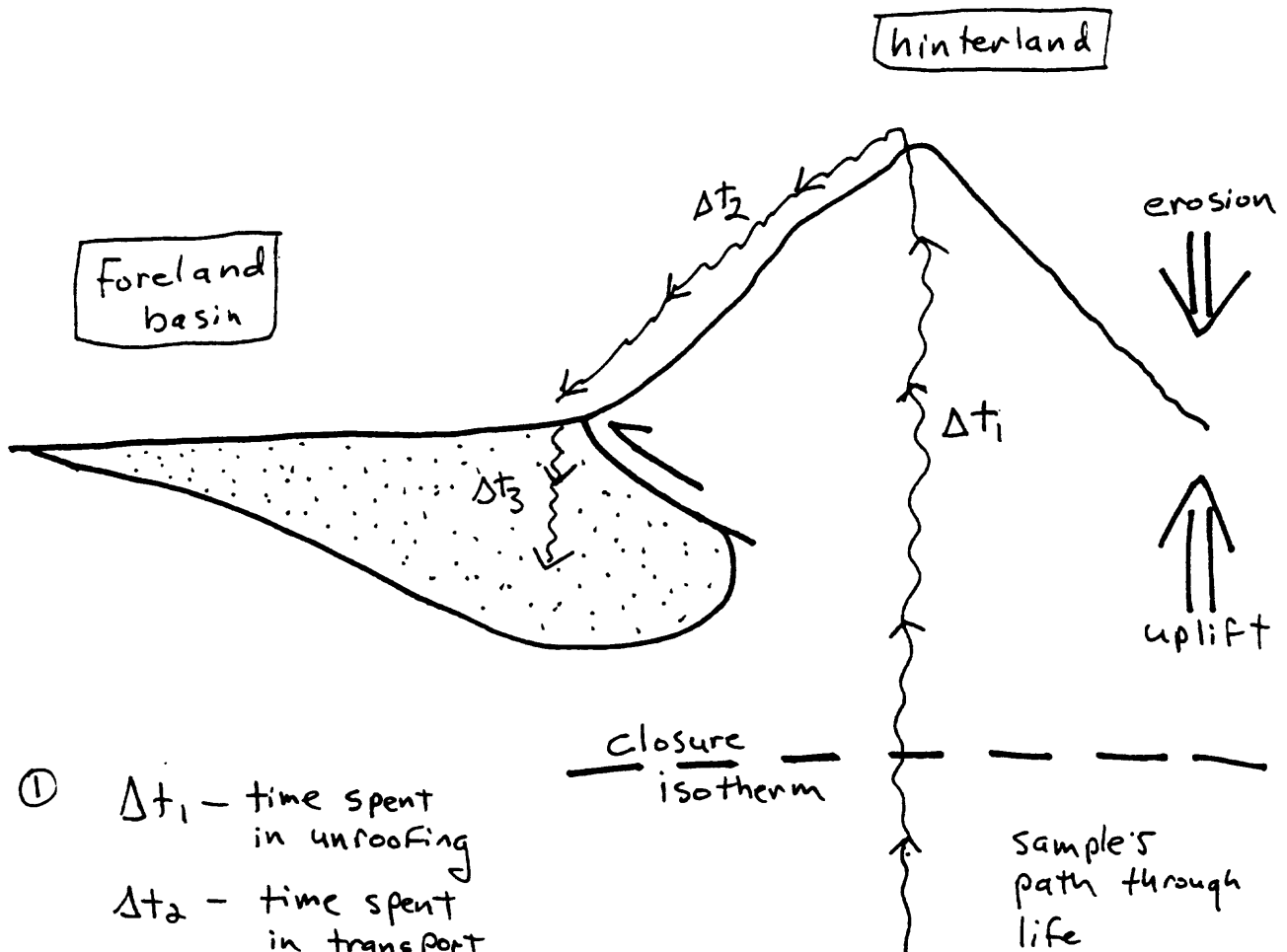
(4) A key element in the success of this study was the detailed magnetic stratigraphy available for the Siwalik Group (see "Fission-Track Dating and Chronostratigraphy," above).

(5) A drawback to the use of zircons in doing studies of young detrital material is the strong dependence of optimum track-etching time on age. Very young grains take a long time to etch,and thus it was necessary to treat each sample twice. Because the differently etched aliquots for each sample will overlap in the age distributions they give, it is not possible to get a single quantitative distribution of all grain ages.

3. References

Baldwin, S. L., Harrison, T. M. and Burke, K., 1986. Fission track evidence for the source of accreted sandstones, Barbados: Tectonics, v. 5, p. 457-468.

Cerveny, P. F., Naeser, N. D., Zeitler, P. K., Naeser, C. W., and Johnson, N. M., 1988, History of uplift and relief of the Himalaya during the past 18 million years: Evidence from fission-track ages of detrital zircons from sandstones of the Siwalik Group. In: Kleinspehn, K. L. and Paola, C. (eds.), New Perspectives in Basin Analysis, Springer, New York, p. 43-61.

Copeland, P. and Harrison, T. M., 1990, Episodic rapid uplift in the Himalaya revealed by ^{40}Ar/^{39}Ar analysis of detrital K-feldspar and muscovite, Bengal Fan: Geology, v. 18, p. 354-357.
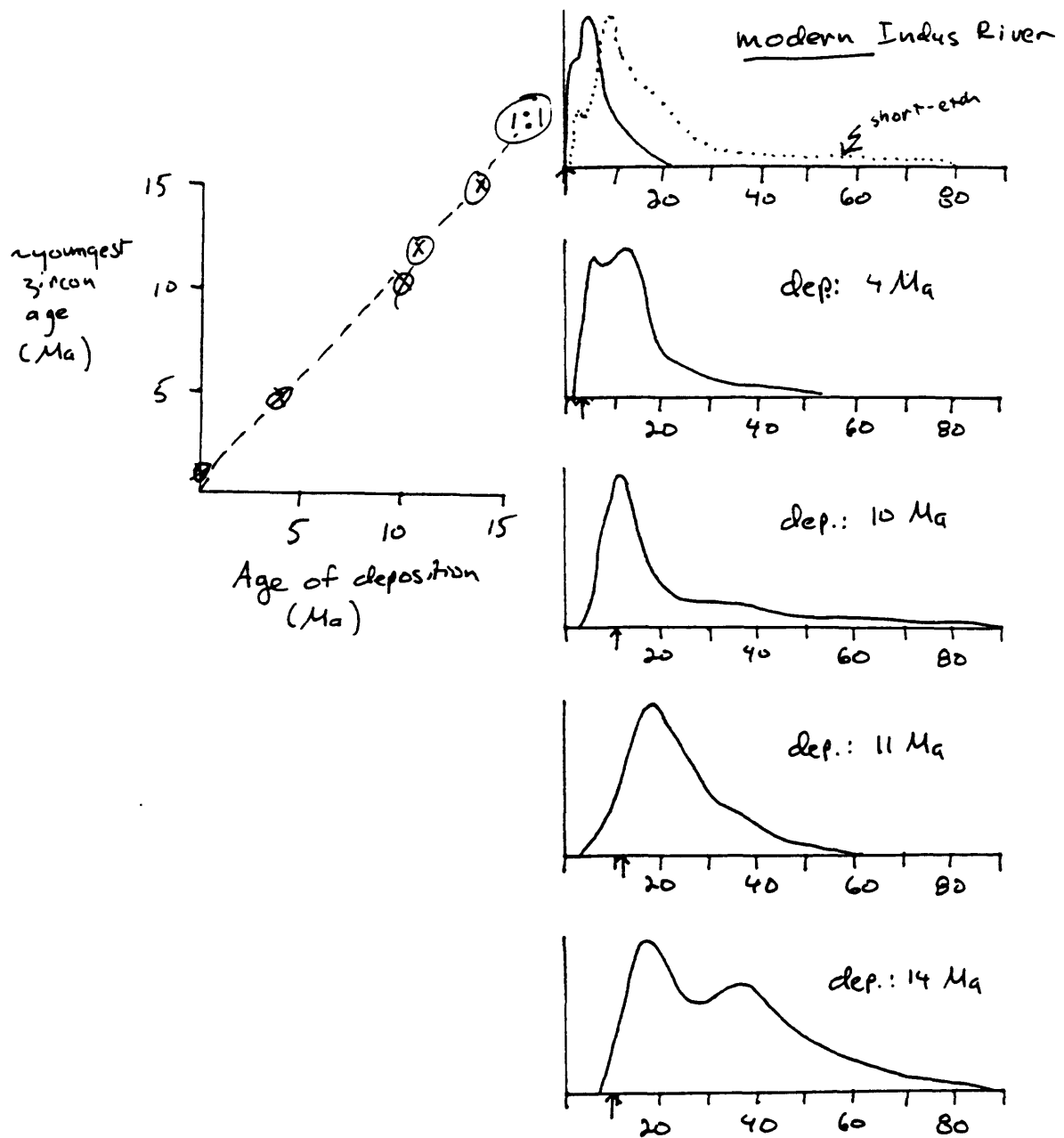
Hurford, A. J., Fitch, F. J., and Clarke, A., 1984, Resolution of the age structure of the detrital zircon populations of two Lower Cretaceous sandstones from the Weald of England by fission-track dating: Geological Magazine, v. 121, p. 269-277.

Johnson, N.M., Opdyke, N.D., Johnson, G.D., Lindsay, E.H., & R.A.K. Tahirkheli, 1982, Magnetic polarity stratigraphy and ages of Siwalik Group rocks of the Potwar Plateau. Pakistan: Palaeogeography, Palaeoclimatology, and Palaeoecology, v. 37, p. 17-42.

Johnson, N.M., Stix, J., Tauxe, L., Cerveny, P.F., & R.A.K. Tahirkheli (1985) Paleomagnetic chronology, fluvial processes and tectonic implications of the Siwalik deposits near Chinji Village, Pakistan: Journal of Geology, v. 93, p. 27-40.

Naeser, N. D., Zeitler, P. K., Naeser, C. W. and Cerveny, P. F., 1987, Provenance studies by fission-track dating_etching and counting procedures: Nuclear Tracks, v. 13, p. 121-126.

Zeitler, P. K., 1985, Cooling history of the NW Himalaya: Tectonics, v. 4, p. 127-151.

Zeitler, P. K., Johnson, N. M., Briggs, N. D. and Naeser, C. W., 1982, Uplift history of the NW Himalaya as recorded by fission-track ages on detrital Siwalik zircons (abstract): Program, Symposium on Mesozoic and Cenozoic Geology (60th Anniversary Meeting, Geological Society of China), Bedaihe, China, p. 109.

Zeitler, P. K., Sutter, J. F., Williams, I. S., Zartman, R. E. & Tahirkheli, R. A. K., 1989, Geochronology and temperature history of the Nanga Parbat-Haramosh Massif, Pakistan. In: Malinconico, L. L. and Lillie, R. J. (eds.) Tectonics of the Western Himalaya, Geological Society of America Special Paper 232, p. 1-22.

hinterland

Foreland basin

erosion

Δt_2

Δt_3

Δt_1

uplift

closure isotherm

sample's path through life

① Δt_1 — time spent in unroofing

Δt_2 — time spent in transport

Δt_3 — time spent in burial

② measured age = $\Delta t_1 + \Delta t_2 + \Delta t_3$

→ For orogenic sedimentation, assume $\Delta t_2 \simeq 0$ m.y.

→ determine Δt_3 from mag. strat., paleo... (= age of sed.)

∴ $\Delta t_1 \simeq$ measured age $- \Delta t_3$

1. Cartoon showing the schematic particle path of a mineral grain through a young orogen.

93

The figure contains the following handwritten labels:

- modern Indus River
- short-etch
- youngest zircon age (Ma)
- 1:1
- Age of deposition (Ma)
- dep: 4 Ma
- dep.: 10 Ma
- dep.: 11 Ma
- dep.: 14 Ma
- note: long-etch data (biased against old ages)

2. Detrital-age spectra for zircons entrained in Siwalik Group sandstones, Trans-Indus region, western Potwar Plateau, Pakistan (data from Cerveny et al., 1988). Age spectra as measured, uncorrected for stratigraphic age. Data are for samples treated using a long etching time; this procedure was designed to ensure that the youngest samples would be sufficiently etched to give good ages. Note that each stratigraphic horizon contains very young zircons whose ages are close to depositional age. As the Siwalik section is at most 3 km thick, and the closure temperature of zircon is ~200°C, thermal resetting is not a viable explanation for this observation.

94

Detrital to Prograde: Pelham dome, central Massachusetts
(R.D. Tucker)

Sedimentary rocks are sensitive indicators of their depositional environment, and their age and provenance are essential constraints to tectonic models of a region. Zircon is a common detrital constituent of most arenites, and it is both a retentive and refractory mineral capable of retaining reliable isotopic age information through crustal recycling events. Because a single grain of zircon may be dated precisely (*e.g.* ± 4 Ma), a spectrum of detrital-grain ages can help to characterize the source rocks of a sedimentary sequence, or to constrain the maximum age of deposition (*i.e.* the age of the youngest detrital grain). In the case of recrystallized and intruded stratified sequences, the minimum age of the sequence may be further constrained by the age of metamorphic minerals or cross-cutting igneous intrusions. Age information of this type may prove invaluable to the geologist interested in on defining the depositional age of sedimentary rocks devoid of fossils, or on resolving the source rocks or terrane affinities of allochthonous sedimentary sequences.

Geologic Setting

A detrital zircon dating study of the metamorphosed quartz-arenites and quartz-wackes in the Pelham dome, central Massachusetts, serves as a useful demonstration of the power of the single-grain dating technique. These sedimentary and intercalated felsic volcanic rocks are the structurally deepest strata exposed in the Bronson Hill antilinorium, and they represent a supracrustal sequence of Late Proterozoic age but whose provenance and terrane affinity is largely unknown (Fig. 10). The stratigraphically deepest unit, the Dry Hill Gneiss, is interpreted by Peter Robinson and workers as a metamorphosed alkali rhyolite (Hodgkins 1985) and it has yielded a U-Pb zircon age of 613 ± 3 Ma (Tucker and Robinson 1990). The Dry Hill Gneiss is overlain gradationally by a thick sequence of metamorphosed sedimentary rocks, including the Poplar Mountain Gneiss, consisting of metamorphosed arkose and quartzite, and its presumed southern-facies equivalent, the Mt. Mineral Formation comprising pelitic schist, quartzite, and amphibolite. The age, tectonic affinity, and metmorphic history of each of these formations is an intriguing issue to geologists of the New England Appalachians as some consider these rocks to be part of Avalon (formerly Africa) that collided with Laurentia in Late Ordovician (Robinson and Hall 1980), Devonian (Osberg 1978), or possibly Carboniferous time (Zen 1983, Wintsch and Sutter 1986, Gromet 1989), whereas others consider it a fragment of Laurentia (McKerrow *et al. in press*) and the stratigraphic "basement" to the Late Ordovician Bronson Hill volcanic arc.

One goal was to define the crystallization age of the volcanic rocks (Dry Hill Gneiss) which have an inherited zircon component, an igneous zircon generation, as well as a component of secondary Pb-loss imposed during kyanite-staurolite grade metamorphism: the challenge here was to remove the component of secondary Pb-loss, and to isolate and analyze as much of the young igneous component, as well as the old inherited component, as possible to attain end-member ages. Another goal was to constrain the depositional age of the stratigraphically highest sedimetary rocks (Poplar

Mtn. and Mt. Mineral formations) which are devoid of fossils, and for which a late Precambrian age is presumed. The last goal was to establish the probable range of source rocks of the sedimentary sequences, through a program of single-grain zircon dating, in the hope that their respective source terranes and provenances may be better understood. As a check of the internal consistency of the results, a number of experiments were designed within the framework of the study so that certain geological interpretations could be tested or eliminated altogether.

Age of the Dry Hill Gneiss and Inherited Zircon Components

Two samples (A and B) of the Dry Hill Gneiss were dated by the multigrain U-Pb zircon technique: one sample (A) yielded an simple discordia with an uppper intercept age of 613 ± 3 Ma interpreted as the crystallization age of the rhyolite protolith. Multigrain zircon analyses of the other sample of Dry Hill Gneiss (B), however, demonstrates the presence of inherited zircon having a minimum average age of 1402 Ma (Fig. 11, Tucker & Robinson 1990). The discordia in the latter sample is defined by five multigrain fractions, with an upper-intercept age of ca. 1747 Ma, which could be interpreted as a mean age of an inherited zircon component if all grains consist of a two-component mixture without an appreciable amount of secondary Pb-loss. Titanite from both samples of Dry Hill Gneiss is concordant at ca. 293 Ma, interpreted as the time of titantite growth, and five zircon analyses from another nearby sample of Dry Hill Gneiss are colinear with a lower-intercept age of ca. 300 Ma, suggesting profound Pb-loss or metamorphic overgrowths at that time.

The presence of inherited zircon was borne-out by etching experiments of polished grain mounts which clearly show their composite nature. To test for the possible presence of inherited components of many ages, 15 single zircon grains were analyzed individually from sample B of the Dry Hill Gneiss which indicated the presence of inherited zircon (Fig. 11).

Figure 11 demonstrates that the inheritance consists of many ages as seen by the resolvable and very different ^{207}Pb/^{206}Pb ages in 15 analyses. Two grains yielded near concordant analyses at the known eruption age of the gneissic protolith (ca. 613 Ma) whereas another two yielded near concordant analyses at the known time of regional metamorphism (ca. 300 Ma, Tucker *et al.* 1988, Tucker and Robinson 1990, Gromet 1989). The latter analyses have depleted Th/U ratios (0.02) suggesting that they are, indeed, single grains of metamorphic zircon containing only a minute component of inheritance (*ca.* 600 Ma or older). All other analyses are grossly discordant with much older ^{207}Pb/^{206}Pb ages, suggesting that they consist of an inherited zircon component with an igneous or metamorphic overgrowth. Because the analyses of known igneous age (*ca.* 600 Ma) have experienced only a trace amount of Pb-loss, it is posssble to *approximate* the inheritance ages by constructing chords through groups of discordant analyses from the range of near primary ages. This method of estimation suggests that three groups of inheritance ages are present: Group I 2850-2550 Ma; Group II 2150-1850 Ma; Group III 1350-1220 Ma.

Detrital Grain Results - The Pelham and Dunlop Brook Quartzites

Two quartzites within the Dry Hill Gneiss (the Pelham Quartzite) were sampled (Fig. 10) which are assummed to have been deposited *ca.* 613 m.y ago, the known age of the Dry Hill Gneiss. Twenty-three of the thirty detrital zircon analyses shown in Fig. 12 are less than 5% discordant indicating that secondary Pb-loss has been nearly eliminated (in rocks of kyanite-staurolite grade) and that the ^{207}Pb/ ^{206}Pb ages are dates of their source rocks, not minimum ages. The sample from Dunlop Brook contained detritus of Archean age, and the age distributions in both samples suggest that the zircon detritus matches closely age groups I,II, III defined above (Fig. 11). No young (< 895 Ma) zircon detritus was discovered in thirty analyses, not even that of the Dry Hill Gneiss with which the quartzites are intecalated; hence their source rocks were probably not of Avalonian or Pan-African affinity. Moreover, two widely separated samples of Pelham quartzite produced reproducible detrital grain ages, indicating that the age groups (I, II, and III) are a reliable signature of the provenance, which was apparently dominated by Archean, and Early to Middle Proterozoic plutonic rocks. Two analyses have model Th/U ratios of 0.07-0.02,suggesting that they were derived from high-grade (granulite facies?) metamorphic rocks (or possibly pegmatites) depleted in thorium (with respect to uranium) over normal igneous values.

Detrital Grain Results - The Mt. Mineral and Poplar Mtn. Quartzites and the Poplar Mountain Gneiss

The detrital zircon ages in the stratigraphically higher quartzites show some similarities with those in the Pelham Quartzites, but also significant differences (Fig. 13). The upper Mt. Mineral quartzite (Fig. 13) yielded a range of detrital zircon ages, most of them concordant, between ca. 1151 Ma and 439 Ma, including detritus of *ca.* 684-604 Ma. Three replicate analyses of the youngest grains, between 454-439 Ma, attest to a distinctive source terrane of this age, most probably the nearby Bronson Hill volcanic arc which has dated rocks between the ages of 465-441 +3/-2 Ma (Tucker and Robinson 1990). The upper Mt. Mineral and Poplar Mtn. quartzites also contain *ca.* 585-600 Ma (Avalonian?) detritus, as well as somewhat older ca. 1540-950 Ma (Grenvillian?) detritus, but not Early Proterozoic and Archean detritus as was found in the Pelham quartzite samples (above). A different age and provenance is thus implied.

The upper Mt. Mineral and Poplar Mtn. quartzites must be Silurian or younger and not late Precambrian as previously presumed. These younger quartzites rest between Proterozoic Dry Hill Gneiss (below) and Late Ordovician gneisses (above, Fig. 10), and hence the interior of the Pelham dome may be a window beneath a major thrust or fold nappe. The upper Mt. Mineral and Poplar Mtn. quartzites contain metamorphic monazite with a U-Pb age of *ca.* 298 Ma, consistent with nearby U-Pb titanite and zircon ages, indicating that a broad area within and outside of the dome was subjected to metamorphic resetting and pegmatite injection in Carboniferous time. This Late Paleozoic recrystallization and deformation episode extends only a short distance east of the Kempfield anticline (Fig. 10), and thus the kyanite-staurolite metamorphic zone within and north of the Pelham dome is a region of Carboniferous metamorphism and deformation superposed on an earlier Devonian pattern not yet fully deduced.

These data demonstrate the power of single-grain zircon dating as a tool to determine the provenance and depositional age of sedimentary rocks, metamorphosed to amphibolite facies grade and devoid of identifiable fossils. Not only has it proved possible to resolve the source-rock ages for kyanite-grade quartzites, but the data demonstrate that petrographically distinctive quartzites are of vastly different age *and provenance*. This discovery has resulted in a dramatic reinterpretation of the local geology, and it is forcing regional geologists to rethink their models concerning the timing of collisional events between Avalonia and Laurentia in the northern Appalachians.
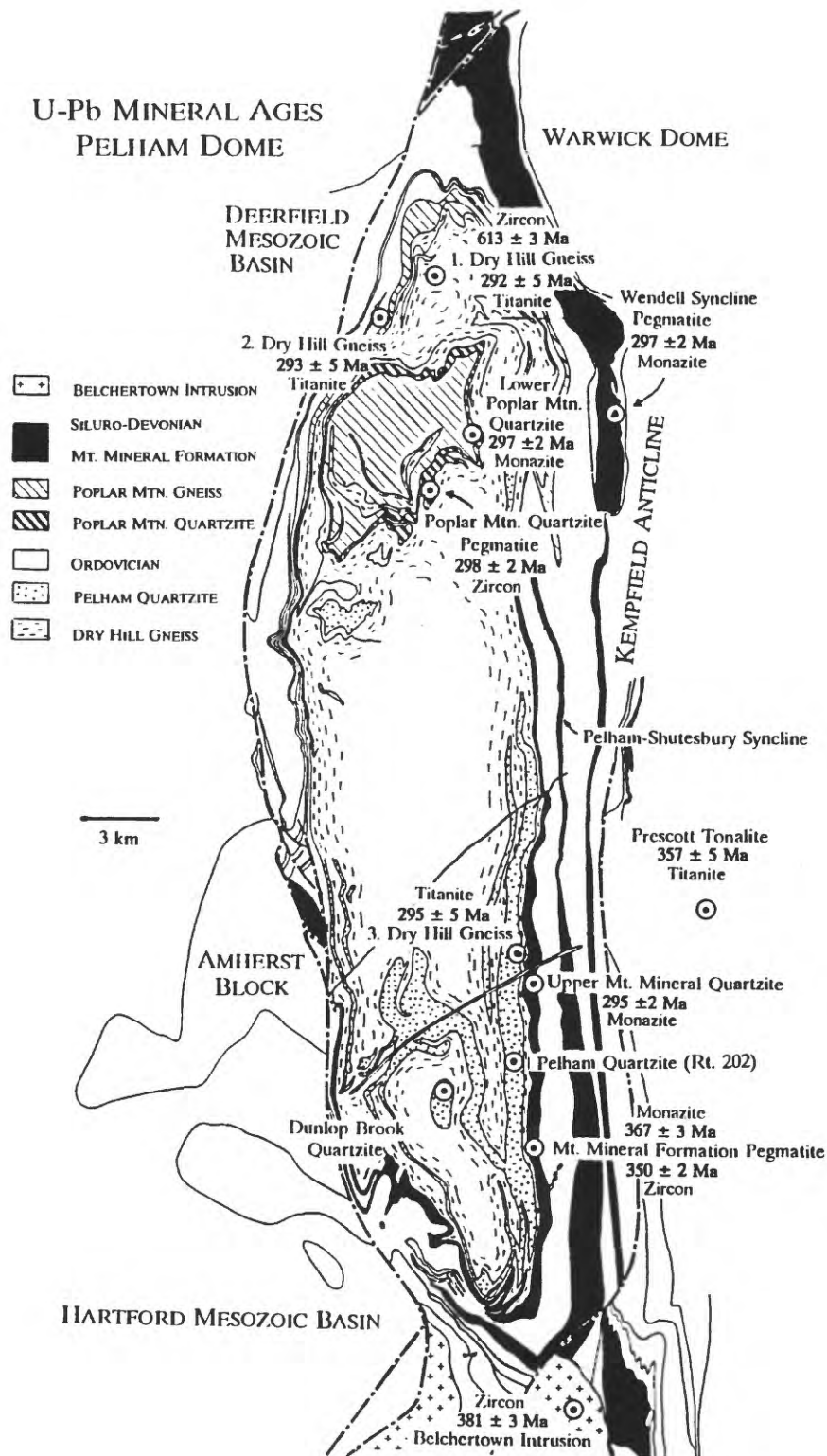
FIGURE 10. Simplified geological map of the Pelham dome, showing the distribution of rock units, grouped according to age, as well as sample localities discussed in the text.

Assignment of a Siluro-Devonian age to the Mt. Mineral Formation is based on the occurrence of Late Ordovician-Early Silurian zircon detritus in the upper quartzite member; Siluro-Devonian strata outside of the dome include the Clough, Fitch, Littleton, and Erving formations. The Pelham quartzites are presumed to be of late Precambrian age, but the Poplar Mtn. gneiss and quartzite are only known to be younger than ca. 584 Ma (age of the youngest detrital grain) and older than 298 Ma (time of metamorphism and pegmatite emplacement).

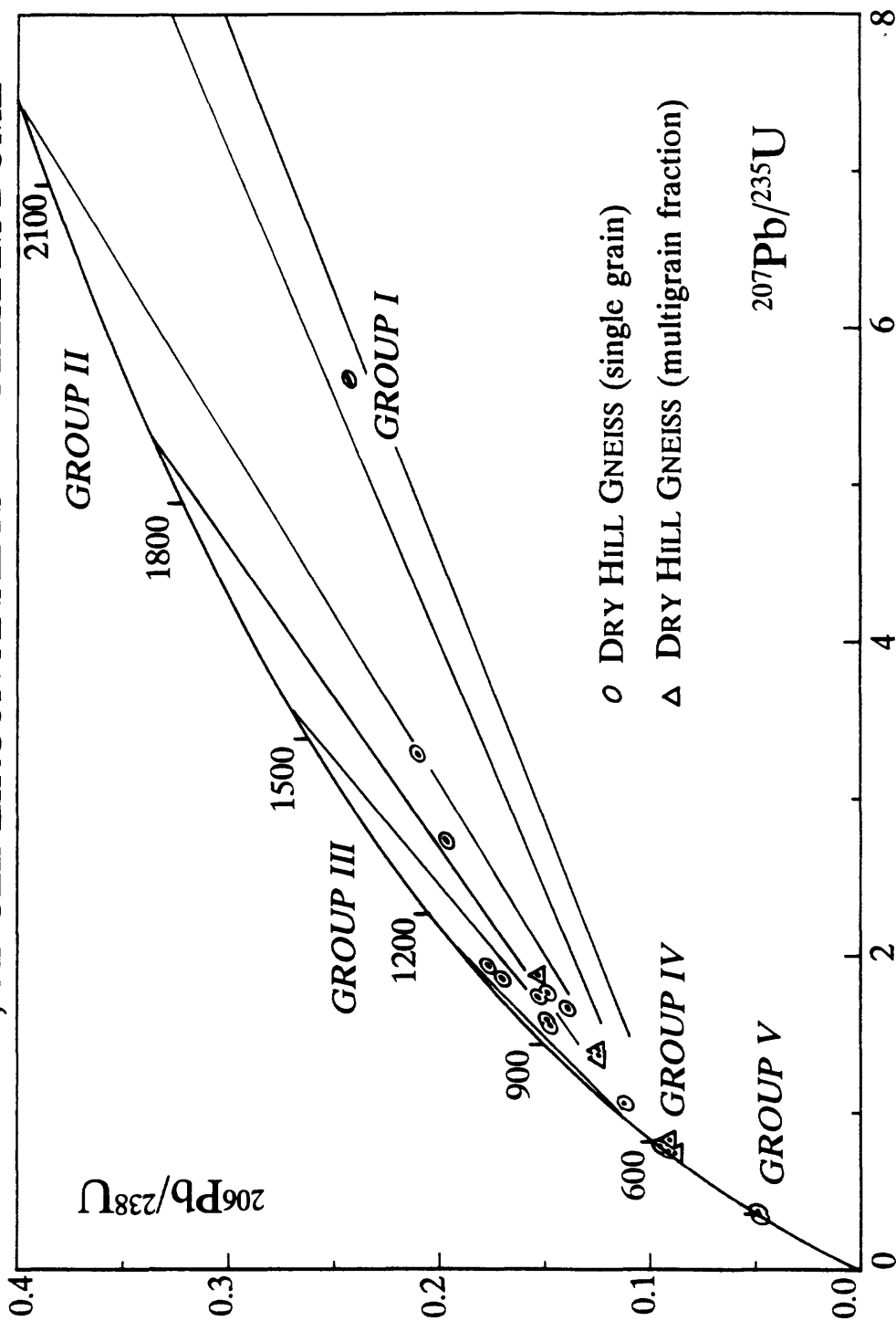# COMPOSITE, SINGLE ZIRCON ANALYSES - PELHAM DOME

FIGURE 11. Concordia diagram of multigrian zircon analyses (triangles) and single-grain zircon analyses (ellipses) from the late Precmabrian (c. 613 Ma) Dry Hill Gneiss, Pelham dome. Multigrain analyses suggest a *mean* minimum age of inheritance of 1407 Ma, whereas single-grain analyses demonstrate that inherited zircon cores with ages ranging between 2850-2550 Ma, 2150-1850 Ma, and 1510-1000 Ma are present. Note two other groups at *ca.* 600 ma and 300 Ma, the known time of igneous emplacement and regional metamorphism, respectively (Tucker and Robinson 1990).
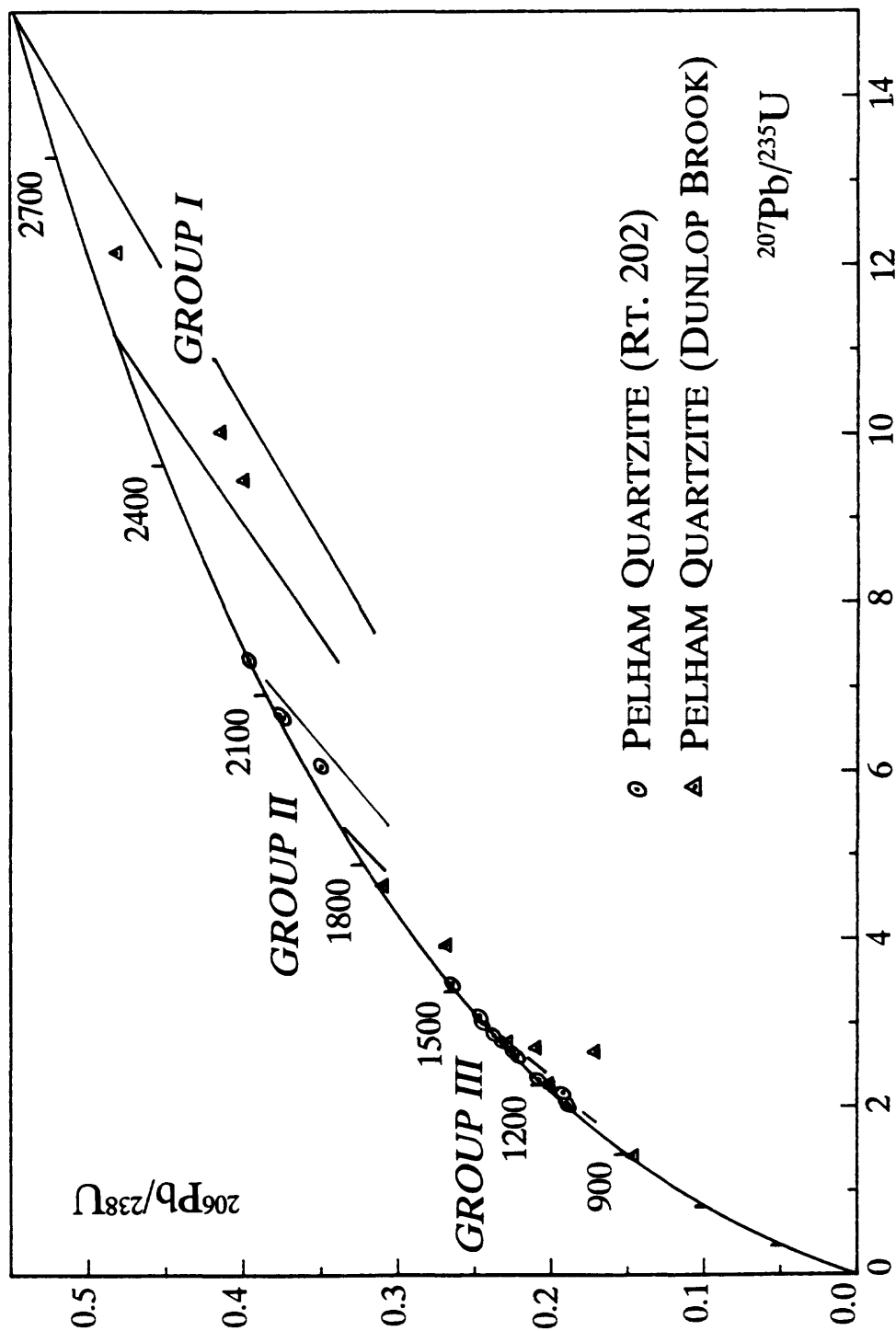
DETRITAL ZIRCON ANALYSES - PELHAM DOME

FIGURE 12. Concordia diagram of single detrital zircons from metamorphosed quartzites (Pelham quartzites) intercalated with late Precambrian Dry Hill Gneiss, Pelham dome, central Massachusetts. Note the near concordance of many analyses, and the replication of age groups defined by the inherited components in composite zircons of the Dry Hill Gneiss (Fig. 11). No young (<895 Ma) detritus was found in 30 analyses, and the oldest grain has a *minimum* ($^{207}Pb/^{206}Pb$) age of 2680 Ma.
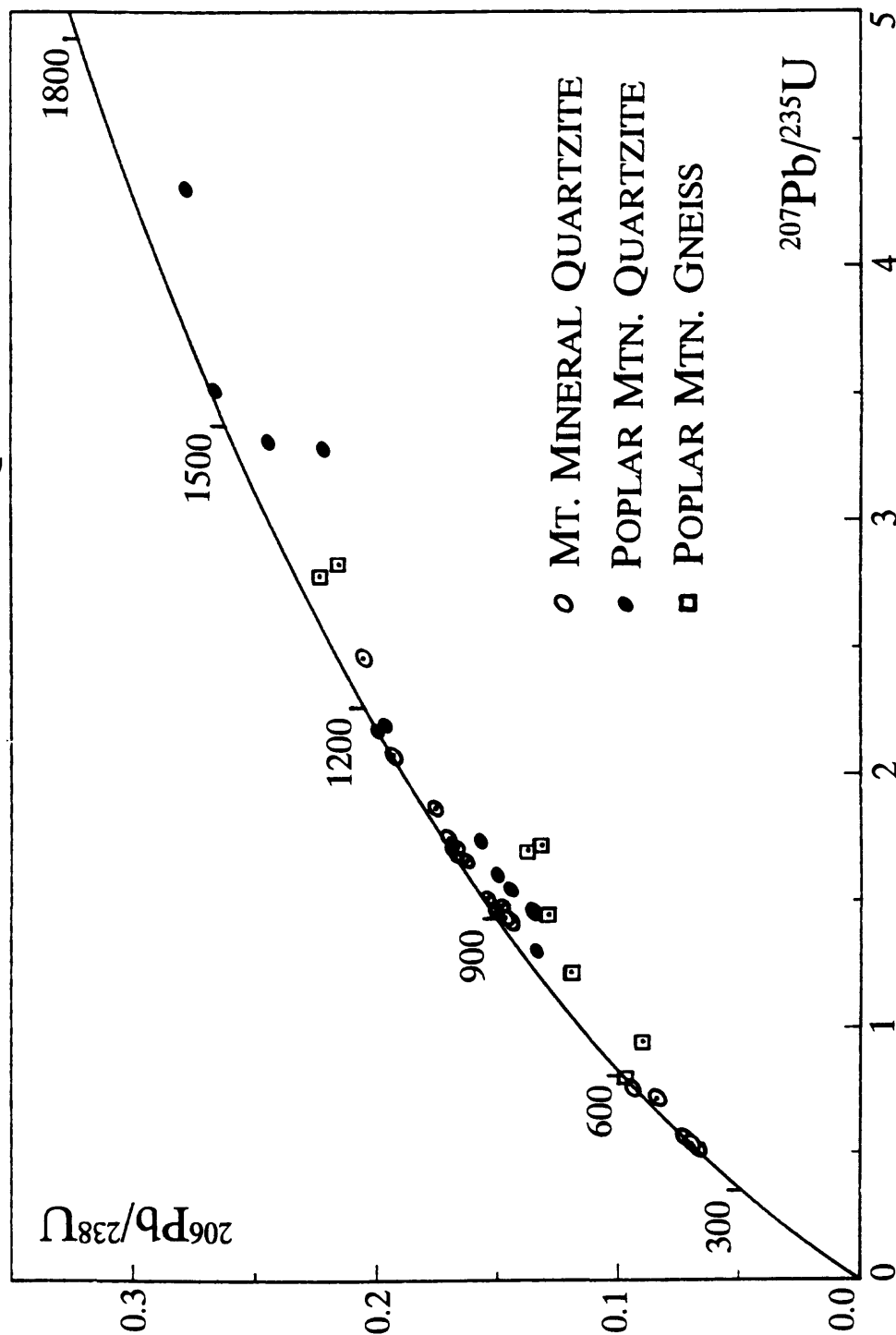
POPLAR MTN. & MT. MINERAL QUARTZITES

FIGURE 13. Concordia diagram of single, detrital zircon analyses from the Poplar Mtn. gneiss and quartzite, and the upper quartzite member of the Mt. Mineral Formation, Pelham dome, central Massachusetts. Most analyses are significantly discordant but, in general, they show slight overlap in age with Group II defined for the Pelham quartzites and Dry Hill Gneiss (Figs. 11 and 12). The majority of concordant analyses from the Poplar Mtn. and Mt. Mineral quartzites indicate that plutonic rocks with ages ranging between 1150-440 Ma were present in their sources.
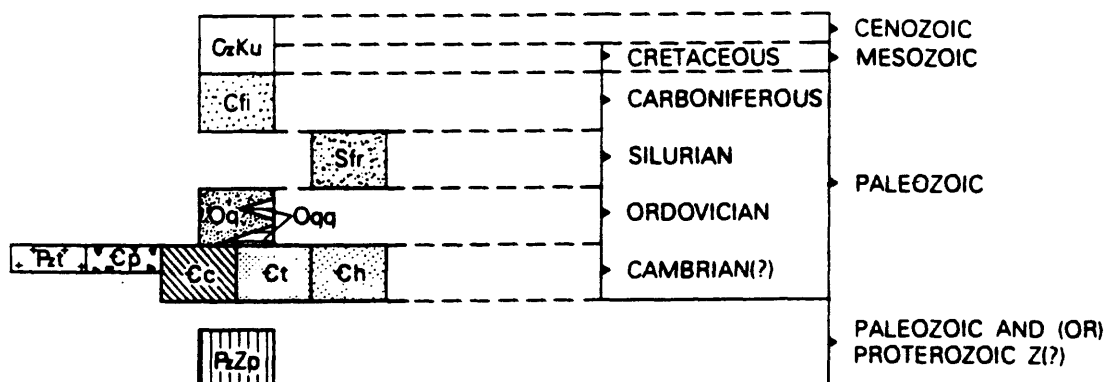
SUTTER, John F., PAVLIDES, Louis, KUNK, Michael J., and
CORTESINI, Henry, Jr., U.S. Geological Survey, Reston, VA 22092
Hornblende $^{40}Ar/^{39}Ar$ ages and cooling-rate studies of muscovite,
biotite, and microcline constrain the age of metamorphism and rates
of uplift in the Piedmont near Fredericksburg. In this area, the
Falls Run Granite Gneiss (FRGG) intruded the Holly Corner Gneiss (HCG),
both were folded, metamorphosed, and then intruded by granitoids of the
Falmouth Intrusive Suite (FIS). Published emplacement ages of 410 Ma
(FRGG) and 300-325 Ma (FIS) bracket the age of deformation and
metamorphism. Regional metamorphic grade in schists (Quantico
Formation) enclosing FRGG and HCG increases from staurolite to
sillimanite. Hornblendes from HCG along this metamorphic gradient
yield ages from 321 Ma (staurolite) to 307 Ma (sillimanite). Assuming
a temperature difference of ~100°C between staurolite and sillimanite
grades, and a constant argon closure temperature for hornblendes along
this gradient, we calculate a slow, postmetamorphic cooling rate of
~7°C/Ma. The argon closure temperature in hornblende at this cooling
rate is probably ~500°C, not far below the lower temperature for
staurolite stability, and thus we interpret the 321 Ma age for
hornblende in staurolite grade rocks to suggest the metamorphism is
Alleghanian. Age spectra for muscovite, biotite, and microcline show
the ~7°C/Ma rate persisted until ~265 Ma. Diffusion gradients in
microcline suggest rocks of the study area cooled from ~130°C starting
at 265 Ma to ~100°C at 243 Ma, a very slow rate of <1.5°C/Ma. This
pronounced change in cooling (uplift?) rate could be related to the
change from convergent to extensional tectonics along this portion of
the eastern margin of North America.
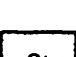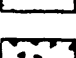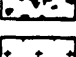
FLOHR, M.J.K. and PAVLIDES, L., U.S. Geological Survey,
National Center 959 (MF) and 928 (LP), Reston, VA 22092
Schists of the Ordovician Quantico Formation (QFS) lie within a refolded
synform in the Piedmont west of Fredericksburg, VA. Metamorphic grade in
these pelitic schists increases from low staurolite on the northwest (NW)
to sillimanite on the southeast (SE). Electron-microprobe compositions
of garnet and coexisting matrix biotite, muscovite, and plagioclase were
obtained from 7 schists collected along this metamorphic gradient. The
easternmost and highest-grade schist came from the metavolcanic Ta River
Metamorphic Suite (TRMS). The Ferry-Spear geothermometer, modified by
Hodges and Spear, and the Ghent and Stout geobarometer were used to
calculate metamorphic temperatures (T) and pressures (P), respectively.

Garnets from QFS are normally zoned with Fe- and Mg-richer rims and
Ca- and Mn-richer cores; garnet from the TRMS sample shows reverse
zoning. Along the NW- to SE-increasing gradient, using garnet core
compositions, T ranges from 487°C on the NW to 615°C on the SE (±50°)
for QFS samples and P ranges from 4.3 to 4.8kb ±1kb for 6 of these
samples; one yielded an anomalous P of 6.7kb. The TRMS sample gave an
unreasonable T of >800°C. A T gradient also was obtained using garnet
rim compositions, with T ranging from 499°C on the NW to 565°C on the SE
(±50°C) for QFS; P ranges from 3.6 to 4.5kb ±1kb. T of 632°-670°C was
calculated for the TRMS sample and although these values are more
uncertain because of the high MnO content of the garnet rims (up to 7.7
wt. %), they are consistent with the trend defined by QFS samples. No
correlation of P with metamorphic gradient was found using either garnet
core or rim compositions. Published hornblende $^{40}Ar/^{39}Ar$ plateau ages
determined for the Holly Corner Gneiss, which is enclosed by QFS, range
from 321 Ma on the NW to 307 Ma on the SE along a closely similar
traverse of the same metamorphic gradient. The general increase of T
from NW to SE, coupled with the general decrease in hornblende ages,
supports a coeval Alleghanian metamorphic event for both formations.

77°37'30" 77°30'00"

38°22'30"

38°15'00"

€p
€c
€c
Oqq
€t
C$_z$Ku
Sfr
€c
Oqq
€h
Berea
Sfr.
€h
Cfi
Oq
Oq
Rappahannock
C$_z$Ku
€h
Sfr
Cfi
Oq
Oq
€h
€h
Sfr
River
Cfi
Oqq
Cfi
C$_z$Ku
€h
C$_z$Ku
€t
Oqq
Oq
C$_z$Ku
€t
Oq
Oq
€t
C$_z$Ku
Oqq
Ni River Res
P$_z$Zp
Sfr
€t
C$_z$Ku
€t
C$_z$Ku
P$_z$Zp
C$_z$Ku
P$_z$Zp
Fredericksburg

SPOTSYLVANIA LINEAMENT

Spotsylvania

0   1 MILE
0   1 KILOMETER

Sk	St
S.C.	F
Sa	

Area of figure 1

7½' QUADRANGLES

Sk - Storck   F - Fredericksburg
St - Stafford   Sa - Spotsylvania
S.C. - Salem Church

104

EXPLANATION

CzKu			CENOZOIC
		CRETACEOUS	MESOZOIC
Cfi		CARBONIFEROUS	
Sfr		SILURIAN	PALEOZOIC
Oq ⊳ Oqq		ORDOVICIAN	
Pzf ⟋€p	€c €t €h	CAMBRIAN(?)	
PzZp			PALEOZOIC AND (OR) PROTEROZOIC Z(?)

CzKu — Coastal Plain sediments: Unconsolidated, upland sand and gravel, terrace, and alluvium and swamp deposits.

Cfi — Falmouth Intrusive Suite: Dikes and sills and small plutons of fine- to medium-grained granitoids, mainly monzogranite to granodiorite and less commonly tonalite.

Sfr — Falls Run Granite Gneiss: Coarse-grained, well foliated, microcline granite gneiss.

Oq / Oqq — Quantico Formation: Gray to black graphitic slate and phyllite to staurolitic schist and biotite-muscovite garnetiferous schist in areas of increased metamorphism. Lenses of micaceous quartzite occur within and locally at its base.

€c — Chopawamsic Formation: Chiefly metavolcanic rocks of felsic, intermediate and mafic compositions interlayered with lesser amounts of meta-epiclastic volcanic rocks and schist.

€t — Ta River Metamorphic Suite: Chiefly amphibolite and amphibolitic gneiss with lesser amounts of biotitic gneiss and schist. In southwest corner of Stafford Quadrangle it includes a large mass of granodiorite gneiss.

€p — Plagiogranitic metatonalite: Medium- to coarse-grained leucocratic to mesocratic quartz-rich meta-intrusive granitoid.

Pzt — Trondhjemitic metatonalite: Fine-grained, allotriomorphic granular, leucocratic granitoid, locally having granophyric texture.

€h — Holly Corner Gneiss: fine- to medium-grained, well foliated, hornblende-biotite gneiss.

PzZp — Po River Metamorphic Suite: Chiefly biotite gneiss with lesser amounts of hornblende gneiss and schist.

Contact — Commonly inferred, dotted where concealed.

Faults — Commonly inferred, dotted where concealed.

Overturned   Upright

Antiform — Showing trace of crestal plane and direction of plunge. Dotted where concealed.

Overturned   Upright

Synform — Showing trace of trough plane and direction of plunge. Dotted where concealed.

105
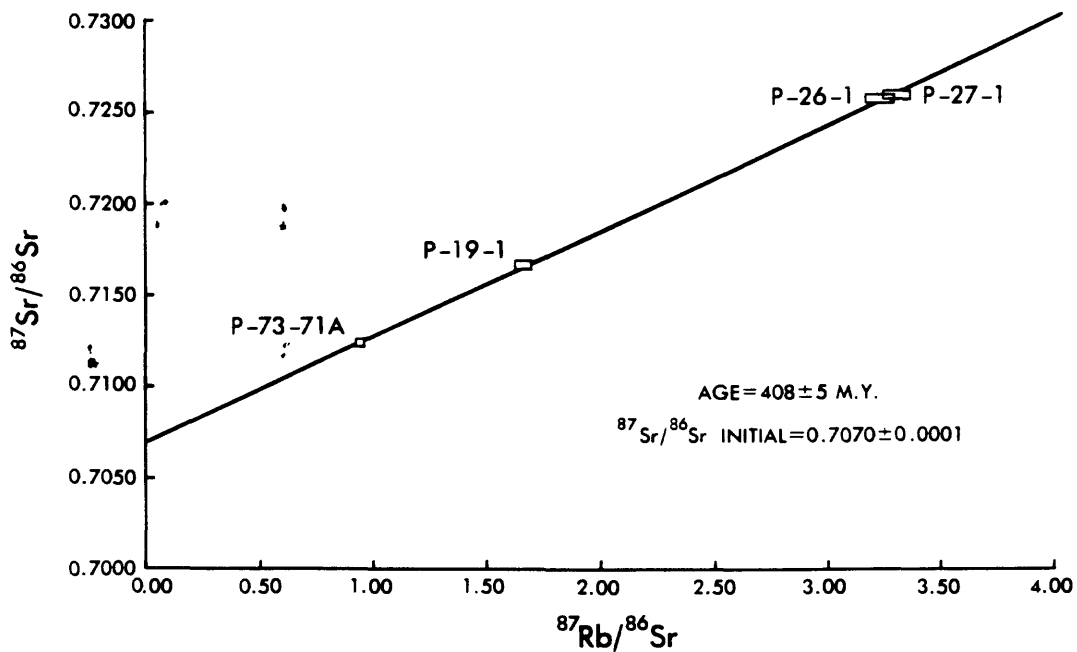
FIGURE 2. – Rb-Sr isochron diagram for the Falls Run Granite Gneiss. For analytical data on samples, see table 2.
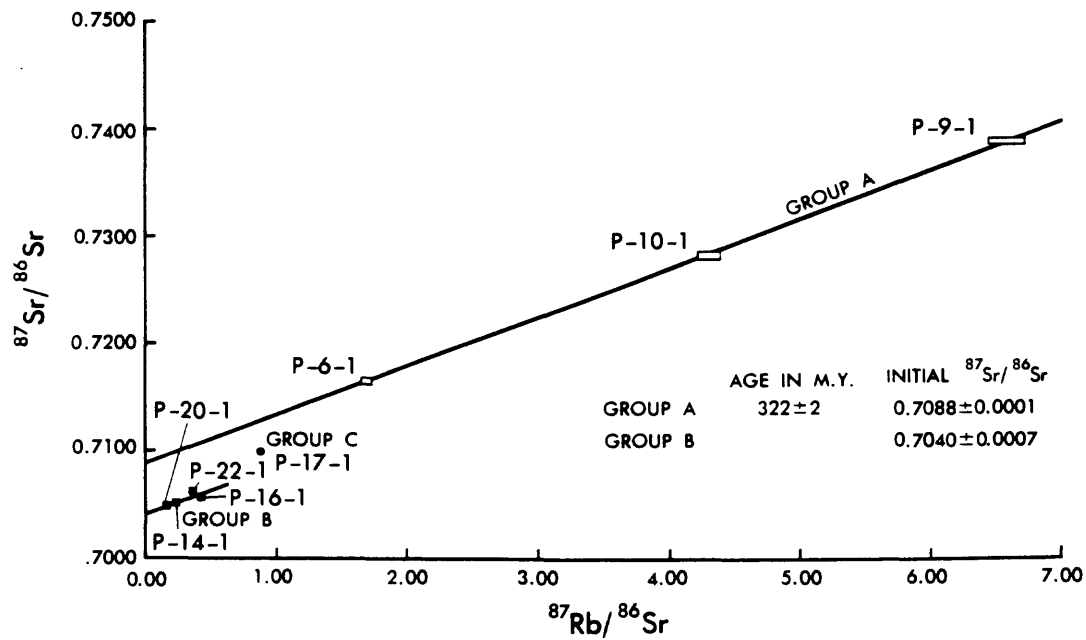
FIGURE 3. – Rb-Sr isochron diagram for the Falmouth Intrusive Suite. For analytical data on samples, see table 2.

HOLLY CORNER GNEISS (€h)

[Regional Gradient - HBL]

NW

Map No.	Sample No.	40/39 Plateau Age
1	72-167	321.3 ± 1.1
2	73-70	319.3 ± 1.2
3	73-66	319.5 ± 1.2
4	75-24	316.1 ± 1.2
5	75-37	318.0 ± 1.1
6	72-140	314.9 ± 1.2
7	75-5	312.3 ± 0.9
8	74-51	306.8 ± 0.9

SE

Increasing Metamorphic Grade

Point Cooling Data:

Age (Ma)

NW End of Traverse:
(9)

HBL = 320
Biot = 297
$Micro_{max}$ = 268
$Micro_{min}$ = 247

SE End of Traverse:
(10)

HBL = 307
MUSC = 282
BIOT = 283
$Micro_{max}$ = 265
$Micro_{min}$ = 243

107

Blank

.

IV - TECTONIC DEVELOPMENT/MINERALIZATION

Avalonian Crustal Assembly
(R.D. Tucker)

The capability to obtain precise isotopic ages of many igneous rocks over most of geological time has increased greatly the ability to resolve geological events on a regional and global scale. An example is given below where the U-Pb method, together with well-established field relationships, has defined precisely the duration of crust-formation and assembly events in the Appalachians of maritime Canada and thereby tested the validity of widely-held plate tectonic models.

The northwest limit of Avalonian (late Precambrian) igneous rocks in Newfoundland has been drawn historically at the Dover Fault and its presumed southern equivalent, the Hermitage Fault (Fig. 14), with the view that Avalon was first juxtaposed with interior elements of the Eastern Crystalline Belt (formerly the Gander and Dunnage Zones, Williams *et al.* 1990) in middle Devonian time, prior to emplacement of the Ackley granite batholith (Dallmeyer *et al.* 1981). New U-Pb isotopic ages (Dunning *et al.* 1990, O'Brien *et al. in press*, Tucker *et al. in prep*) and detailed field mapping (O'Brien and O'Brien 1990) in the region of the Hermitage Flexure and Hermitage peninsula, however, require drastic re-thinking of the model of the Avalon Composite Terrane and its collison with post-Taconia North America. The major results of this research are summarized below and in Figure 15.

Timing of Crustal Assembly, South Newfoundland

1) Detailed mapping and precise geochronology south of the Bay d' Est Fault (Fig. 14) has led to the discovery of an Early-Late Silurian (429 ± 2 Ma to 422 ± 2 Ma) terrestrial volcano-sedimentary succession (the redefined La Poile Group) which rests with local unconformity upon a late Precambrian composite, granitic basement complex (578 ± 10 Ma, the Roti Intrusive Suite), itself intrusive into older amphibolitic gneiss (Grey River Gneiss, 686 +33/-15 Ma) and low-grade sedimentary and volcanic rocks. This composite sub-La Poile Group basement complex (sLPBC) also contains Early Ordovician (495 ± 2 Ma, Ernie Pond Gabbro) intrusive rocks that define the minimum age of pre-Silurian tectonothermal events within the complex (Fig. 15).

2) U-Pb geochronology of key volcanic and plutonic rocks in the type Avalon Zone east of the Hermitage Fault, establishes the synchroneity of Precambrian depositonal, magmatic, and tectonothermal events there with events in the sLPBC (above), thus demonstrating the broader Avalon affinity of the sLPBC. The northwest limit of the sLPBC is the Bay d' Est Fault which places the sLPBC and its Silurian volcano-sedimentary cover over medial Ordovician Dunnage Zone rocks. Juxtaposition of the western margin of Avalon (*s.s.*) with the Dunnage Zone was essentially complete by 420 +2/-1.8 Ma, the time of emplacement of a post-thrusting Late Silurian granite porphyry (Hawks Nest Pond porphyry) (Fig. 15).

3) U-Pb zircon dating of volcanic and plutonic rocks in the area of the Hermitage peninsula yield a remarkably consistent set of ages, directly comparable with the periods of late Precambrian felsic and mafic crust production across the whole of the type Avalon Composite Terrane. The approximate periods of igneous activity are: 680-670 Ma, 630-605 Ma, and 570-550 Ma. Previous attempts to correlate the late Precambrian igneous and sedimentary sequences on the basis of geochemistry alone have proven to be incorrect, as distinct age differences are demonstrated between geochemically similar rocks. Moreover, a new U-Pb zircon age for a rhyolite flow within the Mooring Cove Formation beneath the Rencontre Formation on Chapel Island, places a reliable *maximum* age of 552 ± 2 Ma for the base of the Cambrian system in the proposed North American stratotype section.

4) The observed leading edge of the Avalon Composite Terrane in the Hermitage Flexure region was the locus of widespread magmatism, deformation, and metamorphism between 430-420 Ma that involved the reactivation of fundamental pre-existing structures, some of them of late Precmbrian age. The record of widespread Early Silurian orogenesis, which signalled the arrival of "Avalon" with the Eastern Crystalline Belt, was followed by the emplacement of Late Silurian plutons associated with high-grade metamorphism and sinistral dextral shearing. This was in turn followed by later phases of brittle dextral transpression (Holdsworth 1991) which probably extended well into the Lower Devonian. The brittle Hermitage and Dover faults are related to these later movements, which are broadly coeval with the formation of Early and Middle Devonian molasse-type basins throughout south Newfoundland. Precise U-Pb zircon ages of 390-377 ± 3 Ma for several plutons which clearly post-date this period of brittle and ductile faulting (Chetwynd, François, Pass Island, and Ackley granites), provide only *minimum* age estimates on the the time of linkage of the Avalon and Dunnage terranes. The U-Pb zircon ages are *ca.* 20 Ma older than previous age estimates of these intrusions determined by $^{40}Ar/^{39}Ar$ age spectrum of igneous hornblende (Dallmeyer *et al.* 1981).

LEGEND

Devonian-Carboniferous: porphyritic granite

Silurian: volcanic and plutonic rocks

Cambro-Ordovician: psammite and pelite

Cambro-Ordovician: sedimentary and volcanic rocks

Precambrian (570-540 Ma): volcanic and plutonic rocks

Precambrian (690-600 Ma): volcanic and plutonic rocks

50 km

Dunnage Zone
Gander Zone
Avalon Zone

Dover Fault

HERMITAGE FLEXURE

D'Eist Fault

Bialy Fault

Hermitage Fault

417 +/-2 Ma
577 +/-3 Ma
P€
410 +/-2 Ma
377 +/-2 Ma
565 +/-2 Ma
672 +/-3 Ma
P€
P€
681 +/-2 Ma
378 +/-2 Ma
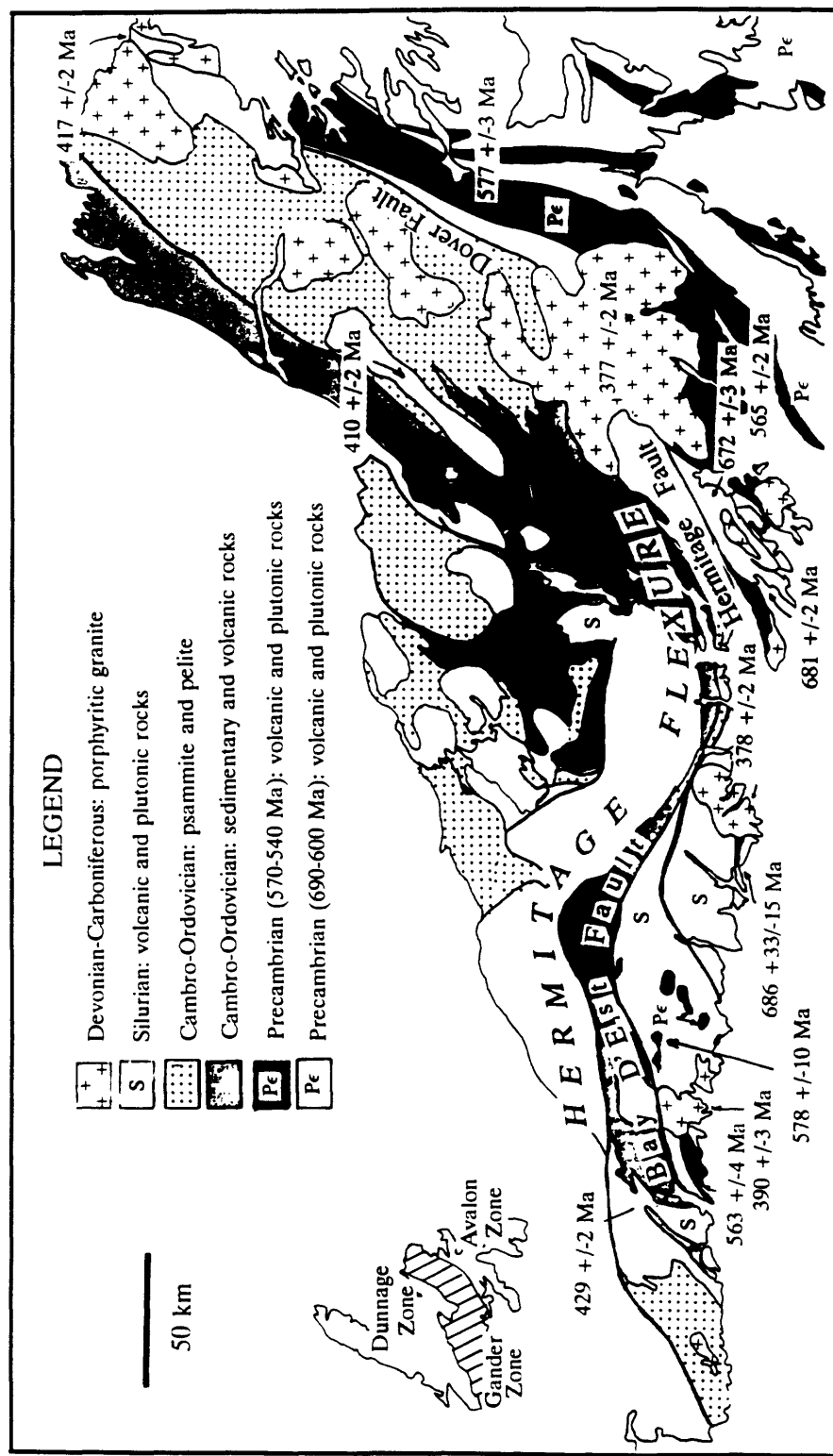686 +33/-15 Ma
578 +/-10 Ma
563 +/-4 Ma
390 +/-3 Ma
429 +/-2 Ma
Pє

FIGURE 14. Geological map of south Newfoundland, simplified after O'Brien and O'Brien 1989, O'Brien et al. *in press*, Dunning *et al.* 1990, and Colman-Sadd *et al.* 1990.
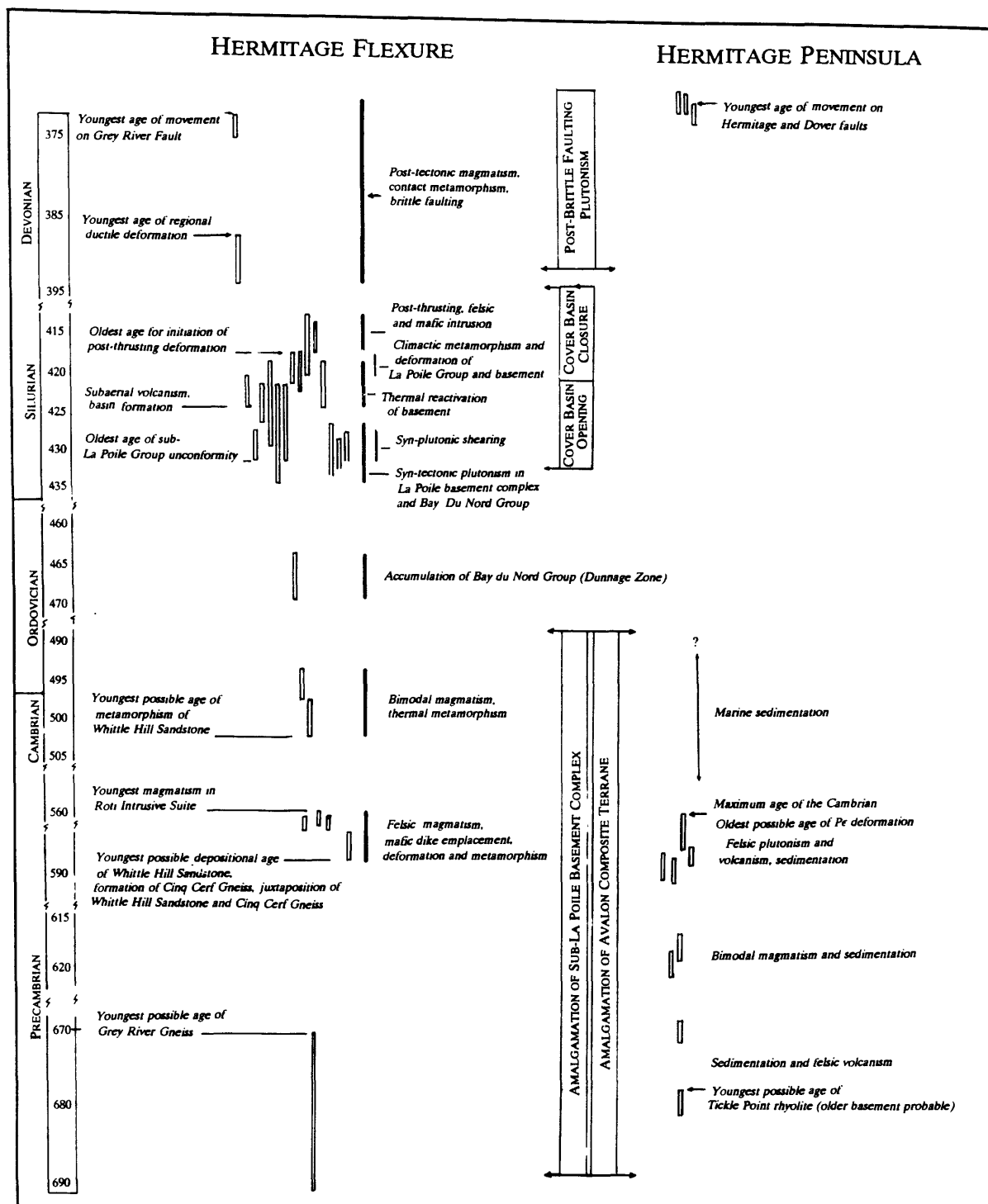
111

FIGURE 15. Timing of major tectonic events in the area of the Hermitage Flexure and Hermitage peninsula. Sources of age information are Dunning *et al.* 1990, Dunning and O'Brien 1989, O'Brien *et al. in press*, and Tucker *et al. in preparation*.

⁴⁰Ar/³⁹Ar and K-Ar data bearing on the metamorphic and tectonic history of western New England

JOHN F. SUTTER
NICHOLAS M. RATCLIFFE } U.S. Geological Survey, Reston, Virginia 22092
SAMUEL B. MUKASA* Department of Geology and Mineralogy, Ohio State University, Columbus, Ohio 43210

ABSTRACT

⁴⁰Ar/³⁹Ar ages of coexisting biotite and hornblende from Proterozoic Y gneisses of the Berkshire and Green Mountain massifs, as well as ⁴⁰Ar/³⁹Ar and K-Ar mineral and whole-rock ages from Paleozoic metamorphic rocks, suggest that the thermal peak for the dominant metamorphic recrystallization in western New England occurred 465 ± 5 m.y. ago (Taconian). Although textural data indicate a complex metamorphic-tectonic history for Paleozoic rocks, no evidence in rocks at least as high as kyanite grade dictates an Acadian age for the Barrovian metamorphism. Available ⁴⁰Ar/³⁹Ar and K-Ar data suggest that the low-grade metamorphism and cleavage formation in Taconic allochthons and the higher-grade metamorphism and emplacement of the Berkshire massif allochthon are Taconian.

⁴⁰Ar/³⁹Ar age data from a poorly defined terrane beginning near the east margin of the Green Mountain massif and extending along the eastern one-third of the Berkshire massif as far south as Otis, Massachusetts, suggest that the area has been retrograded during a metamorphism that peaked at least 376 ± 5 m.y. ago (Acadian).

Available age and petrologic data from western New England indicate the presence of at least three separate metamorphic-structural domains of Taconian age: (1) a small area of relict high-pressure and low-temperature metamorphism in northern Vermont (T-1 domain), (2) a broad area in Vermont and eastern New York of normal Barrovian metamorphism from chlorite to garnet grade and characterized by a gentle metamorphic gradient (T-2 domain), and (3) a rather narrow belt of steep-gradient, Barrovian series metamorphic rocks extending from near the Cortlandt Complex northeastward through Dutchess County, New York, to the Berkshire massif in western Massachusetts (T-3 domain). Areas of maximum metamorphic intensity within the T-3 domain coincide with areas of maximum crustal thickening resulting from imbricate thrusting (Berkshire massif) or from recumbent folding (Manhattan Prong) of remobilized North American continental crust in the later stages of the Taconic orogeny.

INTRODUCTION

The polymetamorphic history of western New England has been the subject of various investigations (see discussion below). This paper is an
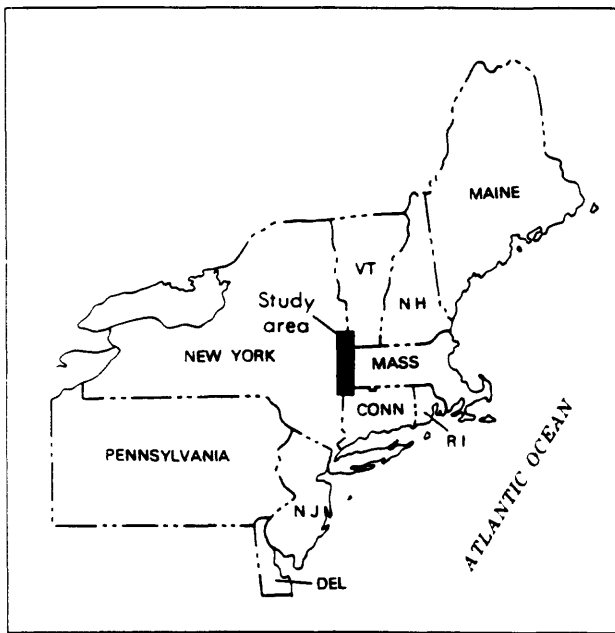
*Present address: Lamont-Doherty Geological Observatory, Palisades, New York 10964.

attempt to integrate all available K-Ar and ⁴⁰Ar/³⁹Ar age data (both published and new results) into a comprehensive picture of the metamorphic history of this area. The general area of study is shown in Figure 1, and data from the following lithotectonic units will be discussed: Taconic allochthons, Green Mountain massif, Berkshire massif, and Paleozoic cover rocks immediately east of the massifs (mainly Hoosac and Rowe-Hawley belts).

Recent geologic studies in western New England have shown that the deformational history of the Taconide belt here is complex. Part of this complexity involves the uncertainty in knowing the relative importance of Taconian as opposed to Acadian dynamothermal effects. About 15 years ago, broad areas of western Massachusetts were thought to have been affected by Acadian metamorphism (Zen, 1967; Ratcliffe, 1969). It was generally agreed that the highest-grade mineral assemblages (garnet to sillimanite zones) are Acadian, although older Taconian features were recognized as important, especially in the chlorite-biotite zone. Large-scale synmetamorphic thrust faulting of the Berkshire massif was recognized, and because the metamorphic isograds of staurolite-kyanite and sillimanite appear to postdate the thrust faulting (Norton, 1967; Ratcliffe, 1965) and seem compatible with thrust-zone textures, this faulting was regarded as Acadian or older.

Recognition of the importance of Taconian metamorphism over a wider area has increased, and structural features have been assigned to the Taconian that formerly were thought to be Acadian. For example, Harwood (1972) observed that a granite of probable Late Ordovician age crosscuts a thrust fault in the Berkshire massif, indicating a Taconian age for at least some of the thrust faults there. Ratcliffe and Harwood (1975) outlined a four-phase Taconian chronology. Formation of crystalloblastic fabrics was important throughout Taconian deformation, but the Taconian deformation and metamorphism culminated in the Middle to Late Ordovician with overthrusting of the Berkshire massif. Northwest-trending F₄ folds developed after the thrusting show evidence of muscovite, biotite, staurolite, garnet, and sillimanite growing across them. Production of these minerals marks, in part, the present distribution of the biotite, garnet, staurolite-kyanite, and sillimanite isograds and previously was assigned to the Acadian (Ratcliffe and Harwood, 1975). The peak of this Barrovian metamorphism was interpreted as Acadian on the basis of (1) the lack of definitive Ordovician ages from any minerals and (2) the proximity of the Berkshire area to Siluro-Devonian strata that are known to have undergone Acadian staurolite-, kyanite-, and sillimanite-grade metamorphism (Hatch, 1975; Norton, 1976). How far west the effects of this Acadian metamorphism extended was not known to Ratcliffe and Harwood

Figure 1. Regional tectonic map and sample locations for new ^{40}Ar/^{39}Ar and K-Ar data presented in this report. (Study area map and explanation are on facing page.)

114

EXPLANATION

(1975). New radiometric age data presented here define the distribution of Taconian versus Acadian metamorphic effects and reveal that the westward extent of Acadian metamorphism is less than previously inferred (Zen, 1967; Ratcliffe, 1969). The new age data also require a revised interpretation of the ages of the various phases of folding and faulting.

SYNOPSIS OF MAJOR TECTONIC FEATURES IN THE TACONIC RANGE AND BERKSHIRE–GREEN MOUNTAIN MASSIFS

Major lithotectonic elements of the region are shown in Figure 1. From structurally lowest to structurally highest, in general from west to east, there are:

A. Precambrian (Proterozoic Y) basement gneiss of the southern Green Mountains and its predominantly Paleozoic clastic-carbonate shelf cover. The suite of autochthonous cover rocks formed as continental shelf sediments on the eastern margin of North America bordering Iapetus. These shelf sediments are capped unconformably by Middle Ordovician black shales and graywacke of the Walloomsac and Snake Hill Formations.

B. Rocks of the Taconic allochthons form the transported part of a preshelf, graben-fill facies and a slope-rise suite of rocks deposited beyond the continental shelf edge in Proterozoic Z through Middle Ordovician time (Bird and Dewey, 1970; Bird, 1975). These allochthons were emplaced starting in the Middle Ordovician, graptolite zone 12–13 (Zen, 1967, p. 68; Berry, 1970). The early allochthons were emplaced as non-metamorphic submarine overthrusts and later ones as progressively harder rock thrusts. The last and tectonically highest slice (Greylock slice) was emplaced synmetamorphically. The Taconic allochthons (other than the Greylock slice) were emplaced prior to imposition of chlorite- through garnet-grade regional metamorphism in the area shown in Figure 1.

C. Proterozoic Y gneiss of the Berkshire massif and its preserved sedimentary cover rocks structurally overlies the carbonate rocks of the autochthon. These rocks were emplaced by thrusting that followed regional metamorphism and cleavage formation in the Taconic allochthons and in the autochthon. The Berkshire massif is separated from the autochthon by major shear zones having a mylonitic fabric. The Berkshire massif consists of multiple, overlapping, and folded fault slices of basement gneiss and intercalated slivers of cover rocks (Ratcliffe and Harwood,
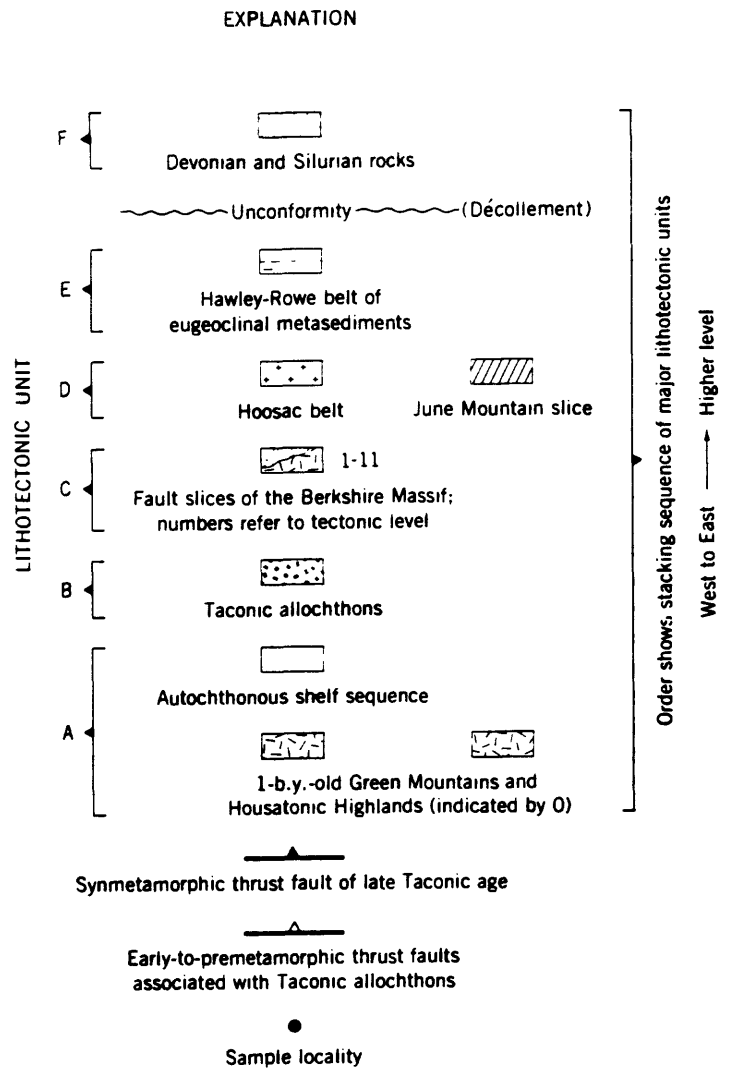
1975) emplaced by strong east-over-west transport that was accompanied by recumbent folding and blastomylonitic fold-thrust fabric. Textures and structures related to the emplacement event have been recognized throughout the massif (Ratcliffe and Harwood, 1975; Ratcliffe and Hatch, 1979, Fig. 5). Translation on the master thrust at the sole of the Berkshire massif is a minimum of 21 km at lat. 42°N (Ratcliffe and Harwood, 1975). Additional structural overlap in the massif accounts for a minimum shortening of the basement by structural overlap of about three times, so that the minimum cumulative overlap of ~60 km is indicated. The leading edge of rocks now representing the Berkshire massif was originally at least 21 km farther east than its present position, and the original width of the massif was at least 60 km.

D. The Hoosac belt east of the Berkshire massif consists of the Proterozoic Z through Cambrian, Hoosac Formation that is transitional in facies between shelf rocks and Taconic slope and rise rocks. These rocks locally rest with unconformity on the highest slices of the Berkshire massif but are largely separated from the basement by a major synmetamorphic detachment zone, the Middlefield thrust–Hoosac Summit thrust.

E. Rowe-Hawley belt: The Hoosac belt is overlain by tectonically intermixed rocks of the Rowe-Hawley belt, containing pods of serpentinite, easterly derived volcanogenic flysch of the Moretown Formation, and Middle Ordovician volcanic rocks and shales of the Hawley Formation. The Whitcomb Summit thrust forms the physical base of this sequence and is believed to conceal the root zone for the Taconic allochthons.

Figure 2. $^{40}Ar/^{39}Ar$ age-spectrum diagrams from Berkshire and Green Mountain traverses. Sample localities shown in simplified version of Figure 1.

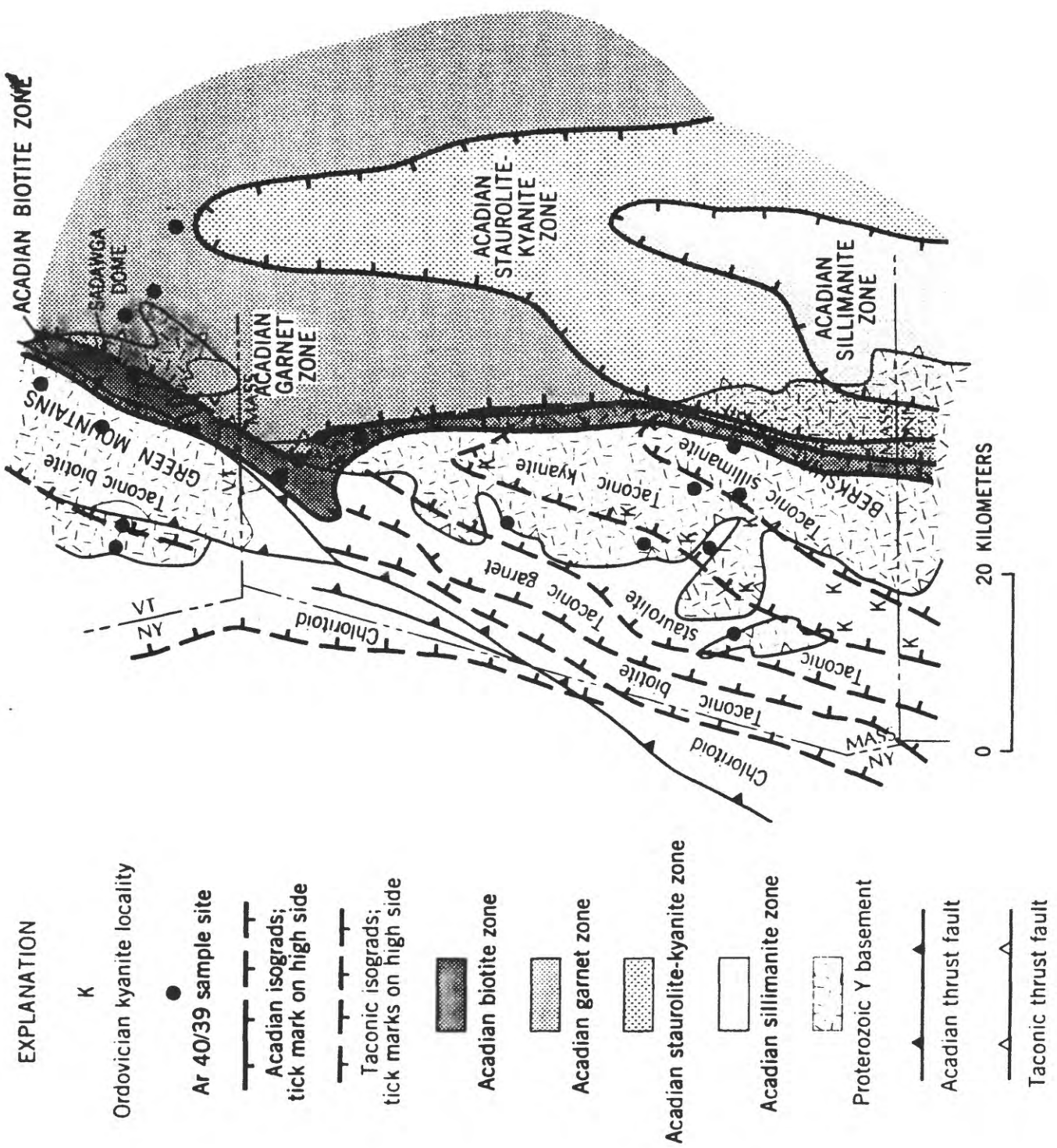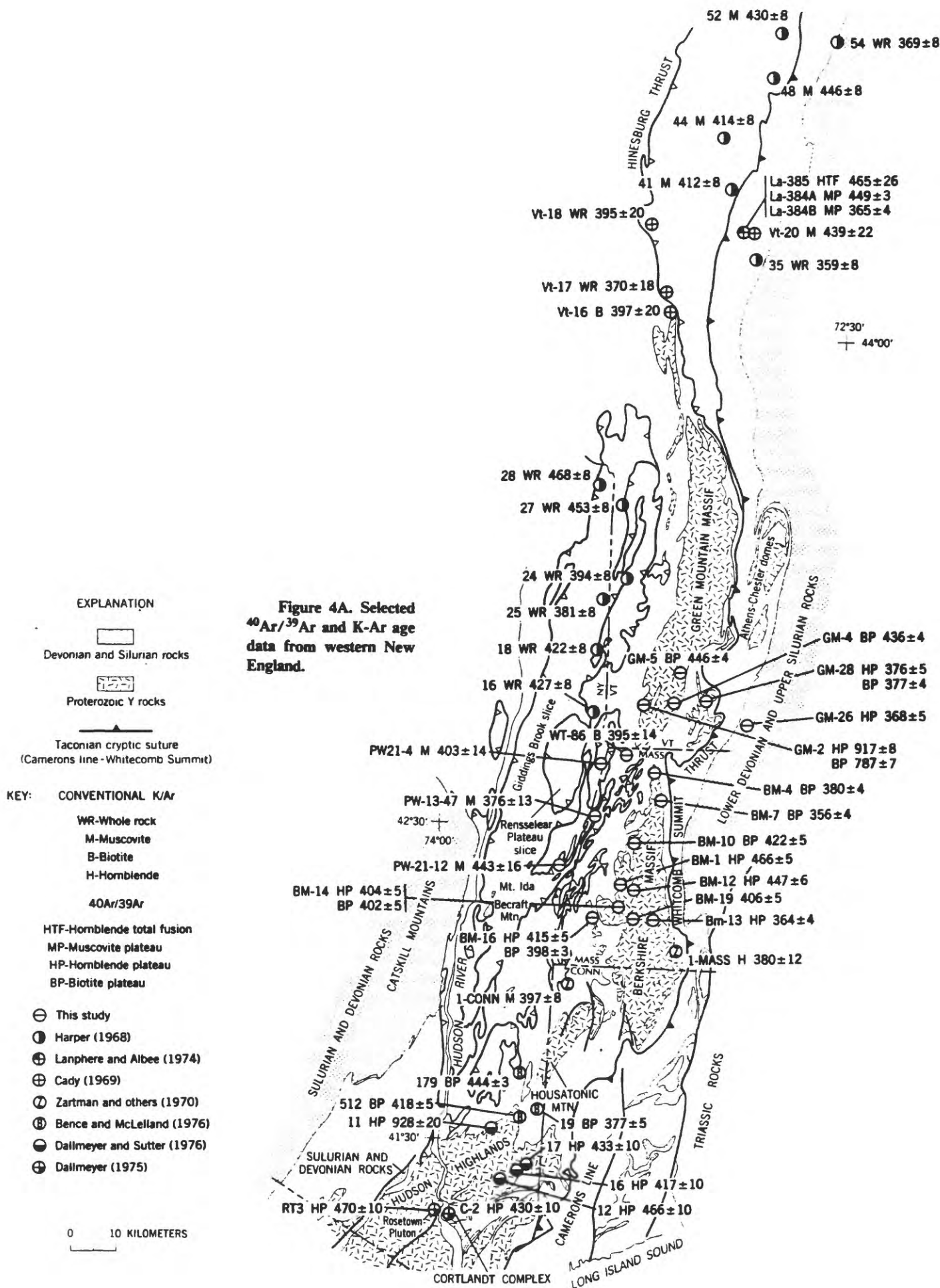Figure 3. New interpretation of Taconian and Acadian metamorphic zones based on $^{40}Ar/$ ^{39}Ar data. The diagram shows possible distribution of preserved Taconian metamorphic zones and areas of Acadian overprinting of biotite grade and higher.

117

Figure 4A. Selected $^{40}Ar/^{39}Ar$ and K-Ar age data from western New England.

52 M 430±8
54 WR 369±8
48 M 446±8
44 M 414±8
41 M 412±8
La-385 HTF 465±26
La-384A MP 449±3
La-384B MP 365±4
Vt-18 WR 395±20
Vt-20 M 439±22
35 WR 359±8
Vt-17 WR 370±18
Vt-16 B 397±20

72°30'
+ 44°00'

28 WR 468±8
27 WR 453±8
24 WR 394±8
25 WR 381±8
18 WR 422±8
GM-4 BP 436±4
GM-5 BP 446±4
GM-28 HP 376±5
BP 377±4
16 WR 427±8
GM-26 HP 368±5
GM-2 HP 917±8
BP 787±7
PW21-4 M 403±14
WT-86 B 395±14
BM-4 BP 380±4
PW-13-47 M 376±13
BM-7 BP 356±4
42°30' +
74°00'
BM-10 BP 422±5
BM-1 HP 466±5
PW-21-12 M 443±16
BM-12 HP 447±6
BM-14 HP 404±5
BP 402±5
BM-19 406±5
Bm-13 HP 364±4
BM-16 HP 415±5
BP 398±3
1-MASS H 380±12
1-CONN M 397±8
179 BP 444±3
512 BP 418±5
11 HP 928±20
41°30'
19 BP 377±5
17 HP 433±10
16 HP 417±10
RT3 HP 470±10
C-2 HP 430±10
12 HP 466±10

HINESBURG THRUST
GREEN MOUNTAIN MASSIF
Athens-Chester domes
LOWER DEVONIAN AND UPPER SILURIAN ROCKS
WHITCOMB SUMMIT THRUST
NY VT
VT MASS
Giddings Brook slice
Rensselear Plateau slice
Mt. Ida
Becraft Mtn
MASS CONN
BERKSHIRE MASSIF
SULURIAN AND DEVONIAN ROCKS
CATSKILL MOUNTAINS
HUDSON RIVER
TRIASSIC ROCKS
HOUSATONIC MTN
HIGHLANDS
SULURIAN AND DEVONIAN ROCKS
HUDSON
Rosetown Pluton
CAMERONS LINE
CORTLANDT COMPLEX
LONG ISLAND SOUND

EXPLANATION

Devonian and Silurian rocks

Proterozoic Y rocks

Taconian cryptic suture
(Camerons line - Whitecomb Summit)

KEY: CONVENTIONAL K/Ar

WR-Whole rock
M-Muscovite
B-Biotite
H-Hornblende

40Ar/39Ar

HTF-Hornblende total fusion
MP-Muscovite plateau
HP-Hornblende plateau
BP-Biotite plateau

⊖ This study
◑ Harper (1968)
⊕ Lanphere and Albee (1974)
⊕ Cady (1969)
⊘ Zartman and others (1970)
Ⓑ Bence and McLelland (1976)
◕ Dallmeyer and Sutter (1976)
⊕ Dallmeyer (1975)

0   10 KILOMETERS

118

Figure 4B. Suggested Taconian and Acadian metamorphic zonation in western New England.

119

SUMMARY DIAGRAM

Relict T-1 high-pressure
low-temperature zone of
Laird and Albee (1981)
≃ 465 m.y.

HH-Hudson Highlands
HM-Housatonic massif
BM-Berkshire massif
GM-Green Mountain massif
C-A-Chester-Athens dome
L.M.-Lincoln Mountain massif

L.M.

NY
T-2

A-1

GM

C-A

Central Vermont
T-2 domain
≃ 460-470 m.y.;
trends N-S

Acadian metamorphic zones Barrovian
st-ky-sill domain

VT
MASS

Taconic chlorite zone rocks T-2

NY

P

BM

T-3

MASS
CONN

A-1

HM

Dutchess Co.- Berkshire T-3
bio to sill domain of this report;
≃ 460-470 m.y.; trends N35°E

⊙ P = Pittsfield, Mass.

HH

0   10 KM

REFERENCES CITED

Alexander, E. C., Jr., Michelson, G. M., and Lanphere, M. A., 1978, MMhb-1: A new $^{40}Ar/^{39}Ar$ dating standard, in Zartman, R. E., ed., Fourth International Conference on Geochronology, Cosmochronology, and Isotope Geology: U.S. Geological Survey Open-File Report 78-701, p. 6–8.

Bence, A. E., and McLelland, J. M., 1976, Progressive metamorphism in Dutchess County, New York: New York State Geological Association, 48th Annual Meeting, Field guidebook, p. B-7-1 to B-7-27.

Berry, W.B.N., 1970, Review of late Middle Ordovician graptolites in eastern New York and Pennsylvania: American Journal of Science, v. 269, p. 304–313.

Bird, J. M., 1975, Late Precambrian graben facies of the northern Appalachians [abs.]: Geological Society of America Abstracts with Programs, v. 7, no. 1, p. 27.

Bird, J. M., and Dewey, J. F., 1970, Lithosphere plate-continental margin tectonics and the evolution of the Appalachian orogen: Geological Society of America Bulletin, v. 81, p. 1031–1060.

Cady, W., 1969, Regional tectonic synthesis of northwestern New England and adjacent Quebec: Geological Society of America Memoir 120, 181 p.

Dallmeyer, R. D., 1975, $^{40}Ar/^{39}Ar$ spectra of biotite and hornblende from the Cortlandt and Rosetown plutons, New York, and their regional implications: Journal of Geology v. 83, no. 5, p. 629–643.

—— 1979, Chronology of igneous and metamorphic activity in south central Maine, in Skehan, J. W., and Osberg, P. H., eds., The Caledonides in the USA, IGCP Project 27: Weston, Massachusetts, Weston Observatory, p. 63–71.

—— 1982, $^{40}Ar/^{39}Ar$ ages from the Narragansett Basin and the southern Rhode Island basement terrane: Their bearing on the extent and chronology of Hercynian tectonothermal events in southern New England: Geological Society of America Bulletin, v. 93, p. 1118–1130.

Dallmeyer, R. D., and Sutter, J. F., 1976, $^{40}Ar/^{39}Ar$ incremental-release ages of biotite and hornblende from variably retrograded basement gneisses of the northeasternmost Reading Prong, New York: Their bearing on early Paleozoic metamorphic history: American Journal of Science, v. 276, no. 6, p. 731–747.

Dallmeyer, R. D., Sutter, J. F., and Baker, D. J., 1975, Incremental $^{40}Ar/^{39}Ar$ ages of biotite and hornblende from the northeastern Reading Prong: Their bearing on late Proterozoic thermal and tectonic history: Geological Society of America Bulletin, v. 86, p. 1435–1443.

Dallmeyer, R. D., and others, 1983, Chronology of tectonothermal activity in the western Avalon Zone of the Newfoundland Appalachians: Canadian Journal of Earth Sciences, v. 20, p. 355–363.

Dalrymple, G. B., and Lanphere, M. A., 1971, $^{40}Ar/^{39}Ar$ technique of K-Ar dating: A comparison with the conventional technique: Earth and Planetary Science Letters, v. 12, no. 3, p. 300–308.

Dalrymple, G. B., and others, 1981, Irradiation of samples for $^{40}Ar/^{39}Ar$ dating using the Geological Survey TRIGA reactor: U.S. Geological Survey Professional Paper 1176, 55 p.

Dodson, M. H., 1973, Closure temperature in cooling geochronological and petrological systems: Contributions to Mineralogy and Petrology, v. 40, p. 259–274.

—— 1979, Theory of cooling ages, in Jager, E., and others, eds., Lectures in isotope geology: New York, Springer-Verlag, p. 194–202.

Doolan, B. L., Drake, J. C., and Crocker, David, 1973, Actinolite and subcalcic hornblende from a greenstone of the Hazen's Notch Formation, Lincoln Mountain quadrangle, Warren, Vermont: Geological Society of America Abstracts with Programs, v. 5, no. 2, p. 157.

Fleck, R. J., Sutter, J. F., and Elliot, D. H., 1977, Interpretation of discordant $^{40}Ar/^{39}Ar$ age spectra of Mesozoic tholeiites from Antarctica: Geochimica et Cosmochimica Acta, v. 41, no. 1, p. 15–32.

Hall, L. M., 1980, Basement-cover relations in western Connecticut and southeastern New York, in Wones, D. R., ed., The Caledonides in the USA, IGCP Project 27: Blacksburg, Virginia, Virginia Polytechnic Institute and the State University Memoir 2, p. 299–306.

Harper, C. T., 1968, Isotopic ages from the Appalachians and their tectonic significance: Canadian Journal of Earth Sciences, v. 5, p. 49–59.

Harrison, T. M., 1981, Diffusion of ^{40}Ar in hornblende: Contributions to Mineralogy and Petrology, v. 78, p. 324–331.

Harrison, T. M., and McDougall, I., 1980, Investigations of an intrusive contact, northwest Nelson, New Zealand—I, Thermal, chronological and isotopic constraints: Geochimica et Cosmochimica Acta, v. 44, p. 1985–2003.

—— 1981, Excess ^{40}Ar in metamorphic rocks from Broken Hill, New South Wales: Implications for $^{40}Ar/^{39}Ar$ age spectra and the thermal history of the region: Earth and Planetary Science Letters, v. 55, p. 123–149.

Harwood, D. S., 1972, Tectonic events in the southwestern part of the Berkshire anticlinorium, Massachusetts and Connecticut: Geological Society of America Abstracts with Programs, v. 4, no. 1, p. 19.

—— 1976, Clinopyroxene-plagioclase symplectite after omphacite and polymetamorphism of allochthonous rocks in northwestern Connecticut: Geological Society of America Abstracts with Programs, v. 8, no. 2, p. 189.

/2/

Harwood, D. S., and Zietz, I., 1974, Configuration of Precambrian rocks in southeastern New York and adjacent New England from aeromagnetic data: Geological Society of America Bulletin, v. 85, p. 181–188.

Hatch, N. L., Jr., 1975, Tectonic, metamorphic and intrusive history of part of the east side of the Berkshire massif, Massachusetts, in Tectonic studies of the Berkshire massif, western Massachusetts, Connecticut, and Vermont: U.S. Geological Survey Professional Paper 888, p. 51–62.

Hunziker, J. C., 1979, Potassium-argon dating, in Jager, E., and others, eds., Lectures in isotope geology: New York, Springer-Verlag, p. 52–76.

Hurley, P. M., and others, 1960, K-Ar and Rb-Sr minimum ages for the Pennsylvanian section in the Narragansett Basin: Geochimica et Cosmochimica Acta, v. 18, p. 247–258.

Karabinos, Paul, 1984, Deformation and metamorphism on the east side of the Green Mountain massif in southern Vermont: Geological Society of America Bulletin, v. 95, p. 584–593.

Kish, S. A., 1982, The application of potassium-argon dating of slates to the study of the metamorphic history of the southern Appalachian Piedmont and Blue Ridge: Geological Society of America Abstracts with Programs, v. 14, nos. 1 and 2, p. 31.

Laird, J., 1977, Phase equilibria in mafic schist and the polymetamorphic history of Vermont [Ph.D. thesis]: Pasadena, California, California Institute of Technology.

Laird, J., and Albee, A. L., 1981, Pressure, temperature, and time indicators in mafic schist: Their application to reconstructing the polymetamorphic history of Vermont: American Journal of Science, v. 281, p. 127–175.

Laird, J., Lanphere, Marvin A., and Albee, Arden L., 1984, Distribution of Ordovician and Devonian metamorphism in mafic and pelitic schists from northern Vermont: American Journal of Science, v. 284, p. 376–413.

Lanphere, M. A., and Albee, A. L., 1974, $^{40}Ar/^{39}Ar$ age measurements in the Worcester Mountains: Evidence of Ordovician and Devonian metamorphic events in northern Vermont: American Journal of Science, v. 274, p. 545–555.

Lanphere, M. A., and Dalrymple, G. B., 1971, A test of the $^{40}Ar/^{39}Ar$ age spectrum technique on some terrestrial materials: Earth and Planetary Science Letters, v. 12, no. 4, p. 359–372.

Lyons, J. B., and Livingston, D. C., 1977, Rb-Sr age of the New Hampshire pluton series: Geological Society of America Bulletin, v. 88, p. 1808–1812.

MacFadyen, J. A., Jr., 1956, The geology of the Bennington area, Vermont: Vermont Geological Survey Bulletin 7, 72 p.

Norton, S. A., 1967, Bedrock geology of the Windsor quadrangle, Massachusetts [Ph.D. thesis]: Cambridge, Massachusetts, Harvard University, 210 p.

—— 1976, Hoosac Formation (Early Cambrian or older) on the east limb of the Berkshire massif, in Page, L. R., ed., Contributions to the stratigraphy of New England: Geological Society of America Memoir 148, p. 357–371.

Ratcliffe, N. M., 1965, Bedrock geology of the Great Barrington area, Massachusetts [Ph.D. thesis]: State College, Pennsylvania, Pennsylvania State University, 213 p.

—— 1969, Stratigraphy and deformational history of rocks of the Taconic Range near Great Barrington, Massachusetts, in New England Intercollegiate Geological Conference, 61st Annual Meeting, Guidebook for field trips in New York, Massachusetts and Vermont: Albany, New York, State University of New York at Albany, p. 2-1 to 2-23.

—— 1975, Cross section of the Berkshire massif at 42°N: Profile of a basement reactivation zone, in New England Intercollegiate Geological Conference, 67th Annual Meeting, Guidebook for field trips in western Massachusetts, northern Connecticut and adjacent areas of New York: New York, City College of C.U.N.Y., Department of Earth and Planetary Sciences, p. 186–216.

—— 1979, Fieldguide to the Chatham and Greylock slices of the Taconic allochthon in western Massachusetts and their relationship to the Hoosac-Rowe sequence, in New England Intercollegiate Geological Conference, 71st Annual Meeting, and New York State Geological Association, 51st Annual Meeting, Guidebook: Troy and Albany, New York, Rensselaer Polytechnic Institute and New York State Geological Survey, p. 388–425.

Ratcliffe, N. M., and Harwood, D. S., 1975, Blastomylonites associated with recumbent folds and overthrusts at the western edge of the Berkshire massif, Connecticut and Massachusetts—A preliminary report, in Tectonic studies of the Berkshire massif, western Massachusetts, Connecticut, and Vermont: U.S. Geological Survey Professional Paper 888, p. 1–19.

Ratcliffe, N. M., and Hatch, N. L., Jr., 1979, A traverse across the Taconide zone in the area of the Berkshire massif, in Skehan, J. W., and others, eds., The Caledonides in the USA, IGCP Project 27: Weston, Massachusetts, Weston Observatory, p. 175–224.

Ratcliffe, N. M., Bender, J. F., and Tracy, R. J., 1983, Tectonic setting, chemical petrology and petrogenesis of the Cortlandt Complex and related igneous rocks of southeastern New York State: Geological Society of America, 1983 Northeastern Section Meeting, Guidebook Field Trip 1, 101 p.

/22

Reynolds, P. H., and Muecke, G. K., 1978, Age studies on slates: Applicability of the $^{40}Ar/^{39}Ar$ stepwise outgassing method: Earth and Planetary Science Letters, v. 40, p. 111-118.

Skehan, J. W., 1961, The Green Mountain anticlinorium in the vicinity of Wilmington and Woodford, Vermont: Vermont Geological Survey Bulletin 17, p. 37-45.

Stanley, R. S., and Ratcliffe, N. M., 1980, Accretionary collapse of the western margin of Iapetus in central New England during the Taconic orogeny: Geological Society of America Abstracts with Programs, v. 12, no. 2, p. 85.

———— in press, Tectonic synthesis of the Taconian orogeny in western New England: Geological Society of America Bulletin.

Steiger, R. H., and Jager, Emilie, 1977, Subcommission on geochronology: Convention on the use of decay constants in geo- and cosmochronology: Earth and Planetary Science Letters, v. 36, no. 3, p. 359-362.

Sutter, J. F., and Smith, T. E., 1979, $^{40}Ar/^{39}Ar$ ages of diabase intrusions from Newark Trend basins in Connecticut and Maryland: Initiation of central Atlantic rifting: American Journal of Science, v. 279, p. 808-831.

Theokritoff, G., 1964, Taconic stratigraphy in northern Washington County, New York: Geological Society of America Bulletin, v. 75, p. 171-190.

Thompson, J. B., Jr., and Norton, S. A., 1968, Paleozoic regional metamorphism in New England and adjacent areas, in Zen, E-An, and others, eds., Studies of Appalachian geology; Northern and maritime: New York, John Wiley and Sons, p. 319-341.

Tracienski, W. E., Jr., 1976, Crossitic amphibole and its possible tectonic significance in the Richmond area, southeastern Quebec, Canada: Canadian Journal of Earth Sciences, v. 13, p. 711-714.

Winkler, H.G.F., 1976, Petrogenesis of metamorphic rocks (4th edition): New York, Springer-Verlag, 334 p.

Zartman, R. E., and others, 1970, A Permian disturbance of K-Ar radiometric ages in New England: Its occurrence and cause: Geological Society of America Bulletin, v. 81, p. 3359-3374.

Zen, E-An, 1967, Time and space relationships of the Taconic allochthon and autochthon: Geological Society of America Special Paper 97, 107 p.

———— 1972, Some revisions in the interpretation of the Taconic allochthon in west-central Vermont: Geological Society of America Bulletin, v. 83, p. 2573-2588.

———— 1981, Metamorphic mineral assemblages of slightly calcic pelitic rocks in and around the Taconic allochthon, southwestern Massachusetts and adjacent Connecticut and New York: U.S. Geological Survey Professional Paper 1113, 128 p.

123

Blank

.

U-Pb Dating of Zircon Overgrowths:
Dating Fluid Flow?
(P.K. Zeitler)

1. Introduction

U-Pb geochronologists have long known that zircons frequently develop overgrowths when they become embroiled in significant geologic events like high-grade metamorphism and partial melting. Although there is a large body of anecdotal information available about the behavior of zircon, it turns out that little quantitative is known about this important mineral in terms of its diffusion kinetics or stability relationships in metamorphic and diagenetic environments. We do have a fairly good body of evidence that suggests that Pb diffusion in zircon is exceptionally sluggish; the slow-cooling closure temperature for Pb in zircon is very high, certainly well above 750°C. Therefore, there's a very good chance that once a zircon grows (for whatever reason at whatever temperature), under most crustal conditions it is likely to retain its age tenaciously.

Until recently, there was little practical that could be done with zircon overgrowths. However, several advances have now opened the door to exploiting such growth zones. First, techniques of U-Pb chemistry and mass spectrometry have improved to the point where single grains and even tiny fragments chiseled from grains can be analyzed with excellent precision; the only drawback in terms of dating overgrowths is one of potential inaccuracy, as one cannot always ensure that an overgrowth is being sampled cleanly. However, a second approach, U-Pb dating via ion microprobe, can do a much better job of ensuring accuracy of sampling, albeit at a considerable cost in precision. To date, the SHRIMP ion probe (housed in Canberra, Australia at the Research School of Earth Sciences of the Australian National University) is the only ion probe capable of geochronologic analyses (several references describing the use of SHRIMP are listed below).

Lately, fluid flow has emerged as a topic of great interest to geologists. Simply to see how feasible the measurements would be, it is worth looking at zircon overgrowths as a potential means of dating flow, even if the theory and data are not yet in place with which we can easily relate specific fluids to specific zircon overgrowths. The case studies that follow represent attempts to date zircon overgrowths developed in high and what may be low temperature systems, respectively.

2. Case Study I. Dating Quartz-Graphite Veins, Bristol, NH

Abstract. Ion-microprobe dating of zircon from quartz-graphite veins at the Bristol, New Hampshire, metamorphic hot spot.
(Zeitler et al., 1990)

INSERT ZEITLER ET AL. 1990 ABSTRACT HERE

Ion-microprobe dating of zircon from quartz-graphite veins at the Bristol, New Hampshire, metamorphic hot spot

Peter K. Zeitler*
Research School of Earth Sciences, Australian National University, G.P.O. Box 4, Canberra, A.C.T. 2601, Australia
Barbara Barreiro, C. Page Chamberlain
Department of Earth Sciences, Dartmouth College, Hanover, New Hampshire 03755
Douglas Rumble III
Geophysical Laboratory, 2801 Upton Street, N.W., Washington, D.C. 20008

ABSTRACT

Detrital zircons entrained in hydrothermal quartz-graphite-rutile veins found near the Bristol, New Hampshire, metamorphic hot spot are overgrown by thin rims. Ion-microprobe analyses of these rims date their growth at 408 ±6 Ma. These measurements quantitatively confirm textural evidence that the graphite veins were emplaced during peak metamorphism associated with the Acadian orogeny, and they provide a direct positive test of the hypothesis, based on petrological and stable-isotope evidence, that the hydrothermal systems responsible for the quartz-graphite veins were also responsible for the hot-spot metamorphism.

INTRODUCTION

In southern New Hampshire, several small granulite facies "hot spots" less than 5 km in diameter are found among the upper amphibolite grade metamorphic rocks of the Merrimack synclinorium (Fig. 1; Chamberlain and Rumble, 1988). Networks of quartz-graphite veins are associated with these hot spots at several localities. Chamberlain and Rumble (1988) have suggested that these veins represent fossil hydrothermal systems active at deep crustal levels during peak metamorphism and that the veins were responsible for the granulite facies conditions found in their immediate vicinity. This hypothesis, if correct, has important implications for our understanding of metamorphic processes, as it would document the transfer during metamorphism of large quantities of fluid across different crustal levels, and it would suggest that advective transfer of heat by fluids can play a significant role in the thermal budget of an orogeny.

The timing of activity within the New Hampshire hot spots relative to Acadian metamorphic and tectonic processes is not well known, because of the difficulty in directly dating the veins and because in central New England there are relatively few dates for Acadian metamorphic processes. The question of timing is, however, of fundamental importance to testing the hypothesis that advective heat transfer can play a significant role during orogeny.

Textural evidence and structural relations suggest that graphite mineralization and hot-spot activity were late- to post-tectonic. Delicate structures present within many graphite veins

were not disturbed by penetrative deformation associated with the Acadian orogeny (Rumble and Hoering, 1986), and in places graphite veins are found to crosscut rocks of the syntectonic new Hampshire Plutonic Series that are ~400–410 m.y. old (Rumble et al., 1986; Lyons and Livingstone, 1977; Barreiro and Aleinikoff, 1985). On the other hand, the lack of retrograde metamorphism in wall rocks of most of the graphite veins provides qualitative evidence that they were emplaced at the same time as, or soon after, peak metamorphic conditions were achieved (Rumble et al., 1986). However, the only quantitative lower limit for the age of graphite mineralization and, implicitly, for the age of metamorphic activity within the hot spots is a Jurassic K-Ar date obtained on illite gouge in a fault that shears graphite (John B. Lyons, 1987, personal commun.).

Quartz-graphite-rutile veins found in the metamorphic hot spot located near Bristol, New Hampshire, contain zircons. In this paper we report our attempts at the U-Pb dating of these zircons, using both conventional methods and the SHRIMP ion microprobe. Our conventional
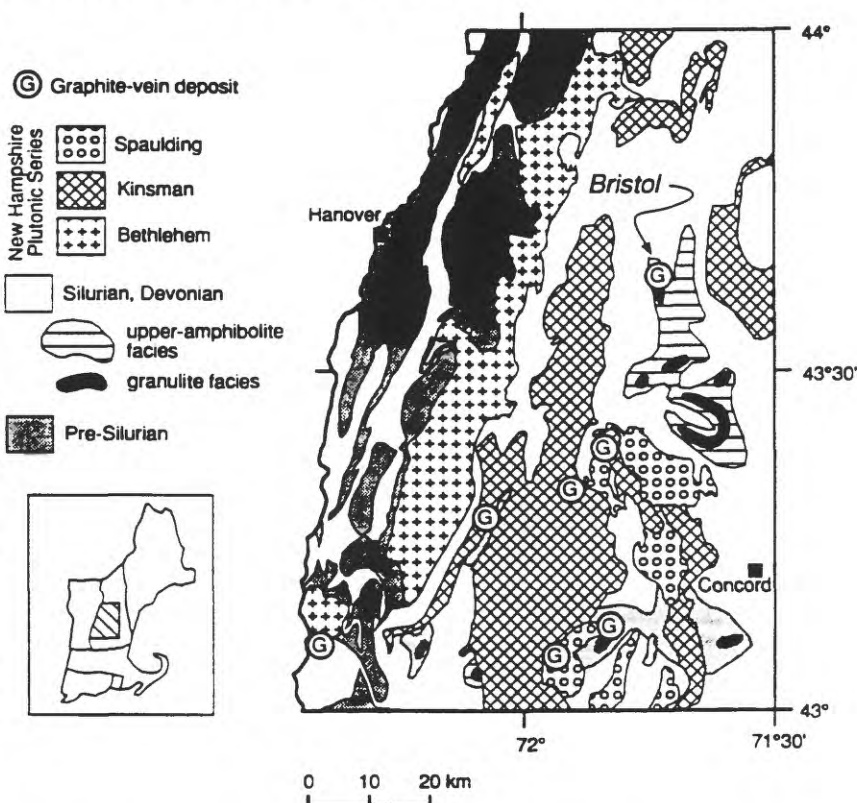

Figure 1. Sketch map of southern New Hampshire, showing location of granulite facies metamorphic hot spots (black) and rocks of New Hampshire Plutonic Series.

*Present address: Department of Geological Sciences, Williams Hall 31, Lehigh University, Bethlehem, Pennsylvania 18015-3188.

126

Summary of main points:

(1) Obtaining an age on the high-temperature hydrothermal system at Bristol is important because this would allow the anomalously high-grade metamorphism found in the region to be linked genetically with the flow of fluids.

(2) Conventional U-Pb dating of the zircons entrained in the quartz veins was of no help in resolving the age of the vein system, because the bulk of the zircon by volume consisted of xenocrystic grains derived from the surrounding metasediments.

(3) SHRIMP analysis revealed there to be substantial overgrowths on many grains. Analysis of these overgrowths showed them to define a coherent, concordant cluster at about 408 ± 6 Ma.

(4) The quoted uncertainty reflects the use of population statistics, which is an advantage one gains when using "single-grain" geochronological methods. However, filtering of the data for outliers was necessary, a process that canmake you very nervous (how does one separate out the components of correlated scatter due to error in common Pb, inheritance, or Pb loss?).

(5) Taken at face value, the age of 408 ± 6 Ma is consistent with recent results which suggest that at least in some regions the Acadian Orogeny took place in the very earliest Devonian.

(6) A weakness of this study is the need to assert that the age we obtained is the age of fluid flow. Yes, xenocrystic zircons entrained in the veins share an overgrowth of common age, but what evidence links those overgrowths to the veins themselves (Occam's Razor really isn't good enough)? What is needed is a means of linking the zircons to the veins geochemically or petrologically--perhaps O-isotopes might be an approach worth pursuing (Kerrich and Wu, 1987).

127

3. Case Study II. Dating Young Overgrowths on Precambrian Zircon, Nanga Parbat Massif, Pakistan

Abstract. U-Pb Dating of Metamorphic Zircon Overgrowths by Means of Depth Profiling with an Ion Microprobe
(Zeitler and Williams, 1988)

By using the SHRIMP ion microprobe in a depth-profiling mode, we have found that zircons from upper-amphibolite facies gneisses of the Nanga Parbat-Haramosh Massif, Pakistan are overgrown by thin, very young, relatively high-U rims. These rims, which surround cores ~ 1850 Ma in age, are only several microns wide, and are marked by low Th/U, high U, and ages of less than 10 Ma. $^{207}Pb/^{235}Pb$ ages are too imprecise to permit meaningful use of Concordia systematics, but there does appear to be real variation in $^{206}Pb/^{238}Pb$ ages from 2 to 10 Ma. Together with an independently determined cooling history obtained using other isotopic systems, the young rim ages imply that zircon overgrowth occurred at temperatures of between 200 and 500°C. Pb loss is not a likely explanation for these data for two reasons. First, zoning profiles across rims are flat, and show no evidence of diffusion. Second, because the Nanga Parbat gneisses cooled below 200°C within the past 2 m.y.,there has been no time for significant radiation damage to accumulate, and estimates of the diffusion rate of Pb in pristine zircon are too low for Pb loss by volume diffusion to be plausible, particularly at low temperatures. The young rims found on the Nanga Parbat zircons probably record a period of post-metamorphic fluid flow, perhaps related to rapid decompression of the Nanga Parbat massif over the past several million years. An important point is that the thin, not easily observed rims on these zircons dominate Concordia systematics, and indicate an age which is younger than that of peak metamorphic temperature.

Summary of main points:

(1) Zircons samples from Precambrian basement gneisses of the Nanga Parbat-Haramosh Massif, Pakistan Himalaya, yield U-Pb ages that are strongly discordant, although discordance of this degree is not unusual. During fission-track and conventional SHRIMP analysis of sectioned grains, it was found that these zircons are mantled by high-U rims.

(2) The rims are very thin, on the order of microns. The only way to analyze them was to use the SHRIMP ion probe, and to use what is for SHRIMP an unconventional mode, involving drilling rather than lateral profiling of a sectioned mount.

(3) The detailed profiling data clearly indicate that the discordance observed in these zircons is due to thin overgrowths, not Pb-loss: profiles in ^{206}Pb are flat at the edges of grains.

(4) The very young rims exert a major control on the Concordia systematics of bulk zircon analyses of Nanga Parabt gneisses, because they are so young and have such high U.

(5) The rims give ages as young as 2 Ma; all ages fall within the range 2 to 14 Ma. At the locality under study, the independently determined thermal history suggests that growth of zircon rims occurred in the temperature range 200-500°C.

5. References

Bristol Hot Spot:

Chamberlain, C.P., and Rumble, D., 1988, Thermal anomalies in a regional metamorphic terrain: An isotopic study of the role of fluids: Journal of Petrology, v. 29, p. 1215-1232.

Dykstra-Eusden, J., and Barreiro, B., 1988, The timing of peak high-grade metamorphism in central-eastern New England: Maritime Sediments and Atlantic Geology, v. 24, 241-255.

Hubacher, F.A., and Lux, D.R., 1987, Timing of Acadian deformation in northeastern Maine: Geology, v. 15, p. 80-83.

Kerrich, R., and Wu, T.-W., 1987, Oxygen isotope relations in zircons: Monitor of primary magmatic $\delta^{18}O$ in altered and metamorphosed granites [abstr.]: Geological Association of Canada Program with Abstracts, v. 12, p. 61.

Lyons, J.B., and Livingstone, D.E., 1977, Rb-Sr age of the New Hampshire plutonic series: Geological Society of America Bulletin, v. 88, p. 1808-1812.

Naylor, R.S., 1971, Acadian orogeny: An abrupt and brief event: Science, v. 172, p. 558-560.

Rumble, D. and Hoering, T.C., 1986, Carbon isotopic geochemistry of graphite vein deposits from New Hampshire, U.S.A.: Geochimica et Cosmochimica Acta, v. 50, p. 1239-1247.

Rumble, D., Duke, E.F., and Hoering, T.C., 1986, Hydrothermal graphite in New Hampshire: Evidence of carbon mobility during regional metamorphism: Geology, v. 14, p. 452-455.

Zeitler, P. K., Barreiro, B., Chamberlain, C. P., and Rumble, D., 1990, Ion-microprobe dating of quartz-graphite veins at the Bristol, New Hampshire, metamorphic hot spot: Geology, v. 18, p. 626-629.

Nanga Parbat, Pakistan:

Zeitler, P. K. and Williams, I. S. 1988, U-Pb dating of metamorphic zircon overgrowths by means of depth profiling with an ion microprobe [abstr.]: EOS (Transactions of the American Geophysical Union), v. 69, p. 464.

Zeitler, P. K., and Chamberlain, C. P., 1991, Petrogenetic and tectonic significance of young leucogranites from the northwestern Himalaya, Pakistan: Tectonics, v. 10, p. 729-741.

Zeitler, P. K., Sutter, J. F., Williams, I. S., Zartman, R. E. & Tahirkheli, R. A. K., 1989, Geochronology and temperature history of the Nanga Parbat-Haramosh Massif, Pakistan. In: Malinconico, L. L. and Lillie, R. J. (eds.) Tectonics of the Western Himalaya, Geological Society of America Special Paper 232, p. 1-22

SHRIMP Ion Probe:

Compston, W.C., Williams, I.S., and Meyer, C., 1984, U-Pb geochronology of zircons from lunar breccia 73217 using a sensitive high mass-resolution ion microprobe: Proceedings of the Fourteenth Lunar and Planetary Science Conference, Part 2, Journal of Geophysical Research, v. 89, suppl., p. B525-534.

Compston, W.C., Kinny, P.D., Williams, I.S., and Foster, J.J., 1986, The age and loss behaviour of zircons from the Isua supracrustal belt as determined by ion microprobe: Earth and Planetary Science Letters, v. 80, p. 71-81.

Cumming, G.L., and Richards, J.R., 1975, Ore lead isotope ratios in a continuously changing earth: Earth and Planetary Science Letters, v. 28, p. 155-171.

Williams, I.S., and Claesson, S., 1987, Isotopic evidence for the Precambrian provenance and Caledonian metamorphism of high grade paragneiss from the Seve Nappes, Scandinavian Caledonides. II. Ion microprobe zircon U-Th-Pb: Contributions to Mineralogy and Petrology, v. 97, p. 205-217.

Williams, I.S., Compston, W., Black, L.P., Ireland, T.R., and Foster, J.J., 1984, Unsupported radiogenic Pb in zircon: a cause of anomalously high Pb-Pb, U-Pb and Th-Pb ages: Contributions to Mineralogy and Petrology, v. 88, p. 322-327.

.
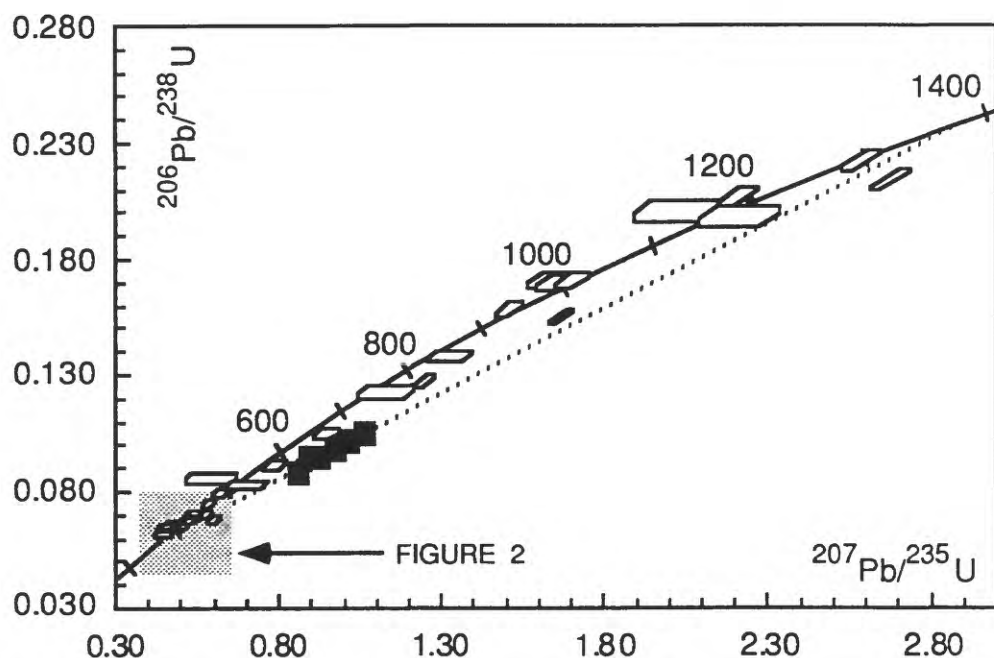
1. Overview of U-Pb results for xenocrystic zircons entrained in quartz-graphite veins at Bristol, New Hampshire. Solid squares show conventional U-Pb results; error boxes (one-sigma) show analyses made using the SHRIMP ion probe. The range of ages obtained with the ion probe is reasonable given the metasedimentary source of the zircons. Note that no effort was made to quantitatively characterize the xenocrystic component. Regression through the conventional data yields a lower intercept of 370 ± 220 Ma.
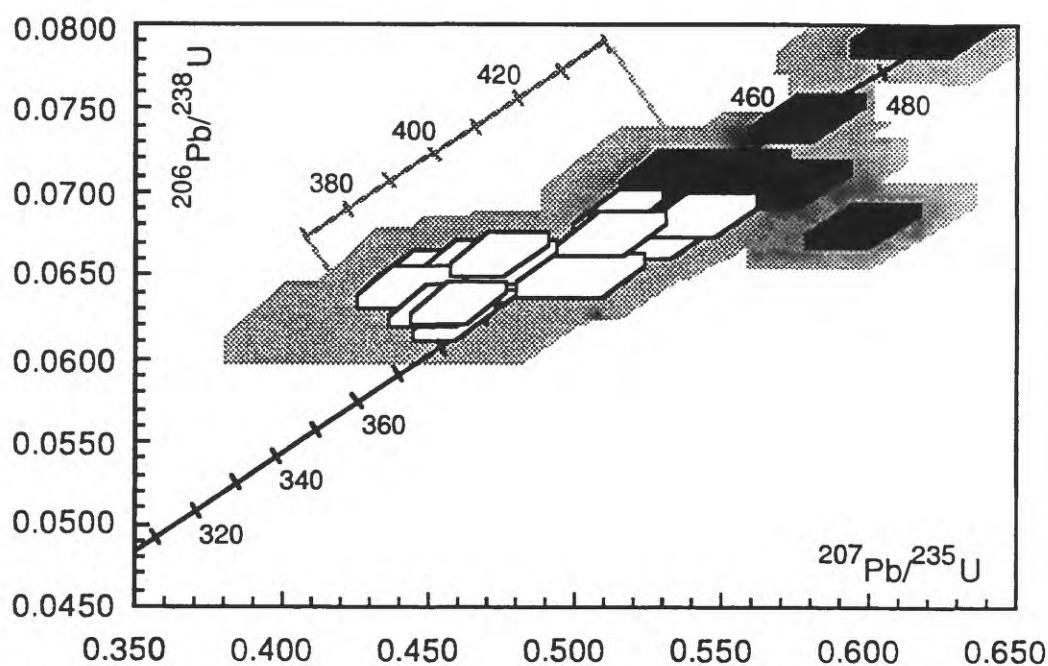

2. Detailed of young SHRIMP analyses from Bristol zircons. Gray boxes give two-sigma errors; white boxes represent those analyses accepted in calculation of age estimate; black error boxes represent analyses that were rejected.
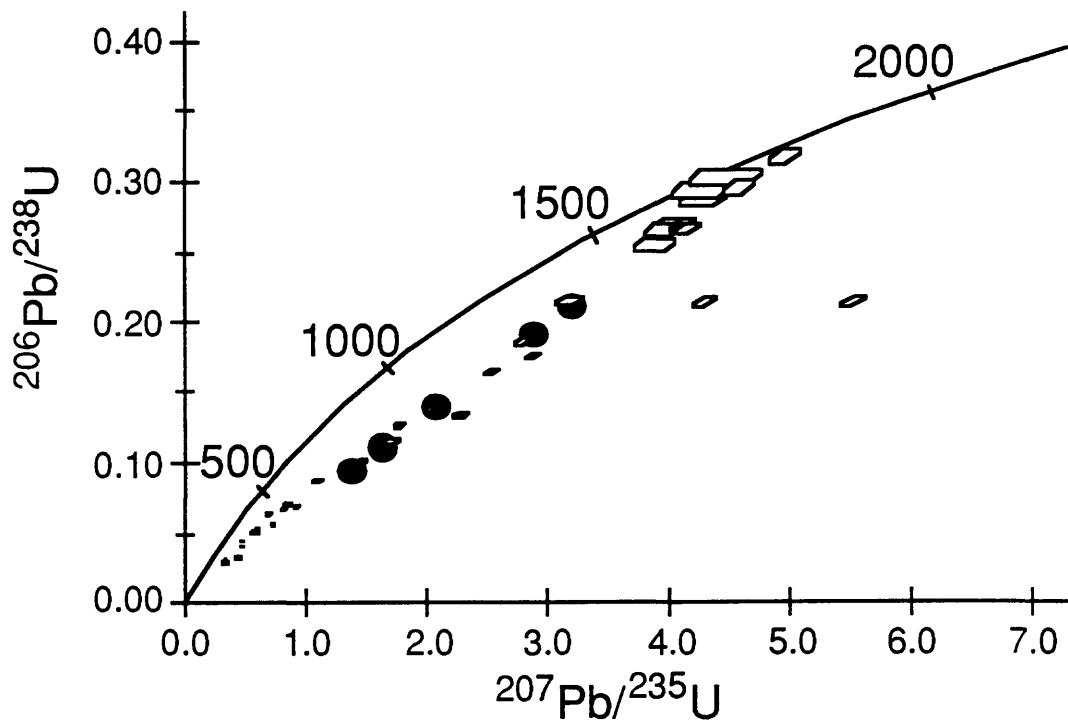
3. Overview of U-Pb results from basement zircons, Nanga Parbat-Haramosh Massif, Pakistan Himalaya. Solid circles are conventional analyses (size of symbol is unrelated to uncertainties, which are much smaller); error boxes show conventional SHRIMP ion probe analyses of sectioned grains. The upper intercept of the discordia trends is about 1850 Ma.
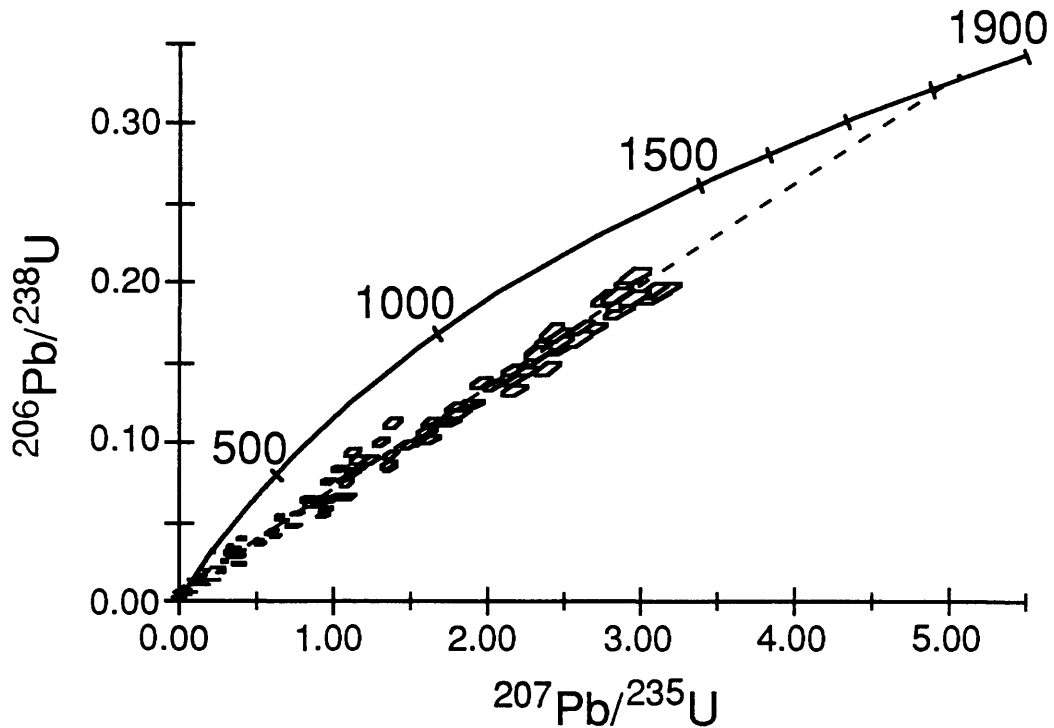
4. Overview of all single-scan data obtained during SHRIMP depth profiling of virtually unpolished, unsectioned zircon grains (normally, seven scans are combined per analysis).

/32
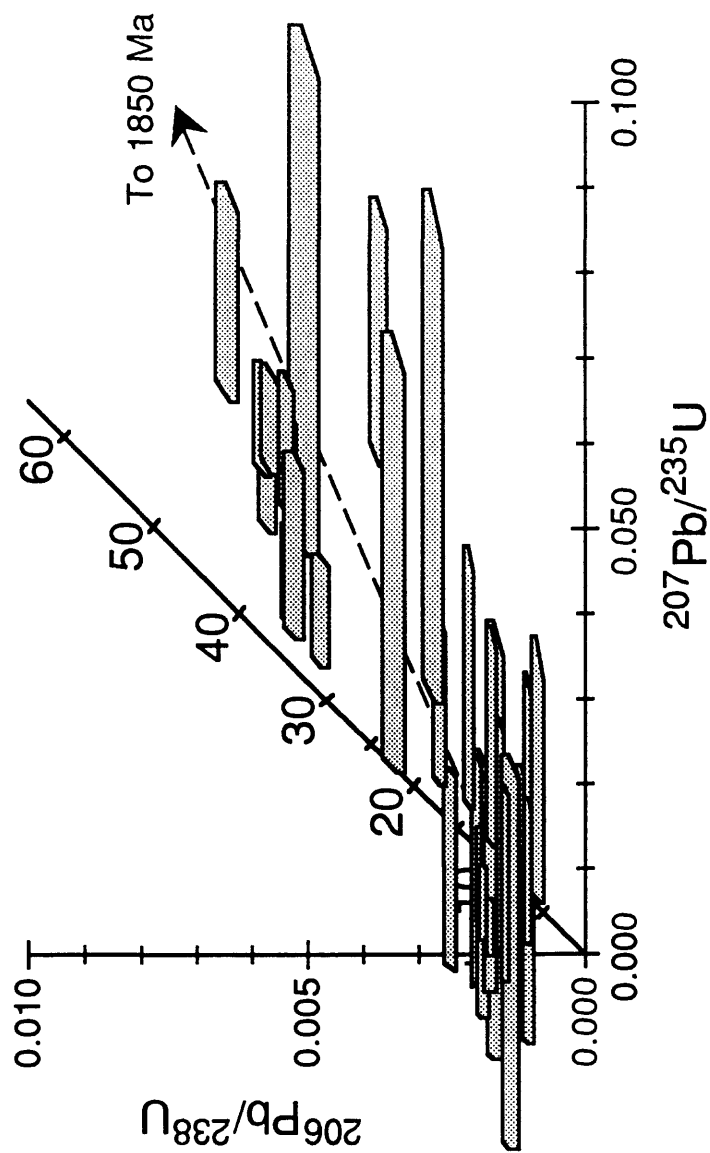
5. Blow-up of young end of Concordia, showing pooled single-scan results. The large x-axis errors reflect the very low ^{207}Pb count rate and the substantial uncertainty in the common lead correction. For reference, arrow shows discordia trend towards 1850 Ma.
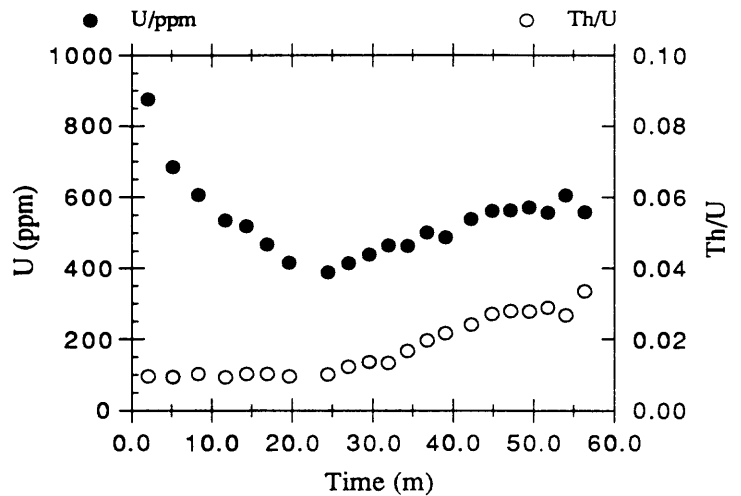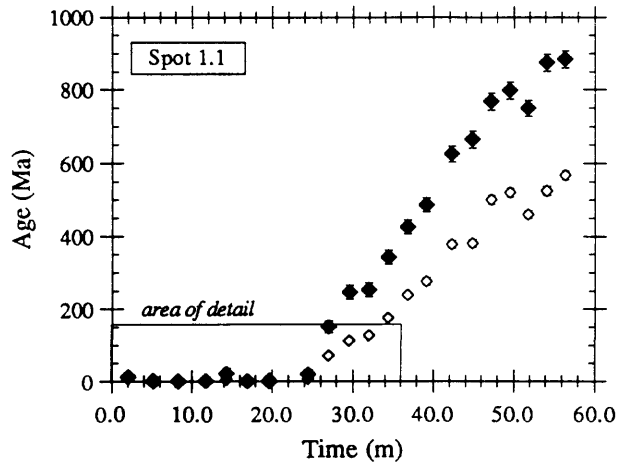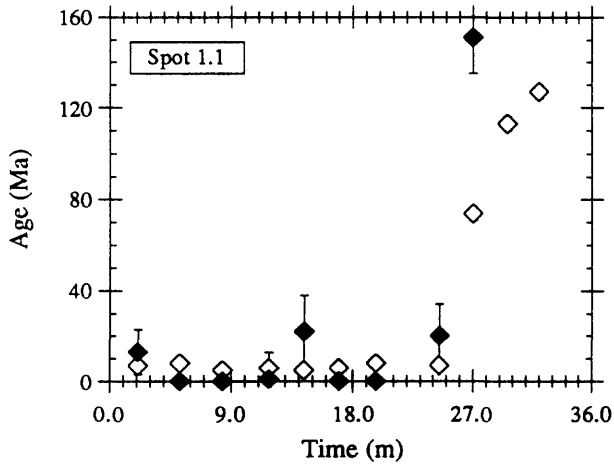
6. SHRIMP depth-profiling data for a single grain. Overview of entire experiment (upper right), details of young ages (upper left), and U and Th/U trends (lower right) are shown. Note the flat profile at the edge of the grain. About 20 minutes of drilling is equivalent to one micron of penetration into a grain.

Thermochronology of Economic Mineral Deposits: Dating the Stages of Mineralization at Panasqueira, Portugal, by High-Precision ^{40}Ar/^{39}Ar Age Spectrum Techniques on Muscovite

LAWRENCE W. SNEE,*

Department of Geology, Oregon State University, Corvallis, Oregon 97331

JOHN F. SUTTER,

U. S. Geological Survey, 981 National Center, Reston, Virginia 22092

AND WILLIAM C. KELLY

Department of Geological Sciences, University of Michigan, Ann Arbor, Michigan 48109

Abstract

^{40}Ar/^{39}Ar age spectrum dates for 13 muscovites have been used to reconstruct the thermal history (thermochronology) of the Panasqueira, Portugal, tin-tungsten deposit, a deposit spatially associated with a belt of Hercynian plutons. Muscovite samples with an age difference as small as 2.2 m.y. (0.7% of the age) are statistically distinct. Statistics are even better for comparison of multiple samples from separate events; that is, a difference of 0.9 m.y. (0.3%) can be resolved in this ~300-m.y.-old deposit. The major tin and tungsten ore-forming stages, which are the oxide-silicate stage, the main sulfide stage, and greisenization, occurred between 296.3 ± 0.8 (1 σ) and 291.6 ± 0.8 m.y. (1 σ). The first substage of the oxide-silicate stage was a short-lived thermal pulse at 296.3 ± 0.6 m.y.; the fluids responsible may have emanated from the known granite cupola. The main sulfide stage was active at 294.5 ± 0.9 m.y. as a slightly longer lived pulse with oldest evidence for this stage (295.8 ± 0.6 m.y.) coming from areas farthest away from the known cupola and youngest evidence (293.5 ± 0.8 m.y.) closest to the cupola. A second substage of the oxide-silicate stage occurred as a short-lived thermal pulse at 292.9 ± 0.7 m.y., synchronous with greisenization of the cupola and alteration of the silica cap at 292.1 ± 0.4 m.y. The duration of activity of the oxide-silicate stage, the main sulfide stage, greisenization, and alteration of the silica cap based on the ages of all 13 muscovites was greater than 4.2 ± 0.5 m.y. (1 σ). Minor argon loss from all dated muscovites occurred during later reheating, probably during the longer lived pyrrhotite alteration stage. A single center, the known cupola, had a prolonged role and was the source for main sulfide stage, oxide-silicate stage II, greisenization, and alteration of the silica cap and possibly oxide-silicate stage I and the pyrrhotite alteration stage; however, a separate source for these latter two stages cannot be ruled out.

This study is an example of a new and powerful application of ^{40}Ar/^{39}Ar age spectrum dating of muscovite. Because of the high precision demonstrated in this study, it is now possible to establish time constraints necessary for solving some of the long-standing problems in economic geology. Beyond this, the unique geologic situation of Panasqueira has allowed us to quantify the thermal characteristics of muscovite. Published fluid inclusion data have been used to estimate a muscovite argon closure temperature of ~325°C during rapid cooling or short reheating and a temperature of ~270°C during slow cooling or extended reheating. Argon-loss patterns displayed by all dated muscovites resulted from reheating after original closure; the mechanism for this argon loss appears to have been argon transport by volume diffusion. Thus, ^{40}Ar/^{39}Ar age spectrum dating of muscovite can be used to evaluate thermal conditions controlling argon diffusion as well as age, duration, and number of episodes of mineralization.

Introduction

ALTHOUGH there have been numerous geochronologic studies of economic mineral deposits, there have been few high-resolution thermochronologic studies of ore-forming processes. Until recently, isotopic techniques have been used only to date ore deposits, but they lacked the precision necessary for measurement of the total duration of mineralization or dating of the separate thermal pulses within an episode of mineralization. Moreover, the effects of chemical and/or thermal alteration on most isotopic systems were so poorly understood that criti-

* Present address: U. S. Geological Survey, Denver Federal Center, Mail Stop 905, Denver, Colorado 80225.
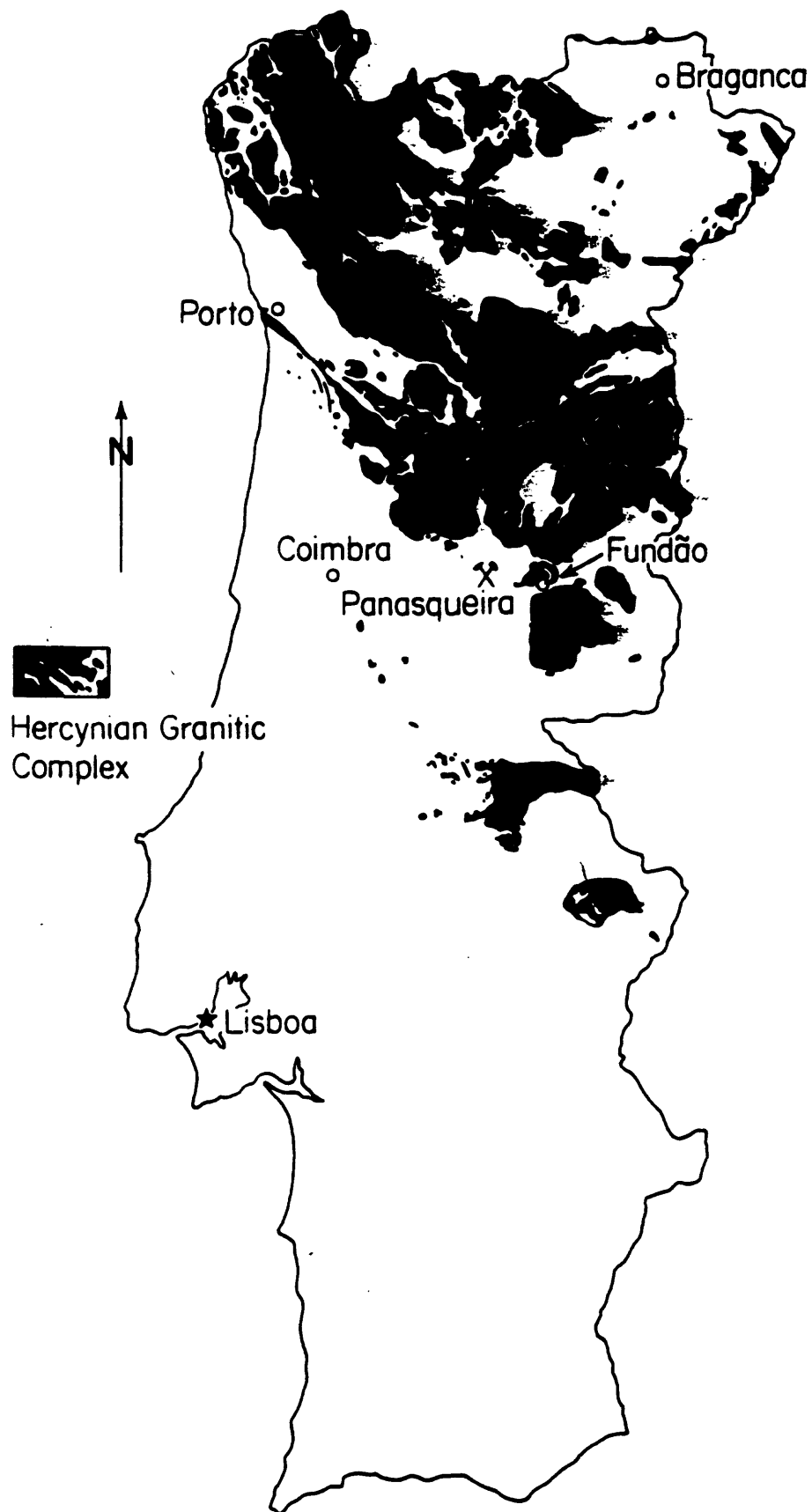
FIG. 1. Map of Portugal showing spatial relation of the Panasqueira mine to the belt of Hercynian granites.
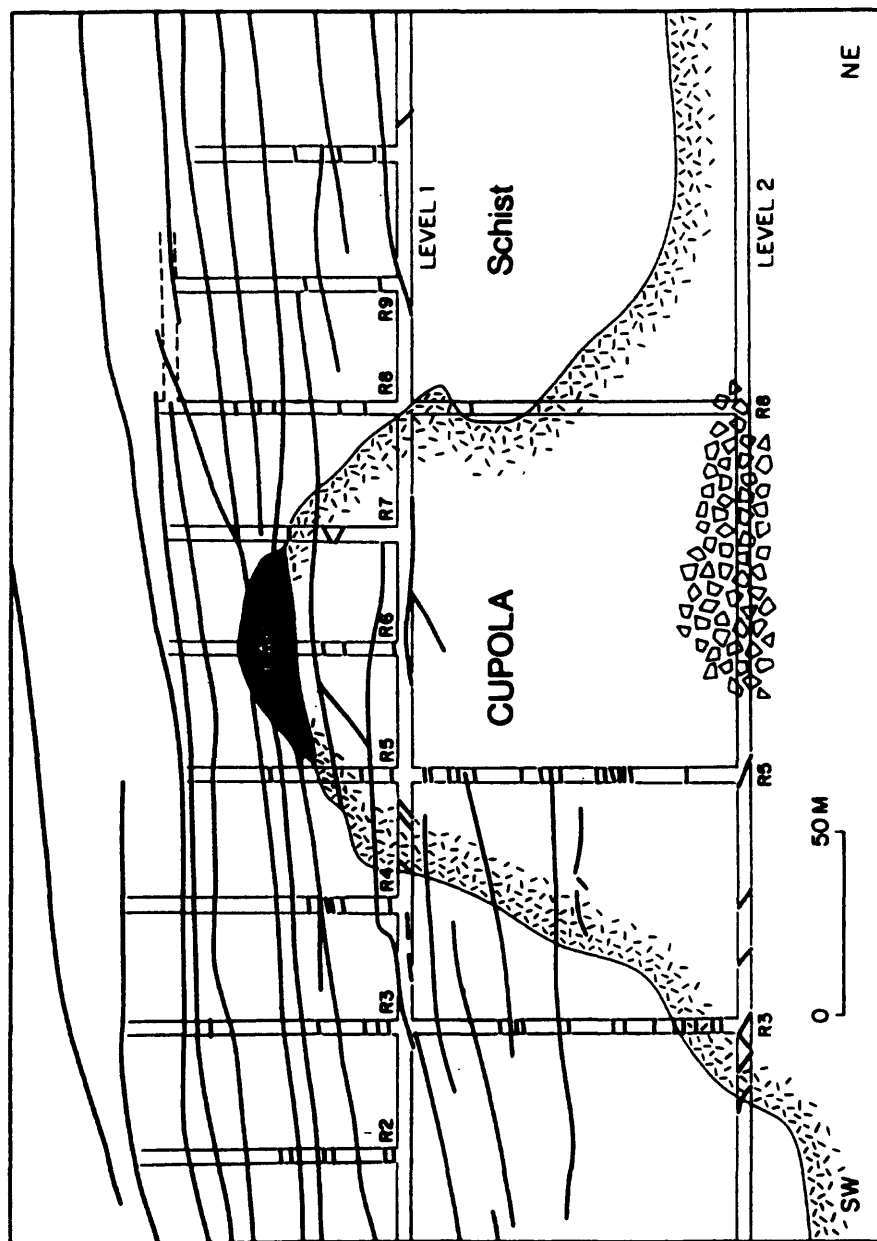
136

FIG. 4. Cross section of the Panasqueira cupola showing the silica cap, crosscutting flat stopes, and zone of abundant xenoliths on level 2.
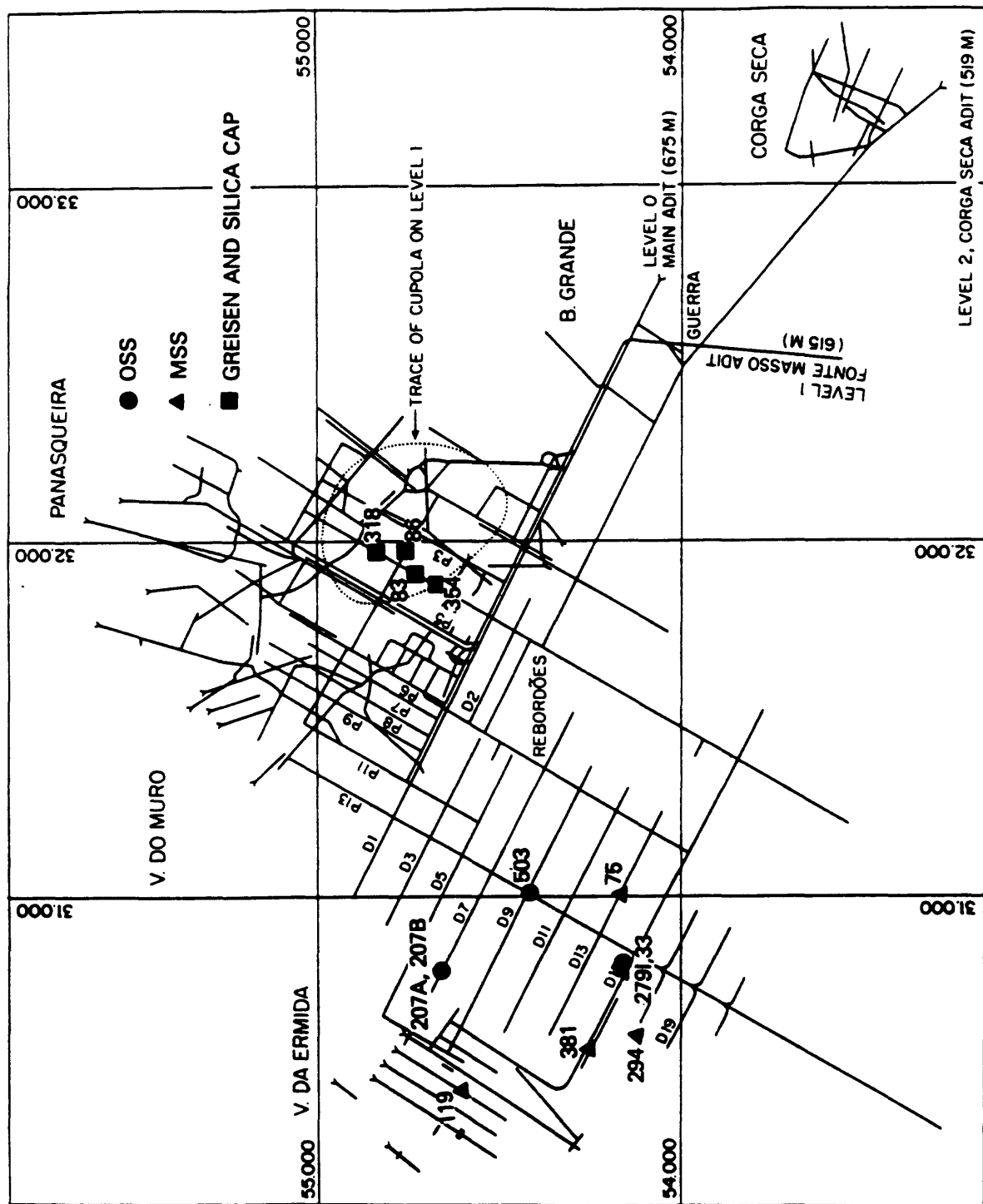
FIG. 5.   Simplified composite level map of the Panasqueira mine showing sample locations. Also shown are principal adits, drives (D), and panels (P) on the main levels 0, 1, and 2. The north-south grid lines are spaced 1 km apart.

138
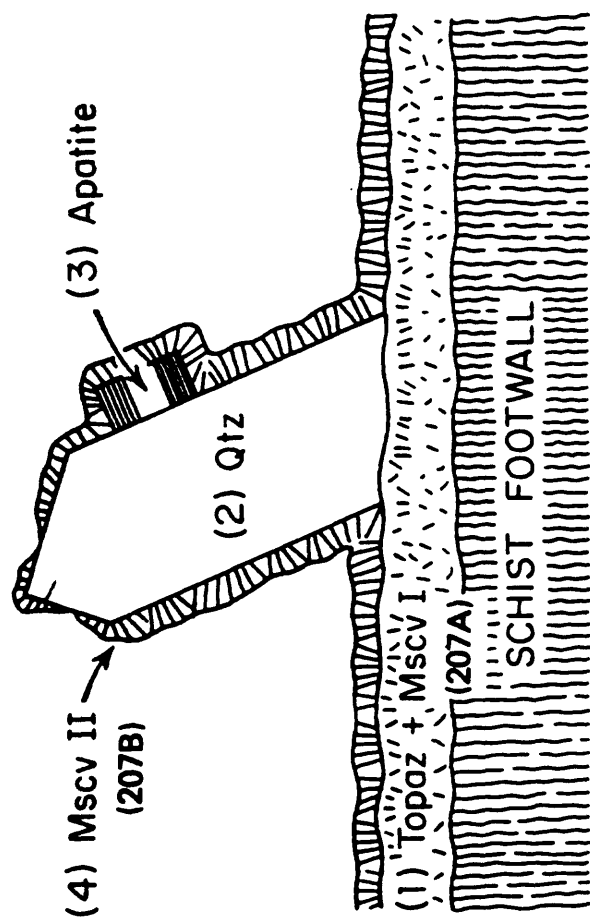
FIG. 6. Diagrammatic cross section of a vein showing the paragenetic relation of samples PGL 207A and PGL 207B.

/39
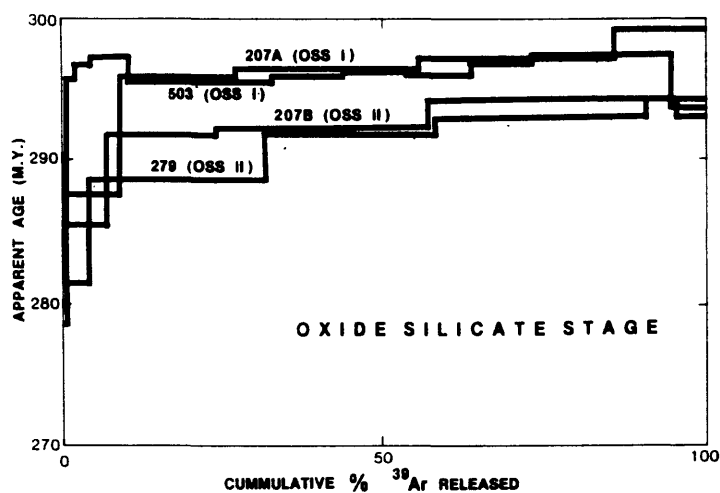
FIG. 7. $^{40}Ar/^{39}Ar$ age spectrum diagrams for oxide-silicate stage I (PGL 503 and PGL 207A) and oxide-silicate stage II (PGL 207B and PGL 279I) muscovites.

FIG. 8. $^{40}Ar/^{39}Ar$ age spectrum diagrams for main sulfide stage muscovites.

FIG. 9. $^{40}Ar/^{39}Ar$ age spectrum diagrams for greisen and altered silica cap muscovites.

140

TABLE 3. Summary of $^{40}Ar/^{39}Ar$ Plateau Ages for Muscovites from Panasqueira, Portugal
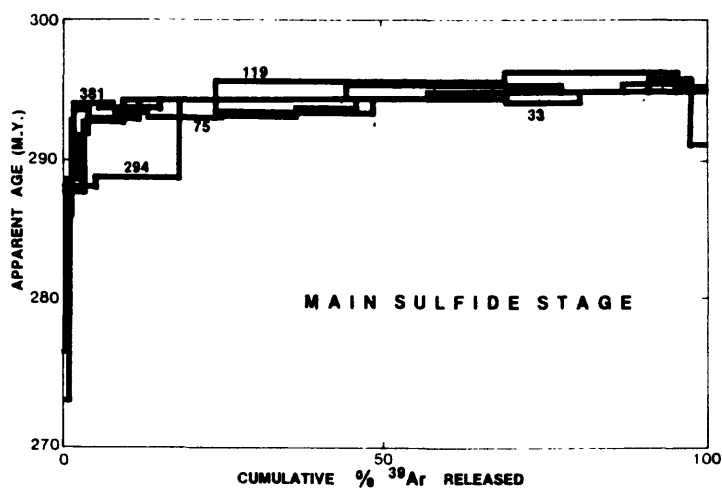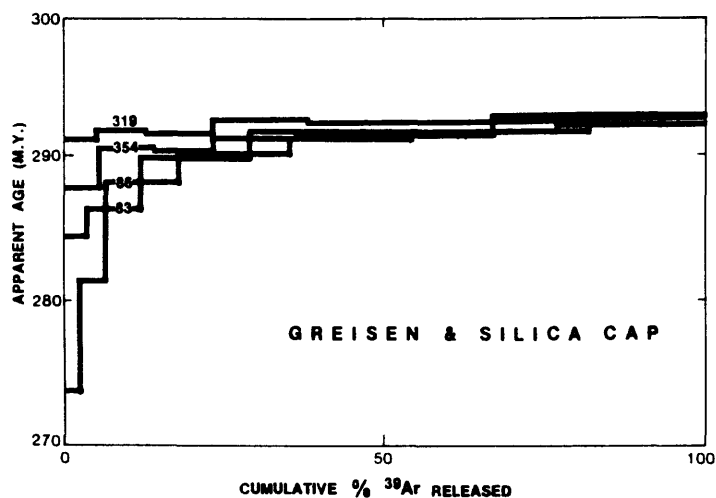
Sample no.	Stage of mineralization	Mean F	Percent of total $^{39}Ar_K$ on plateau	Apparent age (m.y.)
PGL 503	OSS	21.67 ± 0.05	92.5	296.3 ± 0.8
PGL 207A	OSS	21.67 ± 0.05	76.3	296.3 ± 0.8
PGL 207B	OSS	21.43 ± 0.07	71.0	293.3 ± 1.0
PGL 279I	OSS	21.36 ± 0.05	58.7	292.4 ± 0.8
PGL 119	MSS	21.63 ± 0.03	71.4	295.8 ± 0.6
PGL 294	MSS	21.55 ± 0.05	78.1	294.8 ± 0.8
PGL 381	MSS	21.51 ± 0.03	97.4	294.3 ± 0.6
PGL 33	MSS	21.48 ± 0.05	89.6	293.9 ± 0.8
PGL 75	MSS	21.45 ± 0.05	83.3	293.5 ± 0.8
PGL 354	Greisen	21.30 ± 0.06	85.6	291.6 ± 0.8
PGL 83	Greisen	21.35 ± 0.06	70.9	292.3 ± 0.9
PGL 86	Greisen	21.33 ± 0.06	63.9	292.0 ± 0.9
PGL 318	Silica cap	21.36 ± 0.05	100	292.4 ± 0.8

OSS = oxide-silicate stage, MSS = main sulfide stage; F = eq (3) in text

141

OXIDE-
SILICATE
STAGE

296.3 ± 0.6   292.9 ± 0.7
├──○──┤   ├──○──┤
(2)   (2)

MAIN
SULFIDE
STAGE

RANGE
295.8 ± 0.6   293.5 ± 0.8
├─○─┤   ├──○──┤
(1)   (1)
├──○──┤
294.5 ± 0.9
AVE (5)

GREISEN & LATE
MUSCOVITES
IN SILICA CAP

292.1 ± 0.4
├○┤
(4)

ARGON LOSS
EVENT

≤ 292   to   ≥ 274
├─ ─ ─ ─ ─ ─ ─ ─ ─ ─ ─ ─
PYRRHOTITE ALTERATION
STAGE (PAS)

MINIMUN
DURATION
├────────┤
4.2 ± 0.5

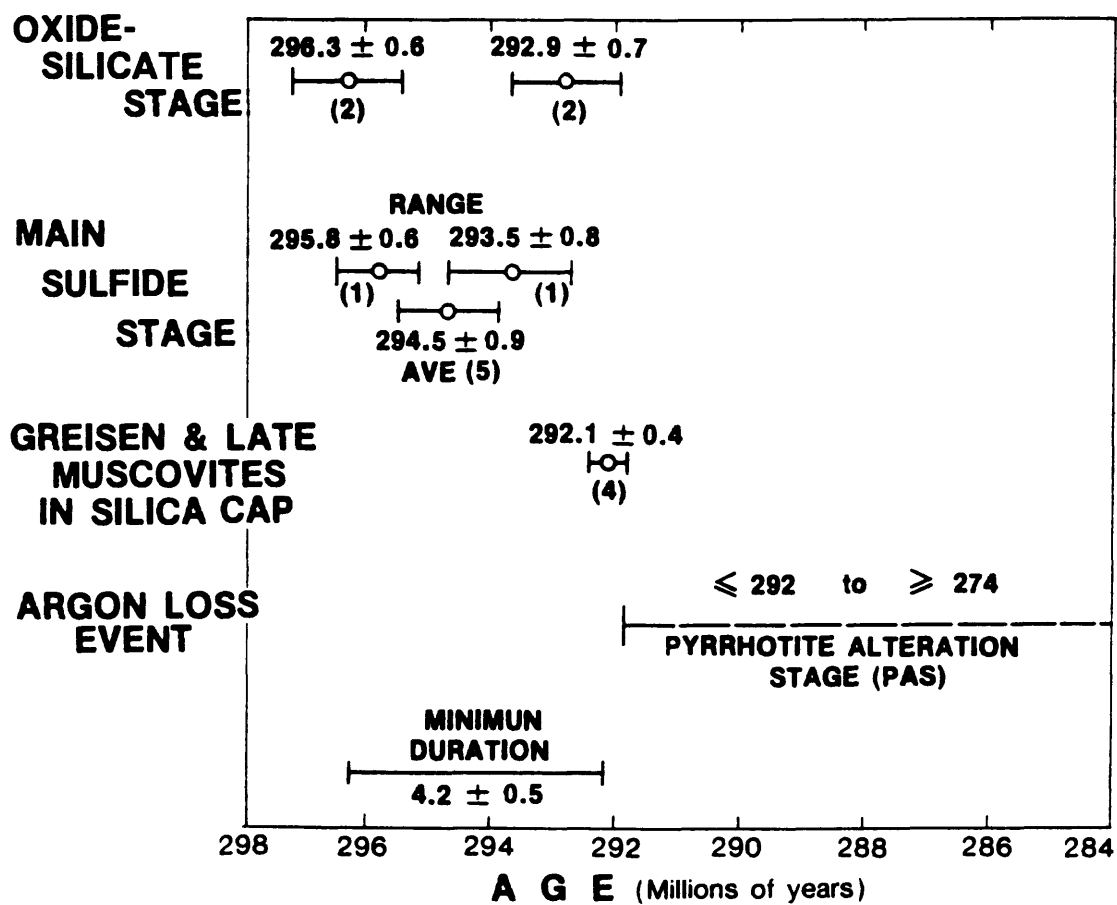298   296   294   292   290   288   286   284

A G E (Millions of years)

FIG. 10.   Revised paragenesis of Panasqueira deposit showing results of detailed $^{40}Ar/^{39}Ar$ geochronology.

142

Summary of thermal activity during mineralization at Panasqueira

The preceding interpretation of $^{40}Ar/^{39}Ar$ age spectrum data is developed below into a geologic interpretation of events at Panasqueira. Our data are limited so this summary is meant only to be a framework that will probably change with additional data.

1. A short-lived thermal pulse, oxide-silicate stage I, occurred at 296.3 ± 0.6 m.y. The source of this activity is unknown, but it may have emanated from the known cupola.

2. A slightly longer lived pulse of activity, the main sulfide stage, occurred about 294.5 ± 0.9 m.y. The oldest evidence for this stage is from Vale da Ermida (295.8 ± 0.6 m.y.) and ages of main sulfide stage muscovites get younger, apparently progressively, to the east. If the source of the main sulfide stage activity was the known cupola, this eastward migration could correspond to a contraction of cupola influence with time during this stage.

3. Another short-lived thermal pulse occurred during oxide-silicate stage II at 292.9 ± 0.7 m.y. This pulse probably emanated from the known cupola where greisenization and alteration of the silica cap occurred at 292.1 ± 0.4 m.y.

4. A ubiquitous, longer lived but lower temperature event, the pyrrhotite alteration stage, occurred sometime between 274 and 292 m.y. The thermal source of this stage is unknown, but since the argon spectrum that records the most argon loss is from the known cupola, the cupola was also the likely thermal source for the pyrrhotite alteration stage.

REFERENCES

Alexander, E. C., Michelson, G. M., and Lanphere, M. A., 1978, A new $^{40}Ar/^{39}Ar$ dating standard: U. S. Geol. Survey Open-File Rept. OF-78-701, p. 6–8.

Bray, C. J., Spooner, E. T. C., Hall, C. M., York, D., Bills, T. M., and Krueger, H. W., 1985, Laser probe $^{40}Ar/^{39}Ar$ and conventional K/Ar dating of illites associated with the McClean uranium deposits, North Saskatchewan, Canada [abs.]: Geol. Soc. America Abstracts with Programs, v. 17, p. 531.

Busink, R. W., 1984, Geochemistry of the Panasqueira tungsten-tin deposit, Portugal: Geol. Ultraiectina, no. 33, 170 p.

Clark, A. H., 1964, Preliminary study of the temperatures and confining pressures of granite emplacement and mineralization, Panasqueira, Portugal: Inst. Mining Metallurgy Trans., v. 73, p. 813–824.

—— 1970, Potassium-argon ages and regional relationships of the Panasqueira tin-tungsten mineralization: Portugal Servicos Geol., Comunicacoes, v. 54, p. 243–261.

Conde, L. N., Pereira, V., Ribeiro, A., and Thadeu, D., 1971, Jazigos hipogenicos de estanhoe e volframio: Guidebook Excursion 7, I Congresso Hispano-Luso-Americano de Geol. Econ., Sept. 19–25, 1971: Lisbon, Direccao Geral de Minase Servicos Geol., 81 p.

Dalrymple, G. B., and Lanphere, M. A., 1969, Potassium-argon dating: San Francisco, W. H. Freeman Co., 251 p.

Dalrymple, G. B., Alexander, E. C., Lanphere, M. A., and Kraker, G. P., 1981, Irradiation of samples for $^{40}Ar/^{39}Ar$ dating using the Geological Survey TRIGA reactor: U. S. Geol. Survey Prof. Paper 1176, 56 p.

Dodson, M. H., 1973, Closure temperature in cooling geochronological and petrological systems: Contr. Mineralogy Petrology, v. 40, p. 259–274.

Fleck, R. J., Sutter, J. F., and Elliot, D. H., 1977, Interpretation of discordant $^{40}Ar/^{39}Ar$ age-spectra of Mesozoic tholeiites from Antarctica: Geochim. et Cosmochim. Acta, v. 41, p. 15–32.

Harrison, T. M., 1981, Diffusion of ^{40}Ar in hornblende: Contr. Mineralogy Petrology, v. 78, p. 324–331.

Harrison, T. M., and McDougall, I., 1980, Investigations of an intrusive contact, northwest Nelson, New Zealand—I, Thermal, chronological and isotopic constraints: Geochim. et Cosmochim. Acta, v. 44, p. 1985–2003.

—— 1982, The thermal significance of potassium feldspar K-Ar ages inferred from $^{40}Ar/^{39}Ar$ age spectra results: Geochim. et Cosmochim. Acta, v. 46, p. 1811–1820.

Kelly, W. C., and Rye, R. O., 1979, Geologic, fluid inclusion, and stable isotope studies of the tin-tungsten deposits of Panasqueira, Portugal: ECON. GEOL., v. 74, p. 1721–1822.

Kulvanich, S., 1975, Micas of the Panasqueira tin-tungsten deposit: Unpub. Masters thesis, Ann Arbor, Univ. Michigan, 64 p.

Lanphere, M. A., and Albee, A. L., 1974, $^{40}Ar/^{39}Ar$ age measurements in the Worcester mountains: Evidence of Ordovician and Devonian metamorphic events in northern Vermont: Am. Jour. Sci., v. 274, p. 545–555.

Lund, K., Snee, L. W., and Evans, K. V., 1986, Age and genesis of precious-metals deposits, Buffalo Hump district, central Idaho: Implications for depth of emplacement of quartz veins: ECON. GEOL., v. 81, p. 990–996.

Merrihue, C. M., and Turner, G., 1966, Potassium-argon dating by activation with fast neutrons: Jour. Geophys. Research, v. 71, p. 2852–2857.

Orev, F. C. d', 1967, Tungsten-tin mineralization and paragenesis in the Panasqueira and Vale da Ermida mining districts, Portugal: Portugal Servicos Geol., Comunicacoes, v. 52, p. 117–167.

Roddick, J. C., 1983, High precision intercalibration of $^{40}Ar/^{39}Ar$ standards: Geochim. et Cosmochim. Acta, v. 47, p. 887–898.

Ruiz, J., Jones, L. M., and Kelly, W. C., 1984, Rubidium-strontium dating of ore deposits: Hosted by Rb-rich rocks, using calcite and other commong Sr-bearing minerals: Geology, v. 12, p. 259–262.

Schermerhorn, L. J. G., 1981, Project ibergranite: Berlin, Freie Univ. Berlin, Inst. Mineralogie, Newsletter No. 1, 9 p.

Skinner, B. J., 1979, The many origins of hydrothermal mineral deposits, in Barnes, H. L., ed., Geochemistry of hydrothermal ore deposits: New York, John Wiley, p. 1–21.

Snee, L. W., 1982, Emplacement and cooling of the Pioneer batholith, southwestern Montana: Unpub. Ph.D. thesis, Columbus, Ohio State Univ., 320 p.

Steiger, R. H., and Jäger, E., 1977, Subcommission on geochronology: Convention on the use of decay constants in geo- and cosmochronology: Earth Planet. Sci. Letters, v. 36, p. 359–362.

Sutter, J. F., Ratcliffe, N. M., and Mukasa, S. B., 1985, $^{40}Ar/^{39}Ar$ and K-Ar bearing on the metamorphic and tectonic history of western New England: Geol. Soc. America Bull., v. 96, p. 123–136.

Thadeu, D., 1951, Geologia do couto mineiro da Panasqueira: Portugal Servicos Geol., Comunicacoes, v. 32, p. 5–64.

Turner, G., 1968, The distribution of potassium and argon in chrondrites, in Ahrens, L. H., ed., Origin and distribution of the elements: New York, Pergamon Press, p. 378–398.

Wallis, W. A., and Roberts, H. V., 1966, Statistics—a new approach, 13th ed.: Toronto, The Free Press, A Corp., 646 p.

144

REFERENCES

Ahrens, L.H., 1946, Determination of the age of minerals by means of the radioactivity of rubidium: Nature 157, 269.

Allègre, C.J., Albarède, F., Grünenfelder, M., and Köppel, V., 1974, $^{238}U/^{206}Pb$ - $^{235}U/^{207}Pb$ - $^{232}Th/^{208}Pb$ zircon geochronology in Alpine and non-Alpine environment: Contrib. Mineral. Petrol. v. 43, 163-194.

Allsopp, H.L., 1961, Rb-Sr age measurements on total rock and separated mineral fractions from the old granite of the central Transvaal: J. Geophys. Res. v. 66, 1499-1508.

Armstrong, R.L., 1966, K-Ar dating of plutonic and volcanic rocks in orogenic belts, in Schaeffer, O.A. and Zähringer, J. (eds.), Potassium-Argon Dating: New York, Springer-Verlag, 117-133.

Beard, B.L., Medaris, L.G., Johnson, C.M. and Brueckner, H.K., 1991, Geochronology and geochemistry of Group A eclogites from the Moldanubian zone of the Bohemian Massif, Czechoslovakia (abstract): Geological Society of Australia Abstracts no. 27, p.8.

Bowring, S.A., Williams, I.S., and Compston, W., 1989, 3.96 Ga gneisses from the Slave province, Northwest Territories, Canada: Geology v.17, 971-975.

Briqueu, L. and de la Boisse, H., 1990, U-Pb geochronology: systematic development of mixing equations and application of Monte Carlo numerical simulation to the error propagaton in the Concordia diagram: Chemical Geology v.88, 69-83.

Brooks, C., Hart, S.R., and Wendt, I., 1972, Realistic use of two-error regresssion treatments as applied to rubidium-strontium data: Reviews of Geophys. and Space Phys. 10m 551-557.

Brueckner, H.K., Bakun-Czubarow, N., Rubenstone, J.L. and Zindler, A., 1991, Converging Sm-Nd mineral ages in eclogites and garnet peridotites from the Caledonides of Norway and the Variscides of Poland and Czechoslovakia: Geological Society of Australia Abstracts no. 27, 14.

Burton, K.W. and O'Nions, R.K., 1991, The thermal evolution of continental crust recorded by crystal growth: Geological Society of Australia Abstracts no. 27, 15.

Cattell, A, Krogh, T.E., and Arndt, N.T., 1984, Conflicting Sm-Nd whole-rock and U-Pb zircon ages for Archean lavas from Newton Township, Abitibi Belt, Ontario: Earth and Planet. Sci. Letters 70, 280-290.

Chen, C.-Y. and Frey, F.A., 1983, Origin of Hawaiian tholeiite and alkali basalt: Nature v. 302, 785-789.

Claesson, S., Pallister, J.S., and Tatsumoto, M., 1984, Samarium-neodymium data on two late Proterozoic ophiolites of Saudia Arabia and implication for crustal and mantle evolution: Contrib. Mineral. Petrol. v. 85, 244-252.

Cohen, A.S., O'Nions, R.K., Siegenthaler, R., and Griffin, W.L., 1988, Chronology of the pressure-temperature history recorded by a granulite terrain: Contrib. Mineral. Petrol. v. 98, 303-311.

Colman-Sadd, S.P., Hayes, J.P., and Knight, I., 1990, Geology of the Island of Newfoundland: Geological Survey Branch, Newfoundland Department of Mines and Energy, 1:1,000,000 color map.

Compston, W., Williams, I.S., and Meyer, C., 1984, U-Pb geochronology of zircons from lunar breccia 73217 using a sensitive high mass-resolution ion microprobe: J. Geophys. Res. 89B, 525-534.

Cortini, M. and Van Calsteren, P.W.C., 1985, Lead isotope differences between whole-rock and phenocrysts in recent lavas from southern Italy: Nature v.314,343-345.

Cumming, G.L., 1969, A recalculation of the age of the solar system: Can. J. Earth Sci. v. 4, 719-735.

Cumming, G.L. and Richards, J.R., 1975, Ore lead in a continuously changing Earth: Earth and Planet. Sci. Letters 28, 155-171.

Cumming, G.L., Rollet, J.S., Rosotti, F.J.C. and Whewell, R.J., 1972, Statistical methods for the computation of stability constants, I. Straight-line fitting of points with correlted errors: J. Chem. Society, Dalton Trans., v. 23, 2652-2658.

Dallmeyer, R.D., Blackwood, R.F., and Odom, A.L., 1981, Age and origin of the Dover Fault: tectonic boundary between the Gander and Avalon zones of the northeastern Newfoundland Appalachians: Canadian Jour. Earth Sciences v.12, 1685-1690.

Davidson, A. and Van Breemen, O., 1988, Baddeleyite-zircon relationships in coronitic metagabbro, Grenville Province, Ontario: implication for geochronology: Contrib. Mineral. Petrol. v. 100, 291-299.

Davis, D.W., 1982, Optimum linear regression and error estimation applied to U-Pb data: Can. J. Earth Sci., v. 19, 2141-2149.

Davis, D.W., Pezutto, F., and Ojakangas, R.W., 1990, The age and provenance of metasedimentary rocks in the Quetico Subprovince, Ontario, from single zircon analyses: implications for Archean sedimentation and tectonics in the Superior Province: Earth and Planet. Sci. Letters v.99, 195-205.

Depaolo, D.J., 1988, Neodymium isotope geochemistry - an introduction: Springer - Verlag, New York, 187 pp.

Dodson, M.H., 1973, Closure temperature in cooling geochronological and petrological systems: Contrib. Mineral. Petrol. v.40,259-274.

Dunning, G.R., O'Brien, S.J., Colman-Saad, S.P., Blackwood, R.F., Dickson, W.L., O'Neill, P.P. and Krogh, T.E., 1990, Silurian orogeny in the Newfoundland Appalachians. Journal of Geology, v.98,895-913.

Dunning, G.R. and O'Brien, S.J., 1989, Late Proterozoic-early Paleozoic crust in the Hermitage flexure, Newfoundland Appalachians: U/Pb ages and tectonic significance: Geology v. 17, 548-551.

Eskola, P., 1921, On the eclogites of Norway: Skrifter Norske Videnskaps-Akademi Oslo I. Matematisk-Naturvitenskapelig Klasse, v.8, 1-118.

Faure, G., 1986, Principles of Isotope Geology (2nd Edition): New York, Wiley, 589 p.

Gebauer, D. and Grünenfelder, M., 1979, U-Th-Pb dating of minerals, in Jäger, E. and Hunziker, J.C., eds., Lectures in Isotope Geology: Berlin, Springer- Verlag, 105-131.

Gebauer, D., Lappin, M.A., Grünenfelder, M., and Wyttenbach, A., 1985, The age and origin of some Norwegian eclogites: a U-Pb zircon and REE study: Chemical Geology v. 52, 227-247.

Goldich, S. S., and Mudrey, Jr., 1972, Dilatancy model for discordant U-Pb zircon ages: in Contributions to Recent Geochemistry and Analytical Chemistry (Vinogradov volume). Moscow: Nauka Publ. Office, pp. 415-418.

Goldschmidt, V.M., 1937, Geochemische verteilungsgesetze der elemente IX: die mengenverh ältnisse der elemente und der atom-arten: Skrifter Norske Videnskaps-Akademi Oslo I. Matematisk-Naturvitenskapelig Klasse v.4, 140 p.

Griffin, W. L. and Brueckner, H. K. 1985, REE, Rb-Sr and Sm-Nd studies of Norwegian eclogites: Chemical Geology v. 52, 249-271.

Griffin, W, L. and Brueckner, H. K. 1980, Caledonian Sm-Nd ages and a crustal origin for Norwegian eclogites: Nature v.285, 319-321.

Griffin, W.L., Austerheim, H., Brastad, K., Bryhni, I., Krill, A.G., Krogh, E.J., Mφrk, M.B.E., Qvale, H., and Tφrudbakken, B., 1985, High-pressure metamorphism in the Scandinavian Caledonides in Gee, D.G. and Sturt, B.A. (eds.), the Celedonide Orogen - Scandinavia and Related Areas: Wiley & Sons, New York, 783-801.

Gromet, L. P. 1989, Avalonian terranes and late Paleozoic tectonism in southeastern New England: Constraints and Problems, in Dallmeyer, R. D. and Keppie, J. D., eds., Terranes in the circum-Atlantic Paleozoic Orogens, Geol. Soc. Amer. Special Pap. 230, 193-211.

Gromet, L. P. 1991, Direct dating of deformational fabrics, in Heaman, L.M. and Ludden, J.L., eds., Application of Radiogenic Isotope Systems to Problems in Geology: Mineral. Assoc. Canada Short-Course Handbook 19, 167-189.

Hahn, O., Strassmann, F. and Walling, E., 1937, Herstellung wägbarer mengen des strontiumisotops 87 als umwandlungsprodukt des rubidiums aus einem kanadischen glimmer: Naturwissenschaften 25, 189.

Hansen, E. C., 1971, Strain facies: Springer-Verlag, New York, 220 pp.

Hanson, G.N. and Gast, P.W., 1967, Kinetic studies in contact metamorphic zones: Geochim. Cosmochim. Acta. 31, 1119-1153.

Hamilton, E.I., 1965, Applied Geochronology: Academic Press, New York, 267 p.

Harper, C.T., 1967, The geological interpretation of potassium-argon ages of metamorphic rocks from the Scottish Caledonides: Scottish J. Geol. v.3, 46-66.

Harrison, T.M. and McDougall, I., 1980, Investigation of an intrusive contact, northwest Nelson, New Zealand - II. Diffusion of radiogenic and excess ^{40}Ar in hornblende revealed by ^{40}Ar/^{39}Ar age spectrum analysis: Geochim. Cosmochim. Acta. 44, 2005-2020.

Hart, S.R., 1964, The petrology and isotopic mineral age relations of a contact zone in the Front Range, Colorado: Journal of Geology 72, 493-525.

Heaman, L.M. and Parrish, R. 1991, U-Pb Geochronology of Accessory Minerals, in Heaman, L.M. and Ludden, J.N., Applications of Radiogenic Isotope Systems to Problems in Geology: Mineral. Assoc. of Canada Short Course Handbook 19, 59-102.

Hildreth, W., Halliday, A.N. and Christiansen, R.L., 1991, Isotopic and chemical evidence concerning the genesis and contamination of basaltic and rhyolitic magma beneath the Yellowstone Plateau Volcanic Field: Journal of Petrology 32, 63-138.

Hodgkins, C.E., 1985, Major and trace element geochemistry and petrology of the late Precambrian Dry Hill Gneiss, Pelham dome, central Massachusetts: Department of Geology and Geography, University of Massachusetts, Contribution 48, 135 p.

Holdsworth, R.E., 1991, The geology and structure of the Gander-Avalon boundary zone in northeastern Newfoundland, in Current Research, Newfoundland Department of Mines and Energy, Report 91-1, 109-126.

Jaffey, A.H., Flynn, K.F., Glendenin, L.E., Bentley, W.C., and Essling, A.M., 1971, Precision measurement of half-lives and specific activities of ^{235}U and ^{238}U: Physical Review C, v.4, 1889-1906.

Johnson, C.M., 1989, Isotopic zonations in silicic magma chambers: Geology v.17, 1136-1139.

Kinney, P.D., Williams, I.S., Froude, D.O. Ireland, T.R., and Compston, W., 1988, Early Archean zircon ages from orthogneisses and anorthosites at Mount Narryer, Western Australia: Precambrian Research v.38, 325-341.

Kober, B., 1986, Whole-grain evaporation for $^{207}Pb/^{206}Pb$ age investigations on single zircons using a double-filament thermal ion source: Contrib. Mineral. Petrol. v.93, 82-90.

Kober, B. 1987, Single-grain evaporation combined with Pb^+ emitter bedding for $^{207}Pb/^{206}Pb$ age investigations using thermal ion mass spectrometry, and implications to zirconology: Contrib. Mineral. Petrol. 96, 63-71.

Krogh, E.J., 1980, Compatible P-T conditions for eclogites and surrounding gneisses in the Kristiansund area, western Norway: Contrib. Mineral. Petrol. v.75, 387-393.

Krogh, T.E., 1973, A low-contamination method for hydrothermal decomposition of zircon and extraction of U and Pb for isotopic age determinations: Geochim. Cosmochim. Acta. v.48, 485-494.

Krogh, T.E. and Davis, G.L., 1974, Alteration in zircons with discordant U-Pb ages: Carnegie Inst. Washington Yearbook 73, 560-567.

Krogh, T. E. 1982a, Improved accuracy of U-Pb zircon ages by the creation of more concordant systems using an air abrasion technique. Geochim. Cosmochim. Acta 46, 637-649.

Krogh, T. E. 1982b, Improved accuracy of U-Pb zircon dating by selection of more concordant fractions using a high-gradient magnetic separation technique. Geochim. Cosmochim. Acta 46, 631-635.

Krogh, T.E. and Keppie, J.D., 1990, Age of detrital zircon and titanite in the Meguma Group, southern Nova Scotia, Canada: clues to the origin of the Meguma Terrane: Tectonophys. v.177, 307-323.

Krogh, T. E., Mysen, B.O. and Davis, G.L., 1974. A Paleozoic age for the primary minerals of a Norwegian eclogite: Carnegie Institution of Washington, Year Book 73, p. 577.

Krogh, T. E., Strong, D.F., O'Brien, S.J., and Papezik, V. S. 1988, Precise U-Pb zircon dates from the Avalon Terrane in Newfoundland. Canadian Journal of Earth Sciences, 25, pp. 442-453.

Lecheminant, A.N. and Heaman, L.M., 1989, Mackenzie igneous events, Canada: middle Proterozoic hotspot magmatism associated with ocean opening: Earth and Planet. Sci. Letters v.96, 38-48.

148

Li Shuguang, Liu Deliang, Chen Yizhi, Hart, S.R., Zhang, G., and Ahang, Z., 1991, Sm-Nd isotopic chronology of the major tectonic events for the Qinling-Dabie orogenic belt: Geol. Soc. of Australia, Abstracts, No. 27, 59.

Ludwig, K.R., 1980, Calculation of uncertainties of U-Pb isotope data: Earth Planet. Sci. Lett., v.46, 212-220.

Ludwig, K.R., 1982a, Programs for filing and plotting U-Pb isotope data for concordia diagrams using an HP-9830 computer and HP-9862 plotter: U.S. Geol. Surv. Open File Report 82-386.

Ludwig, K.R., 1982b, A computer program to convert raw Pb-U-Th isotope ratios to blank-corrected isotope ratios and concentrations, with associated errors and error-correlations: U.S. Geol. Surv. Open File Report 82-820.

Ludwig, K. R. 1985, PBDAT A computer program for processing raw Pb-U-Th isotope data: U. S. Geol. Surv. Open File Report 85-547.

MacDougall, I. and Harrison, T.M., 1988, Geochronology and Thermochronology by the $^{40}Ar/^{39}Ar$ Method. Oxford University, Oxford, 272 p.

MattisonN, J.M., 1987, U-Pb ages of zircons: a basic examination of error propagation: Chemical Geology v. 66, 151-162.

McIntyre, G.A., Brooks, C., Compston, W., and Turek, A., 1966, The statistical assessment of Rb-Sr isochrons: J. Geophys. Res. v.71, 5459-5468.

McKerrow, W.S., Lambert, R. ST. J., and Cocks, L.R.M., 1985, The Ordovician, Silurian, and Devonian periods, in Snelling, N.J. ed., The Chronology of the Geological Record: Brit. Geol. Surv. Memoir 10, 73-80.

Mearns, E.W., 1986, Sm-Nd ages for Norwegian garnet peridotite, in Griffin, W.L., ed., Second International Eclogite Conf., Lithos v.19, 269-278.

Mezger, K, Hanson, G.N. and Bohlen, S.R., 1989, High-precision U-Pb ages of metamorphic rutile: application to the cooling history of high-grade terranes: Earth Planet Sci. Letters 96, 106-118.

Mørk, M. B. E., 1985, A gabbro to eclogite transition on Flemsøy, Sunnmøre, western Norway: Chemical Geology, v.50, 283-310.

Mørk, M. B. E. and MEARNS, E. W. 1986, Sm-Nd isotopic systematics of a gabbro-eclogite transition: Lithos, v.19, 255-267.

Mørk, M. B. E., KULLERUD, K. and STABEL, A. 1988, Sm-Nd dating of Seve eclogites, Norrbotten, Sweden; evidence for early Caledonian (505 Ma): subduction. Contrib. Miner. Petrol. v. 99, 344-351.

Moser, D.E., Krogh, T.E., Heaman, L.M., Hanes, J.A., Helmstaedt, H., 1991, The age and significance of Archean mid-crustal extension in the Kapuskasing Uplift, Superior Province, Canada (abstract): Geol. Soc. Amer. Abstracts with Programs v.23, A134.

Nicolaysen, L. O. 1961, Graphic interpretation of discordant age measurements of metamorphic rocks. Ann. NY Acad. Sci., 92, 198-206.

Oberli, F. and Meier, M., 1991, Age of Eocene-Oligocene boundary in the Marche-Umbria basin, Italy, by high resolution U-Th-Pb dating: Terra abstracts v.3 no.1, 286.

O'Brien, B.H. and O'Brien, S.J., 1989, Re-investigation and re-interpretation of the Silurian La Poile Group of southwestern Newfoundland, in Current Research, Newfoundland Department of Mines and Energy, Report 90-1, 305-316.

O'Brien, B.H., O'Brien, S.J., and Dunning, G.R., in press, Silurian Cover, Late Precambrian - early Ordovician basement, and the chronology of Silurian orogenesis in the Hermitage flexure (Newfoundland Appalachians): Amer. J. Sci. (in press).

Odin, G.S., 1985, Remarks on the numerical scale of Ordovician to Devonian times, inSnelling, N.J. ed., The Chronology of the Geological Record: Brit. Geol. Surv. Memoir 10, 93-98.

Osberg, P.H., 1978, Synthesis of the geology of the northeastern Appalachians, U.S.A.: Geol. Surv. Canada, Paper 78-13, 137-147.

Parrish, R.R, 1990, U-Pb dating of monazite and its application to geological problems: Canadian Jour. Earth Sciences v.27, 1431-1450.

Purdy, J.W. and Jäger, E., 1976, K-Ar ages on rock-forming minerals from the central Alps: Memoir Institute Geol. Min. University of Padova 30, 1-31.

Ramberg, H., 1943, En undersøkelse av Vestrandens regionalmetamorfe bergarter: Norsk Geol. Tidsskr. v. 23, 1-74.

Richard, P., Shimizu, N., and Allègre, C.J., 1976, ^{143}Nd/^{144}Nd, a natural tracer- an application to oceanic basalts: Earth Plan. Sci. Lett. 31, 269-278.

Robinson, P. and Hall, L.M., 1980, Tectonic synthesis of southern New England in Wones. D.R. ed., The Caledonides in the U.S.A.: Department of Geological Sciences, VPI & SU Memoir 2, 73-82.

Roden, M., Parrish, R.R. and Miller, D.S., 1990, The absolute age of the Eifelian Tioga ash bed, Pennsylvania: Journal of Geology v.98, 282-285.

Roddick, J.C., 1987, Generalised numerical error analysis with applications to geochronology and thermodynamics: Geochim. Cosmochim. Acta. v.51, 2129-2135.

Roll, M.A., 1987, Effects of Acadian kyanite-zone metamorphism on relict granulite-facies assemblages, Mount Mineral formation, Pelham dome, Massachusetts: Department of Geology and Geography, University of Massachusetts Contribution no. 60, 202 pp.

Ross, G.M., Parrish, R.R, and Dudás, Ö., 1991, Provenance of the Bonner formation (Belt Supergroup), Montana: insights from U-Pb and Sm-Nd analyses of detrital minerals: Geology 19, 340-343.

Ross, R.J., Naeser, C.W., Izett, G.A., Obradovich, J.D., Bassett, M.G., Hughes, C.P., Cocks, L.R.M., Dean, W.T., Ingham, J.K., Jenkins, C.J., Rickards, R.B., Sheldon, P.R., Toghill, Whittington, H.B. and Zalasiewicz, J., 1982, Fission-track dating of British Ordovician and Silurian stratotypes: Geol. Mag. 119, 135-153.

Ross, R.J., Maeser, C.W., and Izett, G.A., 1976, Apatite fission-track dating of a sample from the type Caradoc (Ordovician) series in England; Geology 4, 505-506.

Samson, S.D., Patchett, P.J., Roddick, J.C. and Parrish, R.R., 1989, Origin and tectonic setting of Ordovician bentonites in North America: isotopic and age constraints: Geol. Soc. America Bull. v.101, 1175-1181.

Schärer, U., Copeland, P., Harrison, T.M. and Searle, M.P., 1990, Age, cooling history, and origin of post-collisional leucogranites in the Karakoram batholith; a multi-system isotope study: Journal of Geology v.98, 233-251.

Shields, W.R., 1960, Comparison of Belgian Congo and synthetic "normal" samples: Table 6 in Appendix A, Report no. 8, National Bureau of Standards (USA) Meeting of the Advisory Committee for Standard Materials and Methods of Measurement, 37 p. (unpublished).

Shirey, S.B., 1991, The Rb-Sr, Sm-Nd and Re-Os isotopic systems: a summary and comparison of their applications to the cosmochronology and geochronology of igneous rocks, in Heaman, L.M. and Ludden, J.N. (eds.) Application of Radiogenic Istope Systems to Problems in Geology: Mineral. Assoc. of Canada Short-Course Handbook 19, 103-162.

Silver, L.T., 1963, The use of cogenetic uranium-lead isotope systems in zircons in geochronology, in Radioactive Dating, International Atomic Energy Agency Symposium, Athens, 279-287.

Silver, L.T. and Deutsch, S., 1963, Uranium-lead isotopic variations in zircon: a case study: Journal of Geology v. 71, 721-758.

Silver, L.T., McKinney, C.R., Deutsch, S., and Bolinger, J., 1963, 1963, Precambrian age determinations in the western San Gabriel mountains, California: J. Geology v.71, 196-214.

Stacey, J.S. and Kramers, J.D., 1975, Approximation of terrestrial lead isotope evolution by a two-sage model: Earth and Planet. Sci. Letters 26, 207-221.

Steiger, R.H. and Jäger, E., 1977, Subcommission on geochronology: convention on the use of decay constants in geo- and cosmochronology: Earth Planet. Sci. Letters 69, 13-29.

Tera, F. and Wasserburg, G.J., 1972, U-Th-Pb systematics in three Apollo 14 basalts and the problem of initial Pb in lunar rocks: Earth and Planet. Sci. Letters v.14, 281-304.

Tilton, G.R., 1960, Volume diffusion as a mechanism for discordant lead ages: Journal of Geophysical Research v.65, 2933-2945.

Tucker, R.D., 1988, Juxtaposition of contrasting terranes in the central Norwegian Caledonides; evidence from U-Pb dating of accessory minerals (abstract): Geol. Soc. Amer. Abstracts with Programs v.20, no.1, 77.

Tucker, R.D., 1986, Geology of the Hemnefjord - Orkanger area, south-central Norway: Norges geologiske undersøkelse v.404, 1-20.

Tucker, R.D. and Krogh, T.E., 1986, Recognition of contrasting crustal segments in the Caledonides of central Norway through U-Pb geochronology (abstract): Geol. Soc. Amer. Abstracts with Programs 19, 872.

Tucker, R.D. and Robinson, R., 1990, Age and setting of the Bronson Hill magmatic arc: a re-evaluation based on new U-Pb zircon ages in southern New England: Geol. Soc. Amer. Bull. v.102, 1404-1419.

Tucker, R.D., Robinson, P. and Hollocher, K.T., 1988, U-Pb zircon, titanite, and monazite dating in "basement" rocks of the Bronson Hill anticlinorium, central Massachusetts (abstract): Geol. Soc. Amer. Abstracts with Programs 7, A216.

Tucker, R.D., Krogh, T.E., and Råheim, A., 1991, Proterozoic evolution and age-province boundaries in the central part of the Western Gneiss Region, Norway; results of U-Pb dating of accessory minerals from Trondheimsfjord to Geiranger, in Gower, C.F., Rivers, T., and Ryan, A.B., Mid-Proterozoic Laurentia-Baltica: Geol. Soc. Canada Special Paper 38, 149-174.

Tucker, R.D., Krogh, T.E., Ross, R.J. and Williams, S.H., 1990, Time-scale calibration by high-precision U-Pb zircon dating of interstratified volcanic ashes in the Ordovician and Lower Silurian stratotypes of Britain: Earth and Planet. Sci. Letters v.100, 51-58.

Tucker, R.D., Råheim, A., Krogh, T.E., and Corfu, F.C., 1987, Uranium-lead zircon and titanite ages from the northern portion of the Western Gneiss Region, south-central Norway: Earth and Planet. Sci. Letters v.81, 203-211.

Van Breemen, O. and Hawkesworth, C.J., 1980, Sm-Nd isotopic study of garnets and their metamorphic host rocks: Trans. of the Royal Society of Edinburgh, Earth Sciences v.71, 97-102.

Vance, D. and O'Nions, R.K., 1990, Isotopic chronometry of zoned garnets: growth kinetics and metamorphic histories: Earth and Planet. Sci. Letters v.97, 227-240.

Wasserburg, G.J., 1963, Diffusion processes in uranium-lead systems: J. Geophys. Res. 68, 4823-4846.

Wetherill, G.W., 1956a, Discordant uranium-lead ages, I: American Geopysical Union Transactions v.37, 320-326.

Wetherill, G.W., 1956b, An interpretation of the Rhodesia and Witwatersrand age patterns: Geochim. Cosmochim. Acta v.9, 290-292.

Wetherill, G.W., 1963, Discordant uranium-lead ages, II. Discordant ages resulting from diffusion of lead and uranium: J. Geophys. Res. v.68, 2957-2965.

Williams, H., 1979, Appalachian orogen in Canada: Canad. Jour. Earth Sciences v.16, 792-807.

Williams, I.S., Compston, W., Black, L.P. Ireland, T.R., and Foster, J.J., 1984, Unsupported radiogenic Pb in zircon: a cause of anomalously high Pb-Pb, U-Pb and Th-Pb ages: Contrib. Mineral. Petrol. v.88, 322-327.

Wintsch, R.P. and Sutter, J.F., 1986, A tectonic model for the Late Peleozoic rocks of southeastern New England: Jour. Geol. v. 94, 459-472.

York, D., 1969, Least squares fitting of a straight line with correlated errors: Earth Planet. Sci. Letters v.5, 320-324.

Zen, E-An, 1983, Exotic terranes in the New England Appalachians - limits, candidates, and ages: a speculative essay, in Hatcher, R.D., Williams, H., and Zietz, I. (eds.), Contributions to the tectonic and geophysics of mountain chains: Geol. Soc. America Memoir 158, 55-81.

Zindler, A., Staudigel, H., Hart, S.R., Endres, R., Goldstein, S., 1983, Nd and Sr isotopic study of a mafic layer from the Ronda ultramafic complex: Nature v. 304, 226-230.

152